1992-05

Composite system stability methods applied to advanced shipboard electric power systems

Amy, John Victor

COMPOSITE SYSTEM STABILITY METHODS APPLIED TO ADVANCED SHIPBOARD ELECTRIC POWER SYSTEMS

by

John Victor Amy Jr.
Naval Engineer
S.M. Electrical Engineering and Computer Science
Massachusetts Institute of Technology
(1990)

B.S. Electrical Engineering
United States Naval Academy
(1983)

Submitted to the Department of
OCEAN ENGINEERING
in Partial Fulfillment of the Requirements
for the Degree of

DOCTOR OF PHILOSOPHY
in the field of

NAVAL ELECTRIC POWER SYSTEMS

at the
MASSACHUSETTS INSTITUTE OF TECHNOLOGY
May 1992

COMPOSITE SYSTEM STABILITY METHODS APPLIED TO ADVANCED SHIPBOARD ELECTRIC POWER SYSTEMS

by

John Victor Amy Jr.

Submitted to the Department of Ocean Engineering on 12 May, 1992 in partial fulfillment of the requirements for the degree of Doctor of Philosophy in the field of Naval Electric Power Systems.

ABSTRACT

Large increases in the complexity of shipboard electric loads as well as development of electric drive, integrated electric drive and pulsed power systems make manifest the present and future importance of naval electric power systems. The most crucial attribute of these systems is their ability to fulfill their function in the presence of "large-signal" perturbations. Fundamental differences between shipboard and commercial electric power systems make all but the most general nonlinear, "large-signal" stability analyses inappropriate for the design and assessment of naval electric power systems. The tightly coupled and compact nature of shipboard systems are best accommodated by composite system stability analyses.

Composite system methods, based upon Lyapunov's direct method, require that each component's stability be represented by a Lyapunov function. A new Lyapunov function which is based upon coenergy is developed for 3-phase synchronous machines. This use of coenergy is generalizable to all electromechanical energy conversion devices. The coenergy-based Lyapunov function is implemented as a "stability organ" which generates waveforms at information terminals of a "device object" in the object oriented simulation environment of WAVESIM. Single generator simulation results are used to acquire a measure of the "over sufficiency" of the coenergy-based Lyapunov function.

Some means of combining the components' Lyapunov functions is necessary with composite system stability criterions. To provide the largest stability region in a Lyapunov function convective derivative space, thereby reducing "over sufficiency", a "time-variant weighted-sum" composite system criterion is developed. This criterion is implemented as a "stability demon" "device object" within the WAVESIM environment. The "stability demon" is tested through RLC circuit simulations and a two-generator simulation. The output of the "stability demon" is suitable for use within an overall system stabilising controller.

Thesis Supervisor: James L. Kirtley Jr., Associate Professor of Electrical Engineering

Thesis Supervisor: Marija D. Ilic, Senior Research Scientist, Department of Electrical Engineering and Computer Science

Acknowledgements

I am deeply grateful to the United States Navy for allowing me to continue my education at M.I.T. and complete this degree. Rich Martin and Dave Young of DARPA, and CAPT Reed and CAPT Graham of NAVSEA 05Z assisted in providing financial support and encouragement for this research. I am most appreciative. A number of people at David Taylor Research Center, Annapolis MD helped me greatly, among them Ed Zivi, Dave Clayton and Henry Hegner. I thank you all very much.

I wish to thank the members of my thesis committee, Professor A.D. Carmichael, Professor M.S. Triantafyllou, Professor J.L. Kirtley Jr. and Dr. M.D. Ilic. I wish to acknowledge, in particular, my two thesis supervisors, Professor Kirtley and Dr. Ilic. Your guidance, encouragement, patience and challenges made this entire effort as enjoyable as it was worthwhile.

I owe a particular debt to my very dear friend, comrade, accomplice, mentor and classmate Dr. Norbert Doerry.--"Thanks Norbs." I also wish to thank my close friend and fellow student Mary Tolikas for her support, help and patience.

"If perhaps I have seen a great distance, it is because I have stood on the shoulders of Giants." - Unknown

My Giants:
Prof. Kirtley
Capt Harry Jackson
Norbert Doerry
Mary Tolikas
Prof. Ogilvie
Dr. Ilic
Prof. Melcher
Capt B.F. Tibbitts
Cdr P. Sullivan
Prof. Carmichael
Cdr R. Celotto
The XIII-A Class of '90
The OE Athena Cluster Regulars
Erv LaForge
Vivian Mizuno
Row
Sr. Regina Clare
Mom and Dad
Rebecca
John III
Christian

Thank you all very much.

Table of Contents

1 Introduction

1.1 Overview of Research Effort

1.1.1 Motivation

The ongoing and significant changes in naval electric power systems reach beyond the bounds of traditional analyses and design methods. Taken with their extant peculiarities, the changes in these systems necessitate improvements in the analysis and design methods which are used. Advanced methods of time domain analysis of multirate, nonlinear, lumped parameter models of electromechanical systems, reference [1.1], have laid the foundation for development of a general "large-signal" stability criterion which is appropriate for advanced naval electric power systems. This new general stability criterion and the advanced time domain analysis techniques will aid the development of advanced nonlinear controls.

The U.S. Navy has stated a desire to develop advanced, integrated naval electric power systems. The capabilities expected of these highly flexible and highly nonlinear power systems demand adaptive, sophisticated nonlinear controls. Virtually all of the dynamic occurrences of interest for shipboard systems stem from "large signal" perturbations. A control regimen addressing these perturbations certainly requires some general stability measure to ensure that control actions are not destabilising. A general, nonlinear "large-signal" stability measure which is wholly appropriate for application to naval electric power systems has not existed. This research addresses this need.

1.1.2 The WAVESIM Environment

The research documented by reference [1.1] establishes a simulation tool, WAVESIM, which uses advanced numerical methods to describe the time-domain behaviour of complex electromechanical systems, such as naval electric power systems. It is capable of representing multirate, tightly coupled, nonlinear systems. Such an analytical capability is required for nonlinear control design.

Additionally, WAVESIM's architecture has the system's components' dynamics modelled within a "device object". Dynamics are not solved on a system level. Hence, a modeller using WAVESIM is free to choose (1) how fundamental the component "device objects" will be and (2) the particular model of a system component that a "device object" uses.

Just as actual components are connected to the rest of a system through physical terminals, so too are the corresponding "device objects" connected by nodal equations in their terminal variables. A very important feature of the WAVESIM environment is the distinction between and accommodation of both normal terminal variables and information terminal variables. A potential and a flow are associated with normal terminals.--Energy transfers occur through normal terminals. Information terminals have only a potential associated with them.--Energy transfers cannot take place at information terminals. Control inputs often take the form of information variables.

Providing information variables from within a "device object" enables construction of a system-wide "large-signal" stability assessor which will provide continuous quantification of stability yet not interfere with the normal terminal variable physics. Such a stability assessor takes advantage of the composite (built up of component "device objects") nature of the system and the flexibility it grants to the modeller. WAVESIM is specifically designed to accommodate the composite nature of naval electric power systems. WAVESIM does not require that a system possess any particular type of "structure".

1.1.3 Research Approach

This research contains two fundamental, interrelated, overlapping tasks. The goal which the two tasks seek to achieve is to develop a composite system stability assessor which uses a general, nonlinear stability criterion to provide an on-line quantification of "large-signal" stability. Whereas the application of this research is naval electric power systems, the algorithms developed here, although general in nature, are implemented within WAVESIM. Furthermore, given the flexible nature of naval electric power systems, no foreknowledge of the interconnection "structure" of the system being studied is assumed.

The first research task is the development and implementation of a "stability organ" for a "device object". A "stability organ" is simply a relationship which generates information variables that a "device object" provides to give an indication of the stability of the "device object". In this research, these variables are a Lyapunov function and its convective derivative.

Development of the "stability organ" includes selecting an appropriate Lyapunov function. Lyapunov's stability methods are based upon sufficient conditions. A poorly selected Lyapunov function may be so "overly sufficient" that its indications are useless. Hence, some assessment of the "over sufficiency" of a Lyapunov function is necessary. Once a Lyapunov function is selected for a specific system component, it must be "coded" within the "device object" representing the system component.

The second research task is to establish a relevant composite system "large-signal" stability criterion. This criterion must use as inputs the outputs of the "stability organs" of participating "device objects". Just as "over sufficiency" issues are critical in the selection of a Lyapunov function for each "stability organ", so too is the derivation of a composite system criterion beset with "over sufficiency" concerns. This criterion also must address the forms of stability which are most relevant to naval electric power systems.

The composite system criterion requires proof of its efficacy. The criterion must be cast into an algorithm which is the basis of the composite system's "stability demon".

This research introduces the "stability organ" and "stability demon" notions which provide an on-line assessment of stability. This on-line assessment is intended as an input to a stabilising controller. The engineering-oriented Lyapunov function which is the basis of the "stability organ" developed in this thesis is generalisable to any electromechanical energy conversion device. The composite system stability criterion which is the basis of the "stability demon" uses a different approach to increasing a system's region of stability within Lyapunov function convective derivative space.

1.2 Overview of Thesis

Chapter 2 provides background material on naval electric power systems and stability analysis methods. Section 2.1 endeavours to provide a glimpse of what advanced shipboard electric power systems will be like. A description of dynamic occurrences of interest is also important. Section 2.2 describes the principles underlying the various methods presently employed for assessing electric power system stability. Section 2.3 takes a concentrated look at a composite system stability method which is quite adaptable to the requirements of naval electric power systems. Section 2.4 is a concise statement of the requirements for a stability criterion for such a system.

Chapter 3 provides the development of the relationships which are the foundation of the two products of this research, a "stability organ" for 3-phase synchronous machines and a composite system "stability demon". Section 3.1 describes the model of a 3-phase synchronous generator which is used and derives the coenergy-based Lyapunov function which is the basis of the "stability organ". Section 3.2 discusses the composite system stability criterion which is implemented as the system-wide "stability demon".

Chapter 4 presents results provided by the "stability organ" and the "stability demon". Section 4.1 shows the output of the "stability organ" for a number of single generator simulations. This output is meant to verify the performance of the "stability organ" and provide a relative measure of the "over sufficiency" of the coenergy-based Lyapunov function. Section 4.2 illustrates the potential of the "time-variant weighted-sum" composite system Lyapunov function which is at the heart of the "stability demon".

Chapter 5 uses both the "stability organ" and "stability demon" to analyse the stability of a two generator system undergoing a short-circuit. One of the generators is conventional, the other superconducting. The analysis is meant to show how the two research products work together within a composite system. The analysis is also of interest because some comparison of the performance of the two generators is possible.

Chapter 6 contains the conclusions regarding this research. Chapter 7 contains the bibliography. Appendices follow.

1.3 References

1.1 Doerry, N.H. "Advanced Numerical Methods for Simulating Nonlinear Multirate Lumped Parameter Models." Thesis, PhD, M.I.T. May 1991.

2 Background

The intent of this chapter is to provide background information on traditional and advanced naval electric power systems and basic electric power system stability analyses. Section 2.1 describes naval electric power systems and relevant dynamic occurrences. Section 2.2 describes the basics of electric power system stability. Section 2.3 provides background on two composite system stability analysis methods. The final section, 2.4, states how well naval electric power system stability analysis needs can be met with the extant methods.

2.1 Naval Electric Power Systems

This discussion has three components. Traditional and advanced naval electric power systems are described independently. As time passes, classification of a contemporary system as traditional or advanced is likely to be somewhat blurred with systems progressively acquiring more of the features attributed to advanced systems. The third component of this discussion focuses on the dynamically "stressfull" environment in which naval electric power systems operate.

2.1.1 Salient Characteristics of Naval Electric Power Systems

The function of naval electric power systems is to supply electric power to the combat, ship control and propulsion, auxiliary and support systems onboard a naval combatant. Given the disastrous consequences of losing power to these loads during combat, after sustaining damage, or while the ship is in a restricted manoeuvring situation, such systems must be robust in the sense of ensuring that vital loads are always supplied. Whereas naval combatants are not typically very large and do not grow in size over their lifetimes, their power systems must achieve a balance between load margin, growth margin, performance criterions and fitting inside of a ship. Historically, electric loads grow by roughly twenty percent over the lifetime of a naval ship. The ship, though, does not grow larger.

Their function and the two broad requirements placed upon them have led to naval electric power systems which are optimised for survivability and minimal weight and volume. These two optimisations continue to be the principal design priorities. They have led to a traditional architecture and the design practices presently employed.

In contrast, commercial electric power systems seek to reliably supply quality electric power to a numerically vast and geographically dispersed set of loads. Furthermore, these power systems seek to discharge this calling at a profit. Hence, the function of the commercial electric power system and the requirements placed upon it have led to a system which is optimised for reliability and minimal operating cost.

The different functions and requirements placed upon naval electric power systems and commercial electric power systems, as well as the different optimisations which these functions and requirements led to, produce electric power systems which are different in some very fundamental ways.--Assumptions which may be true for one, may not be true for the other.

2.1.1.1 Features of Traditional Systems

The function of a naval electric power system and the requirements placed upon it lead to the optimisations discussed above. The traditional architecture that this has led to is a three tiered system. There is the (normal) ship service power system, the emergency (or auxiliary) power system, and the casualty power system. Figure 2.1.1 shows a diagram of a simplified naval electric power system, references [2.1.1] and [2.1.2].

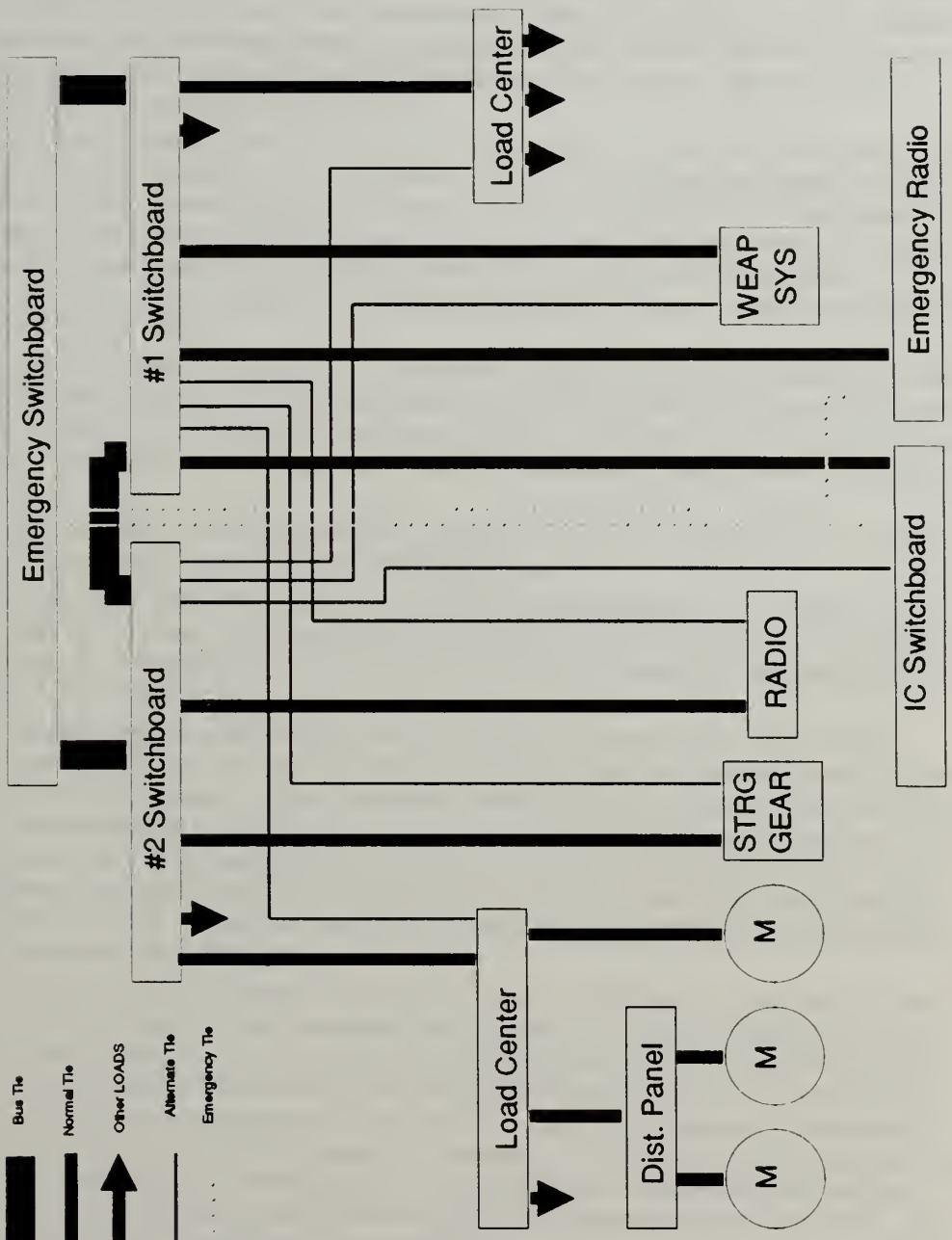

Figure 2.1.1 - An Example of a Traditional Naval Electric Power System

The ship service power system is designed to supply all electric power during all operations from being tied up pierside to general quarters. Ship service generators supply power to the ship service power system. Each generator is connected to a ship service switchboard. The ship service switchboards are connected by bus ties in a ring-bus configuration usually. At low load levels, this permits one generator to supply several switchboards' loads. At higher load levels, this permits paralleling genera-

tors. The generators and their associated switchboards are dispersed throughout the ship fore and aft, port and starboard so that the risk of losing multiple generators/switchboards to a single 'hit' is reduced.

The switchboards provide power to load centers and directly to some individual loads. The load centers, in turn, feed distribution panels and individual loads. Distribution panels supply individual loads. In smaller vessels, load centers are forsaken.--The switchboards provide power to distribution panels and so on. Naval electric power systems are basically radial systems.

The electric loads supplied by the ship service power system fall into one of three categories. The first category is "vital" loads. "Vital" loads have one specific switchboard which is their **normal** supplier of power and a second specific switchboard which is their **alternate** supplier of power. A "vital" load is so important that when its normal switchboard loses power, it is automatically transferred to its alternate switchboard.--That the switching to the alternate supplier is done automatically is what distinguishes "vital" loads.

The second category of loads is "important" loads. "Important" loads also have one specific switchboard which is their normal supplier of power and a second specific switchboard which is their alternate supplier of power. However, when an "important" load's normal switchboard loses power, it must be manually transferred to its alternate switchboard.

The third category of loads contains loads which are not so important and have only one assigned switchboard which supplies power.

On its own, the ship service electric power system endeavours to ensure that "vital" loads will always receive power, thus discharging the function of a naval electric power system. It attempts this by providing two distinct, physically separated power supplies for each "vital" load.

The function of the emergency power system is to ensure that "vital" loads receive electric power when there is a failure of the ship service electric power system (or some part of that system). The emergency power system consists of an emergency generator, an emergency switchboard, and some number of emergency feed lines. The emergency generator is powered by a separate, stand-alone emergency prime mover. The emergency feed lines supply power from the emergency switchboard directly to some emergency loads, examples being the emergency radio transmitter and the internal communications switchboard.

The emergency switchboard plays the key role in fulfilling the function of the emergency power system. The emergency switchboard is usually connected to two ship service switchboards. One of these two switchboards is the primary source of power for the emergency switchboard, the other the alternate source. If both of the emergency switchboard's sources of power are lost, then the emergency generator is automatically started and supplies power. Once one of the ship service switchboards is restored, then the emergency switchboard is automatically transferred back to that power source. It is possible to keep the emergency generator on-line, in parallel, and sharing the load with the ship service generators.

The casualty power system consists of installed vertical risers, installed bulkhead penetrations and designated cabling located throughout the ship in proximity to generators and "vital" loads. This hardware allows manual construction of an ad hoc power system to supply "vital" loads when some part of the power system has been destroyed. In essence, one connects cable directly from a power source to a load.

The operational configuration of the electric power system depends upon the particular operations in which the vessel is engaged. Pierside, the ship service switchboards may be tied together and supplied from a shore power connection. At anchor, the ship service switchboards may be tied together and supplied from a single generator.

During peacetime cruising, the ship service switchboards may be tied together and fed from paralleled generators. Parallel operation is normally used to reduce fuel consumption and avoid "under loading" diesels and gas turbines. At general quarters, the ship service power system is operated in the "split plant" mode. In the "split plant" configuration, all of the switchboards and their associated generators operate independently. This reduces the chance that one 'hit' will interrupt power to all of the ship's loads.

The operational configuration of naval electric power systems involves either a small number (relative to commercial electric power systems) of paralleled generators (maybe even only two), or several independent generator/radially connected load systems. This is true whether the ship service power system, the emergency power system or the casualty power system is being discussed. Given the frequently changing configuration and the number of possible combinations of generators, switchboards, normally or alternately connected load centers, distribution panels and loads, the only constant feature of the naval electric power system is the generators. A given generator could, under a wide range of circumstances, see a full spectrum of load levels and different degrees of participation from a small number of other generators. Considering this fact and the possibility that part of the system may be damaged, the "structure" of a naval electric power system must not always be taken as a "given".

In the design of a warship, the ship's mission is specified first. The combat systems, ship control systems and propulsion systems required to fulfill this mission follow. It is left to the naval electric power system designer to provide a survivable power system which is small enough to fit into the warship. Some design practices have arisen over the years, the system architecture and load categorisation having already been discussed.

Once the major pieces of equipment that will be included in the design of a warship have been identified, the aggregate electric load of these equipments in various operational scenarios is calculated. This load estimation has been done simplistically in the past, reference [2.1.3]. Once the loads are available, the number of generators and their rating can be established.

A major feature of the rating process is the imposition of unequal-load-sharing, load uncertainty and load growth margins, reference [2.1.4]. Once built, naval electric power systems are not very expandable for a number of reasons. Hence, the originally installed electric power system must be capable of adequately handling the growth in load which occurs over thirty years (a typical naval ship lifetime).

The reality of a non-expandable naval electric power system, especially one that will fit inside of a warship, leads to some important characteristics when analysing the behaviour of shipboard systems. First, cable runs are essentially limited by the length of the ship. This means that transmission line dynamics do not play a significant role. Second, the close physical proximity and 'close' electrical proximity of components means that control information is passed very rapidly between parts of the system.

Third, the most profound effect of the constraints and design practices relevant to naval electric power systems is that these issues justifiably conspire to limit generating capacity and rotational inertia. In contrast, commercial electric power systems (speaking here of the U.S.'s) have thousands of generators which all contribute to capacity and inertia. By limiting generating capacity and rotational inertia onboard a warship,

the characteristic of having single loads which are a significant fraction of the generating capacity of the system is added to the already complex nature of naval electric power systems.

Related to the issue of limited generating capacity and rotational inertia is the fact that naval electric power system prime movers are smaller than commercial electric power system prime movers. The smaller prime movers have time constants which are much closer to the generators' electrical time constants than is the case in commercial systems. Time scale separation in commercial electric power systems is well established and yields quite acceptable results. Time scales of naval electric power systems are not so easily separated.--In fact, mechanical and electrical dynamics are very strongly coupled.

Characteristics of Naval Electric Power Systems:
1. Very little rotational inertia relative to loads
2. Fast controls maintain frequency.
3. Shipboard prime movers typically are faster than utilities' relative to dynamic times of interest.
4. Large, dynamic loads relative to generation
5. Generators share loads in proportion to rating.
6. Very fast load-sharing information is provided to all generators.
7. Power electronic switching loads figure considerably.
8. Transmission lines are not nearly as significant as for utilities.
Implications of These Characteristics:
A. Typical electric power system models are not usually appropriate for analysing shipboard dynamics. Higher-order models are necessary both for generators and loads. For example, "Swing" equation assumptions are not met.
B. Some of the mathematical expediencies used in usual electric power system analyses cannot be used with naval electric power systems. "Infinite" buses and "slack" buses do not have manifestations in naval electric power systems. "Constant voltage", "constant frequency" and "constant power" simplifications are invalid usually.
C. Naval electric power systems are very tightly coupled both electrically and with mechanical systems.
D. Faults must be modelled consistently with the characteristics of naval systems.

Table 2.1.1 - Some Characteristics of Traditional Naval Electric Power Systems

The 'small' size, lack of inertia, tight coupling and 'close' electrical proximity of naval electric power systems require fast frequency and voltage controls. During parallel operation, load sharing information is provided to all on-line generators very rapidly. Generator loads are not scheduled; rather, loads are shared in proportion to the generators' ratings. Load flow formulations have little meaning. Further, the primary and secondary levels of control found in commercial systems are not present as such in naval electric power systems.

Loads onboard naval combatants are large, dynamic and rapidly applied. Given the lack of inertia and despite the fast controls, there are large excursions in voltage levels and frequency compared to commercial electric power systems, reference [2.1.5]. Additionally, while the ship service power system and emergency power system attempt to ensure that power is available to "vital" loads, there are interruptions during the switching to alternate sources and during the period of time it takes to start up prime movers, particularly the emergency generator. Constant voltage level, constant frequency, and constant power injection assumptions cannot be made for dynamic analyses.

The foregoing discussion of traditional naval electric power systems is summarised in table 2.1.1.

This characterisation of naval electric power systems is much abbreviated and points out the significant differences between naval electric power systems and commercial electric power systems. The differences stem from different functions with different concomitant optimisations. The differences are driven, at the very least, by the disparate scales of the two types of power system.

2.1.1.2 Features of Advanced Systems

Electric loads on naval ships began as lighting. Electricity then began to be used for ventilation, pumps, heating and radio. In some instances, particularly submarines, electricity was used for propulsion. Around World War II, radar and sonar came into being. Since that time and following the development of computers, the complexity of combat systems has increased vastly. The characterisation of the loads on a warship now includes a large fraction which is power electronic in nature and demands close attention because it is the raison d'être of naval warships. Technological advances and changes in naval warfare have added progressively larger and more troublesome loads to the loads which naval electric power systems support.

The U.S. Navy has recently committed itself to "integrated electric drive" on future combatants. Further, in addition to tieing together an electric propulsion system and a ship service electric power system, research into pulsed electric power systems is underway, reference [2.1.6]. The new demands these will impose upon naval electric power systems further complicate analysis.

In addition to technologically complex and philosophically important loads, "integrated electric drive" implies that the propulsion system and the ship service electric power system are supplied from the same prime movers and may be connected electrically. This interconnection, whether mechanical or electrical, now brings the very large and very dynamic propulsion load into the realm of naval electric power systems. On its own, the propulsion load is a very large and very dynamic load; however, some proposals would further complicate the propulsion load dynamics by feeding it through electronic power converters, references [2.1.7] and [2.1.8].

Figure 2.1.2 shows a simplified diagram of an example advanced naval electric power system. This diagram contains many of the features presently contemplated for inclusion in future naval electric power system designs, references [2.1.6], [2.1.7], [2.1.9] and [2.1.10].

The goal of this research is not to propound or confound the development of "integrated electric drive"; however, its desirability warrants some brief discussion and is founded upon two contentions.

The first contention focuses on cost. An integrated naval electric power system essentially permits conjugation of the propulsion and ship service loads in a manner which allows the most economical operation of the prime movers installed onboard, reference [2.1.7]. This fuel economy translates into reduced tankage requirements, thus reducing the size of the ship. Further, the required number of prime movers decreases, which also augurs reduction in the size of the ship. The current practice of the budgeting offices of the Congress of the United States of America, states that the cost of a ship is in direct proportion to its size, as measured by displacement. Hence, an integrated naval electric power system would reduce the cost of a ship.

The second contention addresses warfighting ability. An integrated naval electric power system directly improves the military effectiveness of a warship as well as enabling the development of some revolutionary concepts in naval warfare, references [2.1.6] and [2.1.9]. The direct improvements in military effectiveness stem from arrangement flexibility and increased "enclaving", reduced signatures, and increased survivability. Integrated naval electric power systems enable the development and employment of such things as rail guns, electrothermal guns, large active sonar among many others. It is these research programs which will require the construction of a pulsed electric power system architecture.

Many attempt to refute the first contention by saying that gear-driven ships have a more efficient transmission at design (full) speed. Some also say that electric drive ships have a higher initial acquisition cost. Hence, the first contention has been and will continue to be assailed.

The second contention draws a lot of fire because there exists no objective measure of military effectiveness. Hence, most would agree that integrated naval electric power systems improve military effectiveness; however, there is little agreement on how much improvement is achieved and whether it is worth the cost, which is yet an unknown.

Now, having cursorily discussed why advanced naval electric power systems are desirable, it is important to examine some of their features.

Three types of prime mover are shown in figure 2.1.2. The propulsion prime movers (STBD and PORT PMOVER) are meant to provide all required propulsion power and various fractions of ship service power. The ratings of the propulsion prime movers are on the order of tens of megaWatts. On a ship the size of a frigate there would be two such prime movers. A ship the size of a destroyer/cruiser would have three or four.

The ship service prime movers (SS PMOVER) are meant to supply ship service power during split plant operations, simultaneous peak ship service electric load and peak propulsion load, and anchored/moored operations. The rating of the ship service prime movers is likely to be between three and five megaWatts. The required number of ship service prime movers is not clear. Similar statements can be made regarding the emergency prime movers (E PMOVER).

The propulsion generators (STBD and PORT PGEN) convert mechanical energy from the propulsion prime movers to electric energy. This electric energy is provided to the electric propulsion system switchboards. The rating of these generators would match that of their prime movers. At high ship speeds, both generators are needed. At lower ship speeds, one generator could supply both switchboards.

The ship service generators could take three forms. First, ship service generators connected to ship service prime movers are conventional. The rating of these generators matches that of their prime movers. Second, in figure 2.1.2, the starboard ship service generator (STBD SSGEN) receives mechanical power from the starboard propulsion prime mover through power take-off gearing (PTO GEAR). This ship ser-

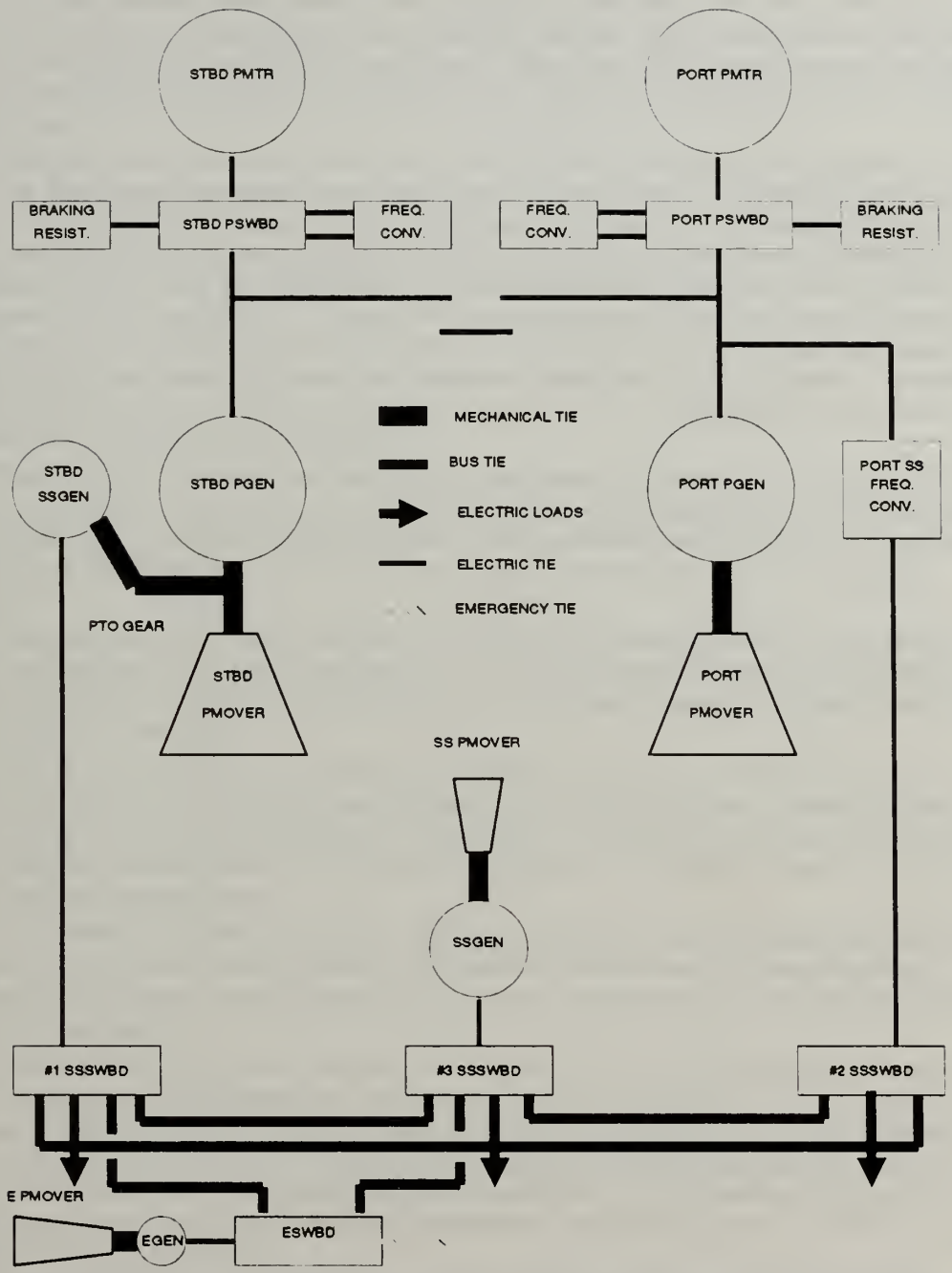

Figure 2.1.2 - An Example of an Advanced Naval Electric Power System

vice generator is mechanically coupled to the propulsion system. Such a generator necessarily includes provisions for variable frequency operation. Third, in figure 2.1.2, the port ship service generator (PORT SS FREQ. CONV.) receives electric power from the port propulsion generator. This ship service generator is electrically coupled to the propulsion system. This electric power is then converted from the propulsion power frequency and voltage to the ship service power frequency and voltage.

Following conversion, the power is supplied to the ship service switchboards. The rating of the frequency conversion equipment would be on the order of the conventional ship service generators.

The ship service switchboards (#n SSSWBD) and emergency switchboards (ESWBD) behave as described in the preceding section. This comprises the ship service power system and is fairly conventional. The role of the propulsion switchboards (STBD and PORT PSWBD) is somewhat more complex than that of the ship service switchboards.

The propulsion motors (STBD and PORT PMTR) take the electric power provided by the propulsion generators and convert it into torque. This torque turns the shaft, which turns the propeller, which generates the thrust, which propels the ship. The power absorbed by the propeller varies according to the rotational speed of the propeller and the velocity of the ship. The relationship between frequency, power, and ship speed is very nonlinear. The propulsion switchboard is the component which, based upon control signals, channels power (1) directly from the propulsion generator to the propulsion motor, (2) from the propulsion generator through power converters (FREQ. CONV.) then to the propulsion motor, or (3) from the propulsion motor to the braking resistors (BRAKING RESIST.).

The foregoing discussion treats the system shown in figure 2.1.2. Figure 2.1.2 is an example which is meant to illustrate features and components which may be present; it does not represent a design practice or even a viable architecture. It illustrates some of the characteristics of the architecture of advanced naval electric power systems.

The architecture of the traditional naval electric power system is three-tiered and caters to the needs of the ship service loads. The architecture of advanced naval electric power systems may well contain ship service power systems with their three-tiered architecture as a subset.

The function of the propulsion power system is to be a survivable source of propulsion power for the ship. The architecture of a propulsion power system is likely to consist of large prime mover/generator sets (large on the scale of naval prime movers), switchboards, power converters, and motors whose rating is fairly close to that of the prime mover/generator sets.

One possible architecture for an aggregate advanced naval electric power system contains a propulsion power system, with its own architecture for ensuring that its function is discharged, coupled to the ship service power system, with its previously discussed architecture.

The function of a pulsed electric power system is to provide pulsed power loads with an extremely high power for a short period of time, reference [2.1.6]. While in very early stages of research and development, one can surmise that such a power system would either exist as (1) a large pulsed load on an integrated naval electric power system with weak limits on pulse repetition rate (PRR), (2) a constant load on the integrated system with energy storage components and strong limits on PRR, or (3) a combination of (1) and (2).

Whereas flexibility is a valued quality in a warship design, the weak limits on PRR will probably draw the eventual selection to (1). Of (1), (2) and (3), (1) would have the greatest impact on the design of the host naval electric power system. Hence, as a worst case view, in fact a view of the likely situation, the effect of chosing (1) is considered.

The implications of chosing (1) are threefold. First, the propulsion power system must be capable of rapidly diverting a large amount of power.--This is not a trivial issue. Second, the propulsion loads must be insensitive to short disruptions in power supply. (This discussion assumes that the ship service power system may not be perturbed.) Third, the control requirements increase in complexity and magnitude.

The implications of the components, features and architecture of advanced naval electric power systems, including pulsed electric power systems, fall into two broad areas. First, the characteristics of traditional naval electric power systems, table 2.1.1, are descriptive of advanced naval electric power systems.--Although for advanced systems, everything is moreso. Second, higher order control must be exercised over the system. This control must be very fast and very adaptive. Hence, to adapt table 2.1.1 to advanced naval electric power systems, one must add emphasis to the existing characteristics and add the requirement for very sophisticated (faster, more adaptive, more sophisticated than commercial electric power system) controls.

2.1.2 Dynamic Occurrences of Interest

Analysis of a naval electric power system rightly focuses on how well it fulfills its function. The selection of the rating of generators ensures that, under static nominal conditions, the power system will fulfill its function. However, the function requires that it be viable in the presence of perturbations as well. Perturbations fall into two categories, deliberate and precipitate.

Deliberate perturbations are perturbations which occur by design. The naval electric power system in question must be inherently able to 'handle' these perturbations. The magnitude of the perturbations can be established beforehand. Four classes of deliberate perturbations warrant discussion. Precipitate perturbations are perturbations whose natures are not known a priori. They are the results of unanticipated or emergency situations. Three classes of precipitate perturbations are considered.

Deliberate Perturbation - Class 1 - Sudden Application and/or Removal of Loads

Warships are frequently required to operate in a responsive fashion. Hence, equipments are suddenly brought on-line, loaded, then taken off-line or load levels suddenly changed. Consider for example the steps taken when a warship goes to general quarters (battle stations). The power system is rapidly switched to split plant operation. The combat systems are energised. The firemain system is sectionalised, requiring most of the large firepumps to be brought on-line.

Going to general quarters is done frequently. It represents a perturbation to the operation of the power system which the power system must inherently be able to accommodate. In a sense, the magnitude of the perturbation is known because the final state of the system is predictable.

The load changes in going to general quarters affect mostly the ship service power system. The combat system load, which is predominantly power electronic in nature, increases dramatically. The firemain load increases. It consists mostly of electric motors and is very dynamic. The motors are big enough that their startup transients and dynamics play a significant role in the greater power system. The "hotel services" loads, such as potable water pumps, galley gear, some ventilation and lighting, decrease.

Going to general quarters is not the only evolution in which large, dynamic changes in the loads occur.--It is illustrative, though. Another example regards the propulsion load. Suppose, to avoid a collision at sea or a grounding, the warship must perform a "crash-back" manoeuvre. During such a manoeuvre, the propulsion motors must

be unloaded completely, stopped, reversed, and then loaded fully. All of this must be performed as rapidly as possible. Bear in mind, the propulsion load is definitely on the order of the generating capacity. "Crash-backs" are performed periodically.

Deliberate Perturbation - Class 2 - Parallel/Split Operation of Generators

It is a normal event to rapidly switch generators from operating in parallel to operating independently and vice versa. Consider again the case of going to general quarters. The power system is immediately shifted to split plant operation. Many of the aspects of this perturbation arise from the rapid loading or unloading of a generator which is entering or leaving parallel operation. Other aspects of this class of deliberate perturbation involve changes in control logic.

Deliberate Perturbation - Class 3 - Varying Frequency Operations

For an ac propulsion system, any large change in the ordered ship speed results in a rapid change in the propulsion motor electrical frequency. This change in frequency is made through the propulsion power system electronic frequency converters and/or the propulsion generators and prime movers. Furthermore, this directly impacts the ship service power system in an integrated naval electric power system. The frequency of the power take-off gear changes the input frequency of the attached ship service generator. The propulsion power system electric frequency input to ship service power electronic converters changes as well.

Changing ordered ship speeds occurs continuously on a warship. Often the speed change is from "bare steerageway" to "ahead flank". Occasionally the speed change is from "ahead flank" to "back full", the "crash back" manoeuvre discussed earlier.

Deliberate Perturbation - Class 4 - Redirecting Large Powers

This type of deliberate perturbation is pondered for pulsed electric power systems of the type discussed in the previous section. If the pulse of power is taken from the propulsion power system, then power must be redirected from the propulsion motors, and possibly the propulsion frequency converters, to the pulsed electric power system loads. This involves maintaining the power output of the propulsion prime movers and generators while simultaneously reducing the power absorption of the propulsion motors to zero and increasing the power to the pulsed power system loads to the peak power level. This class of deliberate perturbation carries elements of the suddenly increasing/decreasing load levels as well as strong control influences.

The timing and extent of precipitate perturbations are not predictable. These perturbations comprise the most important design consideration. While a naval electric power system must be capable of handling deliberate perturbations as a matter of routine, precipitate perturbations are likely to occur when a warship is lethally threatened.--Failure of a naval electric power system in such circumstances is very bad.

Precipitate Perturbation - Class 1 - Ephemeral Power System Effects

This class of perturbation includes occurrences which perturb the naval electric power system without changing the nature of the generating capacity or loads. A prime example of this arises from mechanical shock, reference [2.1.11]. Mechanical shock can result from the effects of ordnance, collision, et cetera. Despite trying to design them to be invulnerable from mechanical shock, circuit breakers will be tripped by mechanical shock.--Tripping the breakers does not change the electric load. It changes the ability of the generator to supply the load. Once the breakers are re-closed, then the system is restored to its pre-perturbed state. Ships are not routinely subjected to mechanical shocks.

Precipitate Perturbation - Class 2 - Damage to the Power System

Whatever the source of damage, naval electric power systems may see an instantaneous change in (removal of) generation capacity, transmission capability, and/or load level. What is more, this type of perturbation does not have an immediate remedy like the preceding class. Ordnance could destroy the majority of loads that a generator is supplying. It could just as easily destroy the generator, leaving loads without their primary power supply. The ordnance could even destroy the tie lines from the generator to the loads without harming either. Weapons effects and collision damage are not predictable.

Precipitate Perturbation - Class 3 - Absence of Control System

For whatever reason, a naval electric power system may be operated manually. That is, all controllers have been disabled. This leaves manual control or no control at all of power system components.

2.1.3 Stability Analyses to Address Relevant Dynamics

Instances of all of the dynamic occurrences of interest discussed in preceding section constitute large perturbations to a power system. The question presented by these large perturbations is whether or not the naval electric power system will be able to carry out its function. Answering this question has fallen within the realm of stability analysis. Sections 2.2 and 2.3 discuss the various stability analyses which are used with electric power systems. This discussion seeks to pose the question of which analysis is most appropriate for assessing the behaviour of naval electric power systems.

Given that the well established time-scale separation found in commercial electric power systems is not present, the dynamic models which must be used in a stability analysis will be different for naval electric power systems. For the most part, a higher order generator model than the "swing" equation model, which is frequently used in commercial electric power system stability studies, is necessary. When considering the behaviour of propulsion power systems, those which use power electronic frequency converters must include the dynamics of the power converter in any dynamic analysis. Considering both propulsion power systems and ship service power systems, motor dynamics are of distinct importance; hence, an accurate dynamic model of the motors is necessary. On the other hand, the same discipline which limits rotational inertia and generation capacity onboard a warship limits the number of loads onboard a warship. Therefore, it is possible, at least in later design stages, to have a complete characterisation of all the loads which are installed. Knowing the loads, appropriate dynamic models of them can be selected for inclusion in stability analyses.

As mentioned earlier, present naval electric power system design margins essentially ensure that steady-state, nominal operation is viable. Once a system configuration is selected for analysis, a "small-signal", "dynamic" stability analysis is used to determine whether the equilibrium state of the system for that configuration is stable in the "small-signal", linear sense.

"Large-signal" perturbations are treated using simulations. Typically a pre-perturbation equilibrium is assessed using dynamic stability (linearised) methods. The anticipated post-perturbation equilibrium is assessed using dynamic stability methods too. Simulations are used to describe how the system transverses state space between the two equilibriums.

Such a series of analyses describes the stability of the naval electric power system in the stated configuration. The simulation results used to assess transient, and the greater "large signal", stability depend upon stated initial conditions. In a sense, the stability characterisation which results from such an analysis is true for only the stated

configuration and initial conditions. This sort of analysis is useful in assessing stability of deliberate perturbations. It is not appropriate for trying to assess stability of precipitate perturbations.

All of the discussion to this point leads to a concise statement of need. A means to characterise the "large signal" stability of an accurately (nonlinearly) modelled naval electric power system which addresses both deliberate and precipitate perturbations must be developed to provide a design criterion which ensures that a naval electric power system fulfills its function. A logical step, once this stability characterisation is obtained, is to use the stability information as a control input for the instances where the uncontrolled system is not stable.

2.1.4 References

2.1.1 Bureau of Naval Personnel. Principles of Naval Engineering. (NAVPERS 10788-B). Washington, D.C.: U.S. Government Printing Office, 1970. Chapter 20.

2.1.2 Division of Engineering & Weapons, U.S.N.A. Introduction to Naval Engineering Systems. Annapolis, MD: U.S. Naval Academy, January 1980. Chapter 4.

2.1.3 Naval Sea Systems Command. Design Data Sheet 310-1 Electrical System Load and Power Analysis for Surface Ships. Washington, D.C.: Naval Sea Systems Command, 1 July 1980.

2.1.4 Department of the Navy, Naval Sea Systems Command. General Specifications for Ships of the United States Navy, Section 300, General Requirements for Electric Plant and Section 320, General Requirements for Electric Power Distribution Systems. Washington, D.C.: Naval Sea Systems Command, 1987.

2.1.5 Department of Defense. Interface Standard for Shipboard Systems, Section 300A, Electric Power, Alternating Current (Metric). (MIL-STD-1399(NAVY)). Washington, D.C. 13 October 1987.

2.1.6 Reed, M.R. "Integrated Electric Drive (IED) - Program Overview." Naval Sea Systems Command (Code 05Z) Presentation, Washington D.C., March 27, 1990.

2.1.7 Casey, J.P. "AC Electric Drive Machinery Design." Arlington, VA, March 14, 1990. (Presented at the 1990 Chesapeake Marine Engineering Symposium, The Society of Naval Architects and Marine Engineers. A General Electric Technical Speech Reprint.)

2.1.8 Hultgren, K.J. "VSCF Cycloconverter Power Equipment A Versatile Technology for Wide Range PDSS." Biloxi, MS, September 27, 1990. (Presented at the 1990 Destroyer, Cruiser & Frigate Technology Symposium, The American Society of Naval Engineers. A General Electric Technical Speech Reprint.)

2.1.9 Doerry, N.H. "ASMS Advanced Surface Machinery Systems." Annapolis, MD, December 13, 1991. (Presented at Naval Reserve Training Lecture.)

2.1.10 Doerry, N.H. "Advanced Numerical Methods for Simulating Nonlinear Multirate Lumped Parameter Models." Thesis, PhD, M.I.T. May 1991.

2.1.11 Department of Defense. MIL-STD-901(NAVY). Washington, D.C.

2.2 Electric Power System Stability Analyses

The intent of this section is to discuss the basic methods used to assess power system stability and their characteristics which impact their relevance to naval electric power systems. For the most part, these methods arose to study the stability of commercial electric power systems. The complexity of the analysis tools that are presently used by utilities vastly exceeds the level of complexity admitted in this discussion. However, this discussion is focused upon the theoretical bases which are common to the more advanced tools.

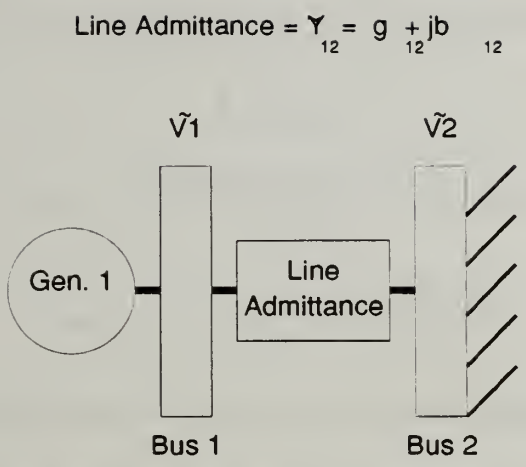

Bus 1 = "Internal" Bus of Generator 1

Bus 2 = "Infinite" Bus

Figure 2.2.1 - Example Power System

As a means of illustrating these methods, an example system is analysed using them. Assume that for the example system, $P-\theta/Q-V$ decoupling is valid. Further assume that synchronous machines can be modelled using the "swing" equation. (The particulars of these assumptions are omitted here. This model of commercial electric power systems is frequently used though.) The example system consists of a synchronous generator supplying electric power through a reactive transmission line to an infinite bus, that is, a three phase voltage source with constant amplitude, constant frequency and constant phase angle. This situation is somewhat analogous to some power system configurations on a Navy ship.

2.2.1 A Common Power System Model

Electric power systems, at least those considered in references [2.2.1]-[2.2.9], contain prime movers driving electric generators. The generators inject power into a system of buses which are interconnected by transmission lines. The electric power is transferred to loads which typically consume a specified real power, which, at load voltages, requires a specific reactive power. These three components, generator, transmission line, and load, comprise the building blocks of electric power systems, at least those treated in the references and in this section.

2.2.1.1 Simple Generator Models

In some stability analyses, generators are represented by a one-axis model. The reasoning is that the excitation voltage is constant. (This ignores excitation systems altogether.) More simplified analyses fix the voltage behind the transient reactance of the generator. The reasoning in this second case is that the field excitation system is ideal and maintains constant field flux. (This neglects excitation control system dyna-

mics.) The equation describing the voltage behind the transient reactance is shown for the case which assumes constant excitation voltage, equation (2.2.1). In virtually all stability analyses, generator resistances and subtransient dynamics are ignored.

$$\frac{T'_{do}}{(x_D - x'_D)}\frac{d}{dt}(e'_q) = -\left(\frac{x_D}{x'_D(x_D - x'_D)}\right)e'_q + \frac{1}{x'_D}v_T\cos(\delta - \theta) + \frac{1}{(x_D - x'_D)}e_{af} \quad (2.2.1)$$

$$\delta = p_p\omega_{rm} \quad (2.2.2)$$

$$m\dot{\omega}_{rm} = P^m - d\omega_{rm} - \left[\frac{v_T^2\sin(2(\delta-\theta))(x'_D - x_Q)}{2x_Q x'_D} + \frac{e'_q v_T\sin(\delta-\theta)}{x'_D}\right] \quad (2.2.3)$$

$$m\dot{\omega}_{rm} = P^m - d\omega_{rm} - \frac{e v_T\sin(\delta-\theta)}{x'_D} \quad (2.2.4)$$

T'_{do} is the direct axis open circuit transient time constant.

x_D is the direct axis synchronous reactance.

x'_D is the direct axis transient reactance.

e'_q is the quadrature axis voltage behind transient reactance.

v_T is the magnitude of the terminal voltage.

δ is the generator rotor (transient voltage) angle.

θ is the terminal voltage angle.

e_{af} is the excitation voltage.

ω_{rm} is the rotor mechanical frequency.

p_p is the number of pole pairs.

m is the inertia of the generator and attached mover.

P^m is the mechanical power input.

d is the mechanical damping of the rotor.

x_Q is the quadrature axis synchronous reactance.

e is the constant voltage behind transient reactance.

The "swing" equation describes the electromechanical behaviour of the generator. Some stability methods allow inclusion of mechanical damping, typically the easily handled (special) cases; most analyses, though, ignore damping. The goal in ignoring damping and resistances is make analysis more tractable, in this case yielding a conservative system. The first "swing" equation, (2.2.3), describes the constant excitation case, the second, (2.2.4), the constant voltage behind transient reactance case.

These two models of generators, (2.2.1, 2.2.2 and 2.2.3) and (2.2.2 and 2.2.4), neglect many details of generator behaviour. The neglected details are not relevant to electro-mechanical stability given the time scale separation in commercial electric power systems.

2.2.1.2 Transmission Line Models

All connections between buses are taken to be transmission lines with a finite, non-zero impedance. Typically, these impedances are described by means of a bus admittance matrix. Complex admittances are used. Of note, complex admittances (and impedances) arise from the steady-state solutions of system equations using Laplace transformations and ignore initial conditions in the formulation of the transfer function.

The conductances that should be present in the bus admittance matrix are usually ignored. Ignoring the resistance of the transmission line eliminates or affects one of the eigenvalues of the system. By ignoring its conductance, the admittance of a given transmission line becomes the inverse of its reactance, a susceptance. A reactance is the product of the steady-state electrical frequency and an inductance.

$$X = \omega_e \cdot L \tag{2.2.5}$$

Few models admit that the transmission line reactances change as frequencies vary. This error is zero in a completely synchronous system, one containing an infinite bus. The error is very small when the rotor speed of a single generator connected to a system with vast inertia varies slightly. For a system where frequencies can vary significantly in transient situations, the value of the transmission line reactances will vary linearly with the speed variations.

The description of an inductor through the use of a complex impedance also obscures the constitutive equation describing its behaviour. Consider now the relationship between the voltage and current of an inductor.

$$v(t) = L\frac{d}{dt}(i(t)) \tag{2.2.6}$$

The Laplace transformation of this equation is simple and direct.

$$V(s) = L(sI(s) - i(0)) \tag{2.2.7}$$

$$s = \alpha + j\omega \tag{2.2.8}$$

$$V(s) = L((\alpha + j\omega)I(s) - i(0)) \tag{2.2.9}$$

$$\frac{V(s)}{I(s)} \neq j(\omega L) = jX \tag{2.2.10}$$

$$\text{rather, } \frac{V(s)}{I(s)} = \alpha L - \frac{Li(0)}{I(s)} + jX \tag{2.2.11}$$

By ignoring the first two terms on the right hand side of equation (2.2.11), a portion of the dynamics of the inductor is lost. This is what is being done with transmission lines in the power system model. It is true, though, that with perfectly (constant frequency and amplitude) sinusoidal waveforms α is zero. The point is that in a stability analysis, the effect of the initial condition term should not be discarded without some justification. In the instance of transmission lines, the steady-state model is being used in a dynamic situation.

2.2.1.3 Load Models

In power system stability studies, loads are usually modelled simplistically. PV buses, PQ buses, and constant impedances are all load models. In the PV bus model, the load absorbs a constant real power at a constant voltage. Such a model represents a load connected directly to a generator terminal bus. A PQ bus model absorbs constant real power and a constant reactive power. Such a load has a constant power factor angle despite voltage variations. Constant impedance models are straightforward, to the point of becoming linear circuit problems. Note, the same argument can be made about a constant, complex impedance load as is made about inductors and reactances in the foregoing discussion on transmission lines. PV and PQ loads are also implicitly linked to steady-state models through their derivation from complex circuit theory (phasors). The frequency dependence of loads is ignored by PV, PQ and constant impedance models. Reference [2.2.4] warns that such dependencies carry great import.

2.2.1.4 Combination of Modelled Dynamics

In the standard power system stability formulation, the four variables of interest are real power flow, P, reactive power flow, Q, bus voltage magnitude, V, and the bus voltage angle, θ. In most of the references, voltage magnitudes, real power flows and reactive power flows are fixed, or solved after the fact. Thus, the only independent variable is the bus voltage angle. Therefore, the system equations for power system stability analysis are quite simply the load flow equations plus the rotor mechanical dynamics and, sometimes, the voltage behind transient reactance dynamics.

What follows is a typical formulation of the system equations as used in contemporary power system stability studies, adapted specifically from reference [2.2.3]. Let there be g generators attached to the system. There are l loads attached to the system. The total number of buses therefore is g + l. The generators are modelled as PV buses, the buses being the "internal" buses. Hence, the voltage angle at the generator buses represents the rotor angle of the generator.

$$m_i\dot{\omega}_{rmi} + d_i\omega_{rmi} = P_i^m - f_i(\underline{\theta}) \qquad i = 1, \ldots, g \tag{2.2.12}$$

$$0 = P_i^{ld} - f_i(\underline{\theta}) \qquad i = g+1, \ldots, g+l \tag{2.2.13}$$

$$f_i(\underline{\theta}) = \sum_{j=1}^{g+l} v_{Ti} v_{Tj} y_{ij} \sin(\theta_i - \theta_j) \qquad i = 1, \ldots, g+l \tag{2.2.14}$$

P_i^{ld} is the real power demand of load i.

y_{ij} is the admittance between i and j.

Note that in the steady-state condition and ignoring mechanical damping, the resulting equations are the load flow equations.

2.2.2 Steady-State Analysis

"Steady-state stability" is the less precise label sometimes given to steady-state analysis. In commercial electric power systems, steady-state analysis refers to assessing the existence of solutions to the steady-state power flow problem. This problem can have no, one or multiple solutions. No solution indicates that the proposed system cannot operate under the specified conditions. One solution indicates that a unique operating point exists. Multiple solutions require further investigation into the characteristics

of each solution.--A stability assessment, per se, is not possible using the results of the steady-state analysis. When structured accordingly, the steady-state analysis solutions provide the equilibriums of the dynamic system. Hence, steady-state analysis can be seen as the first part of the overall stability problem.

Conservation of power implies that the real power provided to the generator is equal to the real power injected at the generator's bus terminal of the transmission line. Equation (2.2.15) is the statement of conservation of power for the example system.

$$P_1^m = P_{12}$$

$$= 3v_{t1}^2 g_{12} - f_{12}\sin(\theta_1) - h_{12}\cos(\theta_1) \qquad (2.2.15)$$

For a lossless transmission line, $g_{12} = 0$ and $h_{12} = 0$.

$$\therefore \quad P_1^m = -f_{12}\sin(\theta_1) = -v_{t1}v_{t2}b_{12}\sin(\theta_1) = v_{t1}v_{t2}|b_{12}|\sin(\theta_1) \qquad (2.2.16)$$

Figure 2.2.2 shows this relationship, (2.2.16), between the real power which is injected into the system and the rotor angle of the generator. In figure 2.2.2, the injected power is normalised using the maximum power, which is equal to $v_{t1}v_{t2}|b_{12}|$. An entirely analogous relationship exists between injected power and terminal voltage magnitudes. The injected power-terminal voltage relationship arises from assuming a constant power factor. This relationship is shown in figure 2.2.3.

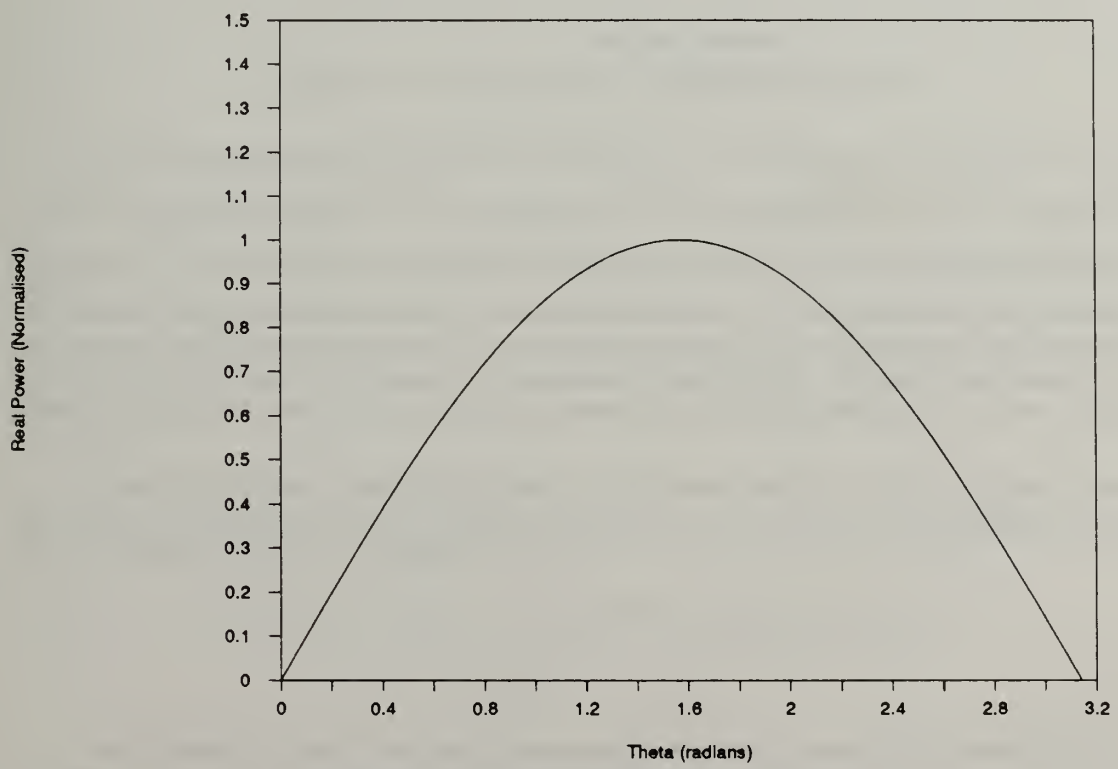

Figure 2.2.2 - Steady-State Power Curve

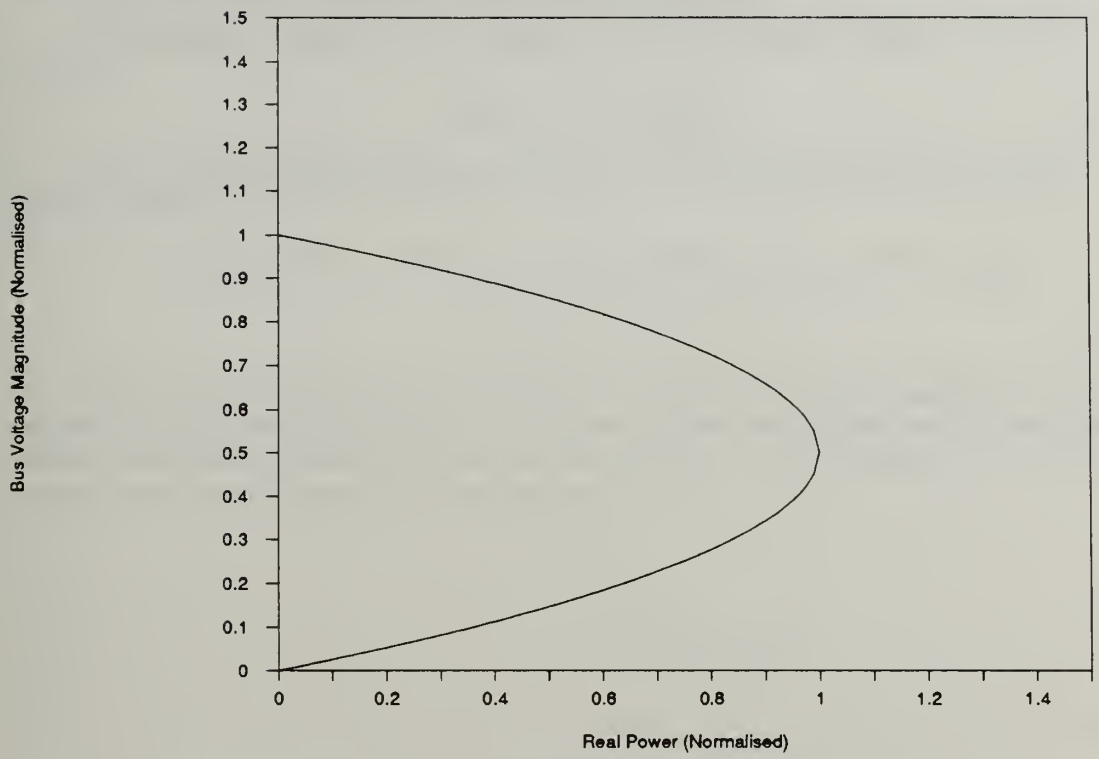

Figure 2.2.3 - Steady-State Voltage/Power Curve

For the generator to provide P_i^m in excess of 1.0 is seen to be impossible in figure 2.2.2. No solution exists for P_i^m in excess of 1.0. For a difference in bus voltage phase angles of $\frac{\pi}{2}$, the generator can provide maximum real power, 1.0, to the transmission line.--One unique solution exists. For powers less than 1.0, the generator can provide the desired real power at one of two bus voltage phase angles.--Multiple solutions exist. Further characterisation of these two solutions is sought later. Similar statements can be made regarding the terminal voltage magnitudes and the injected power in view of figure 2.2.3.

Consider a larger system describable by the same model. In such a system, there are m buses with one generator attached to each bus. The power flow equation for each of the m buses is shown in equation (2.2.17).

$$P_i^m = P_i^{ld} + 3v_{ti}^2 g_{ii} - \sum_{j=1 j \neq i}^{m} [f_{ij}\sin(\theta_i - \theta_j) + h_{ij}\cos(\theta_i - \theta_j)]$$

$$\text{where} \quad i = 1 \ldots m \tag{2.2.17}$$

Any dynamic system, not just systems adhering to the assumptions underlying the models used in the example system, has steady-state equations which must be solved to determine equilibriums. A steady-state analysis of these general equations seeks the same information as in the example system discussed here. Though, not all steady-state equations are the classical "power flow" equations appearing for the example system.

The steady-state equations above are not dynamic equations. To assess stability, a dynamic model is necessary. Under the assumptions mentioned earlier, the $P-\theta/Q-V$ decoupling and "swing" equation assumptions, equations (2.2.18) and (2.2.19) capture the electromechanical dynamics of synchronous machines.

The dynamic equation for the example system, ignoring damping, is simple, (2.2.18).

$$m_1\ddot{\delta}_1 = P_1^m + f_{12}\sin(\delta_1) \tag{2.2.18}$$

For a system with m generators, the general dynamic equations are somewhat more complex, (2.2.19).

$$m_i\ddot{\delta}_i + d_i\dot{\delta}_i = P_i^m - P_i^{ld} - 3e_i^2 g_{ii} + \sum_{j=1 j\neq i}^{m} [f_{ij}\sin(\delta_i-\delta_j) + h_{ij}\cos(\delta_i-\delta_j)]$$

$$\text{for} \quad i = 1\ldots m \tag{2.2.19}$$

This second order model of a synchronous machine is transformed into a system of first order differential equations. The system of first order equations for the example system is shown in equation (2.2.20), the system of first order equations for the electric power system with m generators in equation (2.2.21).

$$\dot{x}_1 = x_2$$

$$\dot{x}_2 = \frac{P_1^m}{m_1} + \frac{f_{12}}{m_1}\sin(x_1)$$

$$\text{where} \quad x_1 = \delta_1 \quad x_2 = \dot{\delta}_1 \tag{2.2.20}$$

$$\dot{x}_i = x_{i+1}$$

$$\dot{x}_{i+1} = \frac{(P_k^m - P_k^{ld} - 3e_k^2 g_{kk})}{m_k} + \frac{1}{m_k}\sum_{j=1 j\neq k}^{m} [f_{kj}\sin(x_i-x_j) + h_{kj}\cos(x_i-x_j)]$$

$$\text{for} \quad k = 1\ldots m \quad \text{where} \quad i = 2(k-1)+1$$

$$x_i = \delta_i \quad x_{i+1} = \dot{\delta}_i \tag{2.2.21}$$

These dynamic equations, now in 'canonical' form, are nonlinear.

2.2.3 Small-Signal Stability Analysis

Dynamic stability is the term defined for electric power systems which corresponds to "small-signal" stability, reference [2.2.11]. This notion of stability is based upon the behaviour of the system in proximity to an equilibrium. Typically, the **nonlinear, dynamic** equations are **linearised** about a specified equilibrium. The resulting linear system is tested for stability using the well established linear stability techniques.

Whereas the linearised system depends not only upon the physical characteristics of the system but also upon the equilibrium about which the linearisation is performed, the linearised dynamics are valid only in a small neighbourhood of the equilibrium. As the state of the system moves away from the equilibrium, so too do the complete (nonlinear) dynamics differ from the linearised dynamics. Hence, dynamic stability is used mainly to assess the effects of small perturbations from an equilibrium.

The equilibrium of the example power system is found by setting the right-hand side of equation (2.2.20) to zero.

$$P_1^m = -f_{12}\sin(\delta_1^e) \tag{2.2.22}$$

Define "small" perturbations of the values of the state variables of the example system from their values at the equilibrium.

$$\bar{x}_1 \equiv \delta_1 - \delta_1^e \quad \bar{x}_2 \equiv \dot{\bar{x}}_1 = \dot{\delta}_1 \tag{2.2.23}$$

This leads to a transformation of the nonlinear dynamic equations into linear dynamic equations. This transformation is based upon a first order Taylor expansion of the $\sin(\bar{x}_1)$ term.

$$\begin{bmatrix} \dot{\bar{x}}_1 \\ \dot{\bar{x}}_2 \end{bmatrix} = \begin{bmatrix} 0 & 1 \\ \dfrac{f_{12}}{m_1}\cos(\delta_1^e) & 0 \end{bmatrix} \cdot \begin{bmatrix} \bar{x}_1 \\ \bar{x}_2 \end{bmatrix} \tag{2.2.24}$$

The characteristic equation of the matrix yields the eigenvalues of the linearised system.

$$\lambda^2 - \frac{f_{12}}{m_1}\cos(\delta_1^e) = 0$$

$$\lambda = \left(-\frac{v_{t1}v_{t2}|b_{12}|}{m_1} \cos\left[\sin^{-1}\left(\frac{P_1^m}{v_{t1}v_{t2}|b_{12}|} \right) \right] \right)^{\frac{1}{2}} \tag{2.2.25}$$

$$\sin^{-1}\left(\frac{P_1^m}{v_{t1}v_{t2}|b_{12}|} \right) < \frac{\pi}{2} \Rightarrow \text{Imaginary } \lambda \rightarrow \text{ stable, oscillatory response}$$

$$\sin^{-1}\left(\frac{P_1^m}{v_{t1}v_{t2}|b_{12}|} \right) > \frac{\pi}{2} \Rightarrow \text{Real, positive and negative } \lambda \rightarrow \text{ unstable response}$$

Relating this result to the steady-state analysis discussed earlier and figure 2.2.2, consider the situation where P_1^m is to be less than 1.0. Two solutions of the steady-state equation exist. One is greater than $\frac{\pi}{2}$; it is an unstable equilibrium. The other solution is less than $\frac{\pi}{2}$; it is a stable equilibrium. For $\frac{\pi}{2}$, no conclusions can be drawn using "small-signal" stability analysis.

The process used here for the example system is the same process that is applied to larger, more complex systems for a "small-signal" stability assessment.

The equilibriums of the nonlinear dynamic equations about which the "small-signal" stability analysis is performed are the equilibriums of the nonlinear system. The linearised system is homotopically equivalent to the nonlinear system in a small neighbourhood of the equilibrium. Hence, provided they are conclusive (that is, no eigenvalues have real parts close to zero), the qualitative stability characterisations of the linearised system are the same as the qualitative stability characterisations of the nonlinear system.

2.2.4 Transient Stability Analysis

Transient stability, a subset of "large-signal" stability, of electric power systems is typically assessed only with great difficulty and indirectly. Given the fact that many power systems are nonlinear, particularly naval electric power systems, evaluating the behaviour of power systems during large excursions from equilibriums requires considering all of the dynamics contained within the **nonlinear, dynamic** equations.

For a long time, the complexity of the power systems and their dynamics defeated such an analysis. Even the definition of stability of a nonlinear system was in question. Hence, the tools for assessing transient stability have been either approximate methods, like the equal area criterion, or indirect methods, such as the use of simulations to study behaviour during large excursions from equilibriums.

A frequently studied transient stability scenario asks the following question. Suppose an electric power system is operating at a steady-state, stable equilibrium. At time t_0, a fault occurs. The fault remains until it is cleared at time t_{cl}. The system after the fault has been cleared, the post-fault system, may be topologically different from the pre-fault system. Will the post-fault system reach an acceptable stable equilibrium?

Scenario:

pre-fault system | faulted system | post-fault system
(equilibrium) t_0 t_{cl}

The means of addressing the transient stability problem are direct methods and indirect methods. Indirect methods are simulations. The solution trajectories of the state variables are computed from the dynamic equations. The behaviour of the solution trajectories determines stability. Direct methods seek to determine stability without having to solve for the solution trajectories.

In practice, the two types of methods are used together. It is impossible, practically speaking, to simulate every conceivable perturbation to an electric power system. Hence, direct methods, typically approximate, provide the cases of greatest concern. Simulations of these cases of greatest concern provide an accurate assessment of stability.

2.2.4.1 Equal Area Criterion

The equal area criterion is a direct method which is essentially a graphical integration of the equations of motion of a lossless electric power system. It is one of the earliest methods used to assess transient stability of nonlinear power systems. Whereas a lossless version of the actual power system is considered by this method, its results are approximate and have been shown to be "overly conservative".

The previously discussed scenario is considered in this analysis. The principal effect of a fault on a one machine system is to change the reactance of the system. Hence, the pre-fault, faulted and post-fault transmission line reactances, b_{12} in the example system, are different. This, in turn, implies that each of the three systems will have different steady-state power curves similar to figure 2.2.2. See figure 2.2.4.

In figure 2.2.4, the effect of the fault upon the steady-state power curves is apparent. Originally, the generator in the example system is supplying P_{out} at a rotor angle of δ_0. At time t_0, the fault occurs. The example system operates with the fault on until t_{cl}. At that time, the rotor angle is δ_{cl}. At t_{cl}, the fault is cleared and the example system begins to operate along the post-fault system curve. δ_{max} represents the largest rotor angle for which the post-fault system possesses a steady-state solution.

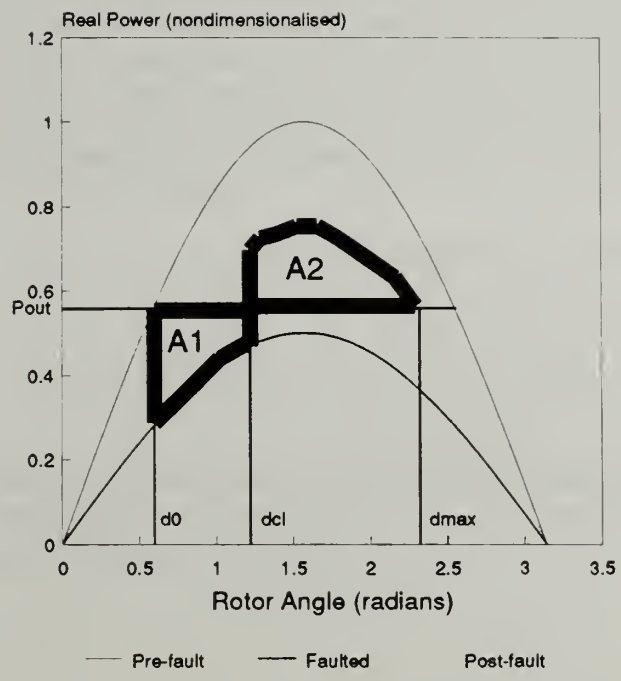

Figure 2.2.4 - Equal Area Criterion

The equal area criterion for transient stability is that area A2 must be larger than A1. The area A1 represents the amount of energy extracted from the synchronous machine during the fault. Area A2 represents the transient energy capacity of the synchronous machine. The value of the time at which area A2 equals A1 is called the critical clearing time, which is the principal concern of many equal area criterion users.

The equal area criterion has its greatest utility when analysing single machine-infinite bus systems, as in the example system, or two machine systems. Multi-machine systems can often be reduced to two "equivalent" machines and this analysis performed.

2.2.4.2 Energy Function Method

The first integral of the dynamic equations, equations (2.2.20) and (2.2.21), which are separable, yields the "energy function". The example system, equation (2.2.20), is easily integrable even in the presence of transfer conductances. However, in the multimachine system, equation (2.2.21), separation of variables and the subsequent integration is not possible if transfer conductances are present. Transfer conductances destroy the symmetric qualities of the power flow expressions in the dynamic equations.

Hence, it had not been possible until the development of an "energy-like" Lyapunov function in reference [2.2.4] to handle systems with transmission line losses. Additionally, the cases of mechanical damping that could be handled were severely limited as well until reference [2.2.4]. Reference [2.2.4] extended the scope of systems which can be analysed using the "energy function" method to include most electric power systems which are adequately described using the "swing" equation dynamic model. Still, let it be noted that this method is tailored to that model.

The "energy function" results from the first integral of the ratio of the two dynamic equations. The "energy function" for the example system is given in equation (2.2.26). It is a continuous, positive definite function of the state variables. The constant of integration is adjusted so that the "energy function" is equal to zero at the stable equilibrium of the example system.

$$V(\dot{\delta}_1, \delta_1) = \frac{1}{2} m_1 \dot{\delta}_1^2 - P_1^m(\delta_1 - \delta_1^e) + f_{12}(\cos\delta_1 - \cos\delta_1^e) \tag{2.2.26}$$

$$\dot{V}(\dot{\delta}_1, \delta_1) = \overline{\nabla} V(\dot{\delta}_1, \delta_1) \cdot \begin{bmatrix} \dot{\delta}_1 \\ \dfrac{P_1^m}{m_1} + \dfrac{f_{12}}{m_1}\sin\delta_1 \end{bmatrix} \equiv 0 \tag{2.2.27}$$

Whereas separation of variables makes the dynamic equations integrable and since the energy along a trajectory is stationary ($\dot{V} = 0$), the "energy function" also represents the phase plane trajectories of $\dot{\delta}_1$ and δ_1.

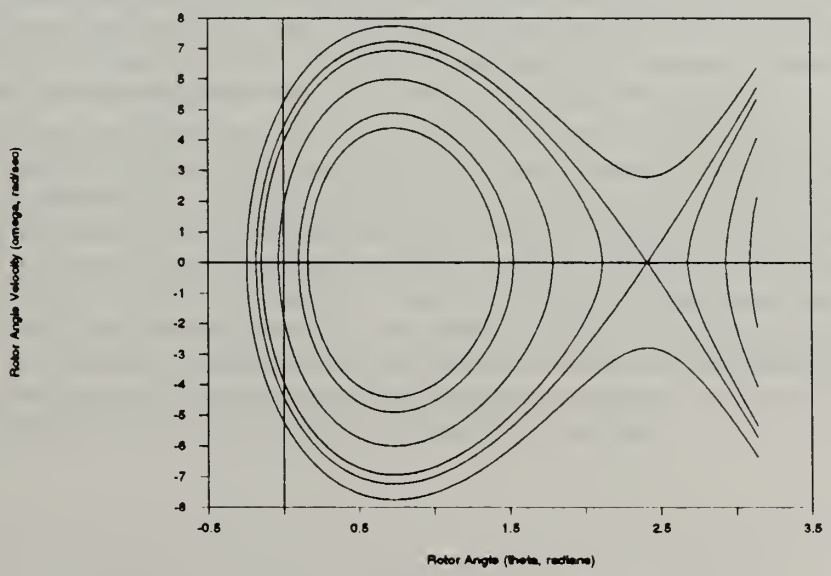

Figure 2.2.5 - Phase Plane Plot of Example System

The "energy function" is developed for the post-fault system because it is the system of interest. Stable behaviour is usually desired in the post-fault system. The equilibriums of the post-fault system, in this case two, lie in the phase plane plot. In figure 2.2.5, the stable equilibrium is at the center of the closed trajectories. The unstable equilibrium is at the intersection of the separatrix and the horizontal axis.

Each trajectory has associated with it a specific energy. Within the separatrix, the trajectories are stable, closed. On and outside of the separatrix, the trajectories are unstable. Hence, the energy associated with the separatrix is the critical energy. The interpretation of the role of this energy is seen in the faulted system. If, while the fault is on, the system acquires enough energy to reach the critical energy by the time the fault is cleared, then the post-fault system's response will be unstable. The time that it takes the faulted system to reach this energy is called the critical clearing time.

Although the "energy function" method is widely used in commercial electric power systems, it is largely a hostage of the underlying "swing" equation dynamic model of the electric power system. In other words, if the relevant dynamics of the system under study are not adequately captured by the "swing" equation model, then the "energy function" method has limited utility.

2.2.4.3 Lyapunov Analyses

Chapter 5.2 of reference [2.2.10] gives the details regarding the use of Lyapunov's direct method. (A more thorough discussion of Lyapunov analysis follows this section.) Simply stated, an equilibrium of a power system is stable in a region about the equilibrium if the convective derivative of the Lyapunov function is non-positive in that locality. Taking this one step further, an equilibrium of a power system is asymptotically stable in a region about the equilibrium if the convective derivative of the Lyapunov function is negative-definite in that locality. Further distinctions regard uniform and global stability.

Hence, to determine if a power system is stable, a candidate Lyapunov function is first selected. Then, the convective derivative of the candidate Lyapunov function is evaluated within a neighbourhood of the equilibrium under scrutiny. The convective derivative of the candidate Lyapunov function is the rate of change of the candidate Lyapunov function with time as the function moves along its state space trajectory. (The convective derivative is also called the substantial derivative or the material derivative or the total derivative.) How this derivative is evaluated varies with the form of the system equations and the person conducting the analysis.

The Lyapunov function used in most of the references ([2.2.2]-[2.2.9]) is a sum of terms meant to represent the energy of the power system. Originally formulated for mechanical systems, the Lyapunov functions used with mechanical systems are usually the sum of the kinetic and potential energies. Similarly, the Lyapunov functions typically used in power system transient stability studies consist of a kinetic and potential energy function. The kinetic energy is relatively straightforward and similar to that found in purely mechanical systems. The potential energy function is less obvious because it is somewhat different from the potential energy of mechanical systems. Some studies also add a force-through-a-displacement energy which will not be discussed. Equation (2.2.28) is just such a Lyapunov function.

$$L(\underline{\theta},\underline{\omega}^g)=\frac{1}{2}\underline{\omega}^{g^T}\cdot\underline{\mathrm{m}}\cdot\underline{\omega}^g+V(\underline{\theta})-\underline{P}^T\cdot\underline{\theta} \tag{2.2.28}$$

$$V(\underline{\theta})=-\sum_{i=1}^{g+l}\sum_{j>i}^{g+l}v_{ti}v_{tj}y_{ij}\cos(\theta_i-\theta_j) \tag{2.2.29}$$

$$\underline{\omega}^g=[\omega_1,\ldots,\omega_g]^T \tag{2.2.30}$$

$$\underline{\theta}=[\theta_1,\ldots,\theta_{g+1}]^T \tag{2.2.31}$$

$$\underline{\mathrm{m}}=\begin{bmatrix} m_1 & 0 & \ldots & 0 \\ 0 & m_2 & \ldots & 0 \\ . & . & & . \\ . & . & & . \\ . & . & & . \\ 0 & 0 & \ldots & m_g \end{bmatrix} \tag{2.2.32}$$

$$\underline{P}=[P_1^m,\ldots,P_{g.}^m P_{g+1}^{ld},\ldots,P_{g+1}^{ld}]^T \tag{2.2.33}$$

Equation (2.2.28) is the actual Lyapunov function. Its right-hand side contains three terms. The first is kinetic energy. The second is the "potential" function, subsequently discussed. The third shows an example of a force-through-a-displacement energy.

Equation (2.2.29) is the potential energy function, or as it is subsequently referred to, the "potential" function. It should be noted that the gradient of the "potential" function with respect to its independent variables, in this case just $\underline{\theta}$, is the load flow equations. $V(\underline{\theta})$ is explicitly constructed so that this is true.--It also fulfills the other requirements for candidate Lyapunov functions. The fact that the load flow equations are the gradient of the "potential" function has an effect on how easily the convective derivative of the Lyapunov function is evaluated.

Equation (2.2.35) shows the convective derivative of a Lyapunov function. Equation (2.2.34) is simply the system equations cast in canonical first order, vector differential form.

$$\dot{\underline{x}}(t)=\underline{f}(\underline{x}(t)) \tag{2.2.34}$$

$$\dot{V}(\underline{x}(t))=\frac{\partial V(\underline{x}(t))}{\partial t}+\overline{\nabla}_x V(\underline{x}(t))\underline{f}(\underline{x}(t)) \tag{2.2.35}$$

The reason for making the load flow equations the gradient of the "potential" function becomes apparent. Evaluating the convective derivative of the typical power system Lyapunov function given in equation (2.2.28) yields the following.

$$\dot{L}(\underline{\theta},\underline{\omega}^g) = \overline{\nabla}_x\left\{\frac{1}{2}\underline{\omega}^{g^T}\cdot\underline{\mathbf{m}}\cdot\underline{\omega}^g + V(\underline{\theta}) - \underline{P}^T\cdot\underline{\theta}\right\}\cdot\{\underline{f}(\underline{\theta},\underline{\omega}^g)\} \tag{2.2.36}$$

$$\underline{f}(\underline{\theta},\underline{\omega}^g) = [\dot{\underline{\theta}}^T \quad \dot{\underline{\omega}}^{g\,T}]^T$$

$$= \begin{bmatrix} \underline{\omega}^g \\ \underline{0} \\ -\frac{d_1}{m_1}\omega_{rm1} + \frac{P_1^m}{m_1} - \frac{1}{m_1}f_1(\underline{\theta}) \\ \cdots \\ -\frac{d_g}{m_g}\omega_{rmg} + \frac{P_g^m}{m_g} - \frac{1}{m_g}f_g(\underline{\theta}) \end{bmatrix} \tag{2.2.37}$$

It is obvious from equation (2.2.36) that the gradient of the "potential" function, $\overline{\nabla}_x V(\underline{\theta})$, will simply be the negative of $\underline{f}(\underline{\theta})$. This vector is then eventually multiplied by itself to yield a negative definite term, at least in the modulo 2π portion of the domain of the angular space.

Other approaches to evaluating the negative semi-definiteness of the convective derivative of equation (2.2.28) use symmetrising matrices or the Jacobian of (2.2.28) and are not discussed further. Any method that can be used to evaluate the negative semi-definiteness or negative definiteness of the convective derivative of the Lyapunov function is permissible.

The kinship between the Lyapunov function, (2.2.28) and (2.2.29), and the "energy function", (2.2.26), should be apparent. In fact, the "energy function" is a valid Lyapunov function. Further, under certain conditions, the equal area criterion represents the "energy function", references [2.2.12] and [2.2.13]. Therefore, all of the methods discussed to this point for determining transient stability are seen to be specific cases of Lyapunov analysis.

2.2.5 Lyapunov Analysis Issues

Nonlinear stability methods based upon Lyapunov's method directly address the thorny issue of "large-signal" stability, including transient stability. Dynamic stability is a specific case of nonlinear stability. In fact, the linearised dynamic system used in a "small-signal" stability analysis is homotopically equivalent to the nonlinear dynamic system from which it is derived. Hence, in a small enough neighbourhood of an equilibrium, linearised and nonlinear behaviour is **identical**. Stability of the linearised system implies the stability of the nonlinear system and vice versa within such a neighbourhood. Steady-state analysis is an even more specialised case of nonlinear stability.--All dynamics are ignored. The steady-state curves correspond to the locus of equilibriums of the nonlinear dynamic system.

The conclusion to be drawn from the foregoing is that examining general nonlinear stability yields more information than is gleaned from steady-state and "small-signal" analyses. Hence, adapting nonlinear stability criterions to a nonlinear dynamic network analysis environment greatly enhances the information available about the electric power system under study.

Power systems are nonlinear, especially shipboard systems. Lyapunov's methods provide a means of assessing nonlinear systems' stability. Reference [2.2.10] is a text describing Lyapunov's methods in detail. It is very important to remember, though, that Lyapunov's methods yield **sufficient** conditions for stability, not necessary conditions for stability. Hence, upon identification of a candidate Lyapunov function, the heart of the "direct" method, a determination that the system is stable is conclusive. However, if a candidate Lyapunov function does not indicate stability, instability cannot be concluded. Hence, the problem arises in the selection of the least "conservative", or least "overly sufficient", Lyapunov function, or even being able to measure the "conservativeness", or "over sufficiency", of a given function.

The "ideal" Lyapunov function accurately captures the magnitude of the δ, of the $\varepsilon - \delta$ stability definition, for the particular system being analysed. Such an "ideal" Lyapunov function is 'minimal' in the sense that it minimises the reduction in the region of stability relative to the largest that δ can be. In contrast, "overly sufficient" Lyapunov functions lead to regions of stability which are smaller than the actual maximum δ of the system.

A further point needs to be made concerning the selection of candidate Lyapunov functions. In a sense, the candidate Lyapunov function can be any function which possesses the required characteristics.--It is only a mathematical tool. Lyapunov was principally concerned with mechanical systems. Lyapunov functions for mechanical systems usually have the physical interpretation of being the energy of the system; although, a physical interpretation is not a necessity just a nicety. The Lyapunov functions used in power systems have likewise been based upon "energy" functions. Although they are not a strict description of the energy within the system.

References [2.2.2]-[2.2.9] all offer distinct Lyapunov functions or expand upon previously developed Lyapunov functions with which to conduct stability analyses of power systems. A common denominator is the fact that all of these methods develop a single candidate Lyapunov function which is a function of **all** of the system's state variables. Some of the methods depend heavily upon the "swing" equation model of electric power systems.

The basics of Lyapunov's theorems are discussed at this point for completeness' sake.

Suppose the system to be analysed can be described as in equation (2.2.38).

$$\dot{\underline{x}}(t) = \underline{f}(\underline{x}, t)$$

$$\underline{x}(0) = \underline{x}_0$$

$$\underline{0} = \underline{f}(\underline{0}, t_1)$$

$$t \geq 0 \qquad (2.2.38)$$

Here, the vector $\underline{x}$ is the state vector. Equilibriums of this system are defined as being the solution of setting $\underline{f}$ equal to zero.

It stands to reason (and can be showed) that **if** one is able to construct a scalar function of the state vector **and** this scalar function of the state vector obeys some conditions which ensure good behaviour **and** this scalar function of the state vector is non-increasing with time, then the equilibrium of the system can be characterised as being stable.

This scalar function is said to be a Lyapunov function. It is usually assigned the letter $V, V(\underline{x})$. $\dot{V}(\underline{x})$ is the rate of change of the Lyapunov function along the system trajectory $\underline{x}(t)$.--This is the convective derivative.

$$\dot{V}(\underline{x},t) = \frac{\partial V}{\partial t} + \overline{\nabla}_x V(\underline{x},t) \cdot \underline{f}(\underline{x},\underline{u},t) \tag{2.2.39}$$

This is a "direct" method for assessing stability because the system trajectory, $\underline{x}(t)$, need not be calculated.

Theorem: The equilibrium $\underline{0}$ at time t_1 of the system (2.2.38) is

A) stable if there exists a continuously differentiable, locally positive definite function V such that

$$\dot{V}(\underline{x},t) \le 0 \quad \forall t \ge t_1 \quad \forall \underline{x} \in B_r \quad \text{for some} \quad B_r$$

B) uniformly stable over $[t_1, \infty)$ if there exists a continuously differentiable, decrescent, locally positive definite function V such that

$$\dot{V}(\underline{x},t) \le 0 \quad \forall t \ge t_1 \quad \forall \underline{x} \in B_r \quad \text{for some} \quad B_r$$

C) uniformly asymptotically stable over $[t_1, \infty)$ if there exists a continuously differentiable, decrescent, locally positive definite function V such that $-\dot{V}$ is a locally positive definite function

D) globally asymptotically stable if there exists a continuously differentiable, decrescent, positive definite function V such that

$$\dot{V}(\underline{x},t) \le -\gamma(\|\underline{x}\|) \quad \forall t \ge t_1 \quad \forall \underline{x} \in \Re^n$$

where $\gamma(\cdot)$ is a function belonging to class K.

The definition of a function belonging to class K given in reference [2.2.10] is adopted here. A continuous function $f: R \to R$ is said to belong to class K if it fulfills three requirements. $f(\cdot)$ is nondecreasing. $f(0) = 0$ and $f(x) > 0 \quad \forall x > 0$.

The definition of a function belonging to class K given in reference [2.2.10] is adopted here. A continuous function $f: R_+ \times R^n \to R$ is said to be decrescent if there exists a function belonging to class K which dominates f.

Thus it would seem that Lyapunov's direct method is relatively simple, requiring only to find the "right" Lyapunov function. However simple and widely applicable it may seem, Lyapunov's direct method is no panacea. Its advantages are that it treats nonlinear, time-varying systems undergoing "large-signal" dynamics. Furthermore, it is a direct method.

Lyapunov's direct method has a number of drawbacks. First, stability findings are qualitative. Second, Lyapunov's conditions are sufficient conditions, not necessary conditions. Third, no general, systematic method exists for generating a Lyapunov function. Fourth, stability must be assessed for each equilibrium separately. Lastly, in the literature, the treatment of inputs, $\underline{u}(t)$, assumes that they are a known function of time.

2.2.6 Relevance to Naval Electric Power System Dynamics

Probably the largest limitation on using the contemporary approaches for assessing transient stability to study naval electric power systems arises from the model of the system which is used.

As mentioned earlier, shipboard systems have finite inertias and strictly limited generating capacity. This leads to potentially large frequency excursions. Advanced shipboard systems forbode large, rapidly applied, short duration loads. This would further exacerbate the frequency excursion issue. As mentioned in the discussion of system modelling, very few of the terms in the conventional models include the frequency dependence of the actual systems. Hence, frequency dynamics would be lost, possibly invalidating the findings of the stability analysis.

The modelling of loads is barely adequate for commercial electric power systems. Naval electric power systems have the advantage that their loads are very finite in extent and number. Hence, a very accurate model of shipboard electric loads is by no means a "holy Grail". A peculiarity of shipboard power systems, for naval combatants particularly, is performance when a significant portion of the system has been damaged by whatever means. Finding an acceptable model that will capture all of the relevant dynamics without carrying along too much baggage is an open issue.

The longest transmission lines in naval electric power systems are short, on the order of 1000ft. Their resistance and inductance are very small. Further, voltages in naval electric power systems are low enough that capacitive transmission line effects are not significant. In essence, loads in naval electric power systems are directly connected to the generators. The "load flow" equations' structure, equation (2.2.17), found in commercial electric power systems, where transmission lines play a crucial role, is not present on warships.

The absence of such a structure highlights the composite nature of naval electric power systems. The close proximity and tight coupling of system components increases the order of the models required to capture all of the relevant dynamics.

Steady-state analysis and "small-signal" stability analysis do have roles in naval electric power system design. To evaluate design performance in the presence of large perturbations, both deliberate and precipitate, requires "large-signal" stability analysis. The equal area criterion and "energy function" method, as well as the other Lyapunov analyses discussed in section 2.2.4.3, are not appropriate because of the underlying model issue.

General Lyapunov stability analysis is capable of handling the "large-signal" perturbations and the higher order nonlinear models required for an accurate assessment of naval electric power system stability. The higher order models, though, place Lyapunov functions within a state space of very high dimensionality. The issue of Lyapunov function selection compounds this complexity.

2.2.7 References

2.2.1 Abed, E.H. and P.P. Varaiya. "Nonlinear oscillations in power systems." Electrical Power and Energy Systems. 1981. pp. 37-43.

2.2.2 Araposthatis, A., S. Sastry, and P. Varaiya. "Analysis of power-flow equation." Electrical Power and Energy Systems. Vol. 3. No. 3. 1981. pp. 115-126.

2.2.3 Araposthatis, A., S. Sastry, and P. Varaiya. "Global Analysis of Swing Dynamics." IEEE Transactions on Circuits and Systems. Vol. CAS-29. No. 10. October, 1982. pp. 673-679.

2.2.4 Kwatny, H.G., L.Y. Bahar, and A.K. Pasrija. "Energy-Like Lyapunov Functions for Power System Stability Analysis." IEEE Transactions on Circuits and Systems. Vol. CAS-32. No. 11. November, 1985. pp. 1140-1149.

2.2.5 Kwatny, H.G., L.Y. Bahar, and A.K. Pasrija. "Static Bifurcations in Electric Power Networks: Loss of Steady-State Stability and Voltage Collapse." IEEE Transactions on Circuits and Systems. Vol. CAS-33. No. 10. October, 1986. pp. 981-991.

2.2.6 Narasimhamurthi, N. and Mohamed T. Musavi. "A Generalized Energy Function for Transient Stability Analysis of Power Systems." IEEE Transactions on Circuits and Systems. Vol. CAS-31. No. 7. July, 1984. pp. 637-645.

2.2.7 Tavora, Carlos J., and Otto J.M. Smith. "Stability Analysis of Power Systems." IEEE Power Engineering Society 1971 Summer Meeting. Portland, Oregon. July 18-23, 1971. (71 TP 591-PWR).

2.2.8 Tsolas, N.A., A. Arapothatis, and P.P. Varaiya. "A Structure Preserving Energy Function for Power System Transient Stability Analysis." IEEE Transactions on Circuits and Systems. Vol. CAS-32. No. 10. October, 1985. pp. 1041-1049.

2.2.9 Willems, Jacques L. "Direct Methods for Transient Stability Studies in Power System Analysis." IEEE Transactions on Automatic Control. Vol. AC-16. No. 4. August, 1971. pp.332-341.

2.2.10 Vidyasagar, M. Nonlinear System Analysis. Englewood Cliffs, New Jersey: Prentice-Hall, Inc. 1978.

2.2.11 Ilic, M. and J. Zaborszky. "Concepts of Stability." IEEE Tutorial Course. Course Text 87EH0262-6-PWR.

2.2.12 Pai, M. Energy Function Analysis for Power System Stability. Kluwer Academic Publications.

2.2.13 Bergen, A. Power Systems Analysis. Englewood Cliffs, NJ: Prentice-Hall, Inc. 1986.

2.3 Composite System Stability Analyses

This section seeks to explore two of the nonlinear methods which have been developed to assess the stability of composite systems. The two criterions given in this section qualify as general nonlinear, "large-signal" stability analyses, as discussed in section 2.2. These methods are relatively general in their application, perhaps moreso than the methods given in section 2.2. They do not depend upon the electric power system model which underlies the stability methods discussed in section 2.2.

2.3.1 Motivation Behind the Composite System Approach

The Lyapunov functions that have been developed for electric power systems, references [2.3.6]-[2.3.13], have usually been monolithic in the sense that the state vector which is the independent variable in the Lyapunov function consists of all of the states of the entire electric power system. For the "swing" equation model, with an m generator system, this means that the Lyapunov function exists in 2m-space. If the system is large, then the problem of interpreting the function and its convective derivative over 2m-space becomes difficult.

Bailey, reference [2.3.1], gives as his motivation the need to reduce the dimensionality of the space in which Lyapunov functions are considered. The need stems from computational complexity. He argues that many relevant, large, complex systems are composed of many simple subsystems which are interconnected. The simple nature of the subsystems combined with an aggregated approach to the interconnections enables a large system, which would have an extremely high order using a monolithic Lyapunov function, to be treated by analysing a number of low order components. Low order systems are frequently handled faster and easier in a computational environment.

The two methods presented next represent an attempt to reduce the order of the space in which Lyapunov functions must be evaluated. They possess the further quality that, as methods, the model and Lyapunov function of each subsystem are left to the user to specify. The methods are not specific to a particular model.

2.3.2 Composite System Stability Criterions

2.3.2.1 Composite Systems

2.3.2.1.1 Linearly Connected Systems

Composite systems are constructed of interconnected components, or subsystems. A subsystem is described by nonlinear equations, references [2.3.1], [2.3.2] and [2.3.3].

$$\dot{\underline{x}}_i = \underline{f}_i(\underline{x}_i, t) + \underline{\mathbf{D}}_i \underline{u}_i$$

$$\underline{y}_i = \underline{\mathbf{H}}_i \underline{x}_i \qquad (2.3.1)$$

If the composite system is comprised of m subsystems, then there will be m such sets of equations. $\underline{x}_i$ represents the n_i states of the i^{th} subsystem. $\underline{u}_i$ represents the m_i inputs to the i^{th} subsystem. $\underline{y}_i$ represents the p_i outputs of the i^{th} subsystem. $\underline{f}_i(\underline{x}_i,t)$ is a n_i-vector valued nonlinear function of the i^{th} state vector and time. The $\underline{\mathbf{D}}_i$ and $\underline{\mathbf{H}}_i$ matrices have the appropriate dimensions to correctly multiply the vectors in equation (2.3.1). The inputs to the i^{th} subsystem are described by equation (2.3.2).

$$\underline{u}_i = \sum_{j=1}^{m} \underline{\mathbf{B}}_{ij} \underline{y}_j + \underline{\mathbf{G}}_i \underline{\mathbf{u}} \qquad (2.3.2)$$

The matrix $\underline{\mathbf{B}}_{ij}$ describes the linear interconnections between the inputs of the ith subsystem and the outputs of the other m-1 subsystems. "Closed-loop" dynamics are accounted for within $\underline{f}_i(\underline{x}_i,t)$; therefore, $\underline{\mathbf{B}}_{ij}$ is zero for i=j. $\underline{u}$ is the vector of exogenous (global) inputs to the composite system. The composite system, assembled from the subsystems, is shown in equation (2.3.3).

$$\dot{\underline{x}}_i = \underline{f}_i(\underline{x}_i, t) + \sum_{j=1}^{m} \underline{\mathbf{C}}_{ij} \underline{x}_j + \underline{\mathbf{K}}_i \underline{u} \qquad i = 1, \ldots, m$$

$$\underline{y} = \underline{h}(\underline{x}, t)$$

$$\text{where} \quad \underline{x} = \begin{bmatrix} \underline{x}_1 \\ \underline{x}_2 \\ \cdot \\ \cdot \\ \cdot \\ \underline{x}_m \end{bmatrix} \quad \underline{y} = \begin{bmatrix} \underline{y}_1 \\ \underline{y}_2 \\ \cdot \\ \cdot \\ \cdot \\ \underline{y}_m \end{bmatrix} \quad \underline{\mathbf{C}}_{ij} = \underline{\mathbf{D}}_i \underline{\mathbf{B}}_{ij} \underline{\mathbf{H}}_j \quad \underline{\mathbf{K}}_i = \underline{\mathbf{D}}_i \underline{\mathbf{G}}_i \qquad (2.3.3)$$

An important feature of this model of a composite system is that the characterisation of the interconnections is known. In other words, the "structure" of the system is a given.

2.3.2.1.2 Assumed Bounds of Subsystem Lyapunov Function

The stability of each of the subsystems is determined through the use of Lyapunov's direct method. The direct method requires identification of a candidate Lyapunov function. Stability assessments stem from the characteristics of the candidate Lyapunov function and its convective derivative. One of the drawbacks of Lyapunov's direct method is "over sufficiency"; hence, the Lyapunov function selected for each subsystem should be minimally "over sufficient". Poorly selected Lyapunov functions lead to crippling "over sufficiency".

Each subsystem has a Lyapunov function which describes its stability. The Lyapunov function of the i^{th} subsystem, $V_i(\underline{x}_i)$, must be a continuously differentiable, locally positive definite function of $\underline{x}_i$, where $\underline{x}_i$ is described by equation (2.3.1). The convective derivative of V_i is evaluated as in equation (2.2.39).

The goal of composite system Lyapunov methods is to characterise the composite system stability on the basis of (1) the subsystems' stability and (2) their interconnections. The requirements on the Lyapunov functions of each of the subsystems indicate that the unforced responses of the subsystems are stable. The bounds of the subsystems' unforced responses provide bounds for the forced responses.

The bounds on the subsystems' Lyapunov functions themselves are in terms of the state variables, $\underline{x}_i$. This is because the Lyapunov functions are solely functions of the state variables. The effect of inputs is seen only in the convective derivatives of the subsystems' Lyapunov functions. Use of this fact is made in establishing bounds on the convective derivatives of the "forced" subsystems.

The authors of references [2.3.1] - [2.3.4] endeavour to determine exponential stability in the large (ESL) and asymptotic stability in the large (ASL) of the composite system. ESL's requirements make it very much like global asymptotic stability (GAS). ASL is just another name for GAS. These two forms of stability are the most demanding. The conditions which the subsystems' Lyapunov functions must fulfill if the subsystems are to be GAS follow.

The equilibrium at the origin, $\underline{x}_i = \underline{0}$, of the unforced subsystem $\underline{x}'_i=\underline{f}_i(\underline{x}_i,t)$, is GAS if there exists a function $V_i(\underline{x}_i,t)$ which is continuously differentiable and which meets conditions 1 and 2 below for positive constants c_{i1}, c_{i2} and c_{i3}. Assume that the solution of $\underline{x}'_i=\underline{f}_i(\underline{x}_i,t)$ exists and is unique.

$$\text{Condition 1} \quad c_{i1}\|\underline{x}_i\|^2 \le V_i(\underline{x}_i,t) \le c_{i2}\|\underline{x}_i\|^2$$

$$\text{Condition 2} \quad \dot{V}_i(\underline{x}_i,t) \le -c_{i3}\|\underline{x}_i\|^2 \qquad (2.3.4)$$

The rest of this discussion assumes that such a function has been identified for all of the subsystems of the composite system. Furthermore, the Lyapunov functions' convective derivatives obey condition 2 for their **unforced** ($\underline{u}_i=\underline{0}$) responses. These two assumptions, which require the unforced subsystems to be GAS, are very sweeping assumptions. However, making these assumptions is necessary if one is trying to obtain results as demanding as proving GAS for a composite system.

In the way of quantifying the requirement that the subsystem Lyapunov functions be continuously differentiable, assume that the subsystem Lyapunov functions meet the further criterion shown in equation (2.3.5). This criterion ensures bounded derivatives with respect to the state variables. This is somewhat more restrictive than the global Lipschitz condition, which is all that is necessary. This requirement represents a source of "over sufficiency".

$$\|\overline{\nabla} V_i(\underline{x}_i,t)\| \le c_{i4}\|\underline{x}_i\| \qquad (c_{i4} > 0) \qquad (2.3.5)$$

2.3.2.2 Vector Lyapunov Function Analysis

The authors of references [2.3.1], [2.3.2] and [2.3.4] develop a stability criterion for a composite system based upon a vector Lyapunov function. The vector Lyapunov function is simply a vector of the subsystems' Lyapunov functions.

$$\underline{V}_v = \begin{bmatrix} V_1(\underline{x}_1, t) \\ \cdot \\ V_i(\underline{x}_i, t) \\ \cdot \\ V_m(\underline{x}_m, t) \end{bmatrix} \tag{2.3.6}$$

Whereas the Lyapunov functions of each of the subsystems satisfy condition 1 of equation (2.3.4), it is ensured that the composite system vector Lyapunov function meets condition 1 of equation (2.3.4) in an element-wise sense. Similar reasoning ensures that the vector Lyapunov function meets the condition on its element-wise gradients. Consequently, the convective derivative of the vector Lyapunov function determines whether the composite system vector Lyapunov function obeys condition 2 of equation (2.3.4). If condition 2 is obeyed, then it is concluded that the composite system is GAS.

$$\dot{\underline{V}}_v = \begin{bmatrix} \dot{V}_1(\underline{x}_1, t) \\ \cdot \\ \dot{V}_i(\underline{x}_i, t) \\ \cdot \\ \dot{V}_m(\underline{x}_m, t) \end{bmatrix} = \begin{bmatrix} \left(\frac{\partial V_1}{\partial t} + \overline{\nabla} V_1^T \underline{f}_1\right) + \overline{\nabla} V_1^T \underline{\mathbf{D}}_1 \underline{u}_1 \\ \cdot \\ \left(\frac{\partial V_i}{\partial t} + \overline{\nabla} V_i^T \underline{f}_i\right) + \overline{\nabla} V_i^T \underline{\mathbf{D}}_i \underline{u}_i \\ \cdot \\ \left(\frac{\partial V_m}{\partial t} + \overline{\nabla} V_m^T \underline{f}_m\right) + \overline{\nabla} V_m^T \underline{\mathbf{D}}_m \underline{u}_m \end{bmatrix} \tag{2.3.7}$$

The first term in the brackets on the far right hand side of equation (2.3.7) can be replaced, inserting the inequality of condition 2 for the subsystems. This step is based upon the supposition that this term is bounded above by the unforced case. This bounding inequality is a source of "over sufficiency". Additionally, the vector products on the far right hand side of equation (2.3.7) can be bounded using vector norms. This bounding inequality is a source of "over sufficiency" as well.

$$\dot{\underline{V}}_v \leq \begin{bmatrix} (-c_{13}\|\underline{x}_1\|^2) + \|\overline{\nabla} V_1\| \, \|\underline{\mathbf{D}}_1 \underline{u}_1\| \\ \cdot \\ (-c_{i3}\|\underline{x}_i\|^2) + \|\overline{\nabla} V_i\| \, \|\underline{\mathbf{D}}_i \underline{u}_i\| \\ \cdot \\ (-c_{m3}\|\underline{x}_m\|^2) + \|\overline{\nabla} V_m\| \, \|\underline{\mathbf{D}}_m \underline{u}_m\| \end{bmatrix} \leq \begin{bmatrix} -c_{13}\|\underline{x}_1\|^2 + c_{14}\|\underline{x}_1\| \sum_{j=1}^{m} \sum_{j \neq 1} \|\underline{\mathbf{C}}_{1j}\|_{\text{induced}} \|\underline{x}_j\| \\ \cdot \\ -c_{i3}\|\underline{x}_i\|^2 + c_{i4}\|\underline{x}_i\| \sum_{j=1}^{m} \sum_{j \neq i} \|\underline{\mathbf{C}}_{ij}\|_{\text{induced}} \|\underline{x}_j\| \\ \cdot \\ -c_{m3}\|\underline{x}_m\|^2 + c_{m4}\|\underline{x}_m\| \sum_{j=1}^{m} \sum_{j \neq m} \|\underline{\mathbf{C}}_{mj}\|_{\text{induced}} \|\underline{x}_j\| \end{bmatrix} \tag{2.3.8}$$

$$\dot{\underline{V}}_v \le \begin{bmatrix} -\frac{c_{13}}{2} & 0 & 0 & 0 & 0 \\ 0 & . & 0 & 0 & 0 \\ 0 & 0 & -\frac{c_{j3}}{2} & 0 & 0 \\ 0 & 0 & 0 & . & 0 \\ 0 & 0 & 0 & 0 & -\frac{c_{m3}}{2} \end{bmatrix} \cdot \begin{bmatrix} \|\underline{x}_1\|^2 \\ . \\ \|\underline{x}_j\|^2 \\ . \\ \|\underline{x}_m\|^2 \end{bmatrix} + \underline{\beta} \tag{2.3.9}$$

$$\underline{\beta} = \begin{bmatrix} -\frac{c_{13}}{2}\|\underline{x}_1\|^2 + c_{14}\|\underline{x}_1\| \sum_{j=1}^{m} \sum_{j\neq 1} \|\underline{C}_{1j}\|_{induced} \|\underline{x}_j\| \\ . \\ -\frac{c_{i3}}{2}\|\underline{x}_i\|^2 + c_{i4}\|\underline{x}_i\| \sum_{j=1}^{m} \sum_{j\neq i} \|\underline{C}_{ij}\|_{induced} \|\underline{x}_j\| \\ . \\ -\frac{c_{m3}}{2}\|\underline{x}_m\|^2 + c_{m4}\|\underline{x}_m\| \sum_{j=1}^{m} \sum_{j\neq m} \|\underline{C}_{mj}\|_{induced} \|\underline{x}_j\| \end{bmatrix} \tag{2.3.10}$$

The vector $\underline{\beta}$ can be simplified by "completing the square" for each of the elements of the vector. "Completing the square" in this application involves use of the triangle inequality. The use of the triangle inequality here is another source of "over sufficiency".

$$\underline{\beta} \le \begin{bmatrix} -\frac{c_{13}}{2}|\underline{x}_1|^2 + c_{14}|\underline{x}_1| \sum_{j=1}^{m} \sum_{j\neq 1} |\underline{C}_{1j}|_{induced} |\underline{x}_j| + \sum_{j=1}^{m} \sum_{j\neq 1} \left(-\sqrt{\frac{c_{13}}{2(m-1)}}|\underline{x}_1| + \sqrt{\frac{(m-1)}{2c_{13}}} c_{14} |\underline{C}_{1j}|_{induced} |\underline{x}_j| \right)^2 \\ . \\ -\frac{c_{i3}}{2}|\underline{x}_i|^2 + c_{i4}|\underline{x}_i| \sum_{j=1}^{m} \sum_{j\neq i} |\underline{C}_{ij}|_{induced} |\underline{x}_j| + \sum_{j=1}^{m} \sum_{j\neq i} \left(-\sqrt{\frac{c_{i3}}{2(m-1)}}|\underline{x}_i| + \sqrt{\frac{(m-1)}{2c_{i3}}} c_{i4} |\underline{C}_{ij}|_{induced} |\underline{x}_j| \right)^2 \\ . \\ -\frac{c_{m3}}{2}|\underline{x}_m|^2 + c_{m4}|\underline{x}_m| \sum_{j=1}^{m} \sum_{j\neq m} |\underline{C}_{mj}|_{induced} |\underline{x}_j| + \sum_{j=1}^{m} \sum_{j\neq m} \left(-\sqrt{\frac{c_{m3}}{2(m-1)}}|\underline{x}_m| + \sqrt{\frac{(m-1)}{2c_{m3}}} c_{m4} |\underline{C}_{mj}|_{induced} |\underline{x}_j| \right)^2 \end{bmatrix} \tag{2.3.11}$$

Simplify equation (2.3.11).

$$\underline{\beta} \le \begin{bmatrix} \sum_{j=1}^{m} \sum_{j\neq 1} \left(\frac{(m-1)}{2c_{13}} c_{14}^2 \|\underline{C}_{1j}\|^2_{induced} \|\underline{x}_j\|^2 \right) \\ . \\ \sum_{j=1}^{m} \sum_{j\neq i} \left(\frac{(m-1)}{2c_{i3}} c_{i4}^2 \|\underline{C}_{ij}\|^2_{induced} \|\underline{x}_j\|^2 \right) \\ . \\ \sum_{j=1}^{m} \sum_{j\neq m} \left(\frac{(m-1)}{2c_{m3}} c_{m4}^2 \|\underline{C}_{mj}\|^2_{induced} \|\underline{x}_j\|^2 \right) \end{bmatrix} \tag{2.3.12}$$

Casting this into the form of the product of a matrix and the vector of the norms-of-the-states-squared yields equation (2.3.13).

$$\underline{\beta} \leq \begin{bmatrix} 0 & \frac{(m-1)c_{14}^2 \| \underline{C}_{12} \|^2_{induced}}{2c_{13}} & \frac{(m-1)c_{14}^2 \| \underline{C}_{13} \|^2_{induced}}{2c_{13}} & \cdot & \frac{(m-1)c_{14}^2 \| \underline{C}_{1j} \|^2_{induced}}{2c_{13}} & \cdot & \frac{(m-1)c_{14}^2 \| \underline{C}_{1m} \|^2_{induced}}{2c_{13}} \\ \frac{(m-1)c_{24}^2 \| \underline{C}_{21} \|^2_{induced}}{2c_{23}} & 0 & \frac{(m-1)c_{24}^2 \| \underline{C}_{23} \|^2_{induced}}{2c_{23}} & \cdot & \frac{(m-1)c_{24}^2 \| \underline{C}_{2j} \|^2_{induced}}{2c_{23}} & \cdot & \frac{(m-1)c_{24}^2 \| \underline{C}_{2m} \|^2_{induced}}{2c_{23}} \\ \frac{(m-1)c_{34}^2 \| \underline{C}_{31} \|^2_{induced}}{2c_{33}} & \frac{(m-1)c_{34}^2 \| \underline{C}_{32} \|^2_{induced}}{2c_{33}} & 0 & \cdot & \frac{(m-1)c_{34}^2 \| \underline{C}_{3j} \|^2_{induced}}{2c_{33}} & \cdot & \frac{(m-1)c_{34}^2 \| \underline{C}_{3m} \|^2_{induced}}{2c_{33}} \\ \cdot & \cdot & \cdot & 0 & \cdot & \cdot & \cdot \\ \frac{(m-1)c_{j4}^2 \| \underline{C}_{j1} \|^2_{induced}}{2c_{j3}} & \frac{(m-1)c_{j4}^2 \| \underline{C}_{j2} \|^2_{induced}}{2c_{j3}} & \frac{(m-1)c_{j4}^2 \| \underline{C}_{j3} \|^2_{induced}}{2c_{j3}} & \cdot & 0 & \cdot & \frac{(m-1)c_{j4}^2 \| \underline{C}_{jm} \|^2_{induced}}{2c_{j3}} \\ \cdot & \cdot & \cdot & \cdot & \cdot & 0 & \cdot \\ \frac{(m-1)c_{m4}^2 \| \underline{C}_{m1} \|^2_{induced}}{2c_{m3}} & \frac{(m-1)c_{m4}^2 \| \underline{C}_{m2} \|^2_{induced}}{2c_{m3}} & \frac{(m-1)c_{m4}^2 \| \underline{C}_{m3} \|^2_{induced}}{2c_{m3}} & \cdot & \frac{(m-1)c_{m4}^2 \| \underline{C}_{mj} \|^2_{induced}}{2c_{m3}} & \cdot & 0 \end{bmatrix} \cdot \begin{bmatrix} \| \underline{x}_1 \|^2 \\ \| \underline{x}_2 \|^2 \\ \| \underline{x}_3 \|^2 \\ \cdot \\ \| \underline{x}_j \|^2 \\ \cdot \\ \| \underline{x}_m \|^2 \end{bmatrix}$$

(2.3.13)

The process of going from equation (2.3.9) to equation (2.3.13) is 'majorisation', reference [2.3.2]. Reference [2.3.2] offers this majorisation as a possible reason why reference [2.3.2] found the vector Lyapunov criterion to be more conservative than the weighted-sum Lyapunov criterion.

$$\underline{\beta} \leq \underline{G} \cdot \underline{\|x\|}^2 \tag{2.3.14}$$

This expression for β, equation (2.3.14), can be substituted into equation (2.3.9). This yields equation (2.3.15).

$$\underline{\dot{V}}_v \leq \begin{bmatrix} -\frac{c_{13}}{2} & 0 & 0 & 0 & 0 \\ 0 & . & 0 & 0 & 0 \\ 0 & 0 & -\frac{c_{j3}}{2} & 0 & 0 \\ 0 & 0 & 0 & . & 0 \\ 0 & 0 & 0 & 0 & -\frac{c_{m3}}{2} \end{bmatrix} \cdot \begin{bmatrix} \|\underline{x}_1\|^2 \\ . \\ \|\underline{x}_j\|^2 \\ . \\ \|\underline{x}_m\|^2 \end{bmatrix} + \underline{G} \cdot \begin{bmatrix} \|\underline{x}_1\|^2 \\ . \\ \|\underline{x}_j\|^2 \\ . \\ \|\underline{x}_m\|^2 \end{bmatrix} \tag{2.3.15}$$

At this point, substituting condition 1 of equation (2.3.4) for each of the subsystem Lyapunov functions allows casting equation (2.3.15) into a matrix differential equation form. The resulting relationship follows directly from condition 1 on the subsystem Lyapunov functions.

$$\underline{\dot{V}}_v \leq \begin{bmatrix} -\frac{c_{13}}{2} & 0 & 0 & 0 & 0 \\ 0 & . & 0 & 0 & 0 \\ 0 & 0 & -\frac{c_{j3}}{2} & 0 & 0 \\ 0 & 0 & 0 & . & 0 \\ 0 & 0 & 0 & 0 & -\frac{c_{m3}}{2} \end{bmatrix} \cdot \begin{bmatrix} \frac{1}{c_{12}} & 0 & 0 & 0 & 0 \\ 0 & . & 0 & 0 & 0 \\ 0 & 0 & \frac{1}{c_{j2}} & 0 & 0 \\ 0 & 0 & 0 & . & 0 \\ 0 & 0 & 0 & 0 & \frac{1}{c_{m2}} \end{bmatrix} \cdot \underline{V}_v + \underline{G} \cdot \begin{bmatrix} \frac{1}{c_{11}} & 0 & 0 & 0 & 0 \\ 0 & . & 0 & 0 & 0 \\ 0 & 0 & \frac{1}{c_{j1}} & 0 & 0 \\ 0 & 0 & 0 & . & 0 \\ 0 & 0 & 0 & 0 & \frac{1}{c_{m1}} \end{bmatrix} \cdot \underline{V}_v \tag{2.3.16}$$

Combining the matrices yields the desired expression, equation (2.3.17).

$$\dot{\underline{V}}_v \le \begin{bmatrix} -\frac{c_{13}}{2c_{12}} & \frac{(m-1)c_{14}^2\|\underline{C}_{12}\|^2_{induced}}{2c_{13}c_{21}} & \frac{(m-1)c_{14}^2\|\underline{C}_{13}\|^2_{induced}}{2c_{13}c_{31}} & \cdot & \frac{(m-1)c_{14}^2\|\underline{C}_{1j}\|^2_{induced}}{2c_{13}c_{j1}} & \cdot & \frac{(m-1)c_{14}^2\|\underline{C}_{1m}\|^2_{induced}}{2c_{13}c_{m1}} \\ \frac{(m-1)c_{24}^2\|\underline{C}_{21}\|^2_{induced}}{2c_{23}c_{11}} & -\frac{c_{23}}{2c_{22}} & \frac{(m-1)c_{24}^2\|\underline{C}_{23}\|^2_{induced}}{2c_{23}c_{31}} & \cdot & \frac{(m-1)c_{24}^2\|\underline{C}_{2j}\|^2_{induced}}{2c_{23}c_{j1}} & \cdot & \frac{(m-1)c_{24}^2\|\underline{C}_{2m}\|^2_{induced}}{2c_{23}c_{m1}} \\ \frac{(m-1)c_{34}^2\|\underline{C}_{31}\|^2_{induced}}{2c_{33}c_{11}} & \frac{(m-1)c_{34}^2\|\underline{C}_{32}\|^2_{induced}}{2c_{33}c_{21}} & -\frac{c_{33}}{2c_{32}} & \cdot & \frac{(m-1)c_{34}^2\|\underline{C}_{3j}\|^2_{induced}}{2c_{33}c_{j1}} & \cdot & \frac{(m-1)c_{34}^2\|\underline{C}_{3m}\|^2_{induced}}{2c_{33}c_{m1}} \\ \cdot & \cdot & \cdot & \cdot & \cdot & \cdot & \cdot \\ \frac{(m-1)c_{j4}^2\|\underline{C}_{j1}\|^2_{induced}}{2c_{j3}c_{11}} & \frac{(m-1)c_{j4}^2\|\underline{C}_{j2}\|^2_{induced}}{2c_{j3}c_{21}} & \frac{(m-1)c_{j4}^2\|\underline{C}_{j3}\|^2_{induced}}{2c_{j3}c_{31}} & \cdot & -\frac{c_{j3}}{2c_{j2}} & \cdot & \frac{(m-1)c_{j4}^2\|\underline{C}_{jm}\|^2_{induced}}{2c_{j3}c_{m1}} \\ \cdot & \cdot & \cdot & \cdot & \cdot & \cdot & \cdot \\ \frac{(m-1)c_{m4}^2\|\underline{C}_{m1}\|^2_{induced}}{2c_{m3}c_{11}} & \frac{(m-1)c_{m4}^2\|\underline{C}_{m2}\|^2_{induced}}{2c_{m3}c_{21}} & \frac{(m-1)c_{m4}^2\|\underline{C}_{m3}\|^2_{induced}}{2c_{m3}c_{31}} & \cdot & \frac{(m-1)c_{m4}^2\|\underline{C}_{mj}\|^2_{induced}}{2c_{m3}c_{j1}} & \cdot & -\frac{c_{m3}}{2c_{m2}} \end{bmatrix} \cdot \underline{V}_v \tag{2.3.17}$$

As described in references [2.3.1] and [2.3.2], if the matrix multiplying $\underline{V}_v$ is stable in the linear stability sense, then the convective derivative of $\underline{V}_v$ obeys condition 2 in an element-wise sense; therefore, the composite system is globally asymptotically stable. Of note, Bailey refers to equation (2.3.17) as the "auxiliary equation". The stability of the matrix multiplying $\underline{V}_v$ constitutes the composite system vector Lyapunov function stability criterion for global asymptotic stability. The matrix multiplying $\underline{V}_v$ is a function of the interconnections of the power system, that is the specific "structure" of the system.

2.3.2.3 Weighted-Sum Lyapunov Function Analysis

The composite system weighted-sum Lyapunov function is the sum of the products of a weighting parameter and the subsystem Lyapunov function for each of the subsystems.

$$V_c(\underline{x},t) = \sum_{i=1}^{m} \alpha_i \cdot V_i(\underline{x}_i,t) \tag{2.3.18}$$

To determine if the composite system is GAS, the composite system weighted-sum Lyapunov function must satisfy conditions 1 and 2 of equation (2.3.4) and the condition of equation (2.3.5).

$$V_c(\underline{x},t) = \sum_{i=1}^{m} \alpha_i \cdot V_i(\underline{x}_i,t)$$

$$\leq \sum_{i=1}^{m} \alpha_i c_{i2} \| \underline{x}_i \|^2$$

$$\leq \max_i\{\alpha_i c_{i2}\} \sum_{i=1}^{m} \| \underline{x}_i \|$$

$$\leq \max_i\{\alpha_i c_{i2}\} \| \underline{x} \|^2$$

$$\text{Similarly,} \quad V_c(\underline{x},t) \geq \min_i\{\alpha_i c_{i1}\} \| \underline{x} \|^2 \tag{2.3.19}$$

Equation (2.3.19) shows that $V_c(\underline{x},t)$ meets condition 1 for GAS. Similar reasoning ensures that the weighted-sum Lyapunov function meets the condition of equation (2.3.5). The composite weighted-sum Lyapunov function must also meet condition 2. Take the exogenous inputs to be zero, $\underline{u}=\underline{0}$.

$$\dot{V}_c(\underline{x},t) = \sum_{i=1}^{m} \alpha_i \dot{V}_i$$

$$= \sum_{i=1}^{m} \left[\alpha_i \left(\frac{\partial V_i}{\partial t} + \overline{\nabla} V_i^T \underline{f}_i \right) + \alpha_i \overline{\nabla} V_i^T \underline{\mathbf{D}}_i \underline{u}_i \right] \tag{2.3.20}$$

As with the vector Lyapunov criterion derivation, the first term in the brackets on the far right hand side of equation (2.3.20) can be replaced, inserting the inequality of condition 2 for the subsystems. This step is based upon the supposition that this term is bounded above by the unforced case. This bounding inequality is a source of "over sufficiency". The use of vector norms to bound the products on the right hand side is the same as in Bailey's derivation, reference [2.3.1], another source of "over sufficiency".

$$\dot{V}_c(\underline{x},t) \le \sum_{i=1}^{m} \{-\alpha_i c_{i3} \| \underline{x}_i \|^2 + \alpha_i \| \overline{\nabla} V_i \| \, \| \underline{D}_i \underline{u}_i \| \}$$

$$\le \sum_{i=1}^{m} \left\{ -\alpha_i c_{i3} \| \underline{x}_i \|^2 + \alpha_i c_{i4} \| \underline{x}_i \| \left\| \sum_{j=1}^{m} \underline{D}_i \underline{B}_{ij} \underline{H}_j \underline{x}_j \right\| \right\}$$

$$\le \sum_{i=1}^{m} \left\{ -\alpha_i c_{i3} \| \underline{x}_i \|^2 + \alpha_i c_{i4} \| \underline{x}_i \| \sum_{j=1}^{m} \sum_{i \ne j} \| \underline{C}_{ij} \|_{\text{induced}} \| \underline{x}_j \| \right\}$$

(2.3.21)

The matrix $\underline{C}_{ij}$ is defined in equation (2.3.3). The induced norm of a matrix is described in equation (2.3.22). This definition of induced norm is taken from reference [2.3.5]. It is not in agreement with the definition of the induced norm given by reference [2.3.2]. The disagreement concerns the fact that an induced norm is defined in terms of a specific vector norm and must be consistent with that vector norm. Reference [2.3.5] is taken here to be correct.

$$\| \underline{A} \|_{\text{induced}} = \sqrt{\lambda_{\max}(\underline{A}^H \cdot \underline{A})}$$

Where $\lambda_{\max}(\cdot)$ = Maximum eigenvalue of given matrix

and $\underline{A}^H$ = Hermitian of matrix $\underline{A}$ (2.3.22)

The induced norm is now used within the expression for the convective derivative of the weighted-sum Lyapunov function. Using the induced norm here is a source of "over sufficiency".

$$\dot{V}_c(\underline{x},t) \le \underline{\| x \|}^T \cdot \begin{pmatrix} -\alpha_1 c_{13} & \cdot & \alpha_1 c_{14} \| \underline{C}_{1j} \|_{\text{induced}} & \cdot & \alpha_1 c_{14} \| \underline{C}_{1m} \|_{\text{induced}} \\ \cdot & \cdot & \cdot & \cdot & \cdot \\ \alpha_j c_{j4} \| \underline{C}_{j1} \|_{\text{induced}} & \cdot & -\alpha_j c_{j3} & \cdot & \alpha_j c_{j4} \| \underline{C}_{jm} \|_{\text{induced}} \\ \cdot & \cdot & \cdot & \cdot & \cdot \\ \alpha_m c_{m4} \| \underline{C}_{m1} \|_{\text{induced}} & \cdot & \alpha_m c_{m4} \| \underline{C}_{mj} \|_{\text{induced}} & \cdot & -\alpha_m c_{m3} \end{pmatrix} \cdot \underline{\| x \|}$$

where $\underline{\| x \|}^T = [\| \underline{x}_1 \|, ., \| \underline{x}_j \|, ., \| \underline{x}_m \|]$ (2.3.23)

An easy transformation, the matrix in equation (2.3.23), called $\underline{R}$, becomes a symmetric matrix, $\underline{S}$.

$$\dot{V}_c(\underline{x},t) \le \underline{\| x \|}^T \cdot \underline{R} \cdot \underline{\| x \|}$$

$$\le \underline{\| x \|}^T \cdot \frac{(\underline{R} + \underline{R}^T)}{2} \cdot \underline{\| x \|}$$

$$\le \underline{\| x \|}^T \cdot \underline{S} \cdot \underline{\| x \|}$$

$$\le \| \underline{\| x \|}^T \| \cdot \| \underline{S} \|_{\text{induced}} \cdot \| \underline{\| x \|} \|$$

$$\le \| \underline{S} \|_{\text{induced}} \cdot \underline{\| x \|}^2 \qquad (2.3.24)$$

For the composite system weighted-sum Lyapunov function to satisfy condition 2, the magnitude of the induced norm of $\underline{S}$ must be bounded.

$$\| \underline{S} \|_{\text{induced}} = \sqrt{\lambda_{max}(\underline{S}^H \cdot \underline{S})}$$

$$= \sqrt{\lambda_{max}(\underline{S}^2)}$$

$$= \sqrt{[\lambda_{max}(\underline{S})]^2}$$

$$= \lambda_{max}(\underline{S}) \qquad (2.3.25)$$

Therefore, for the convective derivative of the composite system weighted-sum Lyapunov function to satisfy condition 2, the relationship in equation (2.3.26) must be true.

$$\lambda_{max}(\underline{S}) < 0 \qquad (2.3.26)$$

This will be true if $\underline{S}$ is negative definite. Hence, the GAS of the composite system hinges upon the negative definiteness of the constructed matrix $\underline{S}$. Just as with the particular composite system vector Lyapunov function criterion discussed in section 2.3.2.2, the composite system weighted-sum Lyapunov function criterion of this section consists of developing a matrix, which is a function of the power system's interconnections ("structure"), that possesses linear stability qualities and, hence, ensures global asymptotic stability.

2.3.3 Limitations of Existing Composite System Stability Criterions

The problem with implementing these two composite system methods is the "over sufficiency" issue. The region of stability, R.O.S., and region of attraction, R.O.A., arising from the composite system methods, if they exist at all, are smaller than should be expected. This would mean that such things as clearing times would be unnecessarily short, perhaps prohibitively so. Identifying the causes of the "over sufficiency" sheds some light on the pervasive extent of this limitation.

The only stability determination which is pursued in references [2.3.1], [2.3.2] and [2.3.3] is that of exponential stability in the large and asymptotic stability (in the large). These are rather strict forms of stability, indicating very well-behaved systems. Electric power systems have, in fact, been known to go unstable, naval electric power systems included. Hence, it may be more worthwhile to establish if a complex electric power system meets the requirements for the weaker forms of stability.

In proving that a system is ESL or ASL, very tight restrictions are placed upon the model.--Namely, the dynamic equations, while not having to be linear, must be reasonably well-behaved functions. Hence, by trying to prove a very strict form of stability, these composite system methods miss the weaker, yet possibly more relevant, forms of stability.

Lyapunov functions (and their convective derivatives) do not have to be quadratic functions or even dominate (or be dominated by) quadratic functions. The reason for choosing quadratic functions is to make the determinations of ESL and ASL tractable.--This is not to say that many electric power systems components do not have worthwhile Lyapunov functions which are quadratic. It may be that in some cases, quadratic Lyapunov functions or quadratic bounding functions may be "overly sufficient".

The substitution of the inequality of condition 2 of equation (2.3.4) into the forced dynamics of the convective derivative of the subsystems' Lyapunov functions is, in essence, using the unforced response to bound the forced response. The validity of this step depends upon the subsystem dynamics being of the form of equation (2.3.1).

$$\dot{V}_{\text{i forced}} = \frac{\partial V_i}{\partial t} + \overline{\nabla} V_i^T \cdot (\underline{f}_i + \underline{\mathbf{D}}_i \underline{u}_i)$$

$$\dot{V}_{\text{i unforced}} = \frac{\partial V_i}{\partial t} + \overline{\nabla} V_i^T \cdot (\underline{f}_i)$$

$$\therefore \quad \dot{V}_{\text{i forced}} = \dot{V}_{\text{i unforced}} + \overline{\nabla} V_i^T \cdot (\underline{\mathbf{D}}_i \underline{u}_i) \tag{2.3.27}$$

$$\text{Condition 2} \quad \Rightarrow \quad \dot{V}_{\text{i forced}} \leq -c_{i3} \| \underline{x}_i \|^2 + \overline{\nabla} V_i^T \cdot (\underline{\mathbf{D}}_i \underline{u}_i)$$

$$\text{Product of Norms} \quad \Rightarrow \quad \dot{V}_{\text{i forced}} \leq -c_{i3} \| \underline{x}_i \|^2 + \| \overline{\nabla} V_i^T \| \cdot \| (\underline{\mathbf{D}}_i \underline{u}_i) \|$$

$$\text{Equation (2.3.5)} \quad \Rightarrow \quad \dot{V}_{\text{i forced}} \leq -c_{i3} \| \underline{x}_i \|^2 + c_{i4} \| \underline{x}_i \| \cdot \| (\underline{\mathbf{D}}_i \underline{u}_i) \| \tag{2.3.28}$$

While this represents a valid bounding of the convective derivative of the subsystems' Lyapunov functions, it also means that the convective derivative is subsequently represented by its upper limit. This represents a source of conservatism ("over sufficiency").

One of the drawbacks of nonlinear analysis is that it is very general (which is also a great strength). Frequently, analysis must resort to the use of limits (bounds). This is often done with norms, for vectors, and induced norms, for matrices. These norms represent a "worst case" sort of mentality, contributing to "over sufficiency" in the Lyapunov criterions. Furthermore, in arithmetic operations, inclusion of norms requires imposition of the "triangle inequality". This is another "worst case" sort of influence, contributing to "over sufficiency" as well.

References [2.3.1] and [2.3.2] do not treat the exogenous inputs to the composite system at all in their derivations of the composite system stability criterions. It is vital in modelling naval electric power systems that exogenous inputs be considered. For example, a typical shipboard exogenous input would be rudder commands given by the deck officer. A different type of exogenous input is sea-state. This input affects the behaviour of the propulsion motors (and just about everything else).

The means of determining stability using the weighted-sum Lyapunov function and the vector Lyapunov function are somewhat similar. Reference [2.3.2], in its derivation of the vector criterion, uses its derivation of the weighted-sum criterion to a point. The weighted-sum criterion derivation includes the weighting factors, the α's. When the vector criterion derivation parts ways with the weighted-sum criterion derivation in reference [2.3.2], the authors of reference [2.3.2] dispense with the weighting factors by setting them equal to one.--This is interesting if one views the weighted-sum Lyapunov function as being related to the vector Lyapunov function. Let V_s denote the weighted-sum Lyapunov function and $\underline{V}_v$ the vector Lyapunov function. Furthermore, let $\underline{\alpha}$ denote the vector of the weights.

$$V_s = \underline{\alpha}^T \cdot \underline{V}_v \tag{2.3.29}$$

This relationship, which is based on the definitions of the respective composite system Lyapunov functions indicates that the weighted-sum Lyapunov function is the projection of the vector Lyapunov function in some direction.

2.3.4 Application of Criterions to Naval Electric Power Systems

To use the specific composite stability methods discussed above, two items are necessary. First, the subsystems' unforced responses must be asymptotically stable. Second, the quantitative nature of the interconnections must be known.--In other words, such an analysis is correct only for the given configuration. The analysis changes if the roster of participating subsystems and/or their interconnections change.

As discussed in section 2.1.1.1, the number of possible configurations of a naval electric power system is vast. How generalisable is an analysis based upon any given structure? Further, section 2.1.3 identifies an eventual need for a stability measure type of input to the control structure of advanced naval electric power systems. If one has an eye on producing an adaptable, sophisticated control architecture which is meant to ensure stable fulfillment of the naval electric power system's function, then the means of monitoring stability must be able to "see beyond" frequently changing configurations. This would seem to disqualify the two composite system stability methods described in this section because of their dependence on knowing a composite system's interconnection structure.

Another serious drawback to using the two composite system stability methods discussed in this section is their "over sufficiency". This "over sufficiency", if adopted, would lead to system designs which would be extremely over conservative. "Over conservativeness" in a naval electric power system design would be crippling.--It would be extremely difficult to minimise weight and volume if too-demanding stability criterions dictated greater system performance than is really necessary.

The composite system stability methods described in this section do have some important merits. Namely, they are not tied to a specific electric power system model which is inappropriate for describing shipboard systems. They are general enough to treat "large-signal" perturbations to a nonlinear system. They do reduce the order of the space in which the system's Lyapunov function exists.

2.3.5 References

2.3.1. Bailey, F.N. "The Application of Lyapunov's Second Method to Interconnected Systems." SIAM Journal of Control. Ser. A. Vol. 3. No. 3. 1965. pp. 443-462.

2.3.2. Michel, A.N. and D.W. Porter. "Stability Analysis of Composite Systems." IEEE Transactions on Automatic Control. Vol. 17. April 1972. pp. 222-226.

2.3.3 Piontkovskii, A.A. and L.D. Rutkovskaya. "Investigation of Certain Stability-Theory Problems by the Vector Lyapunov Function Method." Automation and Remote Control. Vol. 10. 1967. pp. 1422-1429.

2.3.4 Bellman, R. "Vector Lyapunov Functions." SIAM Journal of Control. Ser. A. Vol. 1. No. 1. 1962. pp. 32-34.

2.3.5 Vidyasagar, M. Nonlinear Systems Analysis. Englewood Cliffs, NJ: Prentice-Hall, Inc. 1978.

2.3.6 Araposthatis, A., S. Sastry, and P. Varaiya. "Global Analysis of Swing Dynamics." IEEE Transactions on Circuits and Systems. Vol. CAS-29. No. 10. October 1982.

2.3.7 Kwatny, Harry G., Leon Y. Bahar, Arun K. Pasrija. "Energy-Like Lyapunov Functions for Power System Stability Analysis." IEEE Transactions on Circuits and Systems. Vol. CAS-32. No. 11. November 1985.

2.3.8 Kwatny, Harry G., Leon Y. Bahar, Arun K. Pasrija. "Static Bifurcations in Electric Power Networks: Loss of Steady-State Stability and Voltage Collapse." IEEE Transactions on Circuits and Systems. Vol. CAS-33. No. 10. October 1986.

2.3.9 Narasimhamurthi, Natarajan, Mohamed T. Musavi. "A Generalized Energy Function for Transient Stability Analysis of Power Systems." IEEE Transactions on Circuits and Systems. Vol. CAS-31. No. 7. July 1984.

2.3.10 Siljak, D.D. "Stability of Large-Scale Systems Under Structural Perturbations." IEEE Transactions on Systems, Man, and Cybernetics. Vol. SMC-2. No. 5. November 1972. pp. 657-663.

2.3.11 Tavora, Carlos J., Otto J.M. Smith. "Stability Analysis of Power Systems." IEEE Power Engineering Society 1971 Summer Meeting. Portland, Oregon. July 18-23, 1971. 71 TP 591-PWR.

2.3.12 Tsolas, Nikos A., Aristotle Arapostathis, and Pravin P. Varaiya. "A Structure Preserving Energy Function for Power System Transient Stability Analysis." IEEE Transactions on Circuits and Systems. Vol. CAS-32. No. 10. October 1985.

2.3.13 Willems, Jacques L. "Direct Methods for Transient Stability Studies in Power System Analysis." IEEE Transactions on Automatic Control. Vol. AC-16. No. 4. August 1971.

2.4 Naval Electric Power System Stability Analysis Requirements

This section endeavours to concisely state the need for a composite system stability criterion for the reasons arising from the conclusions in the previous three sections of this chapter.

2.4.1 Stability Analysis Issues

As discussed in section 2.1.2, the dynamic occurrences of interest for the naval electric power system engineer consist of "large-signal" perturbations. Upon review of the discussion in section 2.2, and given the nonlinear nature of naval electric power systems, the presence of "large-signal" perturbations demands "large-signal" stability analysis, section 2.2.4, and not "small-signal" stability analysis, section 2.2.3, or steady-state analysis, section 2.2.2.

Given the imperative nature of fulfilling its function in the presence of large perturbations, deliberate or precipitate, a general nonlinear transient stability design criterion is necessary. Furthermore, some measure of "large-signal" stability soon will be a necessary input if stabilising control schemes are required to ensure fulfillment of a naval electric power system's function.

Beyond stating that "large-signal" stability should be of the greatest interest to naval electric power system engineers, some qualification of the specific form of stability is warranted. It is true that all naval electric power systems have a common equilibrium which is globally asymptotically stable.--Just fuel up a warship; energise all electric equipment; and, let the warship steam in circles indefinitely. It will reach a specific globally asymptotically stable equilibrium, albeit an uninteresting one. It is probably overly-strenuous to attempt to show that operating naval electric power systems have globally asymptotically stable equilibriums. Locally asymptotically stable or even simply stable equilibriums are more likely to be identifiable. Hence, a stability analysis which attempts to prove local asymptotic stability or simple stability is more likely to produce useful results.

The foregoing indicates that the composite system stability methods, as formulated in section 2.3.2, are not appropriate for naval electric power system stability analysis because they try to prove a very strict form of stability that is not likely to exist for shipboard systems.

2.4.2 Modelling Issues

Section 2.1.1 describes naval electric power systems. The conclusion drawn from that discussion is that the models used for commercial electric power systems are not appropriate. Hence, any stability analysis which is based upon the usual commercial electric power system models would not be suitable for analysing naval electric power system stability. Hence, the methods discussed in section 2.2.4 are not appropriate for analysing such systems.

The heavy reliance of the composite stability methods, as formulated in section 2.3.2, on knowing the interconnecting structure of the power system being analysed poses problems. Naval electric power systems change configuration frequently and to significant degrees. A view of the stability of a **process**, not a **structure**, is necessary.

Despite the fact that the composite system stability methods described in section 2.3.2 are too strenuous for naval electric power systems and rely too much on knowing structure, they do permit the analysis of tightly coupled, nonlinear systems like those found on ships. They do not require the system to be describable by any particular electric power system model. Furthermore, they offer the ability to reduce the order of the analysis as well as cater to the composite nature of shipboard systems. This feature would enable incorporation of a stability measure into a future adaptive control architecture for advanced naval electric power systems.

2.4.3 Advanced Stability Criterion Requirements

After surveying the characteristics of naval electric power systems, their stability analysis requirements, conventional electric power system stability analyses, and composite system stability analyses, it is obvious that a method for analysing naval electric power systems must be developed. The method developed in this research adapts the composite system stability framework to the exigencies of naval electric power systems. Namely, only simple stability is assessed. This eliminates the reliance on knowing structure as well as reducing sources of "over sufficiency". Composite system methods lend themselves to available computational tools as well. They are easily incorporated into control architectures too. Hence, the composite system stability criterion developed here treats general, nonlinear, "large-signal" stability in a quantitative manner.

3 Development of a Composite System Stability Assessment

The first section of this chapter describes the development of a Lyapunov function. This Lyapunov function will serve as a component Lyapunov function within a composite system framework. The function is later implemented as a "stability organ" within the WAVESIM simulation environment. Although generalisable, the Lyapunov function developed here is for a synchronous generator.

The second section of this chapter shows the derivation of a composite system stability criterion. It is based upon the notions of vector Lyapunov functions and weighted-sum Lyapunov functions. This criterion forms the basis for an overall composite system stability monitor. The criterion is later implemented as the "stability demon" within the WAVESIM simulation environment.

3.1 Coenergy-Based Lyapunov Function

The goal of this section is to state the model of the synchronous generator which is used in this work and to describe the method for arriving at the coenergy function used as a Lyapunov function. This section also establishes nomenclature.

3.1.1 Lyapunov Function Selection Issues

When pondering the use of Lyapunov's direct method, either with a monolithic Lyapunov function or a composite Lyapunov function, some consideration of the function is necessary. Selection of a function is all important. Lyapunov's theorems provide a means to assess stability using a Lyapunov function; however, no general method is available for finding a Lyapunov function, reference [3.1.1] section 5.2.4. It is worthwhile, though, to consider what the requirements are for a candidate Lyapunov function. Lyapunov's basic stability theorem is given below, reference [3.1.1] section 5.2.1.

Theorem The equilibrium point $\underline{0}$ at time t_0 of the system described by equation (3.1.1) is stable if there exists a continuously differentiable, locally positive-definite function $V(t,\underline{x})$ such that $\dot{V}(t,\underline{x},\underline{u}) \le 0$ for all $t \ge t_0$ and for all $\underline{x} \in B_r$ for some ball B_r.

$$\dot{\underline{x}}(t) = \underline{f}(t,\underline{x}(t)) \qquad t \ge 0 \tag{3.1.1}$$

From the foregoing theorem, only three requirements exist for the candidate Lyapunov function, V . 1) It must be continuously differentiable. (Some have said that this is overly rigorous and that it need only meet the Lipschitz condition.) 2) It must be locally positive definite (about the equilibrium). 3) As implicitly indicated, V must be a function of the state vector $\underline{x}$. Any function which meets these criterions for a system that is described by equation (3.1.1) is a valid candidate Lyapunov function. It is assumed that a solution to equation (3.1.1) exists and is unique.

Rigorously speaking, a 'candidate Lyapunov function' is not called a 'Lyapunov function' unless it meets the criterion placed on its convective derivative. The interpretation given to the ball, B_r, is that B_r is the region about the equilibrium in which the system behaves in a stable fashion. Hence, the locus of points in state space for which $\dot{V}(t,\underline{x},\underline{u}) \le 0$ forms a region of stability about an equilibrium.

Assuming that more than one Lyapunov function exists for a given system, the question arises as to which function is "best". Consider a simple example. Equation (3.1.2) describes the behaviour of the example RLC circuit, figure 3.1.1.

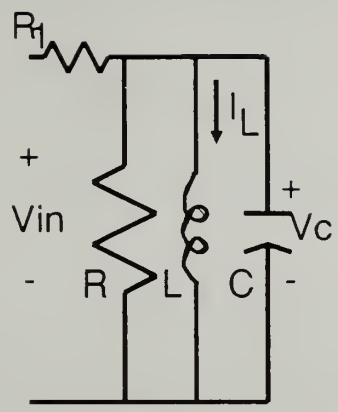

Figure 3.1.1 - Example RLC Circuit

$$\begin{bmatrix} \dot{v}_c \\ \dot{i}_1 \end{bmatrix} = \begin{bmatrix} -\left(\frac{1}{R_1 C} + \frac{1}{RC}\right) & -\frac{1}{C} \\ \frac{1}{L} & 0 \end{bmatrix} \cdot \begin{bmatrix} v_c \\ i_1 \end{bmatrix} + \begin{bmatrix} \left(\frac{1}{R_1 C}\right) \\ 0 \end{bmatrix} \cdot v_{in} \qquad (3.1.2)$$

This is a linear circuit which can be cast into canonical linear form.

$$\underline{x} = \begin{bmatrix} v_c \\ i_1 \end{bmatrix}$$

$$\underline{\mathbf{A}} = \begin{bmatrix} -\left(\frac{1}{R_1 C} + \frac{1}{RC}\right) & -\frac{1}{C} \\ \frac{1}{L} & 0 \end{bmatrix}$$

$$\underline{\mathbf{B}} = \begin{bmatrix} \left(\frac{1}{R_1 C}\right) \\ 0 \end{bmatrix}$$

$$\underline{u} = v_{in}$$

$$\therefore \quad \dot{\underline{x}} = \underline{\mathbf{A}}\underline{x} + \underline{\mathbf{B}}\underline{u} \qquad (3.1.3)$$

This circuit is stable in the sense of linear analysis because, for all positive values of R_1 and R, the real parts of the two eigenvalues of $\underline{\mathbf{A}}$ are negative. (For now, ignore negative resistances, inductances and capacitances.)

Define a first candidate Lyapunov function for the example circuit based upon the energies stored in the inductor and the capacitor.

$$V_1(\underline{x}) = \frac{1}{2} C v_c^2 + \frac{1}{2} L i_1^2 \qquad (3.1.4)$$

In the two-dimensional state space defined by the state variables of the example system, this first candidate Lyapunov function is globally positive definite. To gain a stability assessment, evaluation of the convective derivative of the first candidate Lyapunov function is necessary.

$$\dot{V}_1 = \frac{\partial V_1(\underline{x})}{\partial t} + \overline{\nabla}_{\underline{x}} V_1(\underline{x}) \cdot \underline{f}$$

$$= [C v_c \quad L i_l] \cdot [\underline{A}\underline{x} + \underline{B}u]$$

$$= -\left(\frac{1}{R_1} + \frac{1}{R}\right) v_c^2 + \frac{1}{R_1} v_c v_{in} \tag{3.1.5}$$

For the example circuit to be stable in the sense of Lyapunov, the convective derivative of the first candidate Lyapunov function must be less than or equal to zero.

$$\dot{V}_1 \leq 0$$

$$\text{or} \quad -\left(\frac{1}{R_1} + \frac{1}{R}\right) v_c^2 + \frac{1}{R_1} v_c v_{in} \leq 0 \tag{3.1.6}$$

The last expression, (3.1.6), seems to indicate that the negative-semi-definiteness of $\dot{V}_1$ cannot be concluded. Hence, stability over all of the state space cannot be concluded. This problem arises from the effect that the input voltage has on $\dot{V}_1$. Some values of the input voltage make $\dot{V}_1$ positive, indicating that the stored energy in the system is increasing. If an input voltage dimension is added to the state space, then the region where the negative-semi-definiteness of $\dot{V}_1$ is destroyed is described by (3.1.7).

$$|v_{in}| \geq \left(1 + \frac{R_1}{R}\right) |v_c| \tag{3.1.7}$$

Consider now a second candidate Lyapunov function based upon the total energy put into the parallel elements of the example circuit.

$$V_2(\underline{x}) = \int_0^t \frac{v_c^2}{R} dt + \frac{1}{2} L i_l^2 + \frac{1}{2} C v_c^2 \tag{3.1.8}$$

This function meets the three requirements for the candidate Lyapunov function.

$$V_2(\underline{x}) = \frac{L}{R} \int_0^t v_c \dot{i}_l dt + \frac{1}{2} L i_l^2 + \frac{1}{2} C v_c^2$$

$$= \frac{L}{R} \int_0^{i_l} v_c d\tilde{i}_l + \frac{1}{2} L i_l^2 + \frac{1}{2} C v_c^2$$

$$= \frac{L}{R} v_c i_l + \frac{1}{2} L i_l^2 + \frac{1}{2} C v_c^2 \tag{3.1.9}$$

Now, the convective derivative of the second candidate Lyapunov function is evaluated.

$$\dot{V}_2 = \frac{\partial V_2(\underline{x})}{\partial t} + \overline{\overline{\nabla}}_{\underline{x}} V_2(\underline{x}) \cdot \underline{f}$$

$$= \left[\frac{L}{R} i_1 + C v_c \quad \frac{L}{R} v_c + L i_1 \right] \cdot [\underline{\mathbf{A}x} + \underline{\mathbf{B}u}]$$

$$= \frac{L}{RR_1C} \left\{ -\left[R_1 i_1^2 + \left(1 + \frac{R_1}{R} \right) i_1 v_c + \frac{RC}{L} v_c^2 \right] + \left[i_1 + \frac{RC}{L} v_c^2 \right] v_{in} \right\}$$

(3.1.10)

The region of state space where the convective derivative of the second Lyapunov function is negative semi-definite is less easily seen than that of the first Lyapunov function. Consider only the unforced response of the system, $v_{in} = 0$. In this case, the region of stability indicated by the first Lyapunov function is the entire state space of the example system, which agrees with linear theory. The region of stability indicated by the second Lyapunov function is not the same. Figure 3.1.2 shows the region of stability admitted by the second Lyapunov function.

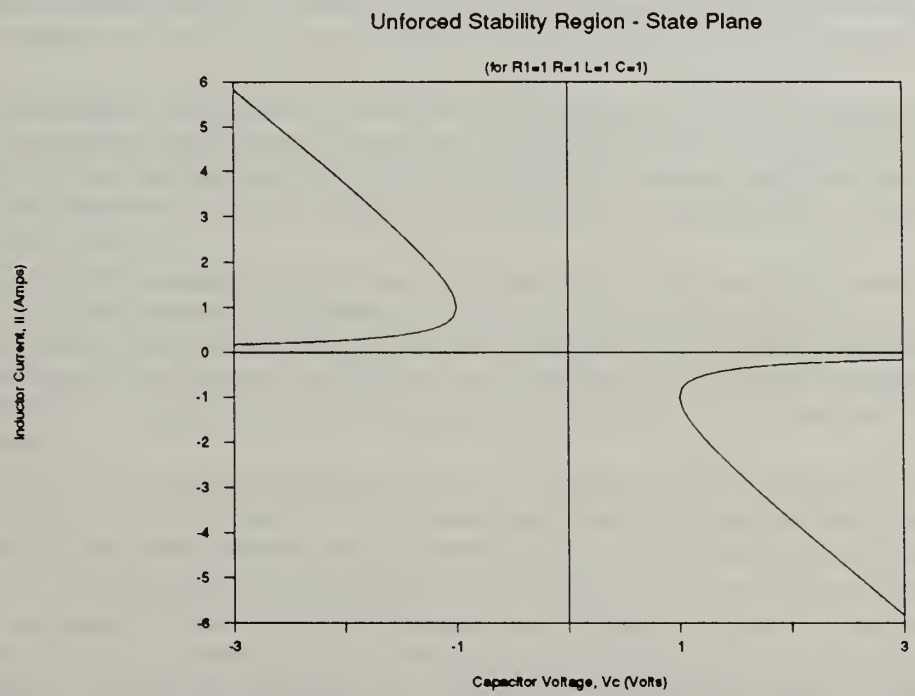

Figure 3.1.2 - RLC Example Second Lyapunov Function Region of Stability

The second Lyapunov function's unforced region of stability consists of the first and third quadrants plus the areas not enclosed by the curves. While the precise area of this unforced region of stability depends upon the circuit parameters, it is less than the unforced region of stability of the first Lyapunov function, which encompasses all of the state space.

In this example, the first Lyapunov function better conveys the stability characteristics of the system. Its unforced region of stability is precisely that which is described using linear theory. The second Lyapunov function does provide a region of stability, which is, in fact, a true region of stability; however, the second Lyapunov function's unforced region of stability is less extensive. The second Lyapunov function is therefore said to be "overly sufficient" or "over-conservative".

The goal, when selecting a candidate Lyapunov function to act as a "device object's" "stability organ", is to chose from the possible candidate Lyapunov functions the one which is least "overly sufficient".

3.1.2 Coenergy in a 3-Phase Synchronous Machine

The issue of using Lyapunov functions in the determination of power system "large-signal" stability is one of chosing the "best" function, which does not appear to have been done yet. A Lyapunov function for a synchronous generator which has strong physical interpretations and gets at the very basis of electromechanical energy conversion is seemingly more likely to be least conservative.

Lumped parameter models are used in the modelling of power system components. The most interesting components for contemporary naval electric power systems engineers, synchronous machines and other electric machines, involve electromechanical energy conversion. The usual method for deriving the torques of electromagnetic origin is to use an application of the conservation of energy or coenergy.

The machine in question is modelled as containing a lossless "coupling field", where the mechanical/electrical interaction takes place. To this "coupling field" is connected electrical and mechanical terminals. Loss mechanisms, and external energy inputs are connected to these terminals. The internal "coupling field", though, is taken to be conservative.

The energy contained within the "coupling field" is stationary in steady-state conditions. In other words, the mechanical power injected into the field is extracted as electric power or vice versa. Energy which is dissipated, as in resistances, or turned into mechanical work is not available to the "coupling field". Stored energies which are not within the "coupling field" do not directly participate in electromechanical energy conversion.

In dynamic situations, stored energies can increase or be expended. Rather than accounting for all of the energy which enters and leaves the machine, emphasis should be placed on the instantaneous energy stored in the machine and its rate of change.

Two principal forms of instability in an electric power system, composed of generators and loads, are loss of synchronisation and voltage collapse. In the former, the generator fails in its essential quality because its frequency does not match the rest of the system's. Hence, mechanical power cannot be converted to electric power. In the latter, the generator fails in its essential quality because its terminal voltage characteristic and that of the rest of the system do not permit electric power to reach the loads. Once again, mechanical power cannot be converted to electric power.

As a brief example of this notion, consider a critical clearing time problem. When generator terminals are opened, none of the electric energy can be extracted through the "coupling field". The mechanical power input which is not dissipated in damping is stored in the rotor's inertia. Armature reaction no longer affects the field flux because the stator currents are zero. Hence, as damper currents die out, the energy stored in the "coupling field" increases.

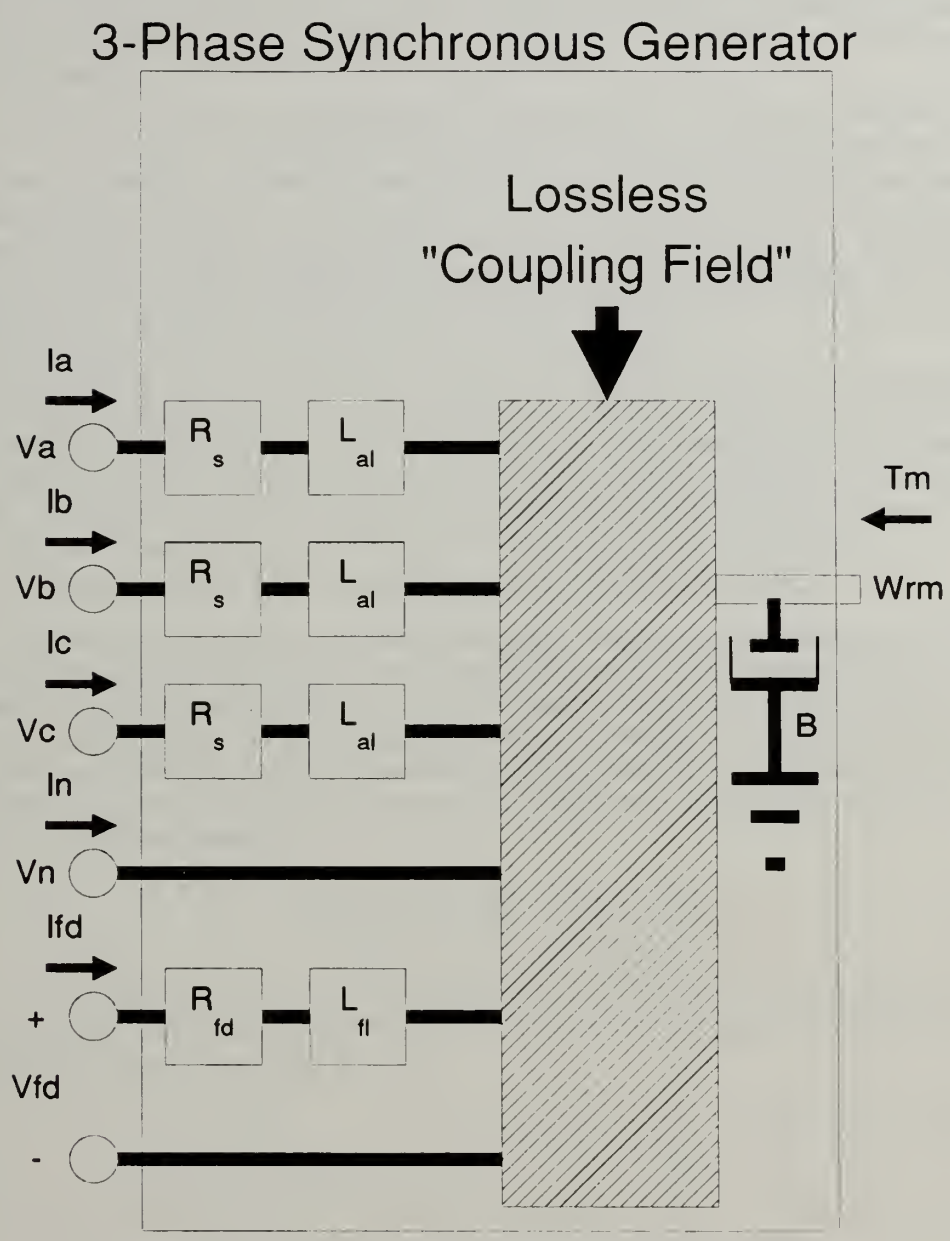

Figure 3.1.3 - Synchronous Generator "Coupling Field"

The issue, when the generator is reconnected, can the excess stored energy be extracted and energy conversion be resumed? To extract the energy as electric power requires the fundamental frequency requirement for energy conversion be met. In other words, the rotor speed cannot be substantially different from synchronous speed. If it is different, then energy cannot be extracted.

The very fundamentals of lumped parameter modelling of electric machines provide the description of the electromechanical energy conversion process and the notion of a "coupling field". Reference [3.1.2], Chapter 3, provides this canonical derivation.--It is not treated in detail here. Rather, the diagram showing the core of the "coupling field" of a generator, figure 3.1.3, provides much of the gist of reference [3.1.2], Chapter 3.

The measure of the conservativeness of the candidate Lyapunov functions which is used in this research is 'critical clearing time'. The critical clearing time for an example system sustaining a casualty is determined precisely through indirect methods, that is, simulations (note-plural). The standard "energy function" method, which represents the basic transient stability analysis for power systems representable by the "swing" equation model, is another method for determining critical clearing time. The critical clearing time derived from this method is usually over-conservative because of the simplifications allowing the use of the "swing" equation model.

The coenergy-based candidate Lyapunov function constitutes the third method used to derive a critical clearing time. The critical clearing times provided by these three different methods are compared. Taking the critical clearing time provided by the simulations to be the most accurate, the conservativeness of the other two methods is gauged. This provides the justification for a declaration of the (relative) conservativeness of the candidate Lyapunov function which is based upon coenergy.

3.1.2.1 3-Phase Synchronous Machine Model in Terminal Variables

To determine the forces of electromagnetic origin and total energy of a 3-phase synchronous machine using the classic energy approach, the magnetic flux within the air-gap of the machine is described as a function of the phase currents and the rotor angle. A magnetically linear machine is assumed outright.--Thus, energy and coenergy are equal. Further, only the fundamental space and time components of the Fourier series expansion of the air-gap fluxes are considered. Symmetric, wye connected stator windings are assumed.

$$\underline{\lambda} = \begin{bmatrix} \underline{\lambda}_{ph} \\ \underline{\lambda}_{R} \end{bmatrix} = \begin{bmatrix} \underline{\mathbf{L}}_{ph} & \underline{\mathbf{M}} \\ \underline{\mathbf{M}}^{T} & \underline{\mathbf{L}}_{R} \end{bmatrix} \begin{bmatrix} \underline{I}_{ph} \\ \underline{I}_{R} \end{bmatrix} \tag{3.1.11}$$

The dependence of the stator inductances on the rotor's position uses the electrical rotor angle, θ_{re}. The stator winding inductances for a general, salient pole, 3-phase machine are given in equation (3.1.12).

$$\underline{\mathbf{L}}_{ph} = \begin{bmatrix} L_{al} + L_{ao} + L_{a2}\cos 2\theta_{re} & -\frac{1}{2}L_{ao} + L_{a2}\cos 2\left(\theta_{re} - \frac{\pi}{3}\right) & -\frac{1}{2}L_{ao} + L_{a2}\cos 2\left(\theta_{re} + \frac{\pi}{3}\right) \\ -\frac{1}{2}L_{ao} + L_{a2}\cos 2\left(\theta_{re} - \frac{\pi}{3}\right) & L_{al} + L_{ao} + L_{a2}\cos 2\left(\theta_{re} - \frac{2\pi}{3}\right) & -\frac{1}{2}L_{ao} + L_{a2}\cos 2(\theta_{re} + \pi) \\ -\frac{1}{2}L_{ao} + L_{a2}\cos 2\left(\theta_{re} + \frac{\pi}{3}\right) & -\frac{1}{2}L_{ao} + L_{a2}\cos 2(\theta_{re} + \pi) & L_{al} + L_{ao} + L_{a2}\cos 2\left(\theta_{re} + \frac{2\pi}{3}\right) \end{bmatrix} \tag{3.1.12}$$

The three inductances that appear in the inductance matrix are L_{al}, L_{ao}, and L_{a2}. L_{al} represents the leakage inductance of a stator phase winding. Whereas the windings are symmetrical, the leakage inductance of each of the phase windings can be said to be equal to that of a-phase, hence the subscript a. L_{ao} is the component of inductance due the stator winding itself and a constant air-gap. L_{a2} is the magnitude of the component of inductance which varies with the rotor position.

The three circuits which represent the rotor are the field winding and two equivalent windings-in-quadrature. The damper windings on the rotor are described by assuming that the actual damper windings consist of two parts. The first is an equivalent winding which is in alignment with the field winding. The second is an equivalent winding which is in quadrature with the field winding.

$$\underline{L}_R = \begin{bmatrix} L_{fl} + L_f & L_{fkd} & 0 \\ L_{fkd} & L_{kdl} + L_{kd} & 0 \\ 0 & 0 & L_{kql} + L_{kq} \end{bmatrix} \tag{3.1.13}$$

Whereas the field winding and the equivalent direct-axis winding of the damper winding are aligned, their fluxes are coupled. The equivalent quadrature-axis winding of the damper is perpendicular to the other windings. Furthermore, the rotor does not experience any time-varying inductances due to saliency in the stator. (It is assumed the stator has no saliency.)

To determine the stator to rotor mutual inductances, the first requirement is to establish a reference for angular displacements. In keeping with reference [3.1.3]'s use of reference directions, the angle θ_{re} represents the angular displacement of the field winding's magnetic axis from the a-phase magnetic axis. The mutual inductances are given in equation (3.1.14). The magnitudes of the mutual inductances, M, L_{akd}, and L_{akq}, are constant.

$$\underline{M} = \begin{bmatrix} M\cos\theta_{re} & L_{akd}\cos\theta_{re} & -L_{akq}\sin\theta_{re} \\ M\cos\left(\theta_{re} - \frac{2\pi}{3}\right) & L_{akd}\cos\left(\theta_{re} - \frac{2\pi}{3}\right) & -L_{akq}\sin\left(\theta_{re} - \frac{2\pi}{3}\right) \\ M\cos\left(\theta_{re} + \frac{2\pi}{3}\right) & L_{akd}\cos\left(\theta_{re} + \frac{2\pi}{3}\right) & -L_{akq}\sin\left(\theta_{re} + \frac{2\pi}{3}\right) \end{bmatrix} \tag{3.1.14}$$

Equation (3.1.11) has now been fully described and is subsequently used to determine the energy in a 3-phase synchronous machine. The stator winding voltage equations contain the resistances of the stator windings and the time-varying flux linkages.

$$\underline{V}_{ph} = \underline{R}_s \cdot \underline{I}_{ph} + \frac{d}{dt}\{\underline{\lambda}_{ph}\}$$

$$= \underline{R}_s \cdot \underline{I}_{ph} + \frac{d}{dt}\{\underline{L}_{ph} \cdot \underline{I}_{ph} + \underline{M} \cdot \underline{I}_R\}$$

$$= \underline{R}_s \cdot \underline{I}_{ph} + \frac{d}{dt}\{\underline{L}_{ph}\} \cdot \underline{I}_{ph} + \underline{L}_{ph} \cdot \frac{d}{dt}\{\underline{I}_{ph}\} + \frac{d}{dt}\{\underline{M}\} \cdot \underline{I}_R + \underline{M} \cdot \frac{d}{dt}\{\underline{I}_R\} \tag{3.1.15}$$

Two items of note appear in equation (3.1.15). First, the structure of the stator resistance matrix is diagonal. The stator resistance per phase is R_s. Secondly, the $\underline{L}_{ph}$ and $\underline{M}$ matrices depend upon the rotor's angular displacement. The rotor's displacement varies with time. Hence, the two matrices have time derivatives that must be considered. Constant rotor speed cannot be assumed. The phase currents are time variant; therefore, they too have time derivatives. The rotor currents, although the field current is "dc", can have time varying values during transients.

The rotor circuits' voltage equations are similar in derivation.

$$\underline{V}_R = \underline{\mathbf{R}}_r \cdot \underline{I}_R + \frac{d}{dt}\{\underline{\lambda}_R\}$$

$$= \underline{\mathbf{R}}_r \cdot \underline{I}_R + \frac{d}{dt}\{\underline{\mathbf{M}}^T \cdot \underline{I}_{ph} + \underline{\mathbf{L}}_R \cdot \underline{I}_R\}$$

$$= \underline{\mathbf{R}}_r \cdot \underline{I}_R + \frac{d}{dt}\{\underline{\mathbf{M}}^T\} \cdot \underline{I}_{ph} + \underline{\mathbf{M}}^T \cdot \frac{d}{dt}\{\underline{I}_{ph}\} + \underline{\mathbf{L}}_R \cdot \frac{d}{dt}\{\underline{I}_R\} \tag{3.1.16}$$

$$\underline{\mathbf{R}}_R = \begin{bmatrix} R_f & 0 & 0 \\ 0 & R_{kd} & 0 \\ 0 & 0 & R_{kq} \end{bmatrix} \tag{3.1.17}$$

Taken together, in terminal variables, the voltage equations of the 3-phase synchronous machine follow.

$$\begin{bmatrix} \underline{V}_{ph} \\ \underline{V}_R \end{bmatrix} = \begin{bmatrix} \underline{\mathbf{R}}_s & \underline{0} \\ \underline{0} & \underline{\mathbf{R}}_r \end{bmatrix} \cdot \begin{bmatrix} \underline{I}_{ph} \\ \underline{I}_R \end{bmatrix} + \frac{d}{dt}\left\{\begin{bmatrix} \underline{\mathbf{L}}_{ph} & \underline{\mathbf{M}} \\ \underline{\mathbf{M}}^T & \underline{\mathbf{L}}_R \end{bmatrix}\right\} \cdot \begin{bmatrix} \underline{I}_{ph} \\ \underline{I}_R \end{bmatrix} + \begin{bmatrix} \underline{\mathbf{L}}_{ph} & \underline{\mathbf{M}} \\ \underline{\mathbf{M}}^T & \underline{\mathbf{L}}_R \end{bmatrix} \cdot \frac{d}{dt}\left\{\begin{bmatrix} \underline{I}_{ph} \\ \underline{I}_R \end{bmatrix}\right\} \tag{3.1.18}$$

To complete the model of a 3-phase synchronous machine in terminal variables, the mechanical dynamics of the rotor must be included. The derivation of the torque of electromagnetic origin is discussed later.

$$\frac{d}{dt}\left\{\begin{bmatrix} \underline{i}_{ph} \\ \underline{i}_R \end{bmatrix}\right\} = \begin{bmatrix} \underline{\mathbf{L}}_{ph} & \underline{\mathbf{M}} \\ \underline{\mathbf{M}}^T & \underline{\mathbf{L}}_R \end{bmatrix}^{-1} \left(\begin{bmatrix} \underline{v}_{ph} \\ \underline{v}_R \end{bmatrix} - \begin{bmatrix} \underline{\mathbf{r}}_s & \underline{0} \\ \underline{0} & \underline{\mathbf{r}}_r \end{bmatrix} \begin{bmatrix} \underline{i}_{ph} \\ \underline{i}_R \end{bmatrix} - \frac{d}{dt}\left\{\begin{bmatrix} \underline{\mathbf{L}}_{ph} & \underline{\mathbf{M}} \\ \underline{\mathbf{M}}^T & \underline{\mathbf{L}}_R \end{bmatrix}\right\} \begin{bmatrix} \underline{i}_{ph} \\ \underline{i}_R \end{bmatrix} \right)$$

$$\frac{d}{dt}\{\theta_{rm}\} = \omega_{rm}$$

$$\frac{d}{dt}\{\omega_{rm}\} = \frac{1}{J}\{T_M + T_E - B\,\omega_{rm}\} \tag{3.1.19}$$

3.1.2.2 3-Phase Synchronous Machine Model in "d-q" Variables

Through the use of Park's transformation, the rotating magnetic field which is generated by the currents in the stator windings is viewed from a reference point on the rotor. Without offering a discussion of Park's transformation, the transformation equations for a 3-phase synchronous machine are given by equations (3.1.20) and (3.1.21). It is vital to this treatment of coenergy that the unitary version of Park's transformation be used.

$$\underline{\mathbf{T}}^T = \underline{\mathbf{T}}^{-1} \tag{3.1.20}$$

$$\therefore \quad \underline{\mathbf{T}} = \sqrt{\frac{2}{3}} \begin{bmatrix} \cos\theta_{re} & \cos\left(\theta_{re} - \frac{2\pi}{3}\right) & \cos\left(\theta_{re} + \frac{2\pi}{3}\right) \\ -\sin\theta_{re} & -\sin\left(\theta_{re} - \frac{2\pi}{3}\right) & -\sin\left(\theta_{re} + \frac{2\pi}{3}\right) \\ \frac{1}{\sqrt{2}} & \frac{1}{\sqrt{2}} & \frac{1}{\sqrt{2}} \end{bmatrix} \qquad (3.1.21)$$

All of the machine's fluxes are described in equation (3.1.11), which is now transformed into d-q quantities and rotor variables.

$$\underline{\lambda}_T = \begin{bmatrix} \underline{\lambda}_{dq} \\ \underline{\lambda}_R \end{bmatrix} = \begin{bmatrix} \underline{\mathbf{T}} \cdot \underline{\mathbf{L}}_{ph} \cdot \underline{\mathbf{T}}^{-1} & \underline{\mathbf{T}} \cdot \underline{\mathbf{M}} \\ \underline{\mathbf{M}}^T \cdot \underline{\mathbf{T}}^{-1} & \underline{\mathbf{L}}_R \end{bmatrix} \cdot \begin{bmatrix} \underline{I}_{dq} \\ \underline{I}_R \end{bmatrix} \qquad (3.1.22)$$

$$\underline{\lambda}_T = \begin{bmatrix} \underline{\lambda}_{dq} \\ \underline{\lambda}_R \end{bmatrix} = \begin{bmatrix} \frac{3}{2}(L_{ao} + L_{a2}) + L_{al} & 0 & 0 & \sqrt{\frac{3}{2}}\, M & \sqrt{\frac{3}{2}}\, L_{akd} & 0 \\ 0 & \frac{3}{2}(L_{ao} - L_{a2}) + L_{al} & 0 & 0 & 0 & \sqrt{\frac{3}{2}}\, L_{akq} \\ 0 & 0 & L_{al} & 0 & 0 & 0 \\ \sqrt{\frac{3}{2}}\, M & 0 & 0 & L_{fl} + L_f & L_{fkd} & 0 \\ \sqrt{\frac{3}{2}}\, L_{akd} & 0 & 0 & L_{fkd} & L_{kdl} + L_{kd} & 0 \\ 0 & \sqrt{\frac{3}{2}}\, L_{akq} & 0 & 0 & 0 & L_{kql} + L_{kq} \end{bmatrix} \cdot \begin{bmatrix} \underline{I}_{dq} \\ \underline{I}_R \end{bmatrix}$$

$$= \underline{\mathbf{L}}_{DQ} \begin{bmatrix} \underline{I}_{dq} \\ \underline{I}_R \end{bmatrix} \qquad (3.1.23)$$

The transformed voltage equations follow.

$$\begin{bmatrix} \underline{V}_{dq} \\ \underline{V}_R \end{bmatrix} = \left(\begin{bmatrix} \underline{\mathbf{R}}_s & \underline{0} \\ \underline{0} & \underline{\mathbf{R}}_R \end{bmatrix} \begin{bmatrix} \underline{I}_{dq} \\ \underline{I}_R \end{bmatrix} + \begin{bmatrix} 0 & -\omega_{re} & 0 & 0 & 0 & 0 \\ \omega_{re} & 0 & 0 & 0 & 0 & 0 \\ 0 & 0 & 0 & 0 & 0 & 0 \\ 0 & 0 & 0 & 0 & 0 & 0 \\ 0 & 0 & 0 & 0 & 0 & 0 \\ 0 & 0 & 0 & 0 & 0 & 0 \end{bmatrix} \begin{bmatrix} \underline{\lambda}_{dq} \\ \underline{\lambda}_R \end{bmatrix} \right) + \frac{d}{dt} \left\{ \begin{bmatrix} \underline{\lambda}_{dq} \\ \underline{\lambda}_R \end{bmatrix} \right\}$$

$$= (\underline{\mathbf{R}} + \underline{\mathbf{B}}_V \underline{\mathbf{L}}_{DQ}) \begin{bmatrix} \underline{I}_{dq} \\ \underline{I}_R \end{bmatrix} + \underline{\mathbf{L}}_{DQ} \frac{d}{dt} \left\{ \begin{bmatrix} \underline{I}_{dq} \\ \underline{I}_R \end{bmatrix} \right\}$$

$$= \left(\underline{\mathbf{R}} + \omega_{re} \begin{bmatrix} 0 & -L_Q & 0 & 0 & 0 & -\sqrt{\frac{3}{2}} L_{akq} \\ L_D & 0 & 0 & \sqrt{\frac{3}{2}} M & \sqrt{\frac{3}{2}} L_{akd} & 0 \\ \underline{0}^{4\times 6} & & & & & \end{bmatrix} \right) \begin{bmatrix} \underline{I}_{dq} \\ \underline{I}_R \end{bmatrix} + \underline{\mathbf{L}}_{DQ} \frac{d}{dt} \left\{ \begin{bmatrix} \underline{I}_{dq} \\ \underline{I}_R \end{bmatrix} \right\}$$

$$= (\underline{\mathbf{R}} + \underline{\mathbf{B}}_{VP}) \begin{bmatrix} \underline{I}_{dq} \\ \underline{I}_R \end{bmatrix} + \underline{\mathbf{L}}_{DQ} \frac{d}{dt} \left\{ \begin{bmatrix} \underline{I}_{dq} \\ \underline{I}_R \end{bmatrix} \right\} \qquad (3.1.24)$$

To complete the model of a 3-phase synchronous machine in d-q variables, the mechanical dynamics of the rotor must be included.

$$\frac{d}{dt} \begin{Bmatrix} \underline{I}_{dq} \\ \underline{I}_R \\ \theta_{rm} \\ \omega_{rm} \end{Bmatrix} = \begin{bmatrix} \underline{\mathbf{L}}_{DQ}^{-1} \left(\begin{bmatrix} \underline{V}_{dq} \\ \underline{V}_R \end{bmatrix} - [\underline{\mathbf{R}} + \underline{\mathbf{B}}_{VP}] \begin{bmatrix} \underline{I}_{dq} \\ \underline{I}_R \end{bmatrix} \right) \\ \omega_{rm} \\ \frac{1}{J} \{ T_M + T_E - B \omega_{rm} \} \end{bmatrix} \qquad (3.1.25)$$

3.1.2.3 Derivation of the Coenergy Using Terminal Variables

The derivation of the total energy and electromagnetic torque is performed using the canonical energy approach. In the model adopted, the flux linkages are functions of currents. Hence, coenergy is used in lieu of energy. This derivation is based upon the notion of a conservative "coupling field", figure 3.1.3. The presence of a conservative "coupling field" permits path independent integration of the state variables. The system is mechanically assembled with electrical inputs equal to zero. Then, the electrical variables are allowed to reach their values one at a time.

$$W'_m = -\int_0^{\theta_{rm}} T_E d\tilde{\theta}_{rm} + \sum_{j=1}^{N} \left[\int_0^{I_j} \lambda_j(I_1, \cdots, I_{j-1}, \tilde{I}_j, 0, \cdots, 0; \theta_{rm}) d\tilde{I}_j \right] \qquad (3.1.26)$$

The integration of the electromagnetic torque is eliminated as it will equal zero. Expansion of equation (3.1.26) yields (3.1.27). When equation (3.1.27) is evaluated and after much simplification, the coenergy can be expressed in vector form, equation (3.1.28).

$$W'_m = \int_0^{I_a} (L_{ao} + L_{a2}\cos 2\theta_{re} + L_{al})\bar{I}_a d\bar{I}_a +$$

$$\int_0^{I_b} \left[\left(-\frac{1}{2}L_{ao} + L_{a2}\cos 2\left(\theta_{re} - \frac{\pi}{3}\right)\right) I_a + \left(L_{ao} + L_{a2}\cos 2\left(\theta_{re} - \frac{2\pi}{3}\right) + L_{al}\right)\bar{I}_b \right] d\bar{I}_b +$$

$$\int_0^{I_c} [\left(-\frac{1}{2}L_{ao} + L_{a2}\cos 2\left(\theta_{re} + \frac{\pi}{3}\right)\right) I_a + \left(-\frac{1}{2}L_{ao} + L_{a2}\cos 2(\theta_{re} + \pi)\right) I_b +$$

$$\left(L_{ao} + L_{a2}\cos 2\left(\theta_{re} + \frac{2\pi}{3}\right) + L_{al}\right)\bar{I}_c] d\bar{I}_c +$$

$$\int_0^{I_f} \left[M\cos(\theta_{re}) I_a + M\cos\left(\theta_{re} - \frac{2\pi}{3}\right) I_b + M\cos\left(\theta_{re} + \frac{2\pi}{3}\right) I_c + (L_f + L_{fl})\bar{I}_f \right] d\bar{I}_f +$$

$$\int_0^{I_{kd}} \left[L_{akd}\cos(\theta_{re}) I_a + L_{akd}\cos\left(\theta_{re} - \frac{2\pi}{3}\right) I_b + L_{akd}\cos\left(\theta_{re} + \frac{2\pi}{3}\right) I_c + L_{fkd} I_f + (L_{kd} + L_{kdl})\bar{I}_{kd} \right] d\bar{I}_{kd} +$$

$$\int_0^{I_{kq}} \left[-L_{akq}\sin(\theta_{re}) I_a - L_{akq}\sin\left(\theta_{re} - \frac{2\pi}{3}\right) I_b - L_{akq}\sin\left(\theta_{re} + \frac{2\pi}{3}\right) I_c + (L_{kq} + L_{kql})\bar{I}_{kq} \right] d\bar{I}_{kq} \tag{3.1.27}$$

$$W'_m = \frac{1}{2}[\underline{I}_{ph}^T \quad \underline{I}_R^T] \begin{bmatrix} \underline{\mathbf{L}}_{ph} & \underline{\mathbf{M}} \\ \underline{\mathbf{M}}^T & \underline{\mathbf{L}}_R \end{bmatrix} \begin{bmatrix} \underline{I}_{ph} \\ \underline{I}_R \end{bmatrix} \tag{3.1.28}$$

For purposes of a subsequent comparison, convert the phase currents in equation (3.1.28) into d-q currents.

$$W'_m = \frac{1}{2}[\underline{I}_{dq}^T \quad \underline{I}_R^T] \begin{bmatrix} \underline{\mathbf{T}} & \underline{\mathbf{0}} \\ \underline{\mathbf{0}} & \underline{\mathbf{I}} \end{bmatrix} \begin{bmatrix} \underline{\mathbf{L}}_{ph} & \underline{\mathbf{M}} \\ \underline{\mathbf{M}}^T & \underline{\mathbf{L}}_R \end{bmatrix} \begin{bmatrix} \underline{\mathbf{T}}^{-1} & \underline{\mathbf{0}} \\ \underline{\mathbf{0}} & \underline{\mathbf{I}} \end{bmatrix} \begin{bmatrix} \underline{I}_{dq} \\ \underline{I}_R \end{bmatrix} \tag{3.1.29}$$

Evaluation of the matrix multiplications in equation (3.1.29) yields the expression, (3.1.30), for the coenergy in terms of d-q currents.

$$W'_m = \frac{1}{2}[\underline{I}_{dq}^T \quad \underline{I}_R^T] \underline{\mathbf{L}}_{DQ} \begin{bmatrix} \underline{I}_{dq} \\ \underline{I}_R \end{bmatrix} \tag{3.1.30}$$

The torque of electromagnetic origin is obtained using the standard approach.

$$T_E = \frac{\partial}{\partial \theta_{rm}} \{W'_m\}$$

$$= \frac{\partial}{\partial \theta_{re}} \{W'_m\} \cdot \frac{\partial \theta_{re}}{\partial \theta_{rm}}$$

$$= p_p \frac{\partial}{\partial \theta_{re}} \{W'_m\} \qquad (3.1.31)$$

After evaluation of (3.1.31) in terms of the terminal, or phase, variables, the torque is found to be a function of the phase currents and rotor electrical angle, (3.1.32).

$$\therefore T_E = p_p \{ \underline{I}_{ph}^T \begin{bmatrix} -L_{a2}\sin 2\theta_{re} & -2L_{a2}\sin 2\left(\theta_{re} - \frac{\pi}{3}\right) & -2L_{a2}\sin 2\left(\theta_{re} + \frac{\pi}{3}\right) \\ 0 & -L_{a2}\sin 2\left(\theta_{re} - \frac{2\pi}{3}\right) & -2L_{a2}\sin 2(\theta_{re} + \pi) \\ 0 & 0 & -L_{a2}\sin 2\left(\theta_{re} + \frac{2\pi}{3}\right) \end{bmatrix} \underline{I}_{ph} +$$

$$\underline{I}_{ph}^T \begin{bmatrix} -M\sin(\theta_{re}) & -L_{akd}\sin(\theta_{re}) & -L_{akq}\cos(\theta_{re}) \\ -M\sin\left(\theta_{re} - \frac{2\pi}{3}\right) & -L_{akd}\sin\left(\theta_{re} - \frac{2\pi}{3}\right) & -L_{akq}\cos\left(\theta_{re} - \frac{2\pi}{3}\right) \\ -M\sin\left(\theta_{re} + \frac{2\pi}{3}\right) & -L_{akd}\sin\left(\theta_{re} + \frac{2\pi}{3}\right) & -L_{akq}\cos\left(\theta_{re} + \frac{2\pi}{3}\right) \end{bmatrix} \underline{I}_R \}$$

(3.1.32)

For purposes of a subsequent comparison, the phase currents in equation (3.1.32) can be transformed into d-q currents. After the transformation and simplification, the electromagnetic torque derived from the coenergy found using terminal variables is expressed in terms of d-q variables, (3.1.33).

$$T_E = p_p \left\{ [I_{dq}^T \quad I_R^T] \begin{bmatrix} 0 & -L_Q & 0 & 0 & 0 & -\sqrt{\frac{3}{2}} L_{akq} \\ L_D & 0 & 0 & \sqrt{\frac{3}{2}} M & \sqrt{\frac{3}{2}} L_{akd} & 0 \\ 0 & 0 & 0 & 0 & 0 & 0 \\ 0 & 0 & 0 & 0 & 0 & 0 \\ 0 & 0 & 0 & 0 & 0 & 0 \\ 0 & 0 & 0 & 0 & 0 & 0 \end{bmatrix} \begin{bmatrix} I_{dq} \\ I_R \end{bmatrix} \right\}$$

$$= p_p \left\{ [I_{dq}^T \quad I_R^T] \underline{\mathbf{B}}_{IP} \begin{bmatrix} I_{dq} \\ I_R \end{bmatrix} \right\}$$

(3.1.33)

3.1.2.4 Derivation of the Coenergy Using "d-q" Variables

Under the assertion that $\underline{\lambda}$ in equation (3.1.11) represents the same physical reality, that is, magnetic field, as $\underline{\lambda}_r$ in equation (3.1.23), then $\underline{\lambda}_r$ can be substituted for $\underline{\lambda}$ in equation (3.1.26). Equation (3.1.34) follows.

$$
\begin{aligned}
W'_{mdq} = &\int_0^{I_d}\left[\frac{3}{2}(L_{ao}+L_{a2})+L_{al}\right]\tilde{I}_d d\tilde{I}_d + \\
&\int_0^{I_q}\left[\frac{3}{2}(L_{ao}-L_{a2})+L_{al}\right]\tilde{I}_q d\tilde{I}_q + \\
&\int_0^{I_o} L_{al}\tilde{I}_o d\tilde{I}_o + \\
&\int_0^{I_f}\left[\sqrt{\frac{3}{2}}\,MI_d+(L_f+L_{fl})\tilde{I}_f\right]d\tilde{I}_f + \\
&\int_0^{I_{kd}}\left[\sqrt{\frac{3}{2}}\,L_{akd}I_d+L_{fkd}I_f+(L_{kd}+L_{kdl})\tilde{I}_{kd}\right]d\tilde{I}_{kd} + \\
&\int_0^{I_{kq}}\left[\sqrt{\frac{3}{2}}\,L_{akq}I_q+(L_{kq}+L_{kql})\tilde{I}_{kq}\right]d\tilde{I}_{kq}
\end{aligned}
\tag{3.1.34}
$$

When equation (3.1.34) is evaluated and simplified, the coenergy can be expressed in vector form, (3.1.35).

$$
W'_{mdq} = \frac{1}{2}\left[\underline{I}_{dq}^{T} \quad \underline{I}_{R}^{T}\right]\underline{L}_{DQ}\begin{bmatrix}\underline{I}_{dq}\\ \underline{I}_{R}\end{bmatrix} \tag{3.1.35}
$$

Comparing equation (3.1.35), which describes $\mathbf{W'}_{mdq}$ (the coenergy calculated from the d-q flux), with equation (3.1.30), which describes $\mathbf{W'}_{m}$ (the coenergy calculated from the terminal flux), indicates that these two coenergies are equal. Hence, the assertion that the flux linkages represent the same field is correct.

It is very important to note that these expressions for the coenergy are easily shown to be positive definite in terms of the state variables. Thus, the coenergy fulfills the first two requirements for a candidate Lyapunov function, section 3.1.1.

Under the assertion regarding the derived coenergy function, transforming the currents back into phase currents should yield the coenergy in terms of the terminal variables and the rotor angle. In d-q variables there is no motion because the rotating magnetic field created by the stator currents is resolved into two stationary (relative to

the rotor) fields. With no motion there is no way to derive the torque of electromagnetic origin. Hence, transformation back into terminal variables should re-introduce angular dependence.

$$W'_{mdq} = \underline{I}_{ph}^{T}\underline{\mathbf{T}}^{T}\begin{bmatrix} \frac{1}{2}\left[\frac{3}{2}(L_{ao}+L_{a2})+L_{al}\right] & 0 & 0 \\ 0 & \frac{1}{2}\left[\frac{3}{2}(L_{ao}-L_{a2})+L_{al}\right] & 0 \\ 0 & 0 & \frac{1}{2}L_{al} \end{bmatrix}\underline{\mathbf{T}}\underline{I}_{ph} +$$

$$\underline{I}_{ph}^{T}\underline{\mathbf{T}}^{T}\begin{bmatrix} \sqrt{\frac{3}{2}}M & \sqrt{\frac{3}{2}}L_{akd} & 0 \\ 0 & 0 & \sqrt{\frac{3}{2}}L_{akq} \\ 0 & 0 & 0 \end{bmatrix}\underline{I}_{R} +$$

$$\underline{I}_{R}^{T}\begin{bmatrix} \frac{1}{2}(L_{fl}+L_{f}) & L_{fkd} & 0 \\ 0 & \frac{1}{2}(L_{kdl}+L_{kd}) & 0 \\ 0 & 0 & \frac{1}{2}(L_{kql}+L_{kq}) \end{bmatrix}\underline{I}_{R} \tag{3.1.36}$$

After carrying out the indicated matrix multiplications in equation (3.1.36) and then simplifying, equation (3.1.37) remains.

$$W'_{mdq} = \frac{1}{2}\begin{bmatrix}\underline{I}_{ph}^{T} & \underline{I}_{R}^{T}\end{bmatrix}\begin{bmatrix}\underline{\mathbf{L}}_{ph} & \underline{\mathbf{M}} \\ \underline{\mathbf{M}}^{T} & \underline{\mathbf{L}}_{R}\end{bmatrix}\begin{bmatrix}\underline{I}_{ph} \\ \underline{I}_{R}\end{bmatrix} \tag{3.1.37}$$

Comparing equation (3.1.37), which describes $\mathbf{W'}_{mdq}$ (the coenergy calculated from the d-q flux), with equation (3.1.38), which describes $\mathbf{W'}_{m}$ (the coenergy calculated from the terminal flux), indicates that these two coenergies are equal. Hence, the assertion of the opening paragraph is again confirmed. Furthermore, angular dependence has been introduced into $\mathbf{W'}_{mdq}$; therefore, its partial derivative can be taken thereby deriving the torque of electromagnetic origin.

$$\mathrm{T}_{E} = p_{p}\frac{\partial}{\partial\theta_{re}}\{W'_{mdq}\} \tag{3.1.38}$$

Evaluating (3.1.38) yields precisely the same result that is given in equation (3.1.33). It is also important to note that equation (3.1.38) can be rewritten in terms of flux linkages and current. After doing so, equation (3.1.39) results.

$$T_E = p_p\left\{\frac{3}{2}L_{a2}I_dI_q + \frac{3}{2}L_{a2}I_qI_d + \sqrt{\frac{3}{2}}\ MI_fI_q + \sqrt{\frac{3}{2}}\ L_{akd}I_{kd}I_q - \sqrt{\frac{3}{2}}\ L_{akq}I_{kq}I_d\right\}$$

$$= p_p\{\lambda_dI_q - \lambda_qI_d\} \tag{3.1.39}$$

This is a familiar and encouraging result. (The factor of three-halves which is frequently shown multiplying this expression arises from a version of Park's transformation which is not the unitary version.)

3.1.2.5 The Rate of Change of Coenergy

To evaluate the rate of change of the coenergy in a 3-phase synchronous machine, it is necessary to evaluate its convective derivative.

$$\dot{W}'_m = \frac{\partial W'_m}{\partial t} + \overline{\nabla}W'_m \cdot \underline{f} \tag{3.1.40}$$

The equivalence of W'_{mdq} (the coenergy calculated from the d-q flux) and W'_m (the coenergy calculated from the terminal flux) has been illustrated. Hence, the latter is taken to represent the coenergy of the synchronous machine, regardless of which currents are taken to be the states. The unitary version of Park's transformation permits this interchangeability.

In equation (3.1.40), coenergy is not an explicit function of time. Hence, its partial derivative with respect to time is zero. The gradient of the coenergy is taken with respect to the states used to describe the coenergy.--In this paper, these states are either the phase currents or the d-q currents and the rotor angle and velocity.

$$\overline{\nabla}_{ph} = \left[\begin{array}{cccccccc} \frac{\partial}{\partial I_a} & \frac{\partial}{\partial I_b} & \frac{\partial}{\partial I_c} & \frac{\partial}{\partial I_f} & \frac{\partial}{\partial I_{kd}} & \frac{\partial}{\partial I_{kq}} & \frac{\partial}{\partial \theta_{rm}} & \frac{\partial}{\partial \omega_{rm}} \end{array}\right]$$

$$\overline{\nabla}_{dq} = \left[\begin{array}{cccccccc} \frac{\partial}{\partial I_d} & \frac{\partial}{\partial I_q} & \frac{\partial}{\partial I_o} & \frac{\partial}{\partial I_f} & \frac{\partial}{\partial I_{kd}} & \frac{\partial}{\partial I_{kq}} & \frac{\partial}{\partial \theta_{rm}} & \frac{\partial}{\partial \omega_{rm}} \end{array}\right] \tag{3.1.41}$$

The vector derivative of the states in equation (3.1.40), $\underline{f}$, comes directly from the equations describing the dynamics of the two models of the 3-phase synchronous machine.

$$\underline{f}_{ph} = \frac{d}{dt}\left\{\begin{bmatrix} \underline{I}_{ph} \\ \underline{I}_R \\ \theta_{rm} \\ \omega_{rm} \end{bmatrix}\right\}$$

$$= \begin{bmatrix} \begin{bmatrix} \underline{L}_{ph} & \underline{M} \\ \underline{M}^T & \underline{L}_R \end{bmatrix}^{-1}\left(\begin{bmatrix} \underline{V}_{ph} \\ \underline{V}_R \end{bmatrix} - \begin{bmatrix} \underline{R}_s & \underline{0} \\ \underline{0} & \underline{R}_r \end{bmatrix}\begin{bmatrix} \underline{I}_{ph} \\ \underline{I}_R \end{bmatrix} - \frac{d}{dt}\left\{\begin{bmatrix} \underline{L}_{ph} & \underline{M} \\ \underline{M}^T & \underline{L}_R \end{bmatrix}\begin{bmatrix} \underline{I}_{ph} \\ \underline{I}_R \end{bmatrix}\right\}\right) \\ \omega_{rm} \\ \frac{1}{J}\{T_M + T_E - B\,\omega_{rm}\} \end{bmatrix} \tag{3.1.42}$$

$$\underline{f}_{dq} = \frac{d}{dt}\left\{\begin{bmatrix} \underline{I}_{dq} \\ \underline{I}_R \\ \theta_{rm} \\ \omega_{rm} \end{bmatrix}\right\}$$

$$= \begin{bmatrix} \underline{\mathbf{L}}_{DQ}^{-1}\left(\begin{bmatrix} \underline{V}_{dq} \\ \underline{V}_R \end{bmatrix} - [\underline{\mathbf{R}} + \underline{\mathbf{B}}_{VP}]\begin{bmatrix} \underline{I}_{dq} \\ \underline{I}_R \end{bmatrix}\right) \\ \omega_{rm} \\ \frac{1}{J}\{T_M + T_E - B\omega_{rm}\} \end{bmatrix} \qquad (3.1.43)$$

Either version of the gradient and the vector derivative can be used in the evaluation of the convective derivative of the coenergy provided that the gradient and the vector derivative used are consistent. Given its time-invariant inductance matrix, the d-q version of the convective derivative is used in this research.

$$\overline{\nabla}_{dq} W'_m = [[\underline{I}_{dq}^T \quad \underline{I}_R^T]\underline{\mathbf{L}}_{DQ} \quad 0 \quad 0] \qquad (3.1.44)$$

The gradient, (3.1.44), is now multiplied by the vector derivative of the state variables, (3.1.43).

$$\dot{W}'_m = [[\underline{I}_{dq}^T \quad \underline{I}_R^T]\underline{\mathbf{L}}_{DQ} \quad 0 \quad 0] \cdot \begin{bmatrix} \underline{\mathbf{L}}_{DQ}^{-1}\left(\begin{bmatrix} \underline{V}_{dq} \\ \underline{V}_R \end{bmatrix} - [\underline{\mathbf{R}} + \underline{\mathbf{B}}_{VP}]\begin{bmatrix} \underline{I}_{dq} \\ \underline{I}_R \end{bmatrix}\right) \\ \omega_{rm} \\ \frac{1}{J}\{T_M + T_E - B\omega_{rm}\} \end{bmatrix}$$

$$= [\underline{I}_{dq}^T \quad \underline{I}_R^T]\begin{bmatrix} \underline{V}_{dq} \\ \underline{V}_R \end{bmatrix} - [\underline{I}_{dq}^T \quad \underline{I}_R^T]\underline{\mathbf{R}}\begin{bmatrix} \underline{I}_{dq} \\ \underline{I}_R \end{bmatrix} - [\underline{I}_{dq}^T \quad \underline{I}_R^T]\underline{\mathbf{B}}_{VP}\begin{bmatrix} \underline{I}_{dq} \\ \underline{I}_R \end{bmatrix} \qquad (3.1.45)$$

A discussion of each of the terms in (3.1.45) is given in the next section.

3.1.2.6 3-Phase Synchronous Machine Coenergy in "d-q" Variables Per-Unitised

The per-unitisation of the system equations in d-q variables is undertaken here. The base power and base voltage are taken as the faceplate ratings of the machine. In this treatment, base voltage is taken to be the rated, peak, line-to-neutral voltage. From base power and base voltage, the other base quantities are calculated. Two "scaling" matrices are also defined.

$$P_B = \frac{3}{2} V_B I_B$$

$$Z_B = \frac{V_B}{I_B}$$

$$T_B = \frac{p_p P_B}{\omega_B} \qquad (3.1.46)$$

$$\underline{\mathbf{V}}_{SC} = \begin{bmatrix} V_B & 0 & 0 & 0 & 0 & 0 \\ 0 & V_B & 0 & 0 & 0 & 0 \\ 0 & 0 & V_B & 0 & 0 & 0 \\ 0 & 0 & 0 & V_{fB} & 0 & 0 \\ 0 & 0 & 0 & 0 & V_{kB} & 0 \\ 0 & 0 & 0 & 0 & 0 & V_{kB} \end{bmatrix}$$

$$\underline{\mathbf{I}}_{SC} = \begin{bmatrix} I_B & 0 & 0 & 0 & 0 & 0 \\ 0 & I_B & 0 & 0 & 0 & 0 \\ 0 & 0 & I_B & 0 & 0 & 0 \\ 0 & 0 & 0 & I_{fB} & 0 & 0 \\ 0 & 0 & 0 & 0 & I_{kB} & 0 \\ 0 & 0 & 0 & 0 & 0 & I_{kB} \end{bmatrix} \qquad (3.1.47)$$

Next, equation (3.1.24) is written in terms of per-unit quantities.

$$\underline{\mathbf{V}}_{SC}\begin{bmatrix} \underline{v}_{dq} \\ \underline{v}_R \end{bmatrix} = \left(\underline{\mathbf{R}} + \omega_{re} \begin{bmatrix} 0 & -L_Q & 0 & 0 & 0 & -\sqrt{\frac{3}{2}}\, L_{akq} \\ L_D & 0 & 0 & \sqrt{\frac{3}{2}}\, M & \sqrt{\frac{3}{2}}\, L_{akd} & 0 \\ \underline{\mathbf{0}}^{4\times 6} & & & & & \end{bmatrix} \right) \underline{\mathbf{I}}_{SC}\begin{bmatrix} \underline{i}_{dq} \\ \underline{i}_R \end{bmatrix} + \underline{\mathbf{L}}_{DQ}\underline{\mathbf{I}}_{SC}\frac{d}{dt}\left\{\begin{bmatrix} \underline{i}_{dq} \\ \underline{i}_R \end{bmatrix}\right\}$$

$$\begin{bmatrix} \underline{v}_{dq} \\ \underline{v}_R \end{bmatrix} = (\underline{\mathbf{V}}_{SC}^{-1}\underline{\mathbf{R}}\underline{\mathbf{I}}_{SC} + \underline{\mathbf{V}}_{SC}^{-1}\underline{\mathbf{B}}_{VP}\underline{\mathbf{I}}_{SC})\begin{bmatrix} \underline{i}_{dq} \\ \underline{i}_R \end{bmatrix} + \underline{\mathbf{V}}_{SC}^{-1}\underline{\mathbf{L}}_{DQ}\underline{\mathbf{I}}_{SC}\frac{d}{dt}\left\{\begin{bmatrix} \underline{i}_{dq} \\ \underline{i}_R \end{bmatrix}\right\}$$

$$\begin{bmatrix} \underline{v}_{dq} \\ \underline{v}_R \end{bmatrix} = (\underline{\mathbf{r}} + \underline{\mathbf{b}}_{VP})\begin{bmatrix} \underline{i}_{dq} \\ \underline{i}_R \end{bmatrix} + \frac{1}{\omega_B}\underline{\mathbf{l}}_{DQ}\frac{d}{dt}\left\{\begin{bmatrix} \underline{i}_{dq} \\ \underline{i}_R \end{bmatrix}\right\}$$

(3.1.48)

The per-unitised matrices follow. Note that the per-unitised inductance matrix, (3.1.51), is symmetric. This has implications which are discussed later.

$$\underline{r} = \begin{bmatrix} \frac{R_s}{Z_B} & 0 & 0 & 0 & 0 & 0 \\ 0 & \frac{R_s}{Z_B} & 0 & 0 & 0 & 0 \\ 0 & 0 & \frac{R_s}{Z_B} & 0 & 0 & 0 \\ 0 & 0 & 0 & \frac{R_f}{Z_{fB}} & 0 & 0 \\ 0 & 0 & 0 & 0 & \frac{R_{kd}}{Z_{kB}} & 0 \\ 0 & 0 & 0 & 0 & 0 & \frac{R_{kq}}{Z_{kB}} \end{bmatrix} \tag{3.1.49}$$

$$\underline{b}_{VP} = \frac{\omega_{re}}{\omega_B} \begin{bmatrix} 0 & -x_Q & 0 & 0 & 0 & -x_{akq} \\ x_D & 0 & 0 & x_{ad} & x_{akd} & 0 \\ 0 & 0 & 0 & 0 & 0 & 0 \\ 0 & 0 & 0 & 0 & 0 & 0 \\ 0 & 0 & 0 & 0 & 0 & 0 \\ 0 & 0 & 0 & 0 & 0 & 0 \end{bmatrix} \tag{3.1.50}$$

$$\underline{l}_{DQ} = \begin{bmatrix} x_D & 0 & 0 & x_{ad} & x_{akd} & 0 \\ 0 & x_Q & 0 & 0 & 0 & x_{akq} \\ 0 & 0 & x_{al} & 0 & 0 & 0 \\ x_{ad} & 0 & 0 & x_F & x_{fkd} & 0 \\ x_{akd} & 0 & 0 & x_{fkd} & x_{KD} & 0 \\ 0 & x_{akq} & 0 & 0 & 0 & x_{KQ} \end{bmatrix} \tag{3.1.51}$$

The elements of the per-unitised inductance matrix are defined in equation (3.1.52). These definitions, along with symmetry, place constraints, (3.1.53), upon the field and damper winding base quantities.

$$x_D = \frac{\omega_B L_D}{Z_B}$$

$$x_Q = \frac{\omega_B L_Q}{Z_B}$$

$$x_{al} = \frac{\omega_B L_{al}}{Z_B}$$

$$x_F = \frac{\omega_B L_F}{Z_{fB}}$$

$$x_{KD} = \frac{\omega_B L_{KD}}{Z_{kB}}$$

$$x_{KQ} = \frac{\omega_B L_{KQ}}{Z_{kB}}$$

$$x_{ad} = \frac{\omega_B I_B}{V_{fB}}\sqrt{\frac{3}{2}}\ M = \frac{\omega_B I_{fB}}{V_B}\sqrt{\frac{3}{2}}\ M$$

$$x_{akd} = \frac{\omega_B I_B}{V_{kB}}\sqrt{\frac{3}{2}}\ L_{akd} = \frac{\omega_B I_{kB}}{V_B}\sqrt{\frac{3}{2}}\ L_{akd}$$

$$x_{akq} = \frac{\omega_B I_B}{V_{kB}}\sqrt{\frac{3}{2}}\ L_{akq} = \frac{\omega_B I_{kB}}{V_B}\sqrt{\frac{3}{2}}\ L_{akq}$$

$$x_{fkd} = \frac{\omega_B I_{fB}}{V_{kB}} L_{fkd} = \frac{\omega_B I_{kB}}{V_{fB}} L_{fkd} \qquad (3.1.52)$$

$$V_B I_B = V_{fB} I_{fB} = V_{kB} I_{kB} \qquad (3.1.53)$$

Usually the products of the field and damper winding base quantities are set equal to the base power. This is not the case here. This slightly different normalisation of the rotor quantities will not affect the dynamic behaviour of the model. Remember, one is free to chose base quantities. This choice of base quantities provides a desirable symmetry.

The final equation to be cast into per-unit form is the rotor mechanical equation. For this, the inertia constant must be defined.

$$H \equiv \frac{\omega_B}{2p_p T_B} J \qquad (3.1.54)$$

Consider the mechanical equation with the electromagnetic torque expanded.

$$J\dot{\omega}_{rm} = T_M + T_E - B\omega_{rm}$$

$$= T_M + p_p\left(\begin{bmatrix} \underline{I}_{dq}^T & \underline{I}_R^T \end{bmatrix} \underline{\mathbf{B}}_I \underline{\mathbf{L}}_{DQ} \begin{bmatrix} \underline{I}_{dq} \\ \underline{I}_R \end{bmatrix} \right) - B\omega_{rm}$$

$$\dot{\omega}_{rm} = \left(\frac{T_B}{J} \right) T^m + \frac{p_p}{J}\left(\begin{bmatrix} \underline{I}_{dq}^T & \underline{I}_R^T \end{bmatrix} \underline{\mathbf{B}}_I \underline{\mathbf{L}}_{DQ} \begin{bmatrix} \underline{I}_{dq} \\ \underline{I}_R \end{bmatrix} \right) - \frac{B}{J}\omega_{rm}$$

$$= \left(\frac{\omega_B}{2p_pH} \right) \left\{ T^m + \begin{bmatrix} \underline{i}_{dq}^T & \underline{i}_R^T \end{bmatrix} \underline{\mathbf{I}}_{SC} \underline{\mathbf{B}}_I \frac{\omega_B}{P_B} \underline{\mathbf{L}}_{DQ} \underline{\mathbf{I}}_{SC} \begin{bmatrix} \underline{i}_{dq} \\ \underline{i}_R \end{bmatrix} \right\} - \frac{B}{J}\omega_{rm}$$

$$= \left(\frac{\omega_B}{2p_pH} \right) \left\{ T^m + \begin{bmatrix} \underline{i}_{dq}^T & \underline{i}_R^T \end{bmatrix} \underline{\mathbf{b}}_{IP} \begin{bmatrix} \underline{i}_{dq} \\ \underline{i}_R \end{bmatrix} \right\} - \frac{B}{J}\omega_{rm} \tag{3.1.55}$$

$$\underline{\mathbf{b}}_{IP} = \frac{2}{3}\underline{\mathbf{B}}_I \underline{\mathbf{l}}_{DQ}$$

$$= \frac{2}{3}\frac{\omega_B}{\omega_{re}}\underline{\mathbf{b}}_{VP} \tag{3.1.56}$$

The vector differential equation of the system can now be written in per-unitised form.

$$\underline{f}_{dq} = \frac{d}{dt}\left\{ \begin{bmatrix} \underline{i}_{dq} \\ \underline{i}_R \\ \theta_{rm} \\ \omega_{rm} \end{bmatrix} \right\}$$

$$= \begin{bmatrix} \omega_B \underline{\mathbf{l}}_{DQ}^{-1}\left(\begin{bmatrix} \underline{v}_{dq} \\ \underline{v}_R \end{bmatrix} - [\underline{\mathbf{r}} + \underline{\mathbf{b}}_{VP}] \begin{bmatrix} \underline{i}_{dq} \\ \underline{i}_R \end{bmatrix} \right) \\ \omega_{rm} \\ \left(\frac{\omega_B}{2p_pH} \right) \left\{ T^m + \begin{bmatrix} \underline{i}_{dq}^T & \underline{i}_R^T \end{bmatrix} \underline{\mathbf{b}}_{IP} \begin{bmatrix} \underline{i}_{dq} \\ \underline{i}_R \end{bmatrix} \right\} - \frac{B}{J}\omega_{rm} \end{bmatrix} \tag{3.1.57}$$

If a per-unitised coenergy function is desired, then a base energy must be defined.

$$E_B \equiv \frac{P_B}{\omega_B} \tag{3.1.58}$$

The base energy normalises the coenergy equation.

$$W'_{mdq} = \frac{1}{2}\begin{bmatrix} \underline{I}_{dq}^{T} & \underline{I}_{R}^{T} \end{bmatrix} \underline{\mathbf{L}}_{DQ} \begin{bmatrix} \underline{I}_{dq} \\ \underline{I}_{R} \end{bmatrix}$$

$$E_B W'_{mdq} = \frac{1}{2}\begin{bmatrix} \underline{i}_{dq}^{T} & \underline{i}_{R}^{T} \end{bmatrix} \underline{\mathbf{I}}_{SC} \underline{\mathbf{L}}_{DQ} \underline{\mathbf{I}}_{SC} \begin{bmatrix} \underline{i}_{dq} \\ \underline{i}_{R} \end{bmatrix}$$

$$w'_{mdq} = \frac{1}{2} \cdot \frac{2}{3}\begin{bmatrix} \underline{i}_{dq}^{T} & \underline{i}_{R}^{T} \end{bmatrix} \underline{\mathbf{I}}_{DQ} \begin{bmatrix} \underline{i}_{dq} \\ \underline{i}_{R} \end{bmatrix} \tag{3.1.59}$$

The convective derivative of the foregoing is normalised as well, (3.1.60).

$$\dot{w}'_{mdq} = \overline{\nabla}_{dq} w'_{mdq} \cdot \underline{f}_{dq}$$

$$= \begin{bmatrix} \frac{2}{3}\begin{bmatrix} \underline{i}_{dq}^{T} & \underline{i}_{R}^{T} \end{bmatrix} \underline{\mathbf{I}}_{DQ} & 0 & 0 \end{bmatrix} \cdot \begin{bmatrix} \omega_B \underline{\mathbf{I}}_{DQ}^{-1} \left(\begin{bmatrix} \underline{v}_{dq} \\ \underline{v}_{R} \end{bmatrix} - [\underline{\mathbf{r}} + \underline{\mathbf{b}}_{VP}] \begin{bmatrix} \underline{i}_{dq} \\ \underline{i}_{R} \end{bmatrix} \right) \\ \omega_{rm} \\ \left(\frac{\omega_B}{2 p_p H} \right) \left\{ T^{m} + \begin{bmatrix} \underline{i}_{dq}^{T} & \underline{i}_{R}^{T} \end{bmatrix} \underline{\mathbf{b}}_{IP} \begin{bmatrix} \underline{i}_{dq} \\ \underline{i}_{R} \end{bmatrix} \right\} - \frac{B}{J} \omega_{rm} \end{bmatrix}$$

$$= \frac{2}{3}\begin{bmatrix} \underline{i}_{dq}^{T} & \underline{i}_{R}^{T} \end{bmatrix} \underline{\mathbf{I}}_{DQ} \omega_B \underline{\mathbf{I}}_{DQ}^{-1} \left(\begin{bmatrix} \underline{v}_{dq} \\ \underline{v}_{R} \end{bmatrix} - [\underline{\mathbf{r}} + \underline{\mathbf{b}}_{VP}] \begin{bmatrix} \underline{i}_{dq} \\ \underline{i}_{R} \end{bmatrix} \right)$$

$$= \frac{2}{3}\omega_B \left\{ \begin{bmatrix} \underline{i}_{dq}^{T} & \underline{i}_{R}^{T} \end{bmatrix} \begin{bmatrix} \underline{v}_{dq} \\ \underline{v}_{R} \end{bmatrix} - \begin{bmatrix} \underline{i}_{dq}^{T} & \underline{i}_{R}^{T} \end{bmatrix} \underline{\mathbf{r}} \begin{bmatrix} \underline{i}_{dq} \\ \underline{i}_{R} \end{bmatrix} - \begin{bmatrix} \underline{i}_{dq}^{T} & \underline{i}_{R}^{T} \end{bmatrix} \frac{3}{2}\frac{\omega_{re}}{\omega_B} \underline{\mathbf{b}}_{IP} \begin{bmatrix} \underline{i}_{dq} \\ \underline{i}_{R} \end{bmatrix} \right\}$$

$$= \frac{2}{3}\omega_B \left\{ \begin{bmatrix} \underline{i}_{dq}^{T} & \underline{i}_{R}^{T} \end{bmatrix} \begin{bmatrix} \underline{v}_{dq} \\ \underline{v}_{R} \end{bmatrix} - \begin{bmatrix} \underline{i}_{dq}^{T} & \underline{i}_{R}^{T} \end{bmatrix} \underline{\mathbf{r}} \begin{bmatrix} \underline{i}_{dq} \\ \underline{i}_{R} \end{bmatrix} \right\} - T^{e} \omega_{re} \tag{3.1.60}$$

Viewing the coenergy as a portion of a candidate Lyapunov function, for the generator to be stable, the convective derivative of the coenergy should be less than or equal to zero. The role of each term in equation (3.1.60) illustrates the influence of each terminal variable on stability.

Current into the generator is taken to be positive; hence, the first term in equation (3.1.60) is positive for electric power going into the generator. This term, when positive, is destabilising. The second term, which is negative definite, represents the internal electrical losses of the generator. As expected, this is stabilising. The third term describes the net mechanical power going into the generator.--It is equal to the negative of the torque of electromagnetic origin in steady state. This term has a positive value in normal generator operation.--Hence, when the prime mover is driving the rotor, this term is positive and destabilising.

3.1.2.7 Coenergy-Based Lyapunov Function Including Inertial Energy

The coenergy function described to this point represents the energy within the generator which participates in electromechanical energy conversion. A form of energy which also participates in transient dynamics is inertial energy. Inertial energy gives indications of whether or not loss of synchronisation instability is occurring.

Besides the physical appeal of including inertial energy within a candidate Lyapunov function, there is also a mathematical appeal. Namely, eight states are shown in the equation representing the synchronous generator, equation (3.1.57). The coenergy function is a globally positive definite function of the six currents. The seventh state variable, the rotor angle, represents a translational degree of freedom and does not contribute to dynamics or stored energy. The eighth state variable is the rotor mechanical speed. Inertial energy is proportional to the square of the mechanical speed. If the constructed candidate Lyapunov function which comprises a "stability organ" is to be a function of **all** the relevant state variables, then inclusion of some positive definite function of the mechanical speed is warranted.

There are several inertial energy relationships which are available. The entire instantaneous rotor inertia can be utilised. Or, rather than accounting for all of the kinetic energy stored within the inertia of the rotor, the inertia associated with the difference between the instantaneous rotor speed and the rated rotor speed can be used as a globally positive definite function of rotor mechanical speed.

$$K.E. = \frac{1}{2} J \omega_{rm}^2$$

$$K.E.(\Delta\omega_{rm}) = \frac{1}{2} J \left(\omega_{rm} - \frac{\omega_B}{p_p} \right)^2 \tag{3.1.61}$$

Equations (3.1.61) are satisfactory components of a candidate Lyapunov function. The inertial energy and the generator's coenergy are not functions of each other. (Their rates of change are related, though.) Hence, no particular significance need be attached to their absolute sum. Rather, if either the coenergy term or the inertial term begins to grow with time, then their scaling should not obscure either term's behaviour. Hence, a scaling factor can be introduced so that when the candidate Lyapunov function is normalised with the base energy, both the coenergy term and the inertial term will be of the same order. Equation (3.1.62) introduces this one possible inertial energy scaling term.

$$K = \left\{ \frac{K.E. \quad at \quad rated \quad speed}{Base \quad Energy} \right\}$$

$$= \left\{ \frac{\frac{1}{2} J \left(\frac{\omega_B}{p_p} \right)^2}{\frac{P_B}{\omega_B}} \right\}$$

$$= H \omega_B \tag{3.1.62}$$

The dimensionless scaling term, K, is used in equations (3.1.63) and (3.1.64).

$$K.E.(\Delta\omega_{rm} E_B) = \frac{1}{K} \cdot \frac{1}{2} J \left(\omega_{rm} - \frac{\omega_B}{p_p} \right)^2$$

$$= E_B \frac{\left(\omega_{rm} - \frac{\omega_B}{p_p} \right)^2}{\left(\frac{\omega_B}{p_p} \right)^2} \tag{3.1.63}$$

$$K.E.(E_B) = \frac{1}{K} \cdot \frac{1}{2} J \omega_{rm}^2$$

$$= E_B \frac{\omega_{rm}^2}{\left(\frac{\omega_B}{P_p}\right)^2} \tag{3.1.64}$$

A last inertial term considers the square of the difference in inertial energy, equation (3.1.65).

$$\Delta K.E.^2 = \frac{1}{2} J \frac{\left(\omega_{rm}^2 - \left(\frac{\omega_B}{P_p}\right)^2\right)^2}{\left(\frac{\omega_B}{P_p}\right)^2} \tag{3.1.65}$$

Any of these inertial terms can be added to the coenergy and the sum used as the "stability organ's" Lyapunov function. The coenergy and inertial energy are positive definite in terms of the states. They are also continuously differentiable. Complete candidate Lyapunov functions can be written and normalised, equations (3.1.66) - (3.1.70).

The equilibrium at the 'origin' is different for several of the given Lyapunov functions, (3.1.66) - (3.1.70). One of the requirements for a valid candidate Lyapunov function is that it be locally positive definite about the particular equilibrium. In most treatments, the equilibrium in question is translated to the origin of state space so that $V(\underline{0}) = 0$. This is true for the Lyapunov functions given by (3.1.66) and (3.1.69). In terms of the rotor mechanical speed, $V(\underline{x}_{eq}) = 0$ for a state vector whose mechanical speed at the equilibrium is the nominal rotor speed in equations (3.1.67), (3.1.68) and (3.1.70). This particular equilibrium is not at the origin. All of the Lyapunov functions, though, are globally positive definite.

$$V'_{m+1} = W'_{mdq} + K.E.$$

$$= \frac{1}{2}[\underline{I}_{dq}^T \quad \underline{I}_R^T]\underline{\mathbf{L}}_{DQ}\begin{bmatrix}\underline{I}_{dq}\\ \underline{I}_R\end{bmatrix} + \frac{1}{2} J \omega_{rm}^2$$

$$E_B v'_{m+1} = \frac{1}{2}[\underline{i}_{dq}^T \quad \underline{i}_R^T]\underline{\mathbf{I}}_{SC}\underline{\mathbf{L}}_{DQ}\underline{\mathbf{I}}_{SC}\begin{bmatrix}\underline{i}_{dq}\\ \underline{i}_R\end{bmatrix} + E_B H \omega_B \frac{\omega_{rm}^2}{\left(\frac{\omega_B}{P_p}\right)^2}$$

$$v'_{m+1} = \frac{1}{3} \cdot [\underline{i}_{dq}^T \quad \underline{i}_R^T]\underline{\mathbf{l}}_{DQ}\begin{bmatrix}\underline{i}_{dq}\\ \underline{i}_R\end{bmatrix} + H \omega_B \frac{\omega_{rm}^2}{\left(\frac{\omega_B}{P_p}\right)^2} \tag{3.1.66}$$

$$V'_{m+2} = W'_{mdq} + K.E.(\Delta\omega_{rm})$$

$$= \frac{1}{2}[\underline{I}_{dq}^{T} \quad \underline{I}_{R}^{T}]\underline{\mathbf{L}}_{DQ}\begin{bmatrix}\underline{I}_{dq}\\ \underline{I}_{R}\end{bmatrix} + \frac{1}{2}J\left(\omega_{rm} - \frac{\omega_B}{p_p}\right)^2$$

$$E_B v'_{m+2} = \frac{1}{2}[\underline{i}_{dq}^{T} \quad \underline{i}_{R}^{T}]\underline{\mathbf{I}}_{SC}\underline{\mathbf{L}}_{DQ}\underline{\mathbf{I}}_{SC}\begin{bmatrix}\underline{i}_{dq}\\ \underline{i}_{R}\end{bmatrix} + E_B H\omega_B \frac{\left(\omega_{rm} - \frac{\omega_B}{p_p}\right)^2}{\left(\frac{\omega_B}{p_p}\right)^2}$$

$$v'_{m+2} = \frac{1}{3}\cdot[\underline{i}_{dq}^{T} \quad \underline{i}_{R}^{T}]\underline{\mathbf{l}}_{DQ}\begin{bmatrix}\underline{i}_{dq}\\ \underline{i}_{R}\end{bmatrix} + H\omega_B \frac{\left(\omega_{rm} - \frac{\omega_B}{p_p}\right)^2}{\left(\frac{\omega_B}{p_p}\right)^2} \qquad (3.1.67)$$

$$V'_{m+3} = W'_{mdq} + K.E.(\Delta\omega_{rm}E_B)$$

$$= \frac{1}{2}[\underline{I}_{dq}^{T} \quad \underline{I}_{R}^{T}]\underline{\mathbf{L}}_{DQ}\begin{bmatrix}\underline{I}_{dq}\\ \underline{I}_{R}\end{bmatrix} + \frac{1}{K}\cdot\frac{1}{2}J\left(\omega_{rm} - \frac{\omega_B}{p_p}\right)^2$$

$$E_B v'_{m+3} = \frac{1}{2}[\underline{i}_{dq}^{T} \quad \underline{i}_{R}^{T}]\underline{\mathbf{I}}_{SC}\underline{\mathbf{L}}_{DQ}\underline{\mathbf{I}}_{SC}\begin{bmatrix}\underline{i}_{dq}\\ \underline{i}_{R}\end{bmatrix} + E_B \frac{\left(\omega_{rm} - \frac{\omega_B}{p_p}\right)^2}{\left(\frac{\omega_B}{p_p}\right)^2}$$

$$v'_{m+3} = \frac{1}{3}\cdot[\underline{i}_{dq}^{T} \quad \underline{i}_{R}^{T}]\underline{\mathbf{l}}_{DQ}\begin{bmatrix}\underline{i}_{dq}\\ \underline{i}_{R}\end{bmatrix} + \frac{\left(\omega_{rm} - \frac{\omega_B}{p_p}\right)^2}{\left(\frac{\omega_B}{p_p}\right)^2} \qquad (3.1.68)$$

$$V'_{m+4} = W'_{mdq} + K.E.(E_B)$$

$$= \frac{1}{2}[\underline{I}_{dq}^{T} \quad \underline{I}_{R}^{T}]\underline{\mathbf{L}}_{DQ}\begin{bmatrix}\underline{I}_{dq}\\ \underline{I}_{R}\end{bmatrix} + \frac{1}{K}\cdot\frac{1}{2}J\omega_{rm}^2$$

$$E_B v'_{m+4} = \frac{1}{2}[\underline{i}_{dq}^{T} \quad \underline{i}_{R}^{T}]\underline{\mathbf{I}}_{SC}\underline{\mathbf{L}}_{DQ}\underline{\mathbf{I}}_{SC}\begin{bmatrix}\underline{i}_{dq}\\ \underline{i}_{R}\end{bmatrix} + E_B \frac{\omega_{rm}^2}{\left(\frac{\omega_B}{p_p}\right)^2}$$

$$v'_{m+4} = \frac{1}{3}\cdot[\underline{i}_{dq}^{T} \quad \underline{i}_{R}^{T}]\underline{\mathbf{l}}_{DQ}\begin{bmatrix}\underline{i}_{dq}\\ \underline{i}_{R}\end{bmatrix} + \frac{\omega_{rm}^2}{\left(\frac{\omega_B}{p_p}\right)^2} \qquad (3.1.69)$$

$$V'_{m+5} = W'_{mdq} + \Delta K.E.^2$$

$$= \frac{1}{2}[\underline{I}_{dq}^T \quad \underline{I}_R^T]\underline{\mathbf{L}}_{DQ}\begin{bmatrix}\underline{I}_{dq}\\ \underline{I}_R\end{bmatrix} + \frac{1}{2}J\frac{\left(\omega_{rm}^2 - \left(\frac{\omega_B}{p_p}\right)^2\right)^2}{\left(\frac{\omega_B}{p_p}\right)^2}$$

$$E_B v'_{m+5} = \frac{1}{2}[\underline{i}_{dq}^T \quad \underline{i}_R^T]\underline{\mathbf{I}}_{SC}\underline{\mathbf{L}}_{DQ}\underline{\mathbf{I}}_{SC}\begin{bmatrix}\underline{i}_{dq}\\ \underline{i}_R\end{bmatrix} + E_B H\omega_B\frac{\left(\omega_{rm}^2 - \left(\frac{\omega_B}{p_p}\right)^2\right)^2}{\left(\frac{\omega_B}{p_p}\right)^4}$$

$$v'_{m+5} = \frac{1}{3}\cdot[\underline{i}_{dq}^T \quad \underline{i}_R^T]\underline{\mathbf{l}}_{DQ}\begin{bmatrix}\underline{i}_{dq}\\ \underline{i}_R\end{bmatrix} + H\omega_B\frac{\left(\omega_{rm}^2 - \left(\frac{\omega_B}{p_p}\right)^2\right)^2}{\left(\frac{\omega_B}{p_p}\right)^4}$$

(3.1.70)

The test for stability comes from the convective derivative of the candidate Lyapunov function.

$$\dot{v}'_{m+1} = \overline{\nabla}_{dq} v'_{m+1}\cdot \underline{f}_{dq}$$

$$= \begin{bmatrix}\frac{2}{3}[\underline{i}_{dq}^T \quad \underline{i}_R^T]\underline{\mathbf{l}}_{DQ} & 0 & 2H\omega_B\frac{\omega_{rm}}{\left(\frac{\omega_B}{p_p}\right)^2}\end{bmatrix}\cdot\begin{bmatrix}\omega_B\underline{\mathbf{l}}_{DQ}^{-1}\left(\begin{bmatrix}\underline{v}_{dq}\\ \underline{v}_R\end{bmatrix} - [\underline{\mathbf{r}} + \underline{\mathbf{b}}_{VP}]\begin{bmatrix}\underline{i}_{dq}\\ \underline{i}_R\end{bmatrix}\right)\\ \omega_{rm}\\ \left(\frac{\omega_B}{2p_pH}\right)\left\{T^m + [\underline{i}_{dq}^T \quad \underline{i}_R^T]\underline{\mathbf{b}}_{IP}\begin{bmatrix}\underline{i}_{dq}\\ \underline{i}_R\end{bmatrix}\right\} - \frac{B}{J}\omega_{rm}\end{bmatrix}$$

$$= \frac{2}{3}\omega_B[\underline{i}_{dq}^T \quad \underline{i}_R^T]\left(\begin{bmatrix}\underline{v}_{dq}\\ \underline{v}_R\end{bmatrix} - [\underline{\mathbf{r}} + \underline{\mathbf{b}}_{VP}]\begin{bmatrix}\underline{i}_{dq}\\ \underline{i}_R\end{bmatrix}\right) + p_p\omega_{rm}\left[T^m + [\underline{i}_{dq}^T \quad \underline{i}_R^T]\underline{\mathbf{b}}_{IP}\begin{bmatrix}\underline{i}_{dq}\\ \underline{i}_R\end{bmatrix} - \frac{B}{T_B}\omega_{rm}\right]$$

(3.1.71)

$$\dot{v}'_{m+2} = \overline{\nabla}_{dq} v'_{m+2} \cdot \underline{f}_{dq}$$

$$= \begin{bmatrix} \frac{2}{3}[\underline{i}_{dq}^{T} \quad \underline{i}_{R}^{T}]\underline{\mathbf{l}}_{DQ} & 0 & 2H\omega_B \dfrac{\left(\omega_{rm} - \frac{\omega_B}{p_p}\right)}{\left(\frac{\omega_B}{p_p}\right)^2} \end{bmatrix} \cdot \begin{bmatrix} \omega_B \underline{\mathbf{l}}_{DQ}^{-1}\left(\begin{bmatrix} \underline{v}_{dq} \\ \underline{v}_R \end{bmatrix} - [\underline{\mathbf{r}} + \underline{\mathbf{b}}_{VP}]\begin{bmatrix} \underline{i}_{dq} \\ \underline{i}_R \end{bmatrix}\right) \\ \omega_{rm} \\ \left(\dfrac{\omega_B}{2p_p H}\right)\left\{T^m + [\underline{i}_{dq}^{T} \quad \underline{i}_{R}^{T}]\underline{\mathbf{b}}_{IP}\begin{bmatrix} \underline{i}_{dq} \\ \underline{i}_R \end{bmatrix}\right\} - \dfrac{B}{J}\omega_{rm} \end{bmatrix}$$

$$= \frac{2}{3}\omega_B[\underline{i}_{dq}^{T} \quad \underline{i}_{R}^{T}]\left(\begin{bmatrix} \underline{v}_{dq} \\ \underline{v}_R \end{bmatrix} - [\underline{\mathbf{r}} + \underline{\mathbf{b}}_{VP}]\begin{bmatrix} \underline{i}_{dq} \\ \underline{i}_R \end{bmatrix}\right) + p_p\left(\omega_{rm} - \frac{\omega_B}{p_p}\right)\left[T^m + [\underline{i}_{dq}^{T} \quad \underline{i}_{R}^{T}]\underline{\mathbf{b}}_{IP}\begin{bmatrix} \underline{i}_{dq} \\ \underline{i}_R \end{bmatrix} - \frac{B}{T_B}\omega_{rm}\right]$$

(3.1.72)

$$\dot{v}'_{m+3} = \overline{\nabla}_{dq} v'_{m+3} \cdot \underline{f}_{dq}$$

$$= \begin{bmatrix} \frac{2}{3}[\underline{i}_{dq}^{T} \quad \underline{i}_{R}^{T}]\underline{\mathbf{l}}_{DQ} & 0 & 2 \cdot \dfrac{\left(\omega_{rm} - \frac{\omega_B}{p_p}\right)}{\left(\frac{\omega_B}{p_p}\right)^2} \end{bmatrix} \cdot \begin{bmatrix} \omega_B \underline{\mathbf{l}}_{DQ}^{-1}\left(\begin{bmatrix} \underline{v}_{dq} \\ \underline{v}_R \end{bmatrix} - [\underline{\mathbf{r}} + \underline{\mathbf{b}}_{VP}]\begin{bmatrix} \underline{i}_{dq} \\ \underline{i}_R \end{bmatrix}\right) \\ \omega_{rm} \\ \left(\dfrac{\omega_B}{2p_p H}\right)\left\{T^m + [\underline{i}_{dq}^{T} \quad \underline{i}_{R}^{T}]\underline{\mathbf{b}}_{IP}\begin{bmatrix} \underline{i}_{dq} \\ \underline{i}_R \end{bmatrix}\right\} - \dfrac{B}{J}\omega_{rm} \end{bmatrix}$$

$$= \frac{2}{3}\omega_B[\underline{i}_{dq}^{T} \quad \underline{i}_{R}^{T}]\left(\begin{bmatrix} \underline{v}_{dq} \\ \underline{v}_R \end{bmatrix} - [\underline{\mathbf{r}} + \underline{\mathbf{b}}_{VP}]\begin{bmatrix} \underline{i}_{dq} \\ \underline{i}_R \end{bmatrix}\right) + \frac{\left(\omega_{rm} - \frac{\omega_B}{p_p}\right)}{\left(H\frac{\omega_B}{p_p}\right)}\left[T^m + [\underline{i}_{dq}^{T} \quad \underline{i}_{R}^{T}]\underline{\mathbf{b}}_{IP}\begin{bmatrix} \underline{i}_{dq} \\ \underline{i}_R \end{bmatrix} - \frac{B}{T_B}\omega_{rm}\right]$$

(3.1.73)

$$\dot{v}'_{m+4} = \overline{\nabla}_{dq} v'_{m+4} \cdot \underline{f}_{dq}$$

$$= \begin{bmatrix} \frac{2}{3}[\underline{i}_{dq}^{T} \quad \underline{i}_{R}^{T}]\underline{\mathbf{l}}_{DQ} & 0 & 2 \cdot \dfrac{\omega_{rm}}{\left(\frac{\omega_B}{p_p}\right)^2} \end{bmatrix} \cdot \begin{bmatrix} \omega_B \underline{\mathbf{l}}_{DQ}^{-1}\left(\begin{bmatrix} \underline{v}_{dq} \\ \underline{v}_R \end{bmatrix} - [\underline{\mathbf{r}} + \underline{\mathbf{b}}_{VP}]\begin{bmatrix} \underline{i}_{dq} \\ \underline{i}_R \end{bmatrix}\right) \\ \omega_{rm} \\ \left(\dfrac{\omega_B}{2p_p H}\right)\left\{T^m + [\underline{i}_{dq}^{T} \quad \underline{i}_{R}^{T}]\underline{\mathbf{b}}_{IP}\begin{bmatrix} \underline{i}_{dq} \\ \underline{i}_R \end{bmatrix}\right\} - \dfrac{B}{J}\omega_{rm} \end{bmatrix}$$

$$= \frac{2}{3}\omega_B[\underline{i}_{dq}^{T} \quad \underline{i}_{R}^{T}]\left(\begin{bmatrix} \underline{v}_{dq} \\ \underline{v}_R \end{bmatrix} - [\underline{\mathbf{r}} + \underline{\mathbf{b}}_{VP}]\begin{bmatrix} \underline{i}_{dq} \\ \underline{i}_R \end{bmatrix}\right) + \frac{\omega_{rm}}{\left(H\frac{\omega_B}{p_p}\right)}\left[T^m + [\underline{i}_{dq}^{T} \quad \underline{i}_{R}^{T}]\underline{\mathbf{b}}_{IP}\begin{bmatrix} \underline{i}_{dq} \\ \underline{i}_R \end{bmatrix} - \frac{B}{T_B}\omega_{rm}\right]$$

(3.1.74)

$$\dot{v}'_{m+5} = \overline{\nabla}_{dq} v'_{m+5} \cdot \underline{f}_{dq}$$

$$= \left[\frac{2}{3}[\underline{i}_{dq}^T \quad \underline{i}_R^T]\underline{\mathbf{l}}_{DQ} \quad 0 \quad 4H\omega_B\omega_{rm} \frac{\left(\omega_{rm}^2 - \left(\frac{\omega_B}{p_p}\right)^2\right)}{\left(\frac{\omega_B}{p_p}\right)^4} \right] \cdot \begin{bmatrix} \omega_B \underline{\mathbf{l}}_{DQ}^{-1} \left(\begin{bmatrix} \underline{v}_{dq} \\ \underline{v}_R \end{bmatrix} - [\underline{\mathbf{r}} + \underline{\mathbf{b}}_{VP}] \begin{bmatrix} \underline{i}_{dq} \\ \underline{i}_R \end{bmatrix} \right) \\ \omega_{rm} \\ \left(\frac{\omega_B}{2p_p H}\right) \left\{ T^m + [\underline{i}_{dq}^T \quad \underline{i}_R^T]\underline{\mathbf{b}}_{IP} \begin{bmatrix} \underline{i}_{dq} \\ \underline{i}_R \end{bmatrix} \right\} - \frac{B}{J}\omega_{rm} \end{bmatrix}$$

$$= \frac{2}{3}\omega_B[\underline{i}_{dq}^T \quad \underline{i}_R^T] \left(\begin{bmatrix} \underline{v}_{dq} \\ \underline{v}_R \end{bmatrix} - [\underline{\mathbf{r}} + \underline{\mathbf{b}}_{VP}] \begin{bmatrix} \underline{i}_{dq} \\ \underline{i}_R \end{bmatrix} \right) + 2p_p\omega_{rm} \frac{\left(\omega_{rm}^2 - \left(\frac{\omega_B}{p_p}\right)^2\right)}{\left(\frac{\omega_M}{p_p}\right)^2} \left[T^m + [\underline{i}_{dq}^T \quad \underline{i}_R^T]\underline{\mathbf{b}}_{IP} \begin{bmatrix} \underline{i}_{dq} \\ \underline{i}_R \end{bmatrix} - \frac{B}{T_B}\omega_{rm} \right]$$

(3.1.75)

These expressions of the coenergy-based candidate Lyapunov functions, (3.1.66)-(3.1.70), and their convective derivatives, (3.1.71)-(3.1.75), are adopted as the relationships underlying the synchronous generator "stability organs" which are evaluated.

3.1.2.8 Inputs in the Coenergy Function Convective Derivative

The vector differential equation, $\underline{f}$, describing the 3-phase synchronous machine, equation (3.1.57), contains input variables, $\underline{u}(t)$. In this case, they are the terminal voltages and mechanical torque. In situations where a machine is temporarily isolated from the rest of a system, some question arises as to which input variables are most appropriate.

Consider a short-circuit critical clearing time, transient stability example. Suppose a generator is supplying power to a system when a symmetric, 3-phase short-circuit is placed across its terminals. First, if only the behaviour of the faulted generator is of interest, then the voltages, $\underline{v}_{dq}$, used in equations (3.1.71) to (3.1.75) for evaluating the convective derivatives, should be set equal to zero, reflecting the short-circuit at the generator's terminals. Second, if the re-connectability of the faulted generator is of interest (the critical clearing time question), then the voltages used in equations (3.1.71) to (3.1.75) should contain information about the system to which the generator would be re-connected.

In the case of the short-circuit example, the relevant system voltage, if substituted for $\underline{v}_{dq}$, would give the convective derivative of the coenergy-based Lyapunov function an interpretation which is extremely relevant to the critical clearing time question. Namely, with system voltages used in lieu of the actual terminal voltages, the coenergy-based Lyapunov function's convective derivative describes the ability of the generator to resume supplying electric power to the system if it were instantaneously re-connected to the system. This version of the convective derivative is subsequently called the "re-connected" derivative.

The negative semi-definiteness of the "re-connected" derivative of the coenergy-based Lyapunov function carries stability interpretations just as the actual convective derivative does. It does, though, capture such effects as loss of synchronisation, which would not be seen if only the actual terminal voltages are used, as in the short-circuit

example. The results yielded by both versions of the convective derivative are examined. Note, though, this issue over input variables arises only when portions of the system are somehow isolated.

3.1.3 Coenergy and Electric Power Systems

The coenergy-based Lyapunov function is an "engineering" Lyapunov function as opposed to a "mathematical" Lyapunov function. Its physical interpretation has very strong appeal for two reasons. First, it captures how well the synchronous machine is converting energy, equation (3.1.60). A positive convective derivative indicates that more energy in entering the machine than is being converted, an unstable situation. A negative convective derivative indicates that, temporarily, the machine is providing more energy than it is receiving, a stable situation. A zero convective derivative indicates stable, steady-state operation; the generator is converting as much energy as it is receiving.

The convective derivative, which gives this telling account of how the generator is performing, is a function only of the generator's parameters, states, and the waveforms at its terminals. It does not depend upon the "interconnection" structure of the rest of the system. This quality is necessary if composite stability measures are contemplated. It corresponds nicely to the nature of naval electric power systems. It also accommodates inclusion in an advanced decentralised stabilising control scheme. Were a single Lyapunov function used to describe the entire power system, then a wealth of information germane to stabilising control of individual components would be lost.

The second reason why the coenergy-based Lyapunov function is so appealing is that it is the actual energy stored in the generator. The success of Lyapunov's direct method for describing the stability of mechanical systems is aided by the fact that determining the actual stored energy of a mechanical system is relatively straightforward. The difficulties encountered in applying Lyapunov's direct method to electric power systems have included describing the actual stored energy of the system.

The actual stored energy of an electric power system is easily derived if the actual stored energies of all of the components are summed. This is not the approach taken in the conventional electric power system Lyapunov functions, equations (2.2.28) and (2.2.29). This usual approach is based upon real power flow, P, and reactive power flow, Q, analyses. P does not represent stored energy at all. Q represents the **amplitude** of a time varying stored energy.--The notions of P and Q arise from steady-state, sinusoidal (complex) analysis with all of the concomitant assumptions, section 2.2.1.2. Although equations (2.2.28) and (2.2.29) have the units of energy and an energy-related interpretation, they do not represent the actual stored energy of the power system.

The coenergy-based Lyapunov function, in fact, represents **all** of the stored energies admitted by the underlying model of the synchronous machine, equation (3.1.57). It includes the energy stored in armature leakage inductances, damper windings, and the field winding. The "swing" equation model, on the other hand, admits only the energy stored in the field winding. The "coupling field" motivated path-independent integration leading to the coenergy expression, equations (3.1.27) & (3.1.28) and (3.1.34) & (3.1.35), is what enables the unique determination of all of the actual stored energy of the synchronous machine. The implication of representing all of the stored energies is that multi-rate energy dynamics are now present.

The presence of multi-rate energy dynamics in the coenergy-based Lyapunov function manifests itself in the form of a superposition of slower responses and faster damped oscillations during dynamic events. Dealing with all of the multi-rate energy information is discussed in greater detail later.

One important feature of the coenergy-based Lyapunov function is that it is general. Since it is based upon a notion universal to all electromechanical energy conversion devices, a coenergy-based Lyapunov function can be developed for any such machine. Hence, it is possible, for example, to derive a function for a polyphase induction motor similar to the one developed here for a synchronous machine. This notion enables all electric machinery components in a composite system to be represented by a Lyapunov function which is based upon that component's actual stored energy.

To capture the stored energy of an entire composite system, all the components' stored energies must appear. The Lyapunov functions representing non-machinery components, such as electronic power converters, tie lines and transformers, must be based upon their stored energies as well. Only when the stored energy of each component is consistently represented will the composite system's stored energy be accurately portrayed. Achieving this goal would go far in improving the performance of Lyapunov's direct method for describing electric power system stability. The coenergy-based Lyapunov function developed here enables fulfillment of that goal.

3.1.3.1 Extraction of Energy Dynamics for a Specified Time-Scale

As mentioned earlier, the coenergy-based Lyapunov function developed in this research includes all of the energy dynamics admitted by the underlying model of the 3-phase synchronous generator, reference [3.1.3]. It is conceivable that some of these energy dynamics may not be relevant if a particular type of stability is being considered. For example, if electromechanical stability is of concern (loss of synchronisation in a critical clearing time scenario), then it may be desirable to overlook the armature and subtransient energy oscillations. Or, if long-term voltage stability is an issue, then energy swings arising from rotor angle oscillations may not be relevant. Hence, some motivation for applying a time-scale 'filter' to the coenergy-based Lyapunov function exists.

One such time-scale 'filter' is based upon averaging the coenergy-based Lyapunov function over a specific interval. The time-scale averaged function varies with time. It represents the average value of the coenergy-based Lyapunov function for a specified period of time preceding time t, equation (3.1.76). See figure 3.1.4.

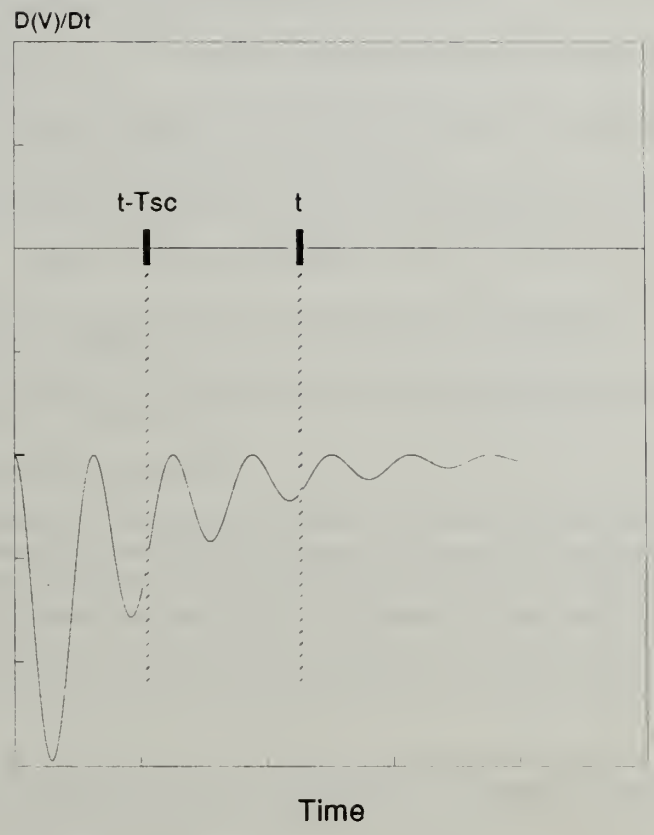

Figure 3.1.4 - Continuous Time-Scale Averaged Function

$$\dot{V}_{\text{Tscavg}}(t) = \frac{1}{T_{sc}} \int_{t-\text{Tsc}}^{t} \dot{V}(\tau) d\tau \qquad (3.1.76)$$

This version of the averaging function is selected because it requires knowing only the previous values of the convective derivative. Otherwise, future values must be known.--This is acceptable for analysis; however, it is not acceptable for inclusion in a control scheme.

The selection of the time-scale of interest is arbitrary, depending only upon the application. For example, equation (3.1.76) can be used to eliminate oscillations arising from armature leakage inductances by chosing the averaging interval, T_{sc}, to be on the order of the armature time constant. To eliminate rotor angle oscillatory behaviour, set T_{sc} to the order of the rotor swing period.

Results of using this averaging function are demonstrated in the next chapter.

3.1.4 References

3.1.1 Vidyasagar, M. Nonlinear Systems Analysis. Englewood Cliffs, NJ: Prentice-Hall, Inc. 1978.

3.1.2 Woodson, H.H. and J.R. Melcher. Electromechanical Dynamics Part I: Discrete Systems. New York, NY: John Wiley & Sons. 1968.

3.1.3 Kirtley, James L. Jr. "Synchronous Machine Dynamic Models." LEES Technical Report TR-87-008. Cambridge, MA: M.I.T. 1987.

3.1.4 Mak, F.K. and M.D. Ilic. "Towards Most Effective Control of Reactive Power Reserves in Electric Machines."

3.1.5 Fitzgerald, A.E., Charles Kingsley Jr. and Stephen D. Umans. Electric Machinery. 4th ed. New York, NY: McGraw-Hill Book Company. 1983.

3.1.6 Kirtley, James L. Jr. "Per-Unit Reactances of Superconducting Synchronous Machinery." Electric Power Systems Engineering Laboratory. Cambridge, MA: M.I.T.

3.1.7 Krause, Paul C. Analysis of Electric Machinery. New York, NY: McGraw-Hill Book Company. 1986.

3.1.8 Matsch, Leander W. Electromagnetic & Electromechanical Machines. 2nd ed. Hagerstown, MD: Harper & Row, Publishers. 1977.

3.1.9 Weil, Susan. "Simulation of Inverter-Driven Six-Phase Synchronous Machines." Thesis, M.S. in E.E. M.I.T. October, 1987.

3.2 Composite System Stability Demon

As discussed in chapter 2, the structure which is present in commercial electric power systems is not present in naval electric power systems. Rather than having generators and loads connected through a series of transmission lines with their concomitant dynamics, naval electric power systems consist of generators and loads virtually directly connected. The coupling between mechanical components and electrical components, and among electrical components further distances the two types of electric power systems.

In fact, viewing naval electric power systems as composite systems comprised of numerous, contiguous components has a lot of appeal. This appeal is especially keen when one considers the frequent changes in configuration of naval electric power systems and the ensuing wide range of dynamics.

Composite systems are systems which are constructed of components which are connected to other components. This notion of components is aligned with the notion of the "device object" within WAVESIM. In the context of naval electric power systems, a component (or its "device object") is a distinct piece of equipment (or that equipment's model), such as a generator, motor, or a gas turbine. In an actual electric power system, the terminals of a component are directly connected to the terminals of other components. Within WAVESIM, the terminal variables of a "device object" are related to the terminal variables of other "device objects" in a way totally analogous to the terminals of the actual component.

A "stability demon" "device object" would correspond to an element within a supervisory level naval electric power system controller. The output of a "stability demon" provides information which is of great utility for a controller seeking to ensure stable transitions between operating points.

As envisioned for application to analysis of naval electric power systems, a "stability demon" takes as inputs the output of each component's "stability organ". A "stability organ's" output is the Lyapunov function and its convective derivative for the specific component. Given these inputs, the "stability demon" is tasked with providing a quantitative measure of the stability of the composite system.

The "stability demon" moves "large-signal" stability measures out of state space and into Lyapunov space. In a composite system where each component is represented by a high-order model, state space has a very large number of dimensions. Lyapunov space, on the other hand, has as many dimensions as the composite system has components. The bias of adopting this perspective is towards ensuring stability through a decentralised scheme. In other words, if components behave in a stable manner, then the composite system will behave in a stable manner.

3.2.1 Development of a Composite System Criterion

A composite system is a fitting way to model naval electric power systems. A composite system is made up of n components which are described in standard form. Each of the n components possesses n_i states. Each of the n state vectors can be described by a system of first order differential equations, (3.2.1).

$$\dot{\underline{x}}_i(t) = \underline{f}_i(\underline{x}_i(t), \underline{u}_i(t), t) \qquad \text{for} \quad i = 1 \ldots n \quad \text{and} \quad t \geq 0 \tag{3.2.1}$$

Some assumptions ensure that $\underline{f}_i$ does not behave poorly, reference [3.2.1]. Assume that $\underline{f}_i$ has a unique solution for all time including and subsequent to time zero. Assume too that each such unique solution corresponds to a unique initial condition. Further, the solution depends continuously upon initial condition. These assumptions are not overly restrictive. Physical systems rarely violate these assumptions.

Each component also possesses a Lyapunov function, V_i, which adequately describes its stability. This component Lyapunov function fulfills all of the requirements for a candidate Lyapunov function. These requirements are discussed in detail in section 3.1.1. To the point, V_i is continuously differentiable, and locally positive definite about equilibrium.

The convective derivative of the component Lyapunov function is negative semi-definite within a region surrounding equilibrium, which is interpreted as a region of stability.

This research adds another restriction to each component's Lyapunov function. A component Lyapunov function must be a function solely of that component's state variables. It must not be a function of a state variable of any other component. This requirement is imposed to allow component-wise differentiation of composite system Lyapunov functions. It is not restrictive, prohibiting 'shared-states' only. The interconnections between components can, should, and do appear in $\underline{f}_i$, equations (3.2.2) - (3.2.4). As the inputs are present in $\underline{f}_i$, they are present in the convective derivative of the component's Lyapunov function as well.

$$V_i = V_i(\underline{x}_i)$$

$$x_{i_k} \neq x_{j_l} \quad \forall \quad j \neq i \quad k \in n_i \quad l \in n_j \tag{3.2.2}$$

$$\underline{f}_i = \underline{f}_i(\underline{x}_i(t), \underline{u}_i(t), t) \qquad \text{for} \quad i = 1 \ldots n \quad \text{and} \quad t \geq 0$$

$$\underline{u}_i = \underline{u}_i(\underline{x}_1, \ldots, \underline{x}_{i-1}, \underline{x}_{i+1}, \ldots, \underline{x}_n, U(t)) \tag{3.2.3}$$

$$\dot{V}_i = \frac{\partial V_i}{\partial t} + \left(\overline{\nabla}_{\underline{x}_i} V_i(\underline{x}_i)\right) \cdot \underline{f}_i(\underline{x}_i, \underline{u}_i, t) \tag{3.2.4}$$

As mentioned in section 2.3.2.3, the means of determining composite system stability using a weighted-sum Lyapunov function or a Lyapunov function vector are somewhat similar. Reference [3.2.2], in its derivation of the vector criterion, uses its derivation of the weighted-sum criterion to a point. The weighted-sum criterion derivation includes the weighting factors, the α's . When the vector criterion derivation parts ways with the weighted-sum criterion derivation in reference [3.2.2], the authors of reference [3.2.2] dispense with the weighting factors by setting them equal to one.--This is interesting if one views the weighted-sum Lyapunov function as being related to the Lyapunov function vector. Let V_s denote the weighted-sum Lyapunov function and $\underline{V}_v$ the Lyapunov function vector. Define $\underline{\alpha}$ as the vector of the weights.

$$V_{ws} = \underline{\alpha}^T \cdot \underline{V}_v \tag{3.2.5}$$

This relationship, which is based on the definitions of the respective composite system Lyapunov functions, section 2.3, indicates that the weighted-sum Lyapunov function is the projection of the Lyapunov function vector in some direction. Development of a weighted-sum Lyapunov function in geometric terms allows reduction of "over sufficiency" in a composite system criterion.

Consider now Lyapunov function space. If each axis in an n dimensional space is assigned to the Lyapunov function of a specific component and since each of the n component Lyapunov functions is continuous, then the locus of points corresponding to the instantaneous values of the component Lyapunov functions represents the trajectory of the composite system through Lyapunov function space. Note, since all of the component Lyapunov functions are at least locally positive definite, the composite system trajectory through Lyapunov function space is usually confined to the 'first quadrant' of the space. Furthermore, the Lyapunov function itself is not the indicator of stability. Hence, little use is made of Lyapunov function space.

Of great interest, though, is Lyapunov function convective derivative space, or subsequently, just **Lyapunov space**.--It is distinct from Lyapunov **function** space, discussed above. Lyapunov space consists of a dimension assigned to each of the n components' Lyapunov function convective derivatives. Zero or negative values of a convective derivative indicate stability. Positive values indicate that stability cannot be concluded. Figure 3.2.1 shows a two dimensional Lyapunov space.

With this Lyapunov space in mind, a series of progressively less conservative composite system stability criterions is presented. Two dimensional Lyapunov space is used as an example because it's easily visualised. The results, though, are generalisable to higher dimensions with a corresponding increase in complexity.

Construct a vector of the convective derivatives of the components' Lyapunov functions. This Lyapunov function convective derivative vector, subsequently referred to as Lyapunov derivative vector, is shown in equation (3.2.6) and follows directly from the Lyapunov function vector discussed in section 2.3.

Figure 3.2.1 - Lyapunov Space (n=2 case)

$$\underline{\dot{V}}_v \equiv \begin{bmatrix} \dot{V}_1 \\ \cdot \\ \dot{V}_i \\ \cdot \\ \dot{V}_n \end{bmatrix} \tag{3.2.6}$$

An element-wise composite system stability criterion demands that all of the components' convective derivatives be non-positive. Hence, $\dot{V}_i \leq 0 \quad \forall i$ must be true for stability to be concluded. This criterion produces a region in Lyapunov space in which stability can be concluded. This stable region in Lyapunov space is shown in figure 3.2.2. The stable region is the cross-hatched, closed third quadrant in n=2 space.

If the trajectory of the Lyapunov derivative vector lies within the stable region, then stability of the composite system can be concluded.

In effect, the element-wise criterion states that each and every component must be stable for the entire system to be stable. If a single component has a positive Lyapunov derivative, does this imply that the composite system, taken as an entity, has gone unstable? No. It means that the stability of the composite system cannot be concluded.

Consider an example, the critical clearing time instability. If a generator is connected to a distribution system, then its failure to regain synchronism would be reflected in an increasing Lyapunov derivative. This one rogue generator would not make the composite system unstable if the inertia and reserve capacity of the entire system is large enough.

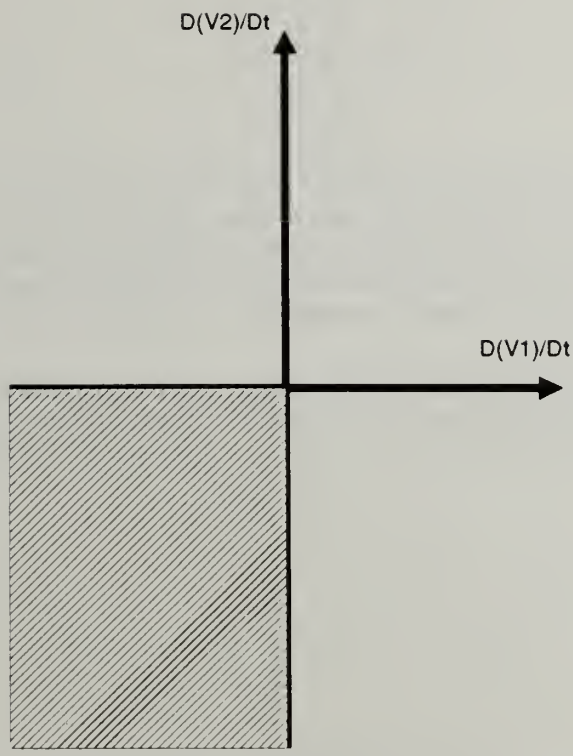

Figure 3.2.2 - Element-Wise Criterion Stable Region in Lyapunov Space (n=2)

It would appear that an element-wise criterion is too conservative, especially when compared with an alternative composite system criterion; this is because each subsystem must be autonomously stable to fulfill this criterion.

Define a composite system candidate Lyapunov function to be the "simple sum" of the components' Lyapunov functions, (3.2.7). Define the composite system state vector to be the vector of components' states, (3.2.8). Lastly, the composite system vector differential equation is a vector of the components' vector differential equations, (3.2.9). These definitions are enabled by the assumption that there are no shared states.

$$V_{ss} \equiv \sum_{i=1}^{n} V_i \tag{3.2.7}$$

$$\underline{x}_{CS} \equiv \begin{bmatrix} \underline{x}_1 \\ \cdot \\ \underline{x}_i \\ \cdot \\ \underline{x}_n \end{bmatrix} \tag{3.2.8}$$

$$\underline{f}_{CS} \equiv \begin{bmatrix} \underline{f}_1 \\ . \\ \underline{f}_i \\ . \\ \underline{f}_n \end{bmatrix} \tag{3.2.9}$$

This "simple sum" of the components' Lyapunov functions is at least a locally positive definite function of the composite system states because each of the components' Lyapunov functions are at least locally positive definite. Similarly, continuously differentiable component Lyapunov functions ensure that their sum is continuously differentiable. Hence, the "simple sum" composite system candidate Lyapunov function is legitimate.

To assess the stability of the composite system requires evaluating the convective derivative of the simple sum, equation (3.2.10). Note, going from line 2 to line 3 in equation (3.2.10) requires the assumption which prohibits shared states.

$$\begin{aligned} \dot{V}_{ss} &= \frac{\partial V_{ss}}{\partial t} + \left(\overline{\nabla}_{\underline{x}_{CS}} V_{ss}\right) \cdot \underline{f}_{CS} \\ &= \sum_{i=1}^{n} \frac{\partial V_i}{\partial t} + \sum_{i=1}^{n} \left(\overline{\nabla}_{\underline{x}_{CS}} V_i\right) \cdot \underline{f}_{CS} \\ &= \sum_{i=1}^{n} \frac{\partial V_i}{\partial t} + \sum_{i=1}^{n} \left(\overline{\nabla}_{\underline{x}_i} V_i\right) \cdot \underline{f}_i \\ &= \sum_{i=1}^{n} \dot{V}_i \end{aligned} \tag{3.2.10}$$

Composite system stability can be concluded if this convective derivative is non-positive, $\dot{V}_{ss} \leq 0$. This criterion has a straightforward geometric interpretation. Consider the n=2 case.

$$\begin{aligned} \dot{V}_{ss} &\leq 0 \\ 0 &\geq \dot{V}_1 + \dot{V}_2 \end{aligned} \tag{3.2.11}$$

The region in Lyapunov space where this "simple sum" criterion is fulfilled is shown cross-hatched in figure 3.2.3. If the trajectory of the Lyapunov derivative vector lies within the stable region, then stability of the composite system can be concluded.

The region where stability can be concluded is the closed half plane shown. For an n=3 system, the boundary of the stability region is a plane, the region itself a half space. This can be generalised into higher dimensions.

It is readily seen that the stability region arising from the "simple sum" criterion, figure 3.2.3, is larger than the stability region admitted by the element-wise criterion, figure 3.2.2. This indicates that the "simple sum" criterion is less conservative than the element-wise criterion.

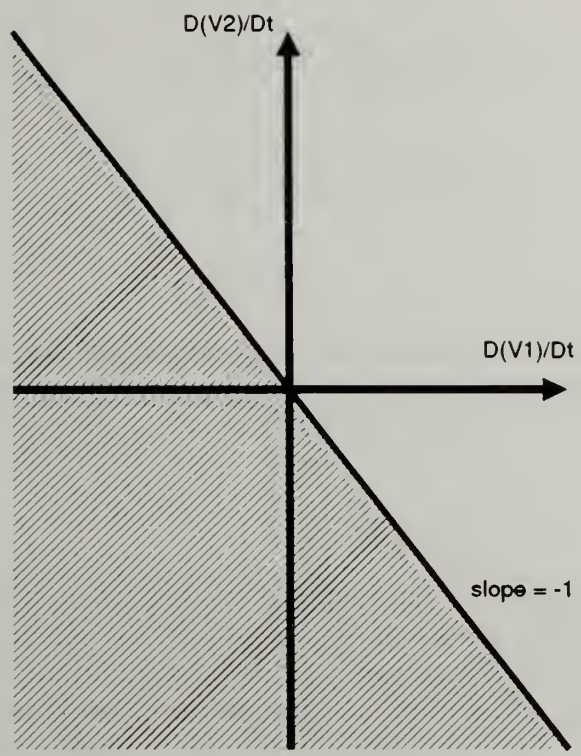

Figure 3.2.3 - "Simple Sum" Criterion Stable Region in Lyapunov Space (n=2)

An improvement in the conservativeness of the "simple sum" criterion is possible. The "simple sum" gives equal weight to all of the composite system components. Consider a weighted-sum criterion.--Its stability region is the same size as that of the "simple sum"; however, if something is known of the behaviour of the components' convective derivatives, then the location of the stable region is adjusted to accommodate the particular components' derivatives' behaviour. The weighted-sum composite system candidate Lyapunov function is defined in equation (3.2.12).

$$V_{ws} \equiv \underline{\alpha}^T \cdot \underline{V}_v \equiv \sum_{i=1}^{n} \alpha_i V_i \qquad (3.2.12)$$

Let the weighting factors, α's , be constants. Whereas the components' Lyapunov functions are continuously differentiable and the α's are constant, the weighted-sum composite system candidate Lyapunov function is continuously differentiable as well. For the candidate Lyapunov function to be positive definite, the α's must be positive and non-zero. Hence, all of the elements of the weighting factor vector, $\underline{\alpha}$, are positive, non-zero constants. If $\underline{\alpha}$ is plotted in Lyapunov space, it will lie in the open 'first quadrant'.

With a constant weighting vector which lies within the open 'first quadrant' of Lyapunov space, the weighted-sum composite system candidate Lyapunov function is seen to be a valid candidate Lyapunov function. To assess stability, its convective derivative must be evaluated.

$$\dot{V}_{ws} = \frac{\partial V_{ws}}{\partial t} + \left(\overline{\nabla}_{\underline{x}_{CS}} V_{ws}\right) \cdot \underline{f}_{CS}$$

$$= \sum_{i=1}^{n} \alpha_i \frac{\partial V_i}{\partial t} + \sum_{i=1}^{n} \alpha_i \left(\overline{\nabla}_{\underline{x}_{CS}} V_i\right) \cdot \underline{f}_{CS}$$

$$= \sum_{i=1}^{n} \alpha_i \frac{\partial V_i}{\partial t} + \sum_{i=1}^{n} \alpha_i \left(\overline{\nabla}_{\underline{x}_i} V_i\right) \cdot \underline{f}_i$$

$$= \sum_{i=1}^{n} \alpha_i \dot{V}_i \qquad (3.2.13)$$

Composite system stability can be concluded if this convective derivative is non-positive, $\dot{V}_{ws} \leq 0$. Just as with the "simple sum" criterion, this criterion has a straightforward geometric interpretation. Consider the n=2 case.

$$\dot{V}_{ws} \leq 0$$

$$0 \geq \alpha_1 \dot{V}_1 + \alpha_2 \dot{V}_2 \qquad (3.2.14)$$

Given a weighting vector $\underline{\alpha}$ in the 'first quadrant' of Lyapunov space, if the Lyapunov derivative vector trajectory lies within the closed half-space defined by a plane perpendicular to $\underline{\alpha}$ and passing through the origin on the side of the plane opposite $\underline{\alpha}$, then stability can be concluded. The region in Lyapunov space where this weighted-sum criterion is fulfilled is shown in figure 3.2.4.

The region where stability can be concluded is the closed half plane shown. This can be generalised into higher dimensions in the same way as the "simple sum" criterion.

As stated, the size of the stability regions are the same for the "simple sum" and weighted-sum criterions. The only advantage derived from using the weighted-sum criterion is rotating the stability region so that the trajectory of the Lyapunov derivative vector remains within the weighted-sum stability region where it would have exited the "simple sum" stability region. The difficulty with this, though, is that something of the behaviour of the Lyapunov derivative vector must be known a priori so that acceptable weighting factors can be chosen.

An "indeterminately-weighted-sum" composite system Lyapunov function criterion uses the behaviour of the trajectory of the Lyapunov derivative vector to determine that a constant weighting vector exists such that the trajectory remains within the stable region of the "indeterminately-weighted-sum" criterion. Consider the two dimensional situation posed in figure 3.2.5.

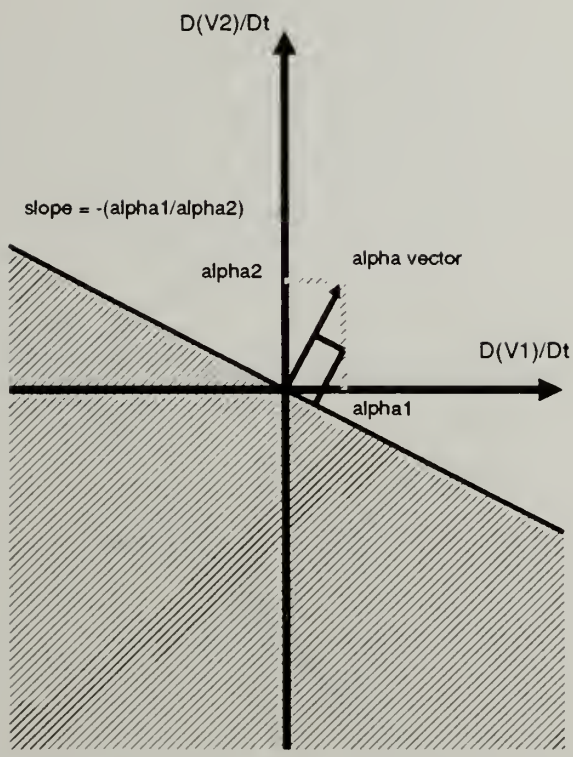

Figure 3.2.4 - Weighted-Sum Criterion Stable Region in Lyapunov Space (n=2)

The curve C in figure 3.2.5 is the trajectory of the Lyapunov derivative vector during some dynamic event. The two dashed lines, A and B, are either tangent to C or bound C and pass through the origin. If C does not enter the closed 'first quadrant', ξ or $\zeta \leq 0$, and the angle subtended by A and B, γ, does not exceed the value of π, then it can be shown that a constant weighting vector, $\underline{\alpha}$, which lies in the open 'first quadrant', exists such that $\dot{V}_{ws} \leq 0$, allowing stability to be concluded.

The "indeterminately-weighted-sum" criterion's stability region is no larger than the "simple sum" or weighted-sum criterions'. It does obviate the need to calculate appropriate weighting factors a priori. For more than two dimensions, though, the angle subtended by C, γ, becomes a solid angle.

Finally, let the weighting vector vary with time. Retain the requirement that the weighting vector be positive and non-zero. This ensures that $V_{ws}(\underline{0}) = 0$. Add the requirement that the time derivative of the weighting vector exists.

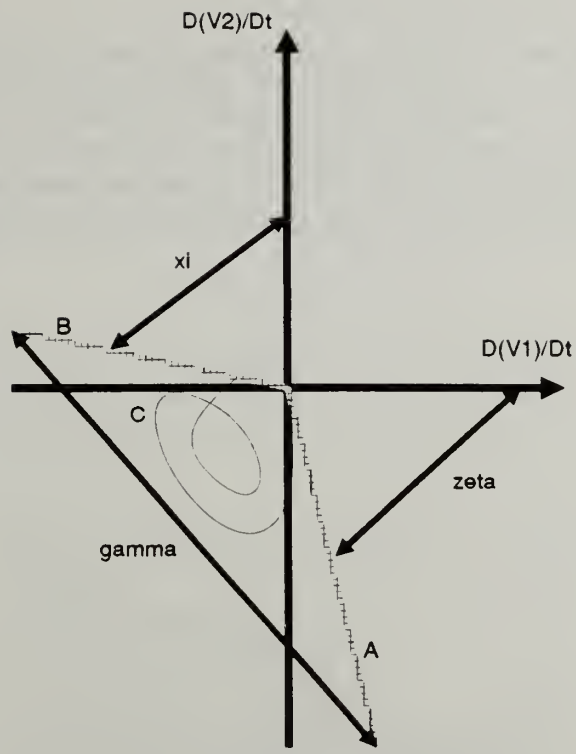

Figure 3.2.5 - "Indeterminately-Weighted-Sum" Criterion in Lyapunov Space (n=2)

$$\underline{\alpha} = \underline{\alpha}(t)$$

$$\alpha_i(t) > 0 \quad \forall i = 1 \ldots n \quad \forall t \geq 0 \tag{3.2.15}$$

The "time-variant weighted-sum" composite system candidate Lyapunov function is identical in form to the weighted-sum composite system Lyapunov function.

$$V_{ws} \equiv \underline{\alpha}^T(t) \cdot \underline{V}_v \equiv \sum_{i=1}^{n} \alpha_i(t) V_i(\underline{x}_i, t) \tag{3.2.16}$$

For the "time-variant weighted-sum" composite system candidate Lyapunov function to be a valid candidate function, $\underline{\alpha}(t)$ must be continuously differentiable, positive and non-zero. Assuming that this is true, evaluation of the convective derivative of the time-variant weighted-sum must be performed.

$$\dot{V}_{ws} = \sum_{i=1}^{n} \alpha_i \left\{ \frac{\partial V_i}{\partial t} + \left(\overline{\nabla}_{\underline{x}_{CS}} V_i \right) \cdot \underline{f}_{CS} \right\} + V_i \cdot \frac{d\alpha_i}{dt}$$

$$= \sum_{i=1}^{n} \alpha_i \dot{V}_i + V_i \dot{\alpha}_i \tag{3.2.17}$$

Where the convective derivative of the time-variant weighted-sum is less than or equal to zero, stability is concluded. For an n=2 case, it is easy to see that the convective derivative yields a stability region larger than the weighted-sum criterion stability region.

$$\dot{V}_{ws} \leq 0$$

$$0 \geq \alpha_1 \dot{V}_1 + V_1 \dot{\alpha}_1 + \alpha_2 \dot{V}_2 + V_2 \dot{\alpha}_2 \qquad (3.2.18)$$

Figure 3.2.6 shows the stability region for the "time-variant weighted-sum" criterion. Two things should be noted. First, the stability region is an instantaneous region. It changes continuously. Figure 3.2.6 amounts to a "snapshot". The slope of the boundary line varies with time as does the y-intercept of the boundary line, $\Sigma(t)$. Second, the Lyapunov derivative vector can lie within a small portion of the 'first quadrant' and still yield a weighted-sum which is non-positive. This is a significant expansion of the region of stability.

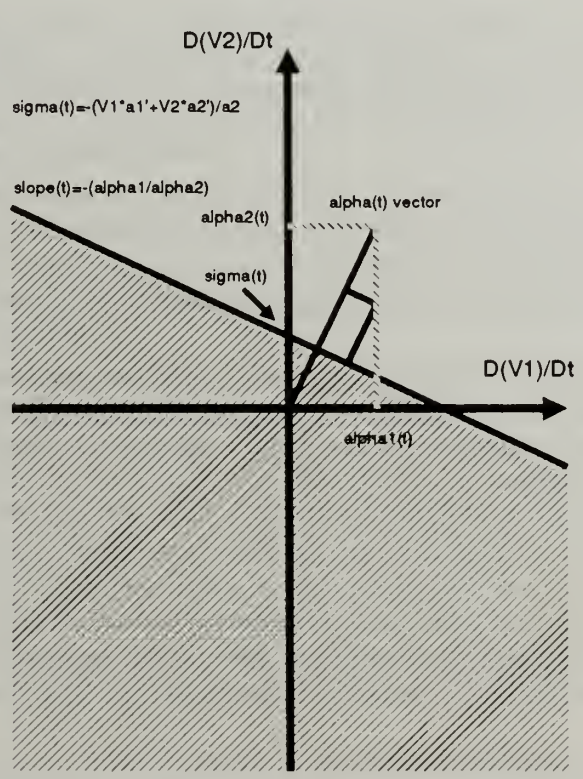

Figure 3.2.6 - "Time-Variant Weighted-Sum" Criterion in Lyapunov Space (n=2)

Two items are important here. The weighting factors, now time-variant, are still constrained to be positive and non-zero. This ensures the positive definiteness of the "time-variant weighted-sum" Lyapunov function. The weighting factors must also be continuously differentiable. This ensures that the "time-variant weighted-sum" Lyapunov function is continuously differentiable. These two items must be true for the "time-variant weighted-sum" Lyapunov function to be a valid candidate. Where these two items are true, the stability region shown in figure 3.2.6 is legitimate.

When selecting a composite system stability criterion for use within a "stability demon", the least conservative criterion is desired. Hence, the last criterion presented, the "time-variant weighted-sum" criterion is adopted for use within this research's "stability demon".

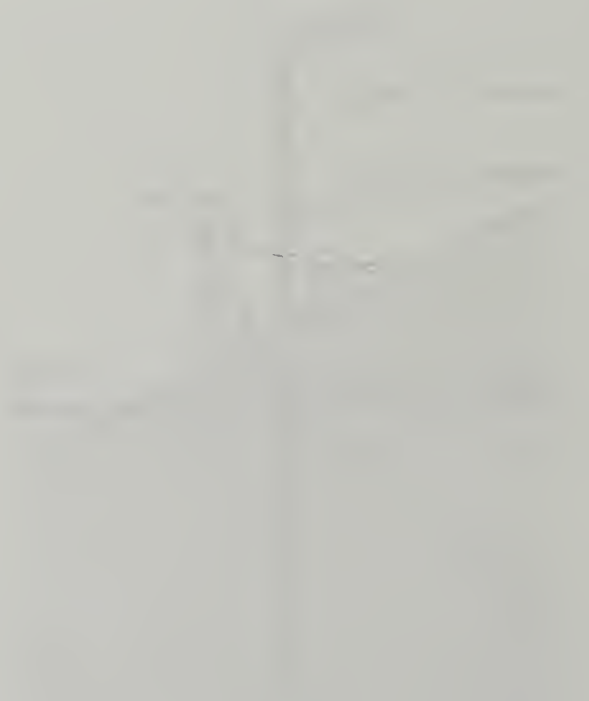

3.2.2 Time-Variant Weighting Vector Issues

The foregoing section establishes the "time-variant weighted-sum" composite system criterion. Here, its implementation as a stability measure is discussed.

Adopting the "time-variant weighted-sum" composite system criterion gives rise to the big issue of choosing the time-variant weighting factors. Examination of the convective derivative of the "time-variant weighted-sum" Lyapunov function shows that there is one equation, (3.2.19), and n unknown $\alpha(t)$'s , and their derivatives. This situation implies that there is a great deal of latitude in selecting $\alpha(t)$'s , provided that they meet the requirements stated in the previous section.

$$0 \geq \dot{V}_{WS} = \sum_{i=1}^{n} \alpha_i \dot{V}_i + V_i \dot{\alpha}_i \tag{3.2.19}$$

The goal of selecting the weighting factors is to expand, to the greatest extent possible, the region of stability. This reduces "over sufficiency". The best means of doing this is not obvious. One means of choosing weighting factors is discussed in detail in this section. This means of finding weighting factors illustrates the issues germane to other means of finding weighting factors.

The first question when pondering how to select the $\alpha(t)$'s is related directly to their use. If the "time-variant weighted-sum" criterion is used solely for a qualitative description of stability, then it is enough to show that valid $\alpha(t)$'s exist. Hence, algorithms would have to search for the weighting factors until they are found or it can be concluded that they do not exist.

In a situation where the composite system is unstable, the algorithm representing the "time-variant weighted-sum" criterion must conclude that no valid $\alpha(t)$'s exist. If the system is on the verge of instability, then finding a systematic way of evaluating the existence of valid weighting factors is very difficult. Such an algorithm could be expected to be very slow and hence unsuitable in a stabilising control environment.

An alternative to the foregoing, if the weighting factors are used for a quantitative characterisation, then a better approach may be to calculate the $\alpha(t)$'s using some pre-selected method. If the pre-selected method provides valid weighting factors, then stability is concluded. Otherwise, the invalid $\alpha(t)$'s indicate that an interpretation that stability cannot be concluded may be acceptable or that a higher-level search must be initiated.

One way of looking at the convective derivative of the time-variant weighted-sum is to see how each component contributes to the weighted-sum. If all of the components' contributions were negative or zero, then the time-variant weighted-sum convective derivative would be less than or equal to zero, indicating stability. Consider the case where each component's contribution to the time-variant weighted-sum is zero. This is the "component neutral" relationship. Equation (3.2.20) defines the contribution of a given component, Ξ_i , to the time-variant weighted-sum's convective derivative.

$$\Xi_i \equiv \alpha_i \dot{V}_i + V_i \dot{\alpha}_i \tag{3.2.20}$$

The "component neutral" relationship sets Ξ_i equal to zero then solves for the $\alpha_i(t)$. If such an $\alpha_i(t)$ exists and meets the requirements for the weighting factors, then the i^{th} component will contribute zero to the composite system's convective derivative.

$$\Xi_i = 0$$

$$0 = \alpha_i \dot{V}_i + V_i \dot{\alpha}_i$$

$$= \frac{\dot{\alpha}_i}{\alpha_i} + \frac{\dot{V}_i}{V_i} \qquad (3.2.21)$$

The final step in equation (3.2.21), division by the product $\alpha_i(t)V_i(t)$, is valid only if $V_i(t)$ is not equal to zero. $\alpha_i(t)$ is non-zero by design. Following the division, integrate (3.2.21) with respect to time.

$$\ln(\alpha_i) + \ln(V_i) = \delta_i$$

$$\therefore \quad \alpha_i = \frac{e^{\delta_i}}{V_i} \qquad (3.2.22)$$

This relationship yields a positive, non-zero weighting factor which makes Ξ_i equal to zero, for non-zero V_i. The term δ_i is the constant which arises from the integration of equation (3.2.21). The value of this constant does have some implications.

Equation (3.2.22) offers an interpretation of the role of the $\alpha(t)$'*s* . Without a weighting factor, a positive convective derivative means that the i^{th} component makes a destabilising contribution to the time-variant weighted-sum. The $\alpha(t)$'*s* can buffer the effect of increasing Lyapunov functions by decreasing. The weighting factors may decrease only so much before they become zero, or negative.--This may be interpreted as a loss of stability. Hence, the $\alpha(t)$'*s* behave like a sort of "stability reserve". If the convective derivative becomes positive, the weighting factor can counteract the destabilising effect, within bounds.

Of immediate concern though, the $\alpha_i(t)$, which results from the "component neutral" relationship, and its derivative are discontinuous for $V_i(t)$ equal to zero. $\alpha_i(t)$ is continuously differentiable; however, all of its derivatives have the same single, isolated, infinite discontinuity. Consideration of $\dot{V}_i(t)$ offers some insight into the role of this discontinuity in the weighting factor and its derivative.

$V_i(t)$ is at least locally positive definite. This means that $V_i(t)$ equal to zero is at least a local minima. Hence, its derivative at that point will always equal zero. Consequently, for $\alpha_i(t)$'s discontinuity point, both terms on the right hand side of equation (3.2.20) are the product of an infinite discontinuity and zero. Temporarily putting aside the weighting factor, the fact that the convective derivative of the component's Lyapunov function is zero at that point is an argument for interpreting the point of discontinuity as being benign.

The constant term δ_i warrants some discussion. In fact, the exponential of this constant plays a role in the "time-variant weighted-sum" Lyapunov function. Equation (3.2.23) shows that the exponential of δ_i is the i^{th} component's contribution to the composite Lyapunov function itself.

$$V_{ws} = \sum_{i=1}^{n} \alpha_i(t) V_i(\underline{x}_i, t)$$

$$= \sum_{i=1}^{n} e^{\delta_i} \qquad (3.2.23)$$

One means of choosing a value for this constant is to decide how much the i^{th} component is going to participate in the "time-variant weighted-sum" Lyapunov function and calculate δ_i accordingly.

The discontinuity at zero values of $V_i(t)$ and the existence of δ_i pose serious problems if the "component neutral" relationship is offered as a closed form means of finding weighting factors. For V_{ws} to be a valid candidate Lyapunov function, it must be locally positive definite; hence, $V_{ws}(\underline{0}) = 0$. The exponential of δ_i is always non-zero. This leads to the characterisation of V_{ws} for an n=1 state space shown in figure 3.2.7.

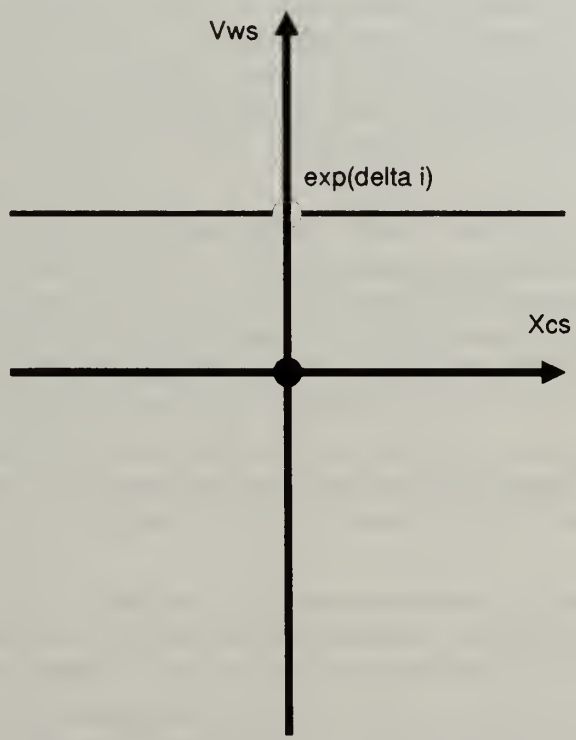

Figure 3.2.7 - The "Component Neutral"'s Lyapunov Function (n=1)

Examining a proof of Lyapunov's direct method, reference [3.2.3], indicates that the discontinuity at zero disqualifies V_{ws} as a candidate Lyapunov function. Hence, any characterisations it provides cannot be trusted. The "component neutral" relationship, by itself, does not yield an appropriate "time-variant weighted-sum" Lyapunov function. It is possible, though, to use the "component neutral" relationship in conjunction with other functions to splice together a suitable time-variant weighting vector.

A "component neutral"-based weighting factor, which makes a component's contribution to the "time-variant weighted-sum" convective derivative equal to zero, has a control implication. Namely, by monitoring only its states, a component's controller can ensure that its contribution toward the composite system's stability is neutral as long as the controller can keep the component within a region of its own state space where the "component neutral" relationship exists.

The "component neutral" relationship ensures conditions under which the "time-variant weighted-sum" Lyapunov function is stationary. This amounts to concluding that the composite system is not moving any farther away from an equilibrium than it already is. In other words, things are not getting worse. This is the case when limit cycles are reached.

Concluding that the composite system is converging towards an equilibrium, asymptotic stability, requires more strenuous conditions than the "component neutral" relationship. The "component neutral" relationship needs the component's Lyapunov function to be continuously differentiable and locally positive definite so that finite escape times are avoided. The composite system's "time-variant weighted-sum" Lyapunov function must possess weighting factors which are continuously differentiable for the same reason.

To show that a composite system is asymptotically stable, at least one component's contribution to the time-variant weighted sum, Ξ_i, must be negative. To expand the stability region of the composite system to the greatest degree possible, which attacks the very heart of the "over sufficiency" issue, should be the guiding principle in the construction of the weighting factors. Choosing $\alpha_i(t)$ to yield a desired Ξ_i would be the job of a "stability demon".

The choice of $\alpha_i(t)$, or a resultant $\alpha_i(t)$, offers a variable for control targeting. Suppose the system controller seeks to ensure that all components are operating as close as possible to the 'third quadrant' in Lyapunov space.--This is the case when all the components are behaving in a stable manner. In this instance, the system controller would produce commands driving the Lyapunov functions and their derivatives so that the resultant $\alpha_i(t)$'s approach 1 and $\dot{\alpha}_i(t)$'s approach 0.

In another control application, suppose that all of the component Lyapunov functions are energy related. Cost optimisations combined with stability requirements may dictate that the controller accept any range of values for $\alpha_i(t)$'s as long as they are nearly constant in time.

It is a simple thing to visualise other scenarios where a system controller could use the information provided by derived weighting factors. Specific relationships for deriving $\alpha_i(t)$'s, given the Lyapunov function and its derivative will arise from specific applications. These relationships, though, must provide $\alpha_i(t)$'s which ensure the legitimacy of the time-variant weighted-sum as a Lyapunov function.

3.2.3 Stability Demon Algorithms

The first "stability demon" developed uses the "component neutral" relationship with allowances for its discontinuity to generate the weighting factors for each component. This provides n equations for n unknowns, the $\alpha_i(t)$'s.

The δ_i'*s* are declared like an initial condition. If the components' Lyapunov functions are energies, then the sum of the exponentials of the δ_i'*s* is the composite system's initial total energy. While the energy may vary with time, the "time-variant weighted-sum" Lyapunov derivative will be constant because it is zero by design.

Implementation of a "component neutral"-based relationship in a WAVESIM "stability demon" encounters three numerical issues. The "component neutral" relationship itself is simple, (3.2.21). However, as equation (3.2.24) shows, α_i is an exponential function of time. WAVESIM can represent variables' waveforms as a series of polynomials. The exponential function has an infinite polynomial series representation. WAVESIM's use of truncated series introduces harmonic distortion.

$$\alpha_i = e^{(\delta_i - \ln V_i)} \tag{3.2.24}$$

This raises issue two. The natural logarithm of the Lyapunov function, or the Lyapunov function as a denominator (3.2.22), does not exist when the Lyapunov function equals zero. This singularity would cause numerical routines to "blow up". As with any numerical computation, WAVESIM solves equations to a desired accuracy, an ε. The algorithms treat numbers whose absolute value is less than ε as being zero.

The final issue is one of simplicity. At least initially, testing the viability of a "component neutral"-based relationship for calculating α'*s* is most easily performed in a manner akin to discrete time methods, WAVESIM's data series waveforms.

3.2.4 References

3.2.1 Vidyasagar, M. Nonlinear System Analysis. Englewood Cliffs, New Jersey: Prentice-Hall, Inc. 1978.

3.2.2 Michel, A.N. and D.W. Porter. "Stability Analysis of Composite Systems." IEEE Transactions on Automatic Control. Vol. 17. April 1972. pp. 222-226.

3.2.3 Wyatt, J. "Qualitative Dynamics of Autonomous Differential Equations. Part I: Closed Orbits and Part II: Stability of Equilibria Via Lyapunov Functions." Lectures 21 & 22. Unpublished Paper from Lectures on Nonlinear Circuit Theory. VLSI Memo No. 84-158. M.I.T., Cambridge, MA. August 1984.

4 Performance of Stability Organ and Stability Demon

This chapter contains results provided by the synchronous generator "stability organ" and the "stability demon". Test cases are presented to both and the results provide a measure of their efficacy.

4.1 Assessment of the Coenergy-Based Stability Organ

The "stability organ" which is developed in section 3.1 is implemented in the form of equations within a synchronous generator "device object". These equations produce output waveforms at information terminals within a WAVESIM simulation. Both the model of the synchronous machine and the "stability organ" equations which are discussed in section 3.1 are shown in a listing of the synchronous generator "device objects" in appendix A.

The output of the "stability organ" during several scenarios illustrates its usefulness with regards to monitoring dynamic behaviour. Lastly, the "stability organ's" prediction of critical clearing time for a specific fault is compared with critical clearing times obtained by other methods.

4.1.1 Steady-State Behaviour

Table 4.1.1 - Example Generator Parameters

Parameters are taken from example machine in reference [4.1].

d-axis mutual reactance	xad	1.8	pu
q-axis mutual reactance	xaq	1.6	pu
stator leakage reactance	xal	0.2	pu
field leakage reactance	xfl	0.225	pu
d-axis damper leakage	xkdl	0.0	pu
q-axis damper leakage	xkql	0.0	pu
stator resistance	rs	0.0177	pu
field resistance	rf	0.00107	pu
d-axis damper resistance	rkd	0.00265	pu
q-axis damper resistance	rkq	0.0212	pu
inertia constant	H	3.0	sec
damping constant	B	0.0	N-m-sec
pole pairs	PP	1	
machine base voltage	VB	367.4	Volts, peak, l-n
machine base power	PB	625000.0	Watts
base frequency	wB	377.0	1/sec
system base voltage	VsB	367.4	Volts, peak, l-n
system base power	PsB	625000.0	Watts

Table 4.1.2 - Steady-State Initial Conditions

d-axis current	id_0	-1.1476	pu
q-axis current	iq_0	-0.4279	pu
"o" current	io_0	0.0	pu
field current	ifd_0	1.8172	pu
d-axis damper current	ikd_0	0.0	pu
q-axis damper current	ikq_0	0.0	pu
rotor electrical angle	θ_{re}	-0.8737	
terminal voltage	vt	0.827	pu
rotor mechanical speed	ω_{rm}	377.0	1/sec
mechanical torque input	Tm	0.85	pu
field voltage	vfd	0.00194	pu

Under steady-state conditions, the "stability organ's" underlying Lyapunov function, the sum of the coenergy and the base energy scaled inertial energy, should be stationary. The constant mechanical power into the generator balances the electric power out and the losses. The machine parameters and initial conditions for this simulation are shown in tables 4.1.1. and 4.1.2. The mechanical torque and field voltage inputs to the generator are held constant.

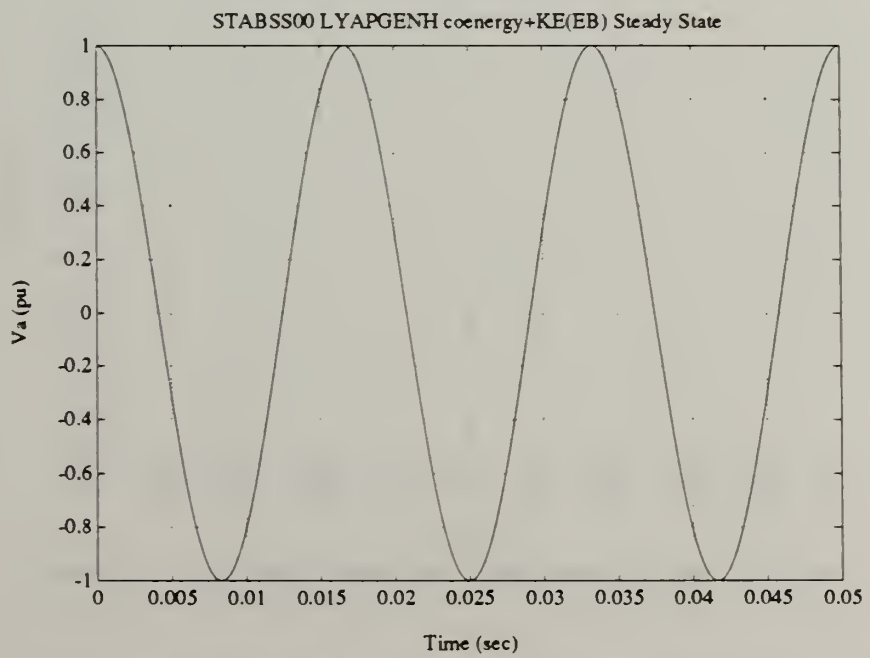

Figure 4.1.1 - Steady-State a-Phase Voltage vs. Time

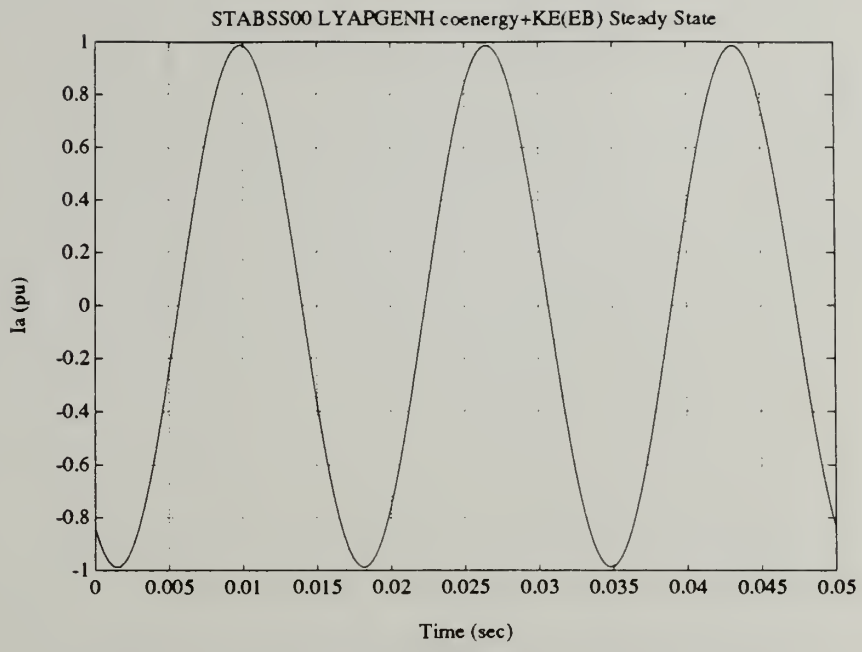

Figure 4.1.2 - Steady-State a-Phase Current vs. Time

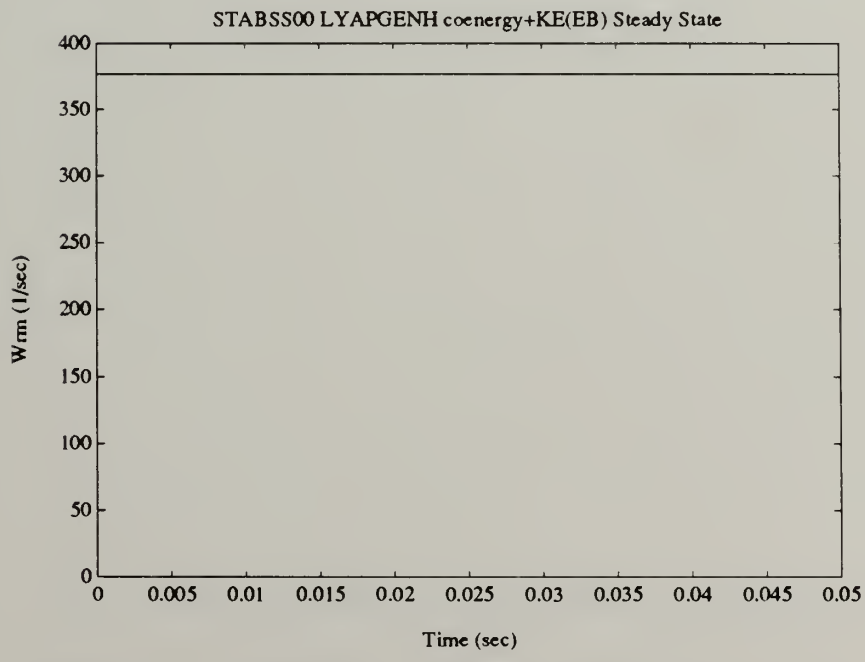

Figure 4.1.3 - Steady-State Rotor Mechanical Speed vs. Time

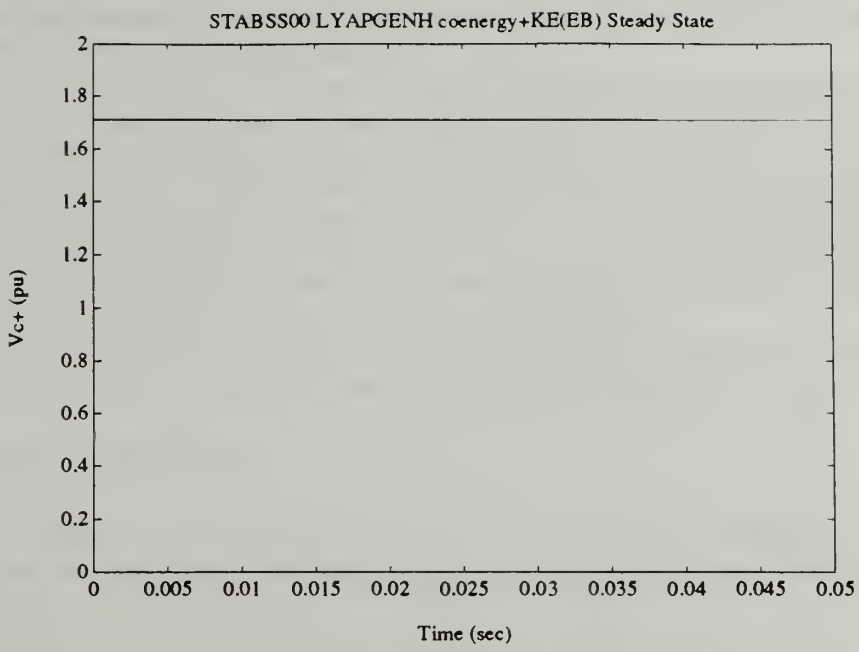

Figure 4.1.4 - Steady-State Lyapunov Function vs. Time

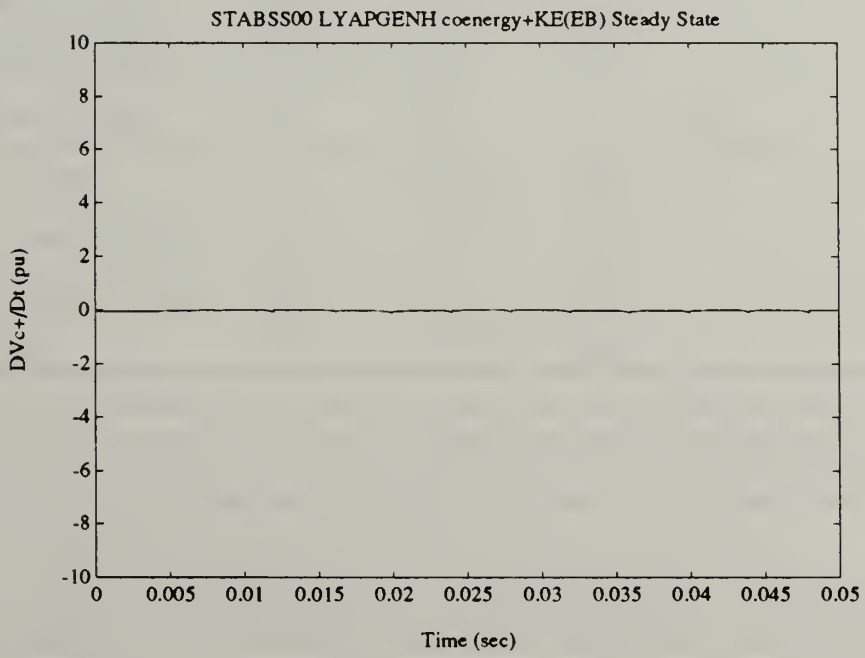

Figure 4.1.5 - Steady-State Lyapunov Derivative vs. Time

In this steady-state simulation, the synchronous generator is supplying rated voltage and current to an infinite bus at 0.85 power factor. All the quantities have been per-unitised as discussed in section 3.1. Figures 4.1.1, 4.1.2 and 4.1.3 all correspond to steady-state for the given load conditions.

Figure 4.1.4 shows the Lyapunov function, coenergy plus scaled inertial energy, produced by the "stability organ" within the generator's "device object". As one would expect for steady-state behaviour, this quantity is stationary in time. The second output of the "stability organ" is the Lyapunov function's convective derivative, figure 4.1.5. This quantity is taken to be the indicator of stability. In this case, it is constant and zero. Hence, stability can be concluded. Figure 4.1.5 contains very small periodic 'notches'. These notches arise from using a truncated Legendre series to represent the perfect sinusoids which are found in steady-state conditions.

The issues of the inputs to the convective derivative, section 3.1.2.8, and time-scale dynamics, 3.1.3.1, are not relevant to steady-state conditions.

4.1.2 Short-Circuit Behaviour

Table 4.1.3 - No-Load Short-Circuit Initial Conditions

d-axis current	id_0	0.0	pu
q-axis current	iq_0	0.0	pu
"o" current	io_0	0.0	pu
field current	ifd_0	0.6799	pu
d-axis damper current	ikd_0	0.0	pu
q-axis damper current	ikq_0	0.0	pu
rotor electrical angle	θ_{re}	0.0	
terminal voltage	vt	0.827	pu
rotor mechanical speed	ω_{rm}	377.0	1/sec
mechanical torque input	Tm	0.0	pu
field voltage	vfd	0.000727	pu

During a symmetrical fault, the three phase terminals of the generator are shorted together. The flux trapped by the stator windings and the flux trapped by the rotor windings give rise to oscillating stored energy levels and oscillating electromagnetic torques, which eventually die away. The small resistances of the stator windings dissipate the trapped flux arising from the stator currents very slowly.

Two short-circuit simulations are shown here. In the first simulation, an unloaded generator is subjected to a symmetric 3-phase fault at time zero. The mechanical torque input to the generator is held constant at zero. This corresponds to the open-circuit, no-load condition. The field voltage is also constant such that the excitation voltage, e_{af}, is unity. Per-unitisation follows section 3.1. The machine parameters for this case are the same as those in table 4.1.1. Initial conditions for this simulation are shown in table 4.1.3.

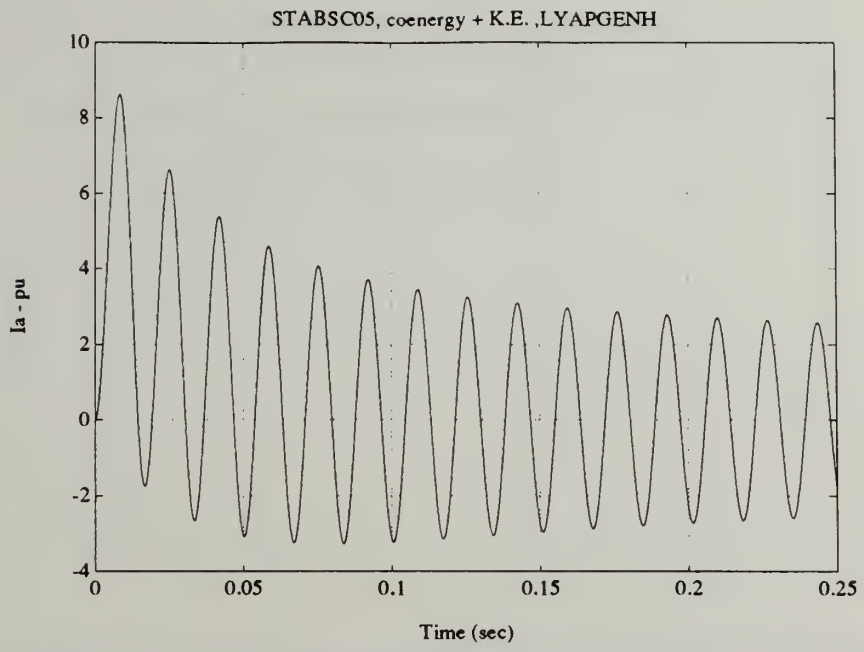

Figure 4.1.6 - No-Load Short-Circuit a-Phase Current vs. Time

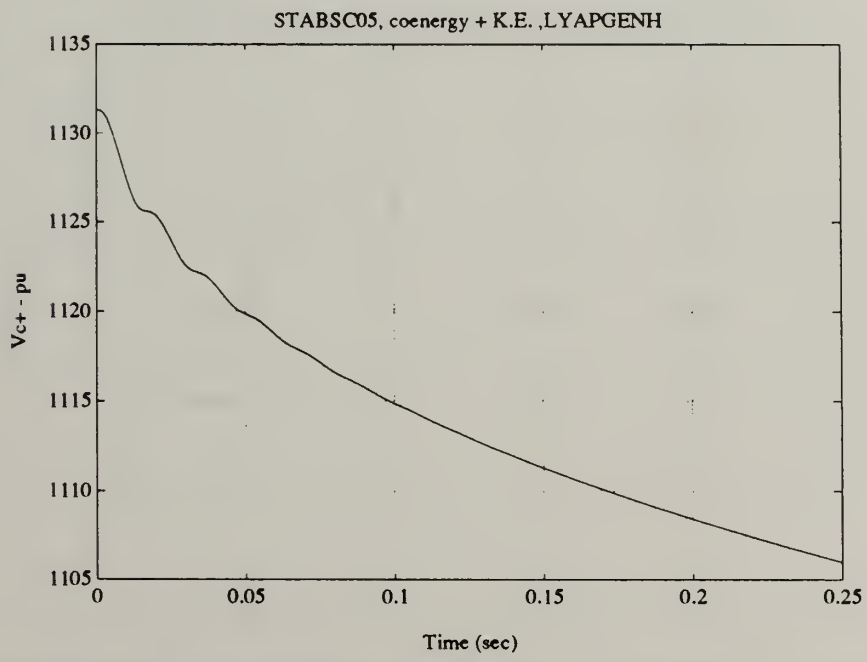

Figure 4.1.7 - No-Load Short-Circuit Lyapunov Function vs. Time

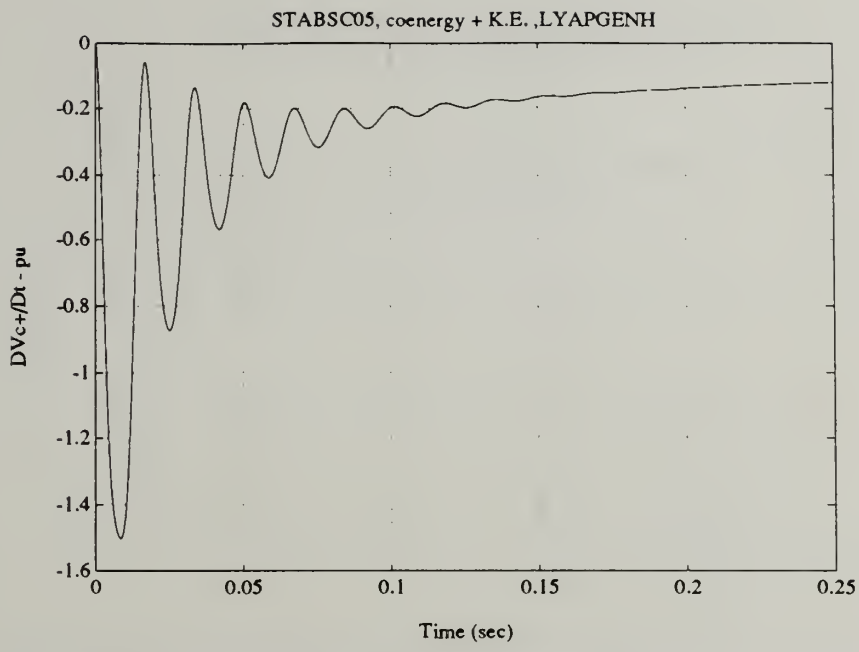

Figure 4.1.8 - No-Load Short-Circuit Lyapunov Derivative vs. Time

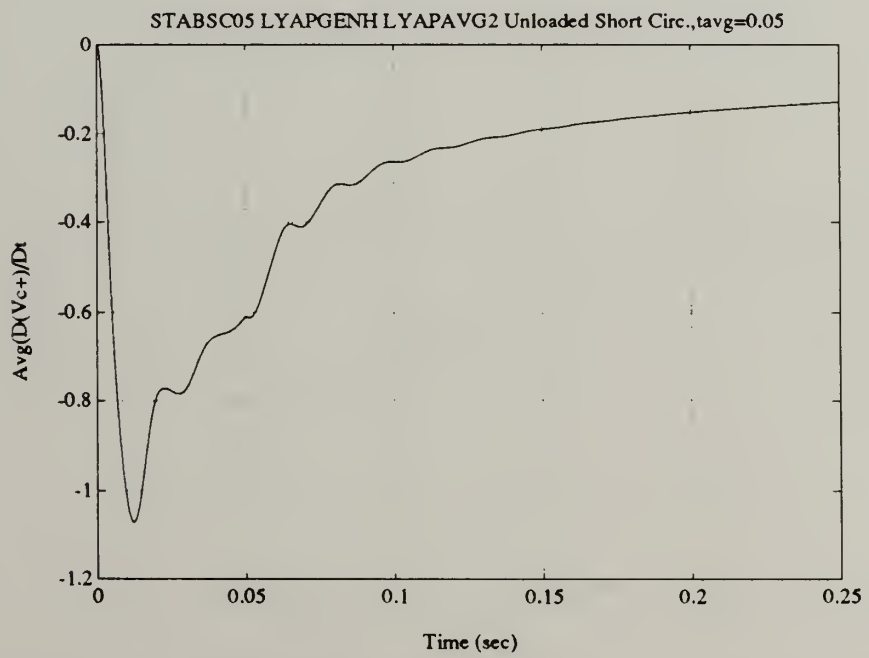

Figure 4.1.9 - No-Load Short-Circuit Averaged Lyapunov Derivative vs. Time (T_{avg} = 0.05 sec)

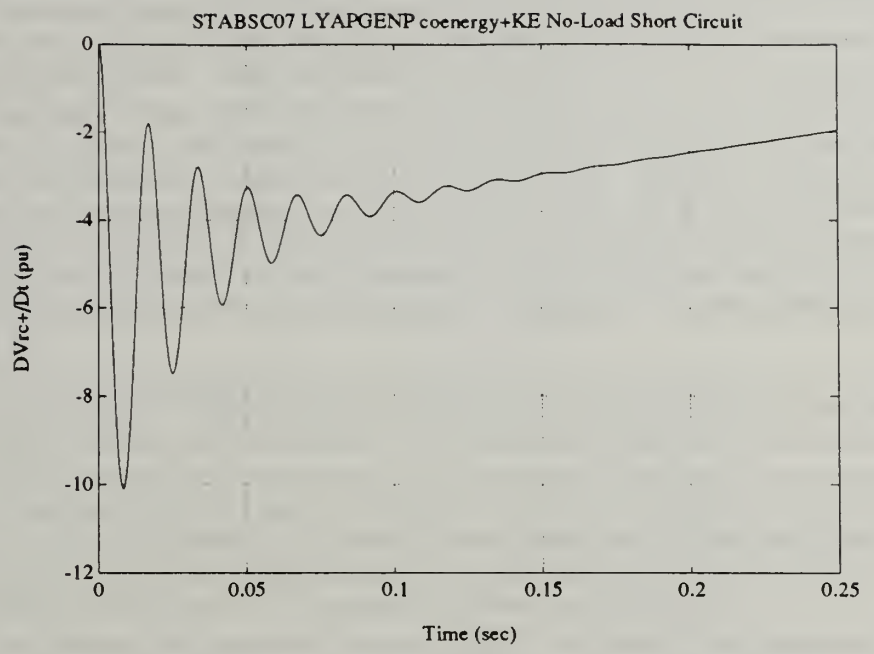

Figure 4.1.10 - No-Load Short-Circuit "Re-connected" Lyapunov Derivative vs. Time

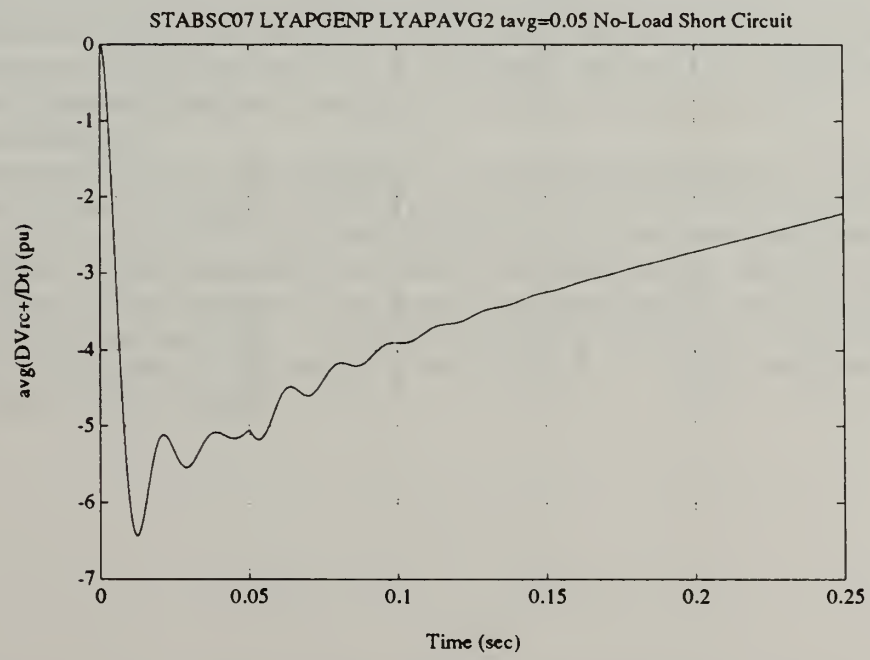

Figure 4.1.11 - No-Load Short-Circuit Averaged "Re-connected" Lyapunov Derivative vs. Time (T_{avg} = 0.05 sec)

The short-circuit current, figure 4.1.6, agrees with accepted short-circuit results, references [4.1] and [4.2]. The decrease in stored-energy depicted by the decreasing Lyapunov function, figure 4.1.7, reflects the fact that there is zero mechanical power input to and zero electric power output from the generator as it dissipates electric power in its winding resistances. This dissipated energy must come from stored energy.

The "stability organ" shown for this first short-circuit simulation is the coenergy plus the inertial energy. See equation (3.1.66). For this simulation, this particular "stability organ" demonstrates a stable response, figure 4.1.8. The other inertial terms did not produce so obviously negative a convective derivative. Both the speed difference kinetic energy relationship, (3.1.67), the base energy normalised kinetic energy relationship, (3.1.68), and the others as well, possessed convective derivatives which were dominated by the large electromagnetic energy oscillations.--See the discussion in section 3.1.3.1.

The time-scale averaging discussed in section 3.1.3.1 is applied to the Lyapunov derivative output of the "stability organ", figure 4.1.9 and figure 4.1.11. An averaging window of 0.05 seconds is used because it is somewhat longer than the armature time constant, 0.03 seconds. In this instance, the time-scale averaging attenuates the amplitude of oscillations, which is seen by comparing figures 4.1.8 and 4.1.9 and figures 4.1.10 and 4.1.11. The envelope of the electromagnetic oscillations has a time constant on the order of the armature time constant. The averaging function is carried out by a routine called LYAPAVG2.m. This routine is listed in Appendix A.

Two versions of the generator "device object", one which uses actual terminal voltages and one which uses "re-connected" voltages (This is discussed in section 3.1.2.8.), are used with this simulation. The nature of the convective derivative of the Lyapunov function is different for these two cases, the "re-connected" version providing the better transient stability (critical clearing time) information, figure 4.1.10. If its behaviour, isolated from the rest of the system, is of interest, the version which uses the actual terminal voltages accurately portrays the generator's stored energy. The generator "device object" which contains the "re-connected" version of the convective derivative of the Lyapunov function, coenergy plus inertial energy, is LYAPGENP.m and is shown in Appendix A.

In the second short-circuit simulation, the synchronous generator is supplying rated current at rated voltage at a 0.85 lagging power factor when a symmetric 3-phase fault occurs, at time zero. The mechanical torque input to the generator is held at 0.85 of rated torque. This corresponds to the rated voltage and current, 0.85pf condition. The field voltage is held constant at the value which produces the correct terminal voltage at the loaded condition. Per-unitisation follows section 3.1. The machine parameters for this case are the same as those in table 4.1.1. Initial conditions for this simulation are shown in table 4.1.4.

Table 4.1.4 - 0.85pf Load Short-Circuit Initial Conditions

d-axis current	id_0	-1.1476	pu
q-axis current	iq_0	-0.4279	pu
"o" current	io_0	0.0	pu
field current	ifd_0	1.8172	pu
d-axis damper current	ikd_0	0.0	pu
q-axis damper current	ikq_0	0.0	pu
rotor electrical angle	θ_{re}	-0.8737	
terminal voltage	vt	0.827	pu
rotor mechanical speed	ω_{rm}	377.0	1/sec
mechanical torque input	Tm	0.85	pu
field voltage	vfd	0.00194	pu

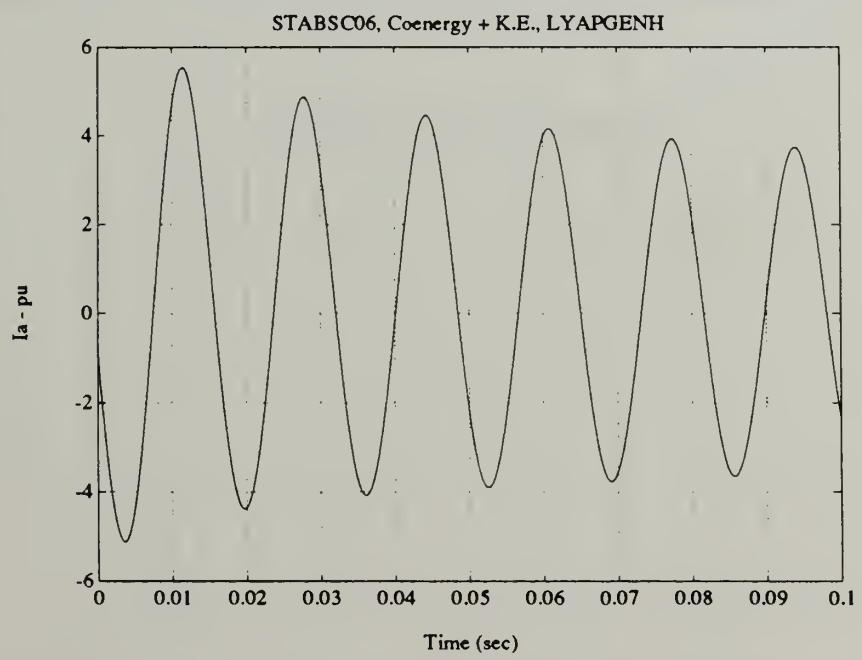

Figure 4.1.12 - 0.85pf Load Short-Circuit a-Phase Current vs. Time

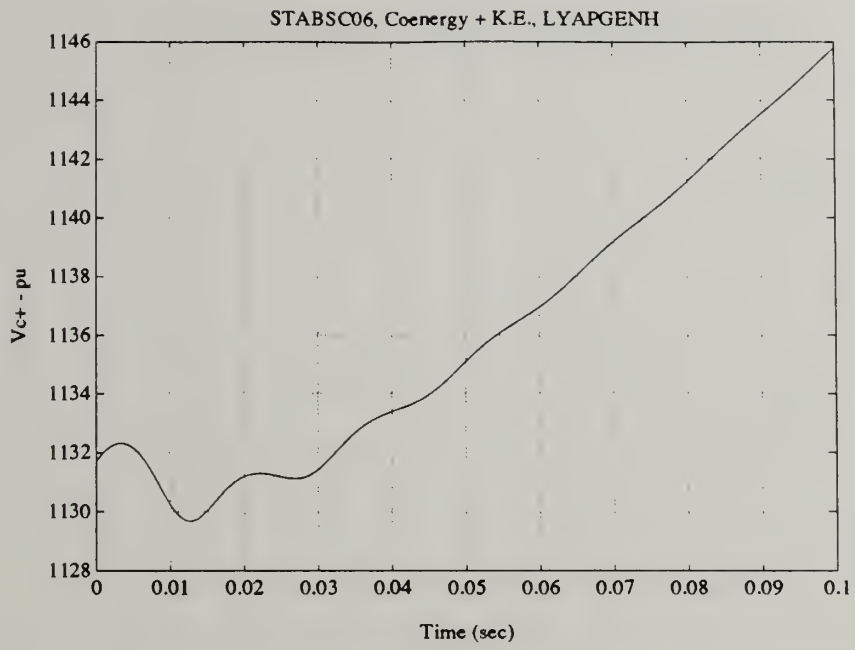

Figure 4.1.13 - 0.85pf Load Short-Circuit Lyapunov Function vs. Time

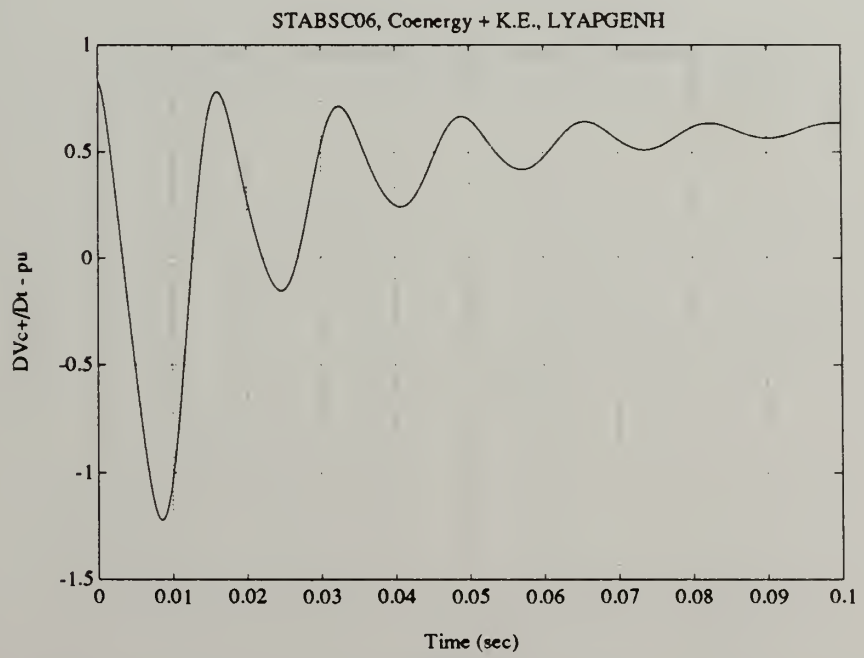

Figure 4.1.14 - 0.85pf Load Short-Circuit Lyapunov Derivative vs. Time

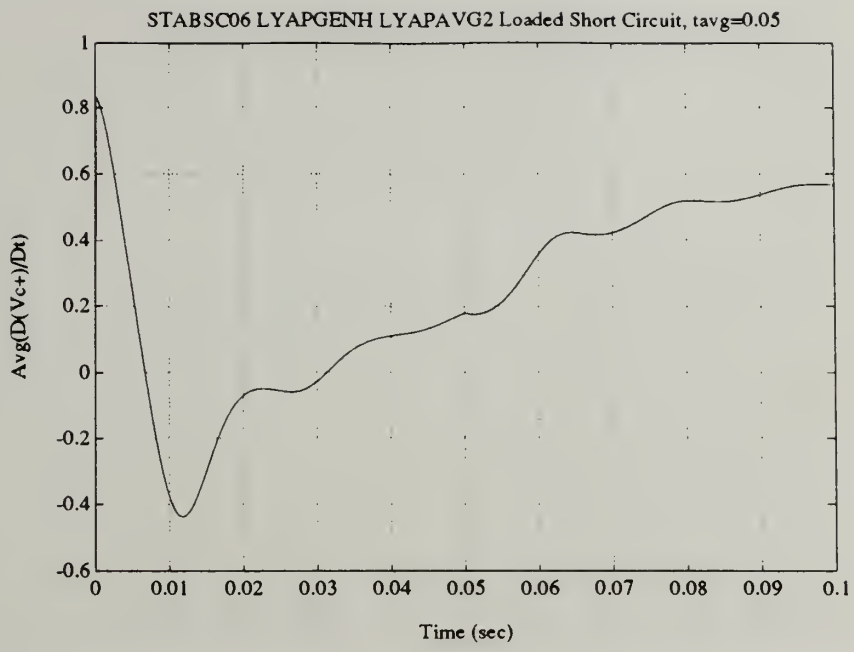

Figure 4.1.15 - 0.85pf Load Short-Circuit Averaged Lyapunov Derivative vs. Time (T_{avg} = 0.05 sec)

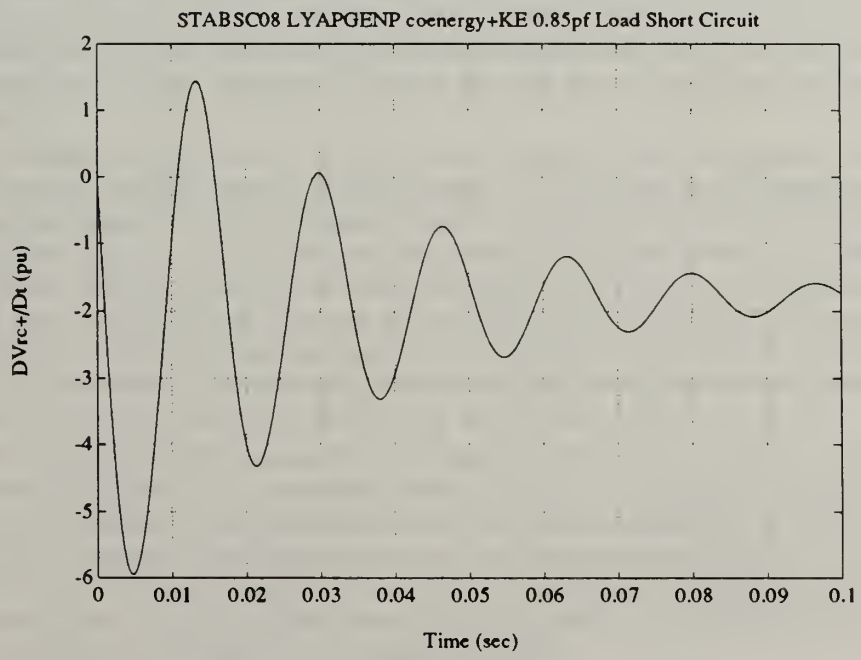

Figure 4.1.16 - 0.85pf Load Short-Circuit "Re-connected" Lyapunov Derivative vs. Time

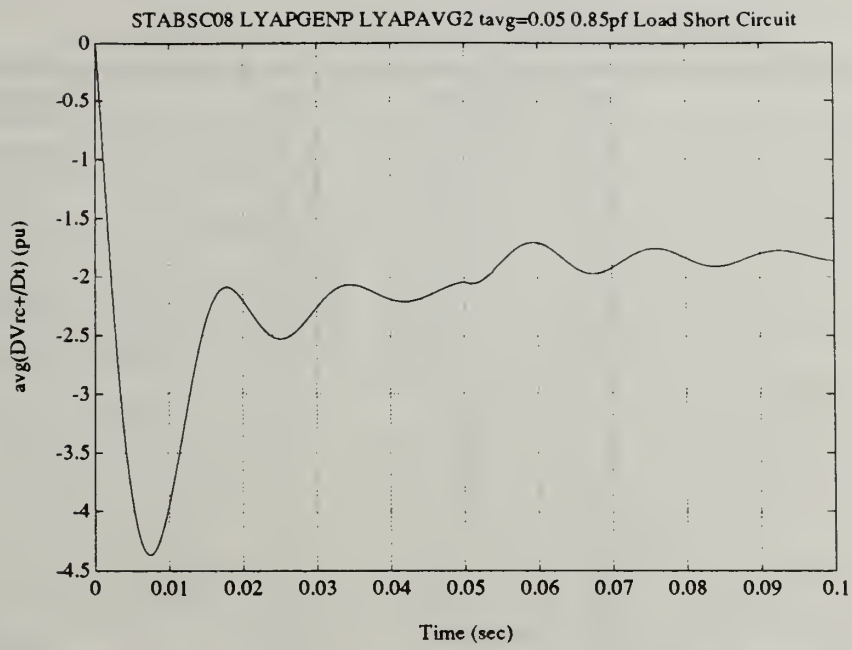

Figure 4.1.17 - 0.85pf Load Short-Circuit Averaged "Re-connected" Lyapunov Derivative vs. Time (T_{avg} = 0.05 sec)

The short-circuit current is what one would expect, figure 4.1.12. The oscillating increase in stored-energy depicted by figure 4.1.13 reflects the fact that there is 0.85 (pu) mechanical power input to and zero electric power output from the generator. It can only dissipate electric power in its winding resistances, which are very small. Hence, virtually all of the mechanical power into the generator must be stored in the rotor's inertia.

The "stability organ" shown for this second short-circuit simulation is also the coenergy plus the inertial energy. See equation (3.1.66). For this simulation, this particular "stability organ" does not demonstrate a response which allows one to conclude stability, figure 4.1.14. The convective derivative in this case shows the strong influence of the input torque. Time-scale averaging of figure 4.1.14, figure 4.1.15, does not permit any conclusions to be made about stability either. Here too, an averaging window of 0.05 seconds is used because it is somewhat longer than the armature time constant, 0.03 seconds. The averaging attenuates the amplitude of oscillations, which is seen by comparing figures 4.1.14 and 4.1.15 and figures 4.1.16 and 4.1.17.

In this simulation, the time-scale averaged "re-connected" version of the Lyapunov derivative, figure 4.1.17, provides a better picture of the transient stability of the generator. The averaging eliminates the very fast electromagnetic oscillations. The "re-connected" version of the derivative captures the generator's ability to resume supplying electric power to the system. Were this simulation continued for a longer time, an indication of the critical clearing time could be obtained by finding where the Lyapunov derivative of figure 4.1.17 becomes positive.

4.1.3 Step-Load Behaviour

Table 4.1.5 - Step-Load Initial Conditions

d-axis current	id_0	-1.1476	pu
q-axis current	iq_0	-0.4279	pu
"o" current	io_0	0.0	pu
field current	ifd_0	1.8172	pu
d-axis damper current	ikd_0	0.0	pu
q-axis damper current	ikq_0	0.0	pu
rotor electrical angle	θ_{re}	-0.8737	
terminal voltage	vt	0.827	pu
rotor mechanical speed	ω_{rm}	377.0	1/sec
mechanical torque input	Tm	0.35	pu
field voltage	vfd	0.00194	pu

The generator in this case is initially supplying 0.85 per-unit power to an infinite bus. The terminal voltage and currents are both at their rated values. The mechanical power into the generator is suddenly reduced to 0.35 per-unit at time zero. The generator remains connected to the infinite bus. The field excitation is held constant at the 0.85 load level. The machine parameters for this case are the same as those in table 4.1.1. Initial conditions for this simulation are shown in table 4.1.5.

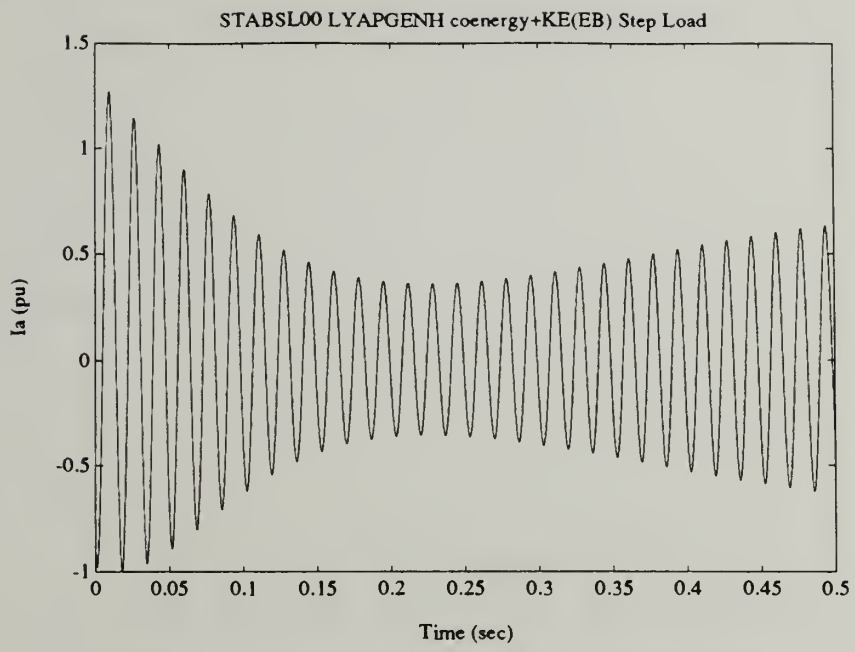

Figure 4.1.18 - Step-Load a-Phase Current vs. Time

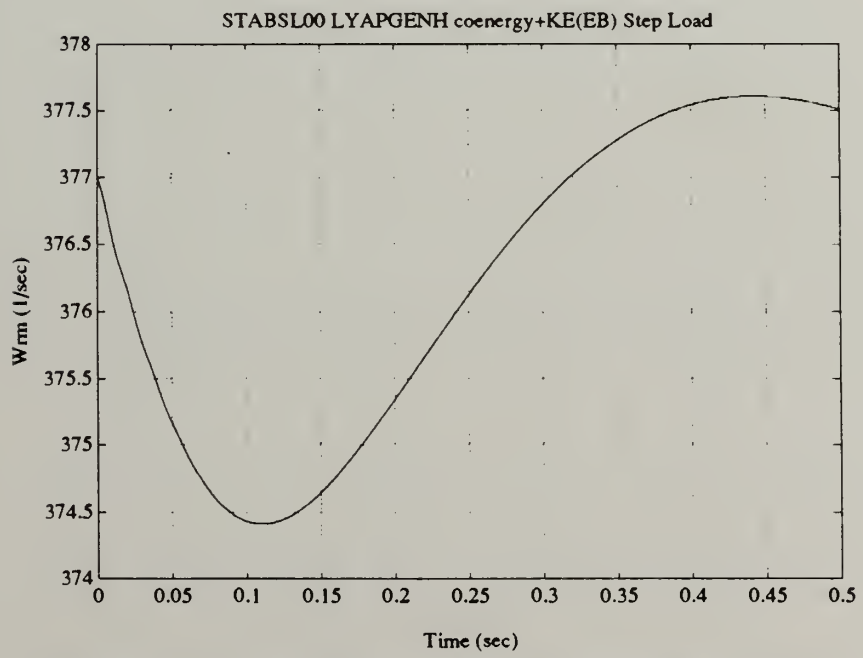

Figure 4.1.19 - Step-Load Rotor Mechanical Speed vs. Time

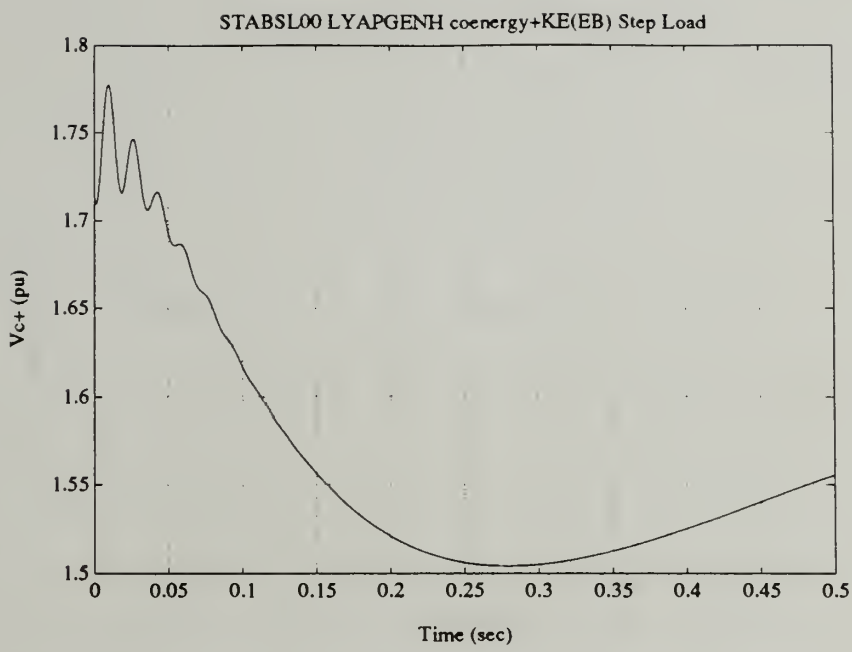

Figure 4.1.20 - Step-Load Lyapunov Function vs. Time

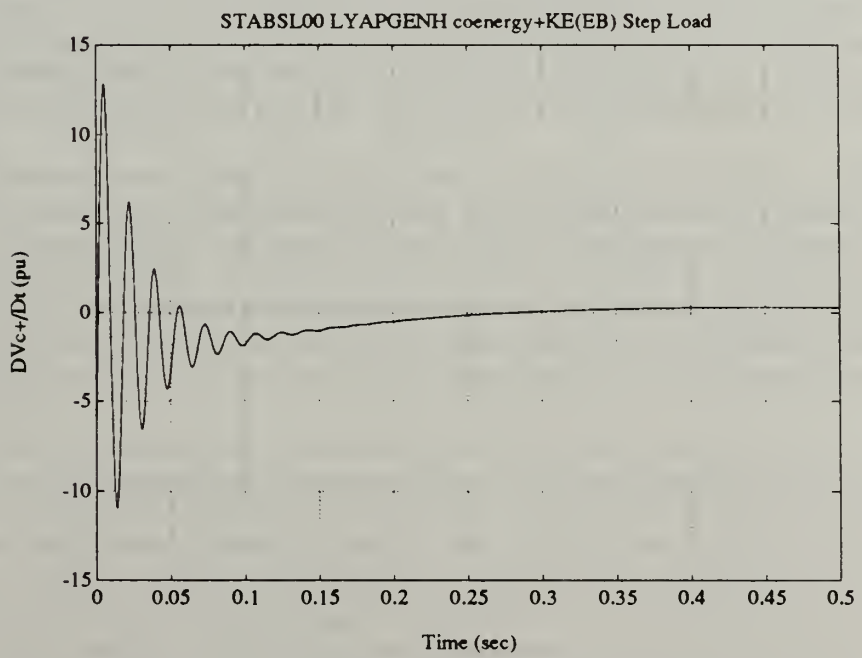

Figure 4.1.21 - Step-Load Lyapunov Derivative vs. Time

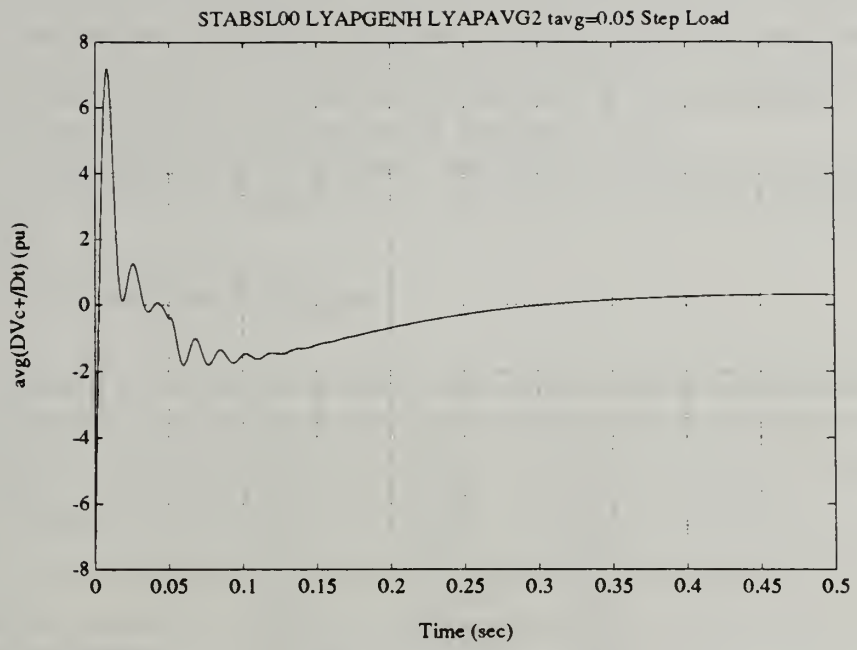

Figure 4.1.22 - Step-Load Averaged Lyapunov Derivative vs. Time (T_{avg} = 0.05 sec)

The step-load current illustrates the unloading effect, figure 4.1.18. The subtransient time constant, 0.2 seconds, is also evident. Oscillations in the rotor mechanical speed, figure 4.1.19, reflect oscillations in electromagnetic torque which arise from damper winding currents. The stored-energy, depicted by figure 4.1.20, possesses three distinct characteristics. First, the initial oscillations in the Lyapunov function, figure 4.1.20, die away with a time constant on the order of the armature time constant, 0.03 seconds.

The second item of note is the decrease in the Lyapunov function over the first half of the simulation. During this segment, the terminal current decreases to accommodate the new load that the generator can supply. The decrease in stored energy results from the presence of damper currents, which increase in an attempt maintain constant flux. The currents generate an electromagnetic torque which, combined with the step decrease in the mechanical torque input, produces a rotor deceleration. The damper currents die out over a period corresponding to the subtransient time constant, 0.2 seconds.

The third characteristic of the time behaviour of the Lyapunov function is the increase over the second half of the simulation. This increase reflects the rebounding terminal currents and the dying damper currents. The rotor's kinetic energy, stemming from speed oscillations, varies in a similar way to the electromagnetic energy.

The "stability organ" shown for this second short-circuit simulation is the coenergy plus base energy scaled inertial energy. See equation (3.1.69). For this simulation, this particular "stability organ" does not demonstrate a response which allows one to conclude stability, figure 4.1.21. The Lyapunov derivative in this case is dominated by the initial electromagnetic oscillations. Selection of a different inertial energy relationship, such as the kinetic energy itself, yields different results. This choice of inertial energy term foreshadows the discussion in the next section.

Time-scale averaging of figure 4.1.21, figure 4.1.22, does not permit any conclusions to be made about stability either. An averaging window of 0.05 seconds is used because it is somewhat longer than the armature time constant, 0.03 seconds. The averaging attenuates the amplitude of oscillations, which is seen by comparing figures 4.1.21 and 4.1.22. However, even attenuation of the amplitude of the electromagnetic energy oscillations does not overcome the dominance of the electromagnetic effects which results from the base energy scaling of the kinetic energy.

In this simulation, the "re-connected" version of the Lyapunov derivative is irrelevant because the generator terminals remain connected to the system throughout the dynamic event.

4.1.4 Critical Clearing Time Prediction

Table 4.1.6 - 0.85pf Load Open-Circuit Initial Conditions

d-axis current	id_0	0.0	pu
q-axis current	iq_0	0.0	pu
"o" current	io_0	0.0	pu
field current	ifd_0	1.814	pu
d-axis damper current	ikd_0	-1.151	pu
q-axis damper current	ikq_0	-0.420	pu
rotor electrical angle	θ_{re}	-0.8737	
terminal voltage	vt	0.827	pu
rotor mechanical speed	ω_{rm}	377.0	1/sec
mechanical torque input	Tm	0.85	pu
field voltage	vfd	0.00194	pu

The critical clearing time prediction to be made considers the case of a synchronous generator supplying rated current and voltage to an infinite bus at 0.85pf. At time zero, its stator terminals are suddenly open-circuited. Input torque and field voltage remain constant. How long the generator can remain open-circuited before it can no longer be successfully re-connected to the system is sought. The critical clearing times predicted by the various "stability organs" are compared with ones predicted by other methods in the next section.

Critical clearing time determinations are frequently sought for short-circuit faults as opposed to open-circuit faults. This is the case for the system considered in the next chapter. An open-circuit critical clearing time is sought in this section for two reasons.

First, stator currents are zero. Consequently, the electromagnetic energy oscillations arising from armature leakages are not present. Hence, the coenergy is solely a function of rotor currents. Whereas the coenergy is formulated in the "d-q" reference frame, section 3.1.2.4, the coenergy should not contain any oscillations. Determination of negative semi-definiteness of the Lyapunov functions' convective derivatives will be easier.

Second, for naval electric power systems in particular (and especially those with gas turbine prime movers), open-circuit faults have dangerous implications. Gas turbines typically are light-weight, implying small inertias. A sudden loss in load, as happens when the generator being supplied is open-circuited, admits the real possibility of catastrophic turbine overspeed. Open-circuit faults are an important design consideration because their imposition is foreseeable on naval combatants.

The machine parameters in table 4.1.1 are used in this case. The initial conditions are shown in table 4.1.6. As mentioned, the terminal voltages and currents are at their rated values. The generator is providing power to an infinite bus at 0.85pf, lagging, when its terminals are suddenly opened. The mechanical torque input and field excitation are held constant at the pre-fault levels.

Three modelling issues arise for this particular simulation. First, the imposition of zero stator currents makes the stator's "d", "q", and "o" axis flux linkages' dynamic equations algebraic equations. This permits reduction in the order of the generator's dynamic model.

Second, for a direct comparison of critical clearing times with reference [4.1], the dynamic model of the generator used in reference [4.1], which uses the "voltages behind reactances" as states, is adopted. For the two reasons given here, the "device object" implementing this model is used for the open-circuit simulations. The listing of this "device object", LYAPGENK.m, is shown in Appendix A.

The third modelling issue confronts initial conditions. Most circuit breakers open when the current encounters a zero-crossing. Hence, for 3-phase tie lines, breaker openings occur over a significant fraction of a cycle. In this set of simulations, the opening is assumed to occur instantaneously. In practice, this is imposed by a step change in the rotor currents at time zero. The currents used as initial conditions are the currents at $t=0^+$.

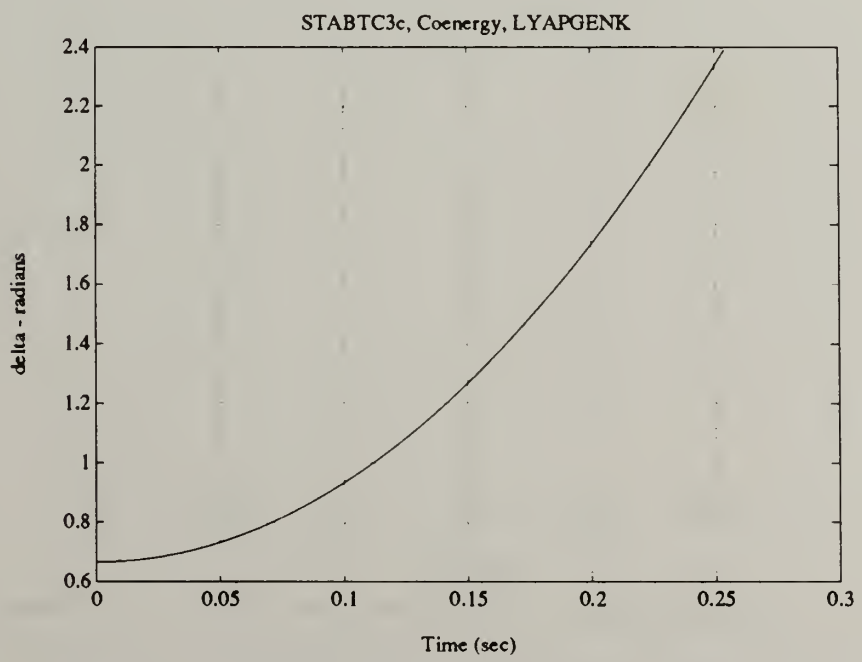

Figure 4.1.23 - 0.85pf Load Open-Circuit Rotor Angle vs. Time

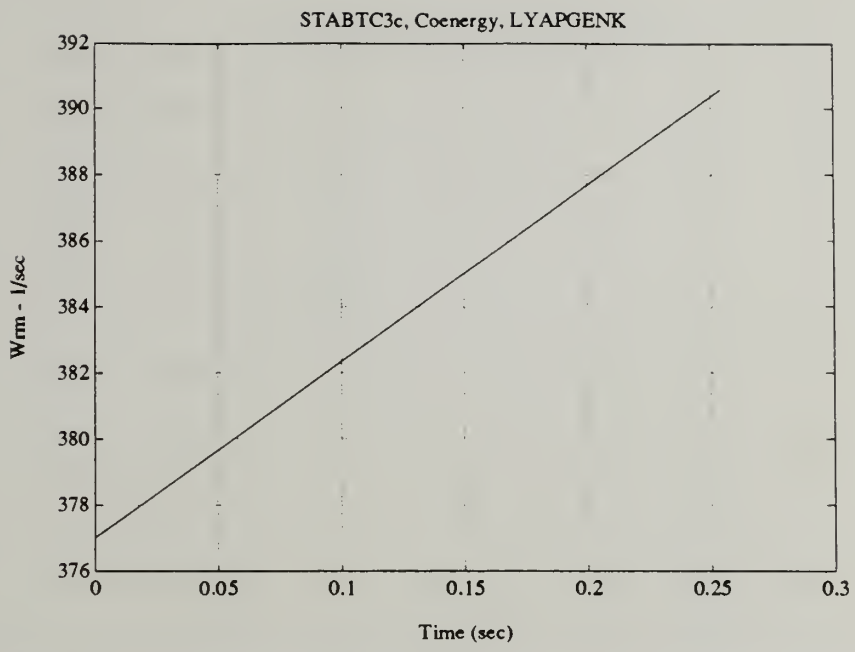

Figure 4.1.24 - 0.85pf Load Open-Circuit Rotor Mechanical Speed vs. Time

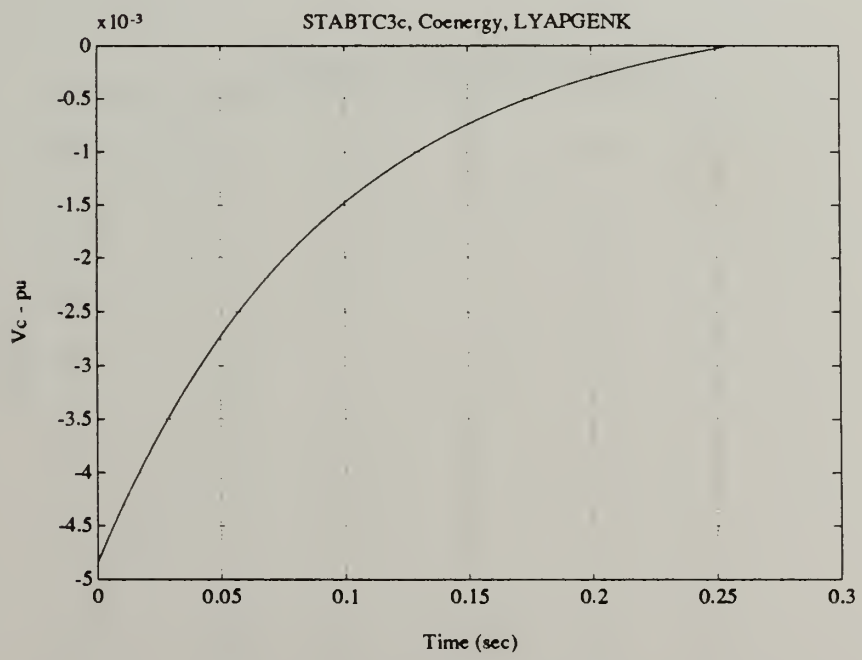

Figure 4.1.25 - 0.85pf Load Open-Circuit Coenergy Derivative vs. Time

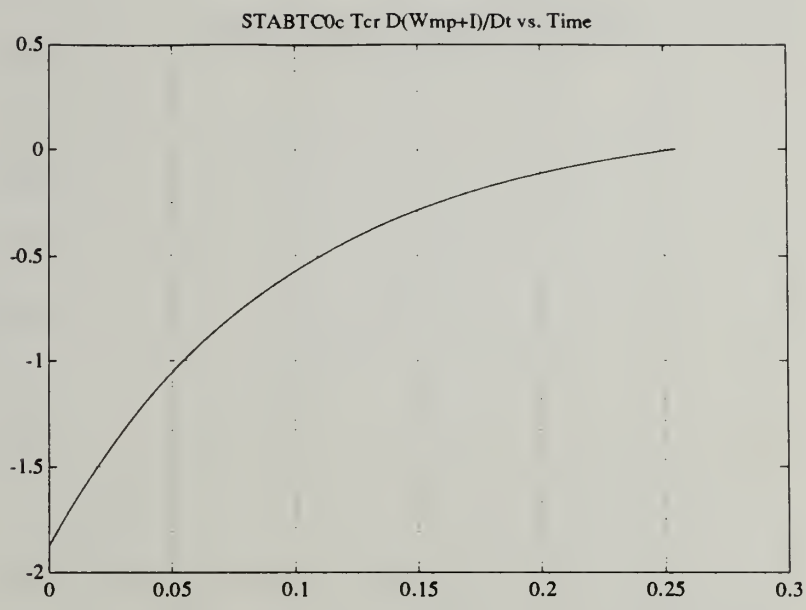

Figure 4.1.26 - 0.85pf Load Open-Circuit V(Coenergy + K.E.($\Delta\omega_{rm}$ E_B)) Derivative vs. Time

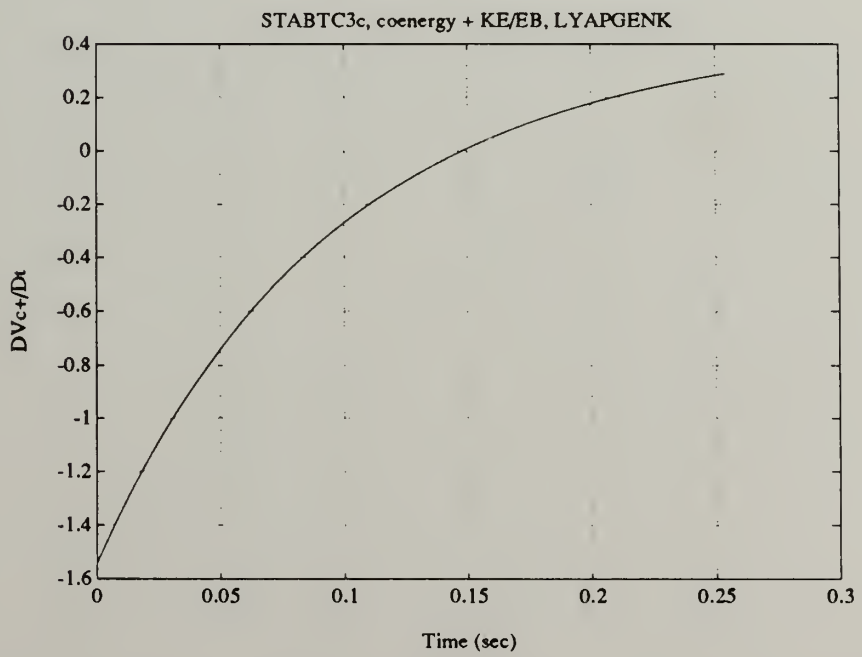

Figure 4.1.27 - 0.85pf Load Open-Circuit V(Coenergy + K.E.(E_B)) Derivative vs. Time

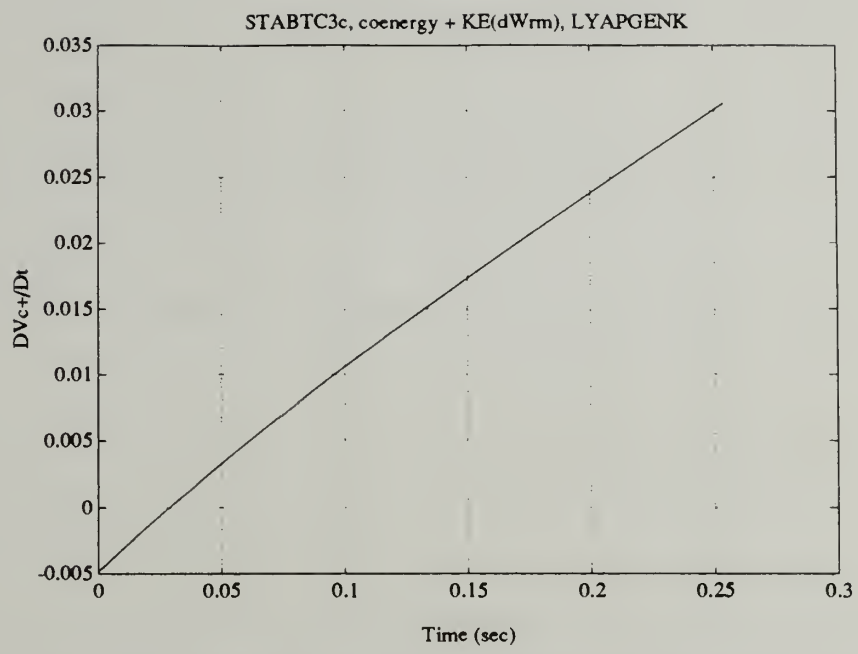

Figure 4.1.28 - 0.85pf Load Open-Circuit V(Coenergy + K.E.($\Delta\omega_{rm}$)) Derivative vs. Time

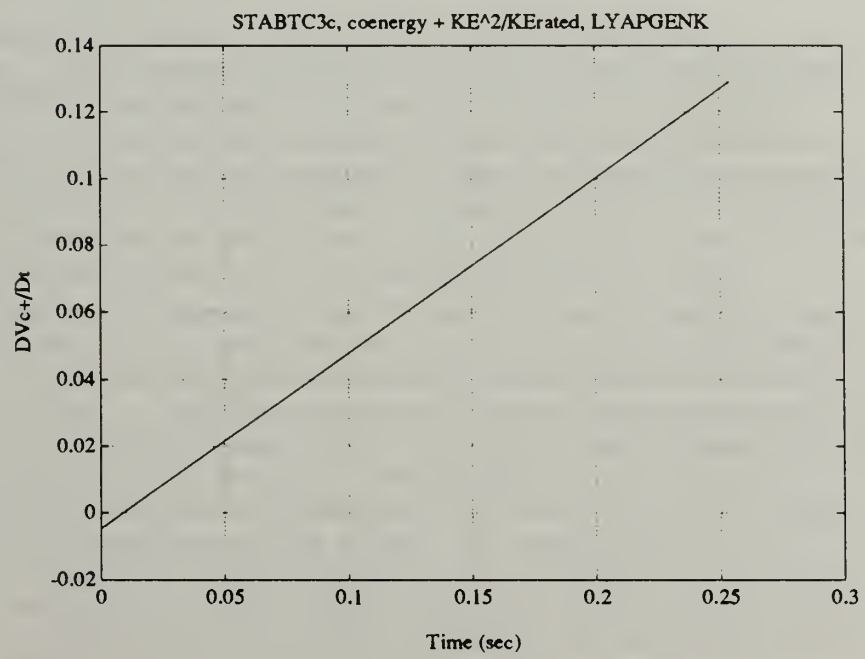

Figure 4.1.29 - 0.85pf Load Open-Circuit V(Coenergy + $\Delta K.E.^2$) Derivative vs. Time

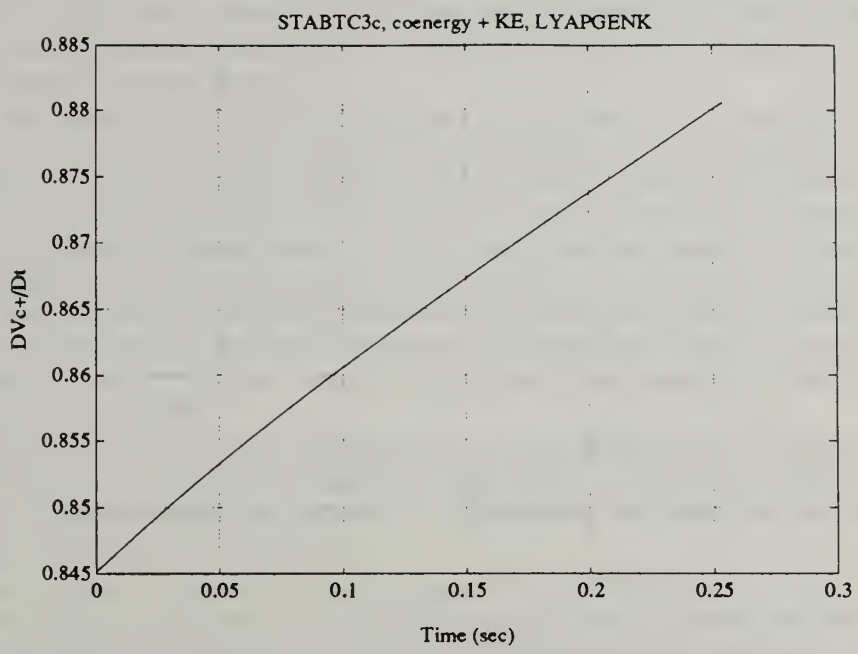

Figure 4.1.30 - 0.85pf Load Open-Circuit V(Coenergy + K.E.) Derivative vs. Time

The rotor angle, figure 4.1.23, and rotor mechanical speed, figure 4.1.24, correspond to the behaviour of the open-circuited generator for the period of time during which the fault is imposed. The behaviour after the fault has been cleared is not examined for this analysis.

Each of the inertial terms (3.1.66)-(3.1.70) provided different critical clearing time predictions. Each is shown, figures 4.1.26 to 4.1.30. The principal differences stem from the relative magnitudes of the coenergy and inertial energy terms.

The plot of the convective derivative of just the coenergy shows that it is decaying, figure 4.1.25. In fact, its (negative) derivative asymptotically approaches zero. This reflects the decay of the currents in the damper windings. It is this plot that points out the need to include an inertial term to account for rotor acceleration. Looking at this plot alone would mislead one into concluding stability for all time.

The second convective derivative shown is the rate of change of the coenergy plus the kinetic energy of the speed difference scaled to the electric base energy, figure 4.1.26. This Lyapunov derivative indicates that stable behaviour cannot be concluded after 0.253 seconds. The third convective derivative combines the rate of change of coenergy and the rate of change of the base energy normalised inertial energy. It yields a maximum time of 0.115 seconds for concluding stability, figure 4.1.27. The fourth convective derivative, which is based upon the kinetic energy of the speed change, predicts a lapse of conclusive stability at time 0.09 seconds, figure 4.1.28. The fifth convective derivative, based upon the square of the instantaneous kinetic energy divided by the rated kinetic energy, ends conclusive stability at time 0.01 seconds, figure 4.1.29. The sixth convective derivative, which is simply the sum of coenergy and kinetic energy, indicates conclusive stability at no time at all, figure 4.1.30.

Based on the above, the least "overly sufficient" prediction of the time when stability can no longer be concluded is 0.253 seconds, figure 4.1.26. It is important to note here that this prediction is based solely on the rate of change of an energy-related function. It is not directly related to the ability of the generator to regain synchronism with a constant frequency network.

For the open-circuit fault dealt with here, the notion of "re-connected" Lyapunov derivatives is irrelevant. The premise behind use of the system voltages in the convective derivative of the Lyapunov function is that since the generator is inductive, currents cannot change instantaneously but voltages can. The "re-connected" convective derivative provides the instantaneous value of the Lyapunov derivative were the system voltage suddenly applied to the synchronous generator's terminals. For the open-circuit fault, currents are zero. Since they cannot change instantaneously, the voltage which is applied to the terminals is irrelevant because it is multiplied by zero. Consequently, the critical clearing time prediction found in this section is independent of the version of convective derivative used.

The fact that zero stator currents leads to no oscillations in the Lyapunov derivatives precludes the necessity for time-scale averaging. This means that the critical clearing time predictions of this section are independent of issues surrounding the selection of an averaging time-scale.

This example makes very clear the issue of "over sufficiency". The coenergy, by itself, is not a valid candidate Lyapunov function because it ignores the mechanical speed. All of the other functions are valid candidate Lyapunov functions. Whereas they are valid, the fact that the results provided by some of the functions are less useful than those provided by others stresses the importance of Lyapunov function selection.

The Lyapunov functions which yield very short critical times are not wrong. They are overly cautious in this particular instance. The longest predicted time, though, is conclusive.

4.1.5 Comparison of Critical Clearing Time Predictions

For the case of the 0.85pf open-circuit critical clearing time prediction for the generator of table 4.1.1, the times predicted by the various Lyapunov functions which make up the synchronous generator "device object's" "stability organ" range from 0.0 seconds to 0.253 seconds. These times are obtained by running one simulation for each of the respective "stability organs". The behaviour after the fault has been cleared does not need to be observed.

Presently, the most accurate way to determine critical clearing time is through simulation(s). Rather than using trial and error to hit upon the actual critical clearing time, the two approximate, though direct, methods discussed in section 2.2.4 are used to obtain a first, approximate time which is refined through subsequent simulations.

The equal area criterion provides one approximate critical clearing time. This method is admittedly approximate. The simplifying assumptions which make it tractable lead to conservative results. The specific method described in reference [4.2] is used in this case. The equal area criterion derived critical clearing time in the case of the generator of table 4.1.1 for the transient event of section 4.1.4 is 0.209 seconds.

The "energy function" method also provides an approximate critical clearing time. This method's simplifying assumptions also lead to slightly conservative results. The method of reference [4.3] is used in this case. Its critical clearing time prediction is 0.226 seconds.

The actual critical clearing time, established by simulations in reference [4.1] and confirmed using WAVESIM simulations in conjunction with this research is 0.253 seconds. The one Lyapunov function based upon differential speed inertial energy scaled to the base electric energy provided this same time prediction. For this particular type of fault, the other Lyapunov functions were even more conservative than the approximate methods.

4.2 Assessment of Composite System Stability Demon

A frequently studied electric circuit is the parallel RLC circuit. Such a circuit is discussed in section 3.1.1. Figure 3.1.1 shows the RLC circuit which is shown below as well. Table 4.2.1 contains the parameter values of the circuit components used in the simulations within this section.

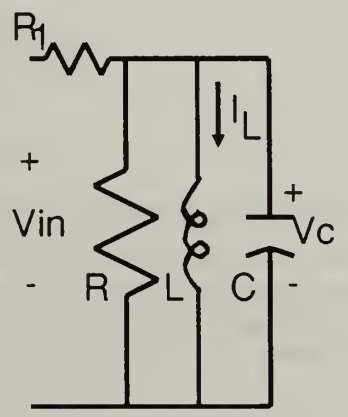

Figure 4.2.1 - Example RLC Circuit

Table 4.2.1 - RLC Parameter Values		
R1	10.0	Ohms
R	1.0	Ohms
L	1.0	Henries
C	2.0	Farads

Because its behaviour is rather well understood, this circuit is chosen as a means to test the "stability demon" "device object". The results provided by the "stability demon" are compared with the known stability characteristics of this system. Furthermore, this system possesses just two states. Hence, its Lyapunov space is two-dimensional and, therefore, easily visualisable.

To test the "stability demon", an inductor "device object" which contains a "stability organ" and a capacitor "device object" which contains a "stability organ" had to be coded. The inductor and capacitor are treated as separate components in this analysis. Appendix A contains a file listing of the inductor and capacitor "device objects" which contain the respective "stability organs". In both cases, stored energy is the Lyapunov function.

In section 3.1.1, two Lyapunov functions are developed for the RLC circuit. Those two Lyapunov functions are monolithic in the sense that one Lyapunov function is used to describe the entire system. In this "stability demon" test, the Lyapunov function representing the inductor is distinct from the Lyapunov function representing the capacitor. The RLC circuit is being modelled as a composite system.

The "stability demon" used in these tests calculates the weighting factors using a "component neutral"-based relationship, equation (3.2.21). Its "device object" file listing is given in appendix B.

4.2.1 Stable Composite RLC Circuit Performance

Table 4.2.2 - Unforced Initial Conditions		
I_L	1.0	Amps
V_c	1e-5	Volts
V_{in}	0.0	Volts ($\forall t \geq 0$)
δ_1	1.6487	
δ_1	1.6487	

In this first simulation, the RLC circuit is given a non-zero initial state vector. The input voltage is zero. Hence, this is the unforced response of the RLC circuit. As this is a linearly stable circuit, the output of the "stability demon" should indicate such. Table 4.2.2 contains the initial conditions for this simulation.

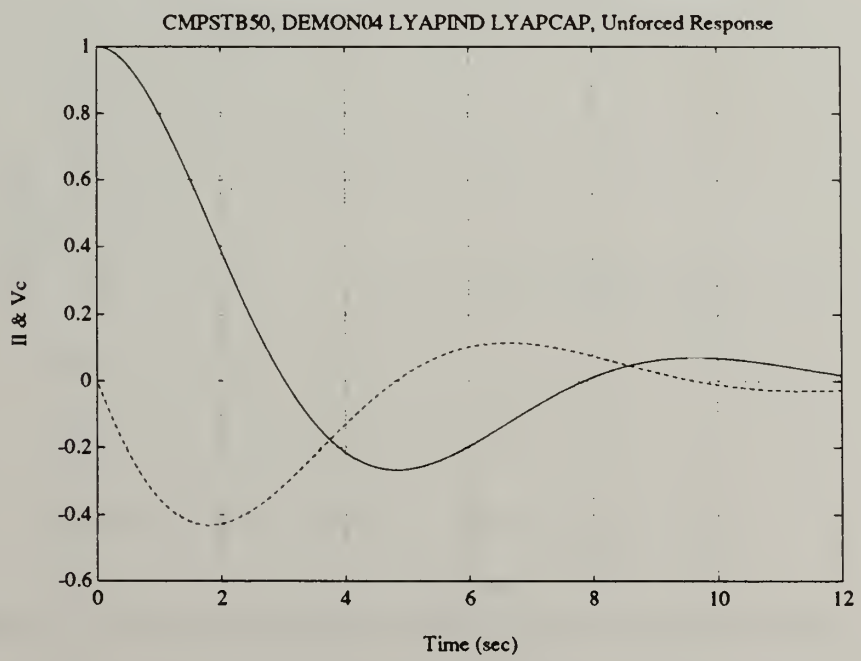

Figure 4.2.2 - RLC Unforced Response (I_L & V_c vs. Time)

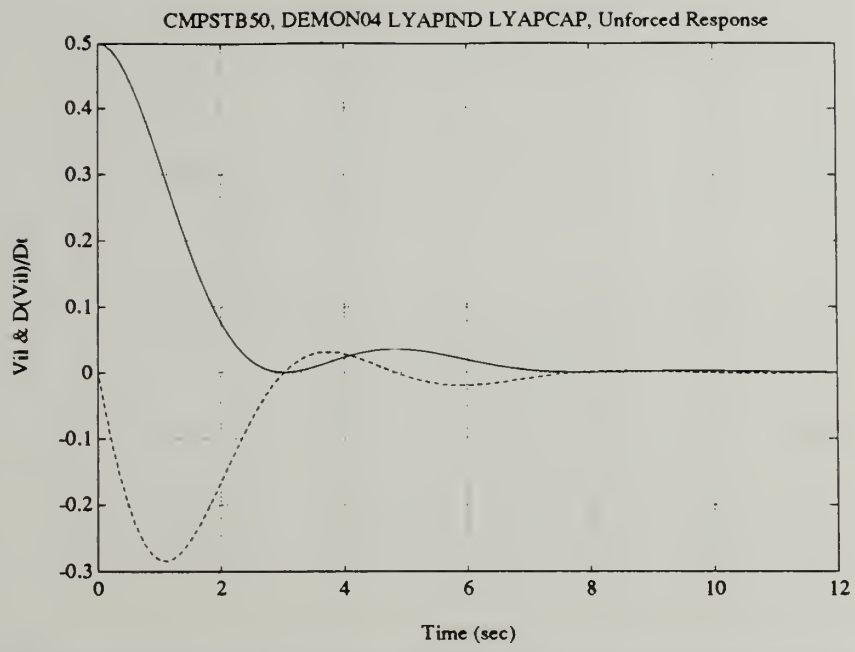

Figure 4.2.3 - Unforced Inductor Lyapunov Output (V_1 and $D(V_1)/Dt$ vs. Time)

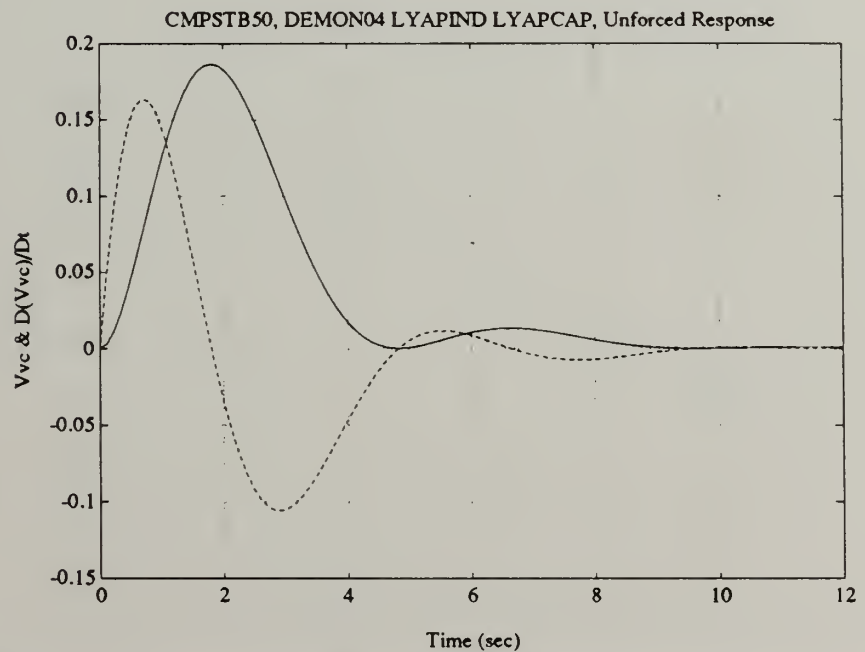

Figure 4.2.4 - Unforced Capacitor Lyapunov Output (V_2 and $D(V_2)/Dt$ vs. Time)

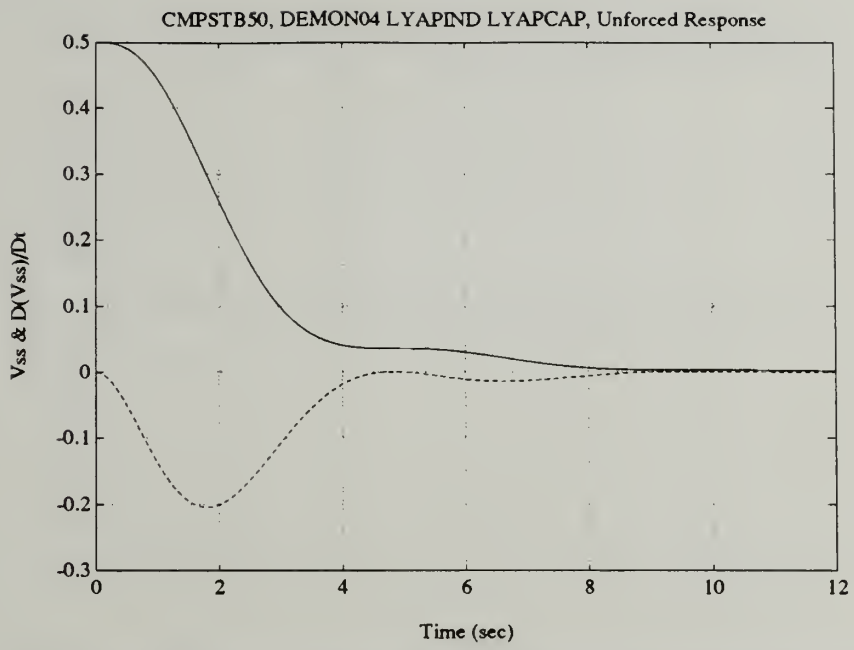

Figure 4.2.5 - Unforced "Simple Sum" Lyapunov Output (V_{ss} and $D(V_{ss})/Dt$ vs. Time)

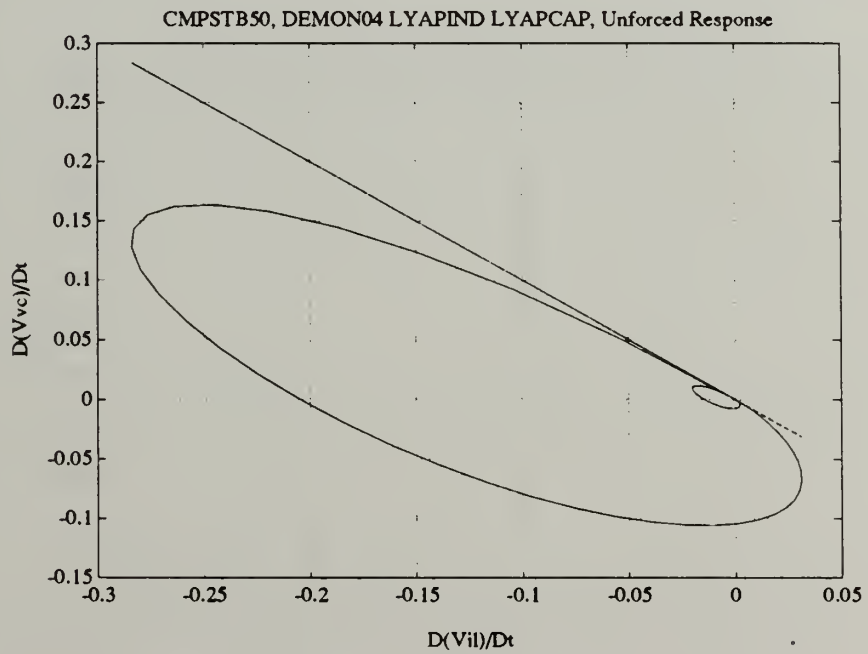

Figure 4.2.6 - Unforced Lyapunov Space Trajectory ($D(V_2)/Dt$ vs. $D(V_1)/Dt$)

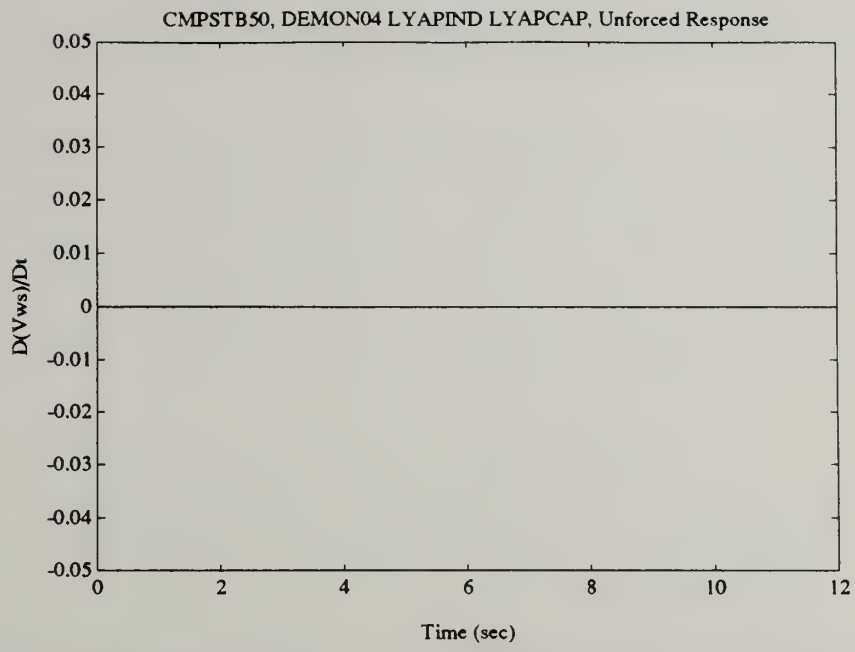

Figure 4.2.7 - Unforced "Time-Variant Weighted-Sum" Lyapunov Derivative ($D(V_{ws})/Dt$ vs. Time)

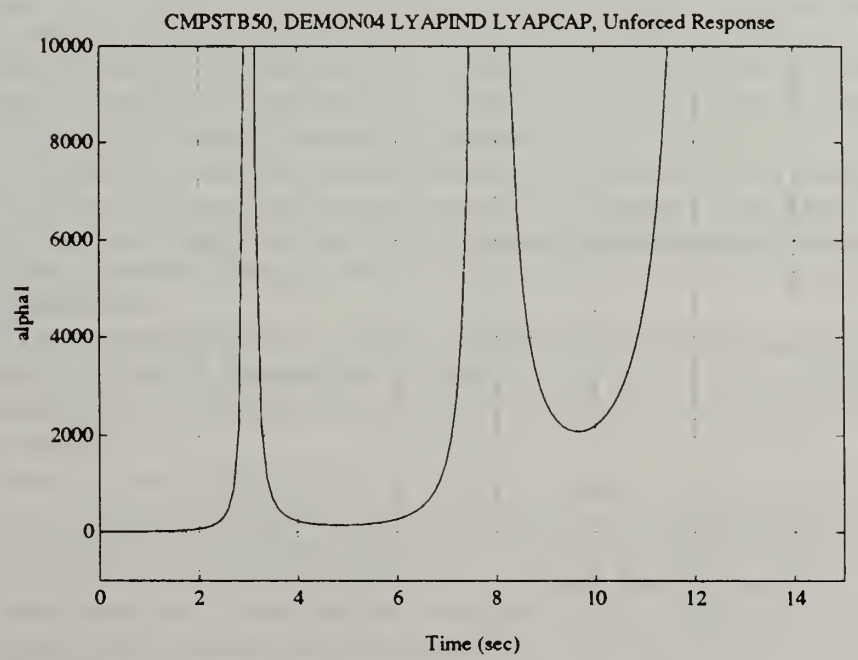

Figure 4.2.8 - Unforced Time-Variant Weighting Factor (α_1 vs. Time)

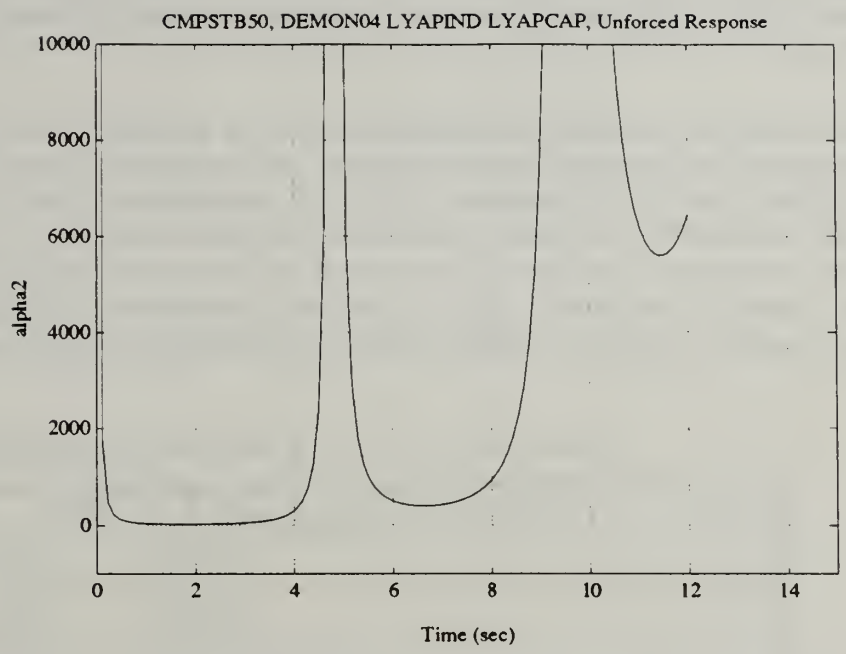

Figure 4.2.9 - Unforced Time-Variant Weighting Factor (α_2 vs. Time)

Figure 4.2.2 shows the behaviour of the inductor current and capacitor voltage, the two state variables, during the unforced response. The oscillations arise from the fact that this is an underdamped circuit. Figure 4.2.3 shows the output of the inductor's "stability organ", the stored energy and its convective derivative over time. Figure 4.2.4 shows the same quantities for the capacitor. Note, zero points of the Lyapunov function (stored energy) coincide with positive going zero points of the Lyapunov function's convective derivative. This is discussed in section 3.2.2.

It is interesting to consider that the inductor and capacitor in this simulation have non-negative values. Hence, their behaviour could be expected to be stable. However, both of their Lyapunov functions' convective derivatives are positive for significant periods of time. In an oscillating system, a Lyapunov function based upon energy must reflect the oscillations.

The first composite stability measure obtained is the "simple sum" of the two Lyapunov outputs. Figure 4.2.5 shows the "simple sum" composite Lyapunov function and its convective derivative. This sum's convective derivative is negative semi-definite, indicating stability.

The closed curve in figure 4.2.6 is the Lyapunov space trajectory of the composite RLC system. The line in the figure is the stability region border discussed in conjunction with figure 3.2.3. The unforced behaviour of this linearly-stable RLC circuit does not meet the element wise criterion for stability. It does, though, meet the "simple sum", weighted-sum, and "indeterminately-weighted-sum" criterions of section 3.2.1. This is consistent with the statement in section 3.1.1 that, for this circuit, the unforced response region of stability is all of state space.

Whereas the "stability demon" employed for this test is based upon the "component neutral" relationship, the convective derivative of the "time-variant weighted-sum" Lyapunov function should be identically zero for all time. Figure 4.2.7 shows that this is so. Figures 4.2.8 and 4.2.9 show the respective time-variant weighting factors, the α'*s*.

The points where the α'*s* grow asymptotically large are the points where the Lyapunov function itself goes to zero. As implemented here, though, the Lyapunov function never actually reaches zero, but, rather, becomes smaller than a specified tolerance, an ε. The α'*s* for such a value of the Lyapunov function are based upon the value of ε. This behaviour and the discussion in section 3.2.2 indicate that when an α is "small", the corresponding component's stability is "small". When an α is "large", the corresponding component is behaving in a stable fashion. In a sense, α here quantifies stability.

4.2.2 Step-Response Composite RLC Circuit Performance

Table 4.2.3 - Step Input Initial Conditions		
I_L	0.0	Amps
V_c	0.0	Volts
V_{in}	10.0	Volts ($\forall t \geq 0$)
δ_1	1.6487	
δ_1	1.6487	

In this simulation, the RLC circuit is given a zero initial state vector. The input voltage is a step input at time zero. Hence, this is the step response of the RLC circuit. As this is a linearly stable circuit with bounded input, the output of the "stability demon" should indicate a bounded response. Table 4.2.3 contains the initial conditions for this simulation.

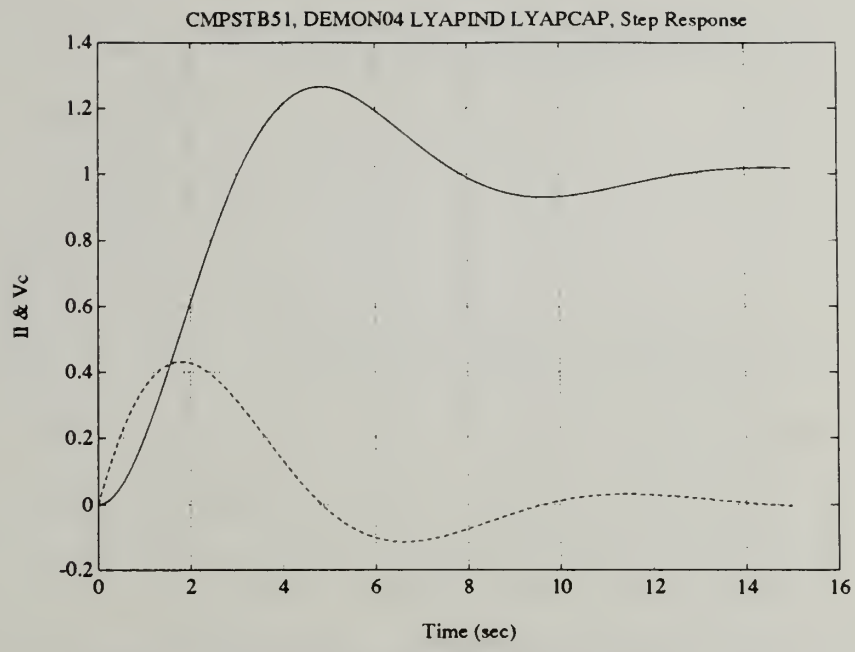

Figure 4.2.10 - RLC Step Response (I_L & V_c vs. Time)

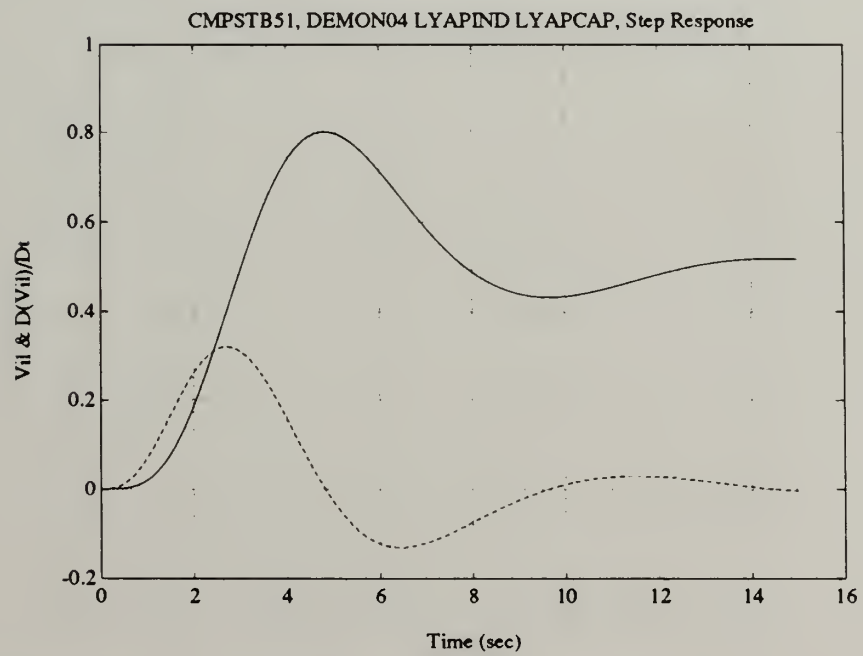

Figure 4.2.11 - Step Response Inductor Lyapunov Output (V_1 and $D(V_1)/Dt$ vs. Time)

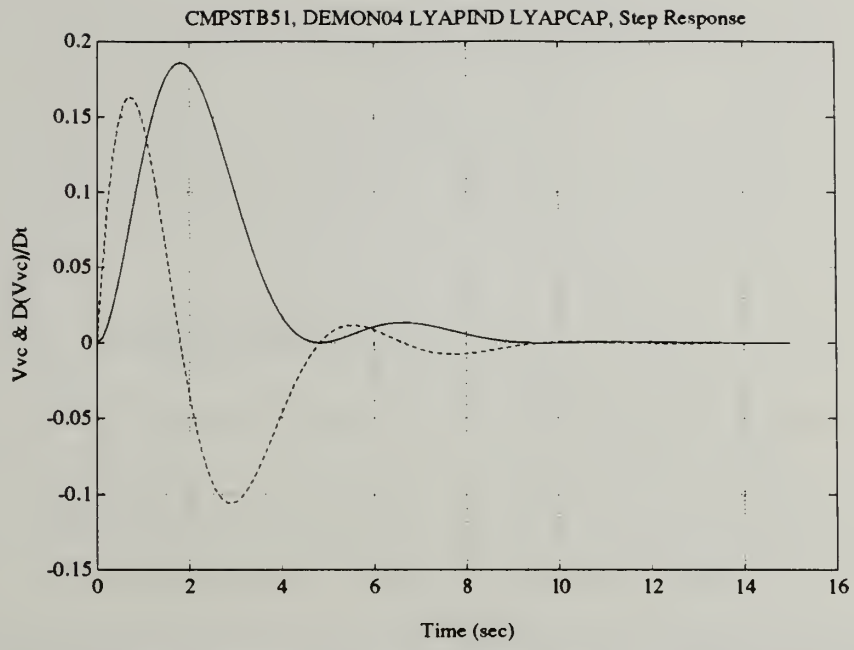

Figure 4.2.12 - Step Response Capacitor Lyapunov Output (V_2 and $D(V_2)/Dt$ vs. Time)

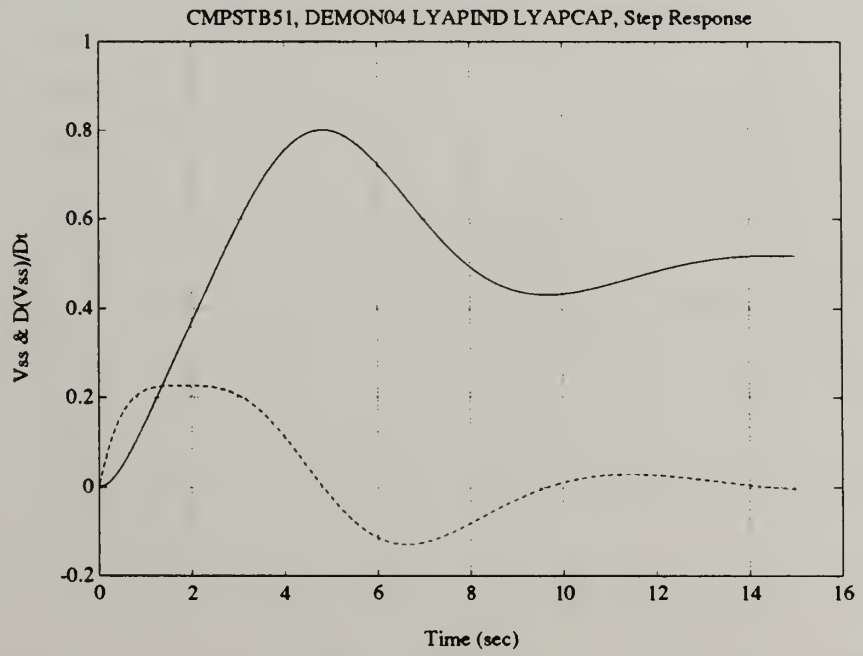

Figure 4.2.13 - Step Response "Simple Sum" Lyapunov Output (V_{ss} and $D(V_{ss})/Dt$ vs. Time)

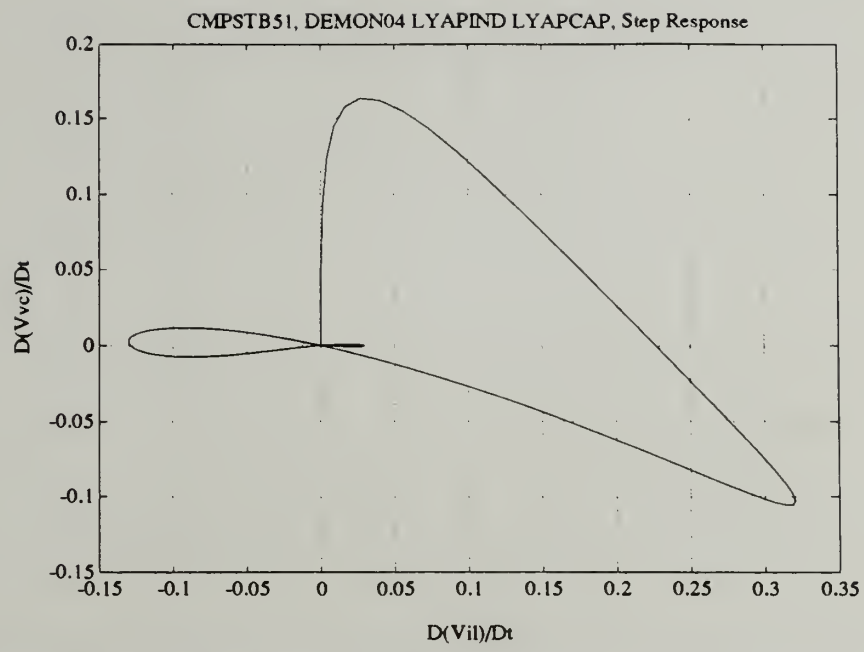

Figure 4.2.14 - Step Response Lyapunov Space Trajectory ($D(V_2)/Dt$ vs. $D(V_1)/Dt$)

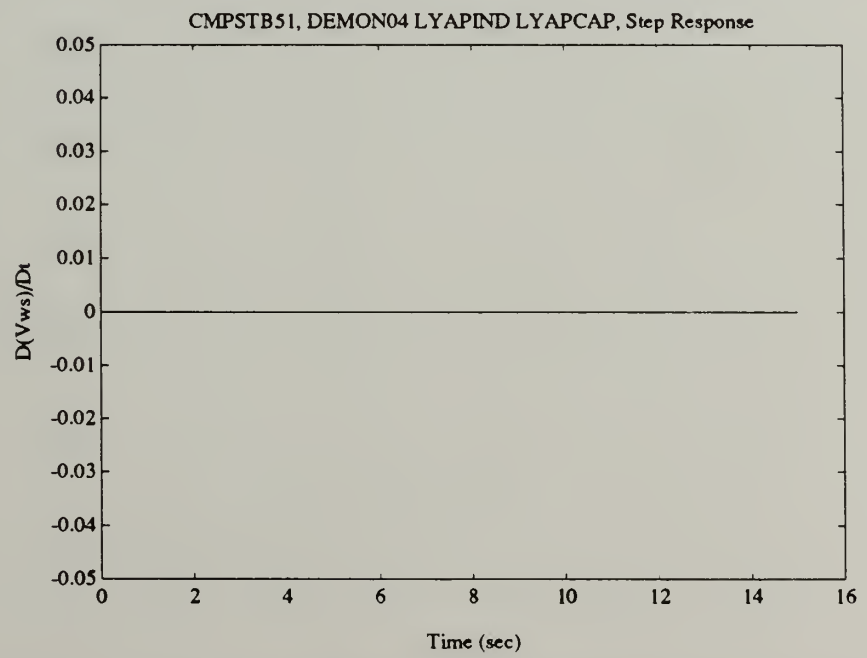

Figure 4.2.15 - Step Response "Time-Variant Weighted-Sum" Lyapunov Derivative ($D(V_{ws})/Dt$ vs. Time)

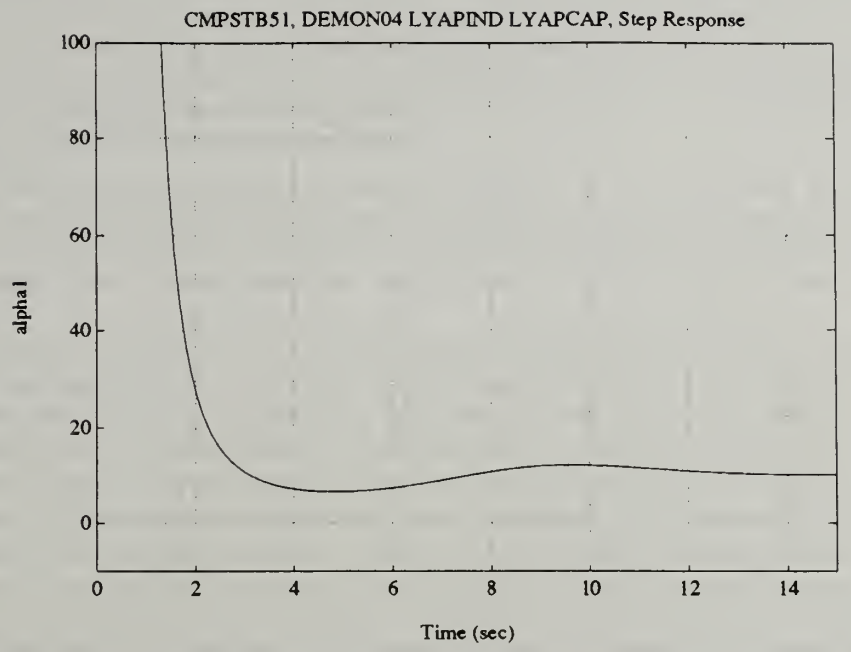

Figure 4.2.16 - Step Response Time-Variant Weighting Factor (α_1 vs. Time)

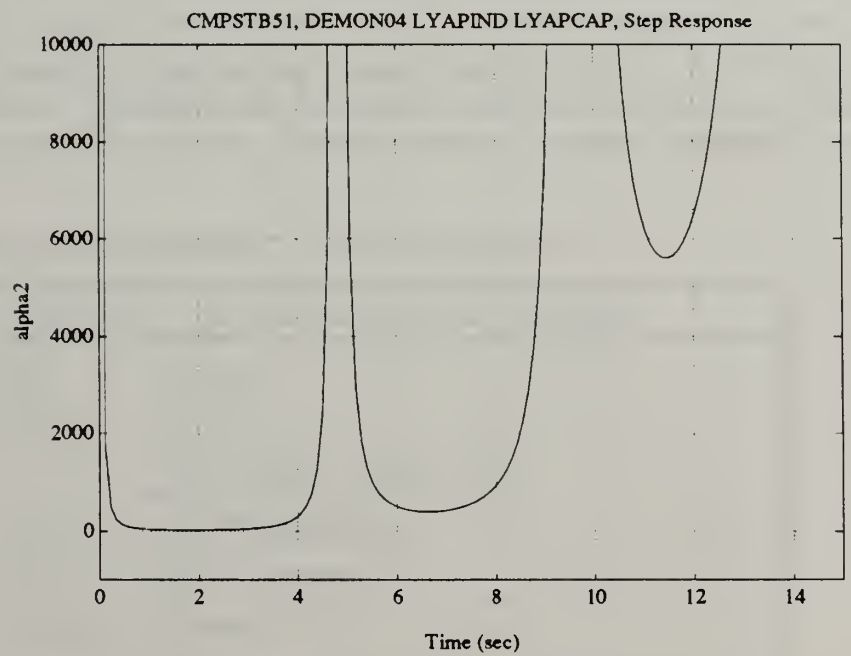

Figure 4.2.17 - Step Response Time-Variant Weighting Factor (α_2 vs. Time)

Figure 4.2.10 shows the behaviour of the inductor current and capacitor voltage, the two state variables, during the step input response. The oscillations arise from the fact that this is an underdamped circuit. Figure 4.2.11 shows the output of the inductor's "stability organ", the stored energy and its convective derivative over time. Figure 4.2.12 shows the same quantities for the capacitor. Note, here too that the zero points of the Lyapunov function (stored energy) coincide with positive going zero points of the Lyapunov function's convective derivative.

The first composite stability measure obtained is the "simple sum" of the two Lyapunov outputs. Figure 4.2.13 shows the "simple sum" composite Lyapunov function and its convective derivative. This sum's convective derivative is certainly not negative semi-definite. Hence, based upon the "simple sum" criterion, stability cannot be concluded.

The curve in figure 4.2.14 is the Lyapunov space trajectory of the composite RLC system. The step response behaviour of this linearly-stable RLC circuit does not meet the element wise criterion for stability. Nor does it meet the "simple sum", weighted-sum, and "indeterminately-weighted-sum" criterions of section 3.2.1. This is because the Lyapunov space trajectory enters the 'first quadrant' of Lyapunov space. Hence, none of the criterions mentioned allows stability to be concluded for this case.

Whereas the "stability demon" employed for this test is based upon the "component neutral" relationship, the convective derivative of the time-variant weighted-sum Lyapunov function should be identically zero for all time, despite the temporary incursion into the 'first quadrant' of Lyapunov space. Figure 4.2.15 shows that this is so. Figures 4.2.16 and 4.2.17 show the respective time-variant weighting factors, the α'*s*.

The points where the α'*s* grow asymptotically large are the points where the Lyapunov function itself goes to zero. Whereas the inductor's Lyapunov function is approaching a steady-state, non-zero value, α_1 does not display asymptotic behaviour. Since the capacitor is approaching a steady-state, zero value, α_2 does display asymptotic behaviour. This behaviour is consistent with the behaviour noted during the unforced response discussion. In this example too, $\underline{\alpha}$ tends to quantify stability in some sense.

4.2.3 Resonant Composite RLC Circuit Performance

Table 4.2.4 - Resonant Input Initial Conditions		
I_L	0.0	Amps
V_c	0.0	Volts
V_{in}		Sinusoidal Voltage Source
	10.0	Volts (amplitude)
	0.71	sec^{-1} (frequency)
	1.5708	phase
δ_1	1.6487	
δ_1	1.6487	

In this simulation, the RLC circuit is given a zero initial state vector. The input voltage is a sine wave whose frequency is very close to the resonant frequency, $\omega_n = \frac{1}{\sqrt{2}}$. Were the input frequency set exactly equal to the resonant frequency, then a singular system would exist and WAVESIM's current method of solution, Newton-Raphson, fails. As this is a linearly stable circuit with bounded input, the output of the "stability demon" should indicate a bounded response. Table 4.2.4 contains the initial conditions for this simulation.

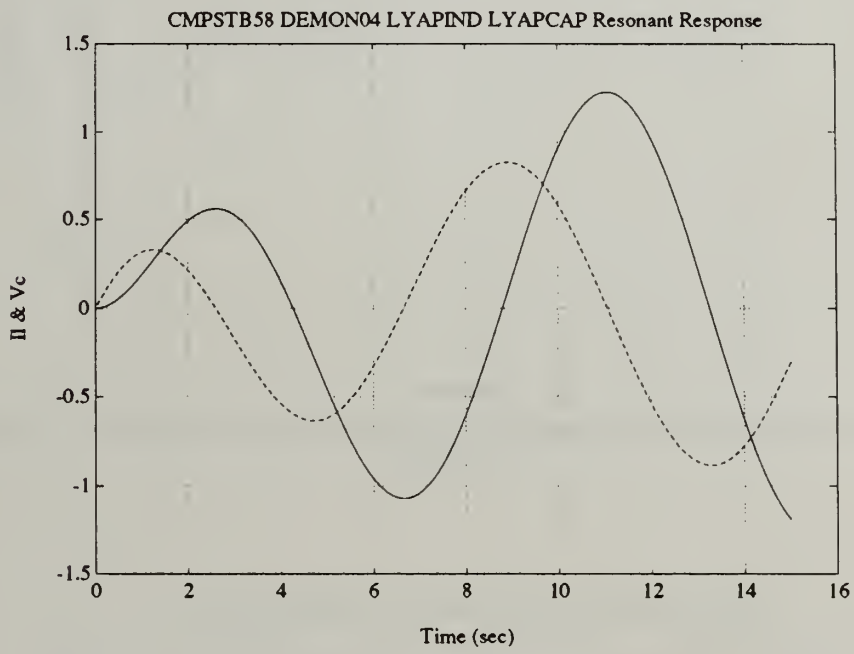

Figure 4.2.18 - RLC Resonant Response (I_L & V_c vs. Time)

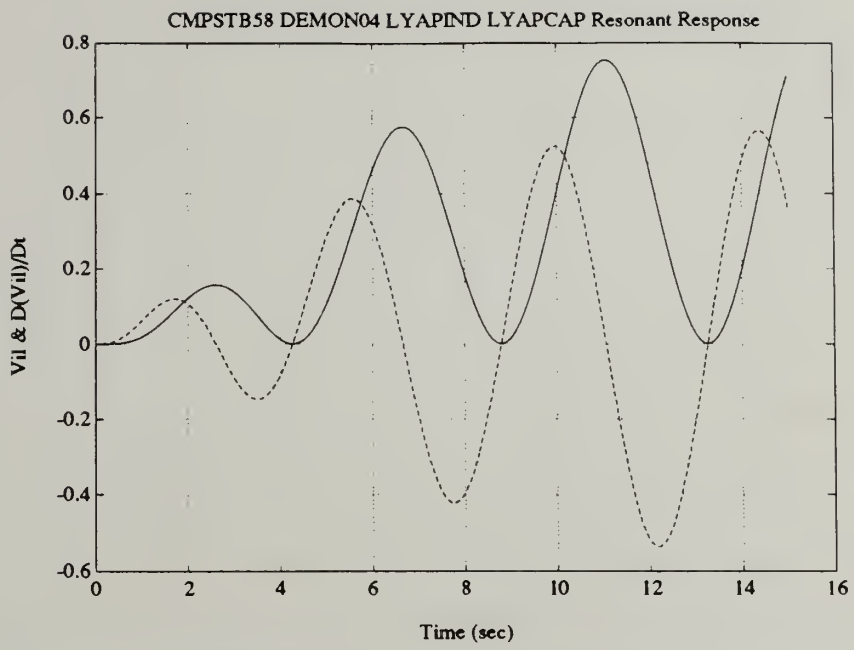

Figure 4.2.19 - Resonant Response Inductor Lyapunov Output (V_1 and $D(V_1)/Dt$ vs. Time)

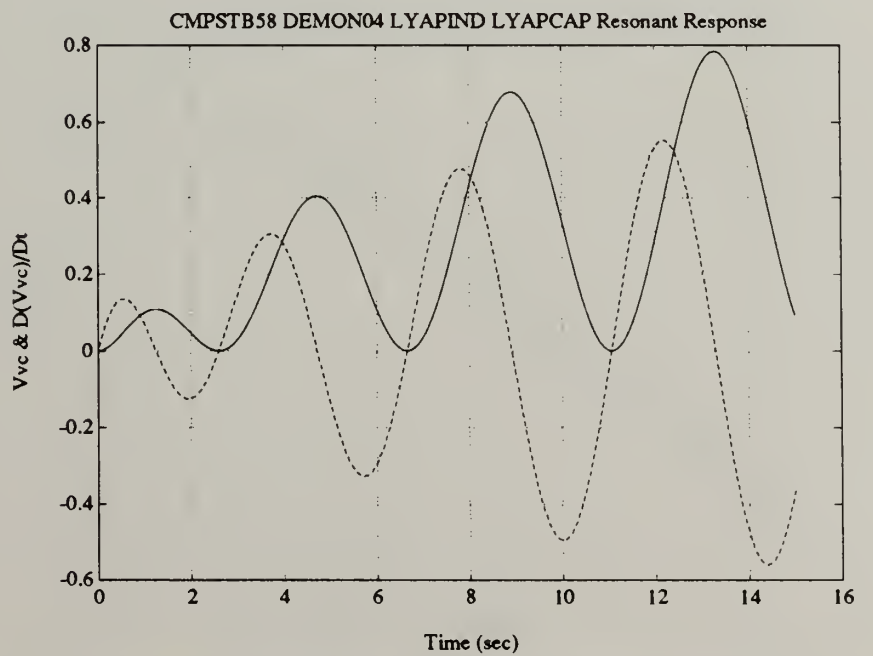

Figure 4.2.20 - Resonant Response Capacitor Lyapunov Output (V_2 and $D(V_2)/Dt$ vs. Time)

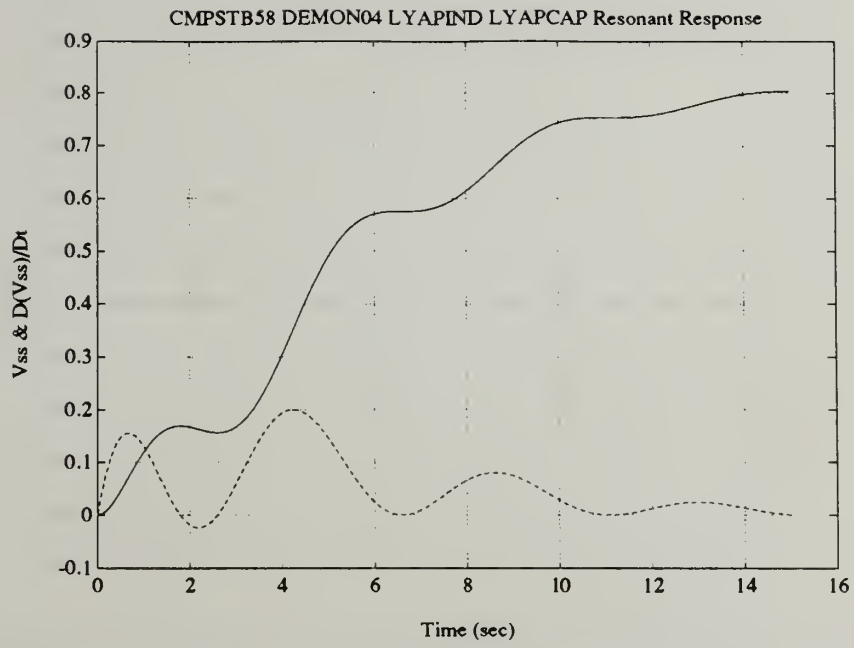

Figure 4.2.21 - Resonant Response "Simple Sum" Lyapunov Output (V_{ss} and $D(V_{ss})/Dt$ vs. Time)

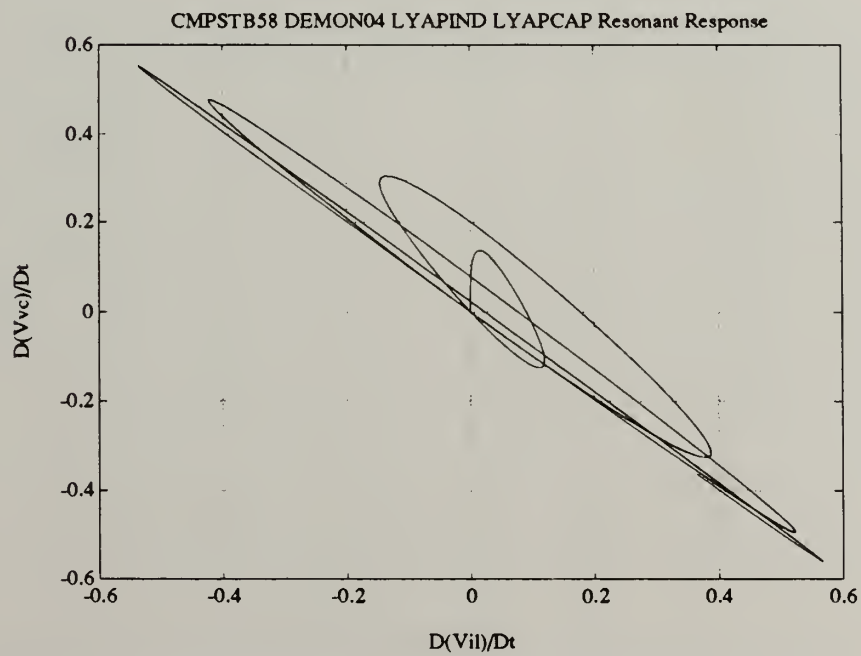

Figure 4.2.22 - Resonant Response Lyapunov Space Trajectory ($D(V_2)/Dt$ vs. $D(V_1)/Dt$)

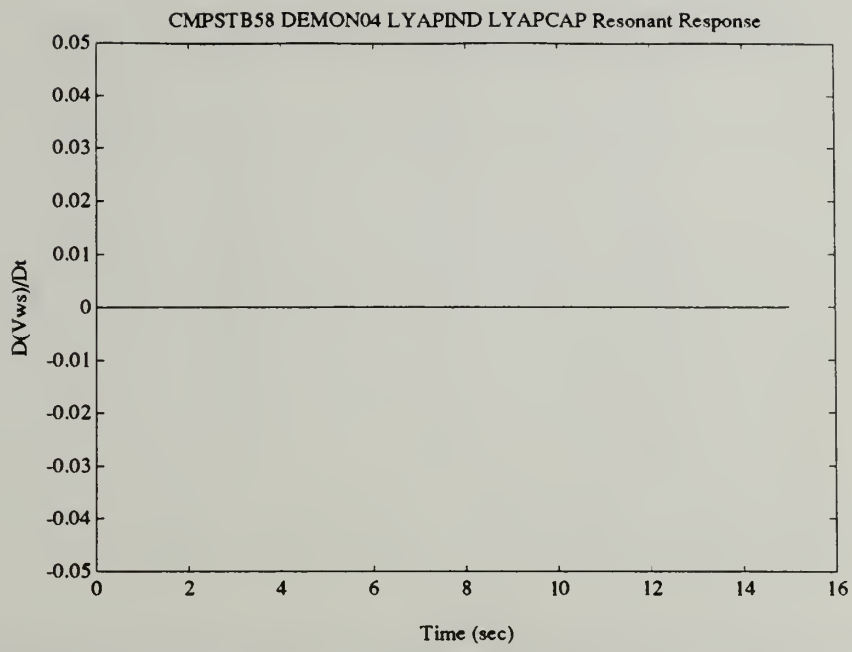

Figure 4.2.23 - Resonant Response "Time-Variant Weighted-Sum" Lyapunov Derivative ($D(V_{ws})/Dt$ vs. Time)

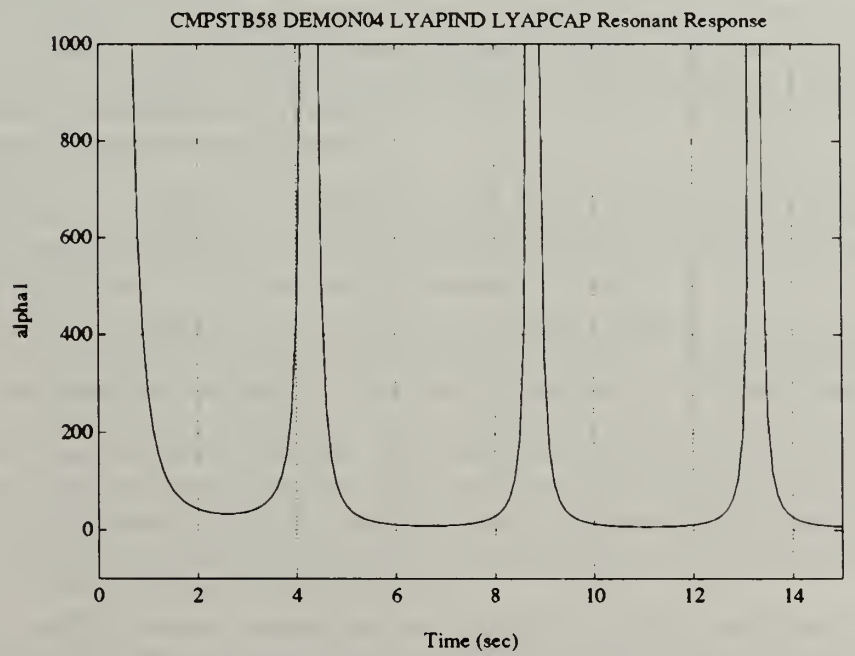

Figure 4.2.24 - Resonant Response Time-Variant Weighting Factor (α_1 vs. Time)

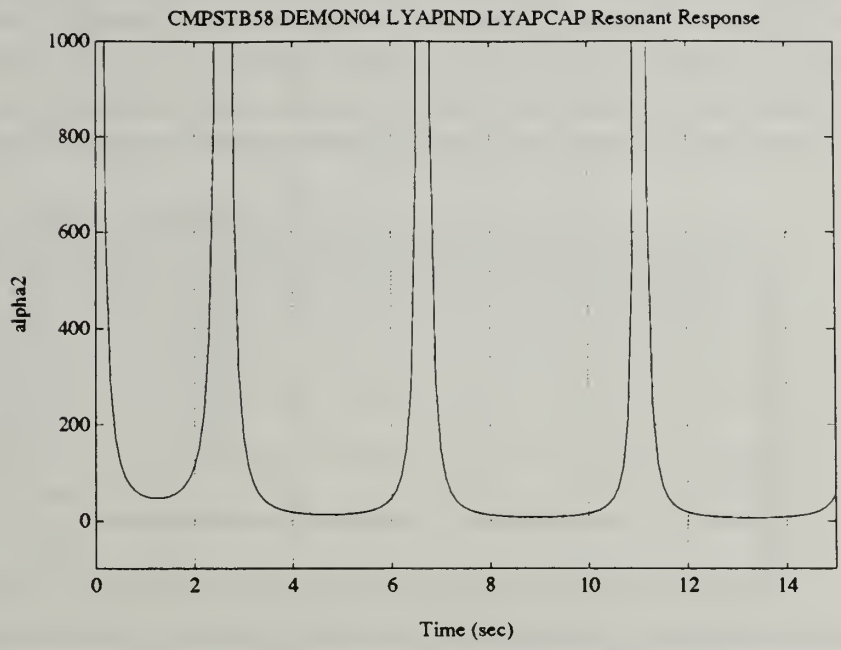

Figure 4.2.25 - Resonant Response Time-Variant Weighting Factor (α_2 vs. Time)

Figure 4.2.18 shows the behaviour of the inductor current and capacitor voltage, the two state variables. The growing oscillations arise from the fact that this is an underdamped circuit being excited with a near-resonant input. Figure 4.2.19 shows the output of the inductor's "stability organ", the stored energy and its convective derivative over time. Figure 4.2.20 shows the same quantities for the capacitor. Both "stability organs" indicate increasing, oscillatory behaviour. Here too the zero points of the Lyapunov function (stored energy) coincide with positive going zero points of the Lyapunov function's convective derivative.

Figure 4.2.21 shows the "simple sum" composite Lyapunov function and its convective derivative. This sum's convective derivative is certainly not negative semi-definite. The stored energy is mostly increasing, though, at a decreasing rate. Based upon the "simple sum" criterion, stability cannot be concluded.

The curve in figure 4.2.22 is the Lyapunov space trajectory of the composite RLC system. The resonant behaviour of this linearly-stable RLC circuit does not meet the element wise criterion for stability. Nor does it meet the "simple sum", weighted-sum, and "indeterminately-weighted-sum" criterions of section 3.2.1. This is because the Lyapunov space trajectory enters the 'first quadrant' of Lyapunov space. Hence, none of the criterions mentioned allows stability to be concluded for this case. Indeed, the Lyapunov space trajectory of the composite system appears to be approaching a limit cycle. The limit cycle trajectory passes along either side of the boundary line given for the "simple sum" criterion in section 3.2.1.

The "stability demon" employed here is based upon the "component neutral" relationship; therefore, the convective derivative of the "time-variant weighted-sum" Lyapunov function should be identically zero for all time, despite the repeated, though temporary, incursions into the 'first quadrant' of Lyapunov space. Figure 4.2.23 shows that this is so. Figures 4.2.24 and 4.2.25 show the respective time-variant weighting factors, the α'*s*..

The points where the α's grow asymptotically large are once again seen to be the points where the Lyapunov function itself goes to zero. Whereas the inductor's Lyapunov function is approaching a limit cycle, α_1 displays periodic asymptotic behaviour. The capacitor and hence, α_2, displays similar behaviour. Temporarily overlooking the peaks in the weighting factors, one can see an overall decline in the value of the α's.. $\underline{\alpha}$ quantifies the tenuous, limit cycle type of stability present in this case.

4.2.4 Time-Variant Composite RLC Circuit Performance

Table 4.2.5 - Time Variant Circuit Inputs and Initial Conditions		
I_L	1.0	Amps
V_c	1e-5	Volts
V_{in}	0.0	Volts
δ_1	1.6487	
δ_1	1.6487	

In this simulation, the RLC circuit is given a non-zero initial state vector. The input voltage is zero. The parallel resistor, R in figure 4.2.1, changes resistance 8.0 seconds into the simulation. It changes from a value of 1.0 Ohms, as given in table 4.2.1, to a value of -1.0 Ohms. The negative resistance causes the circuit to possess positive, real-valued eigenvalues. This presages an exponentially increasing response. Table 4.2.5 contains the initial conditions for this simulation.

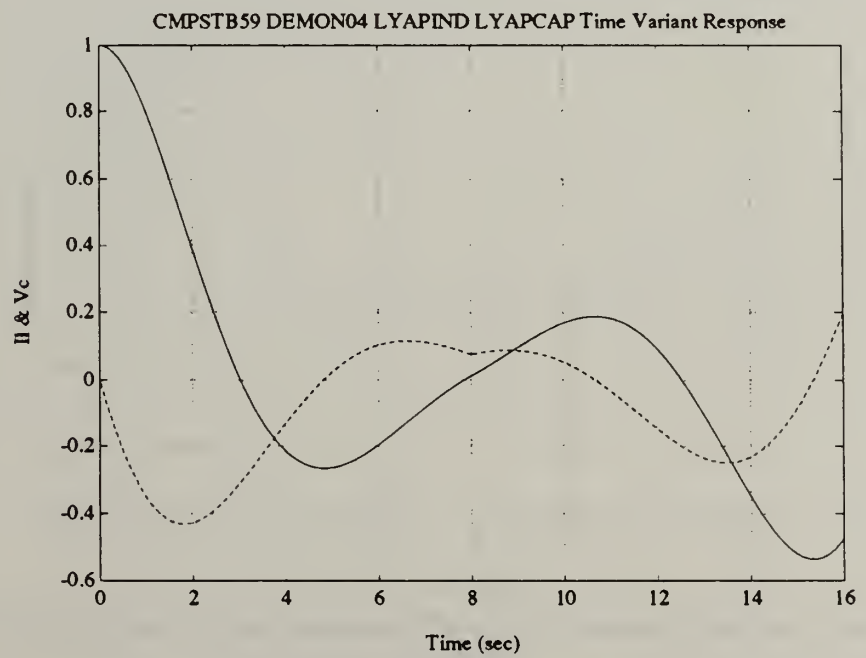

Figure 4.2.26 - RLC Time-Variant Response (I_L & V_c vs. Time)

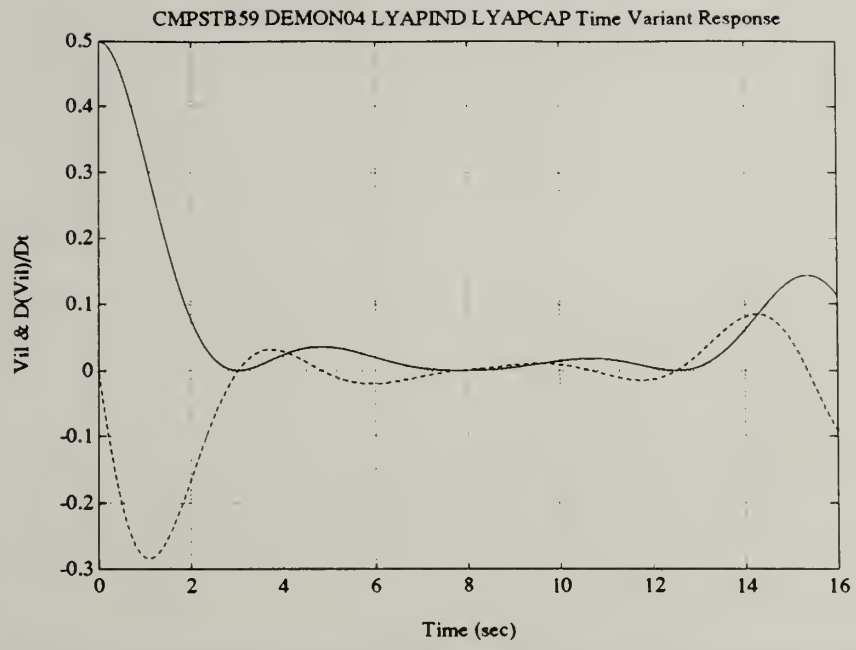

Figure 4.2.27 - Time-Variant Response Inductor Lyapunov Output (V_1 and $D(V_1)/Dt$ vs. Time)

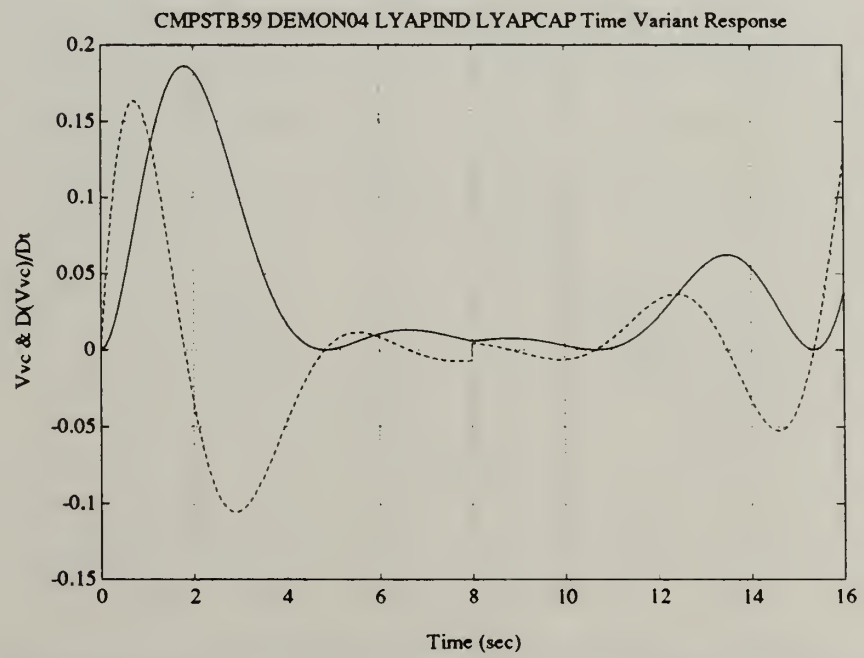

Figure 4.2.28 - Time-Variant Response Capacitor Lyapunov Output (V_2 and $D(V_2)/Dt$ vs. Time)

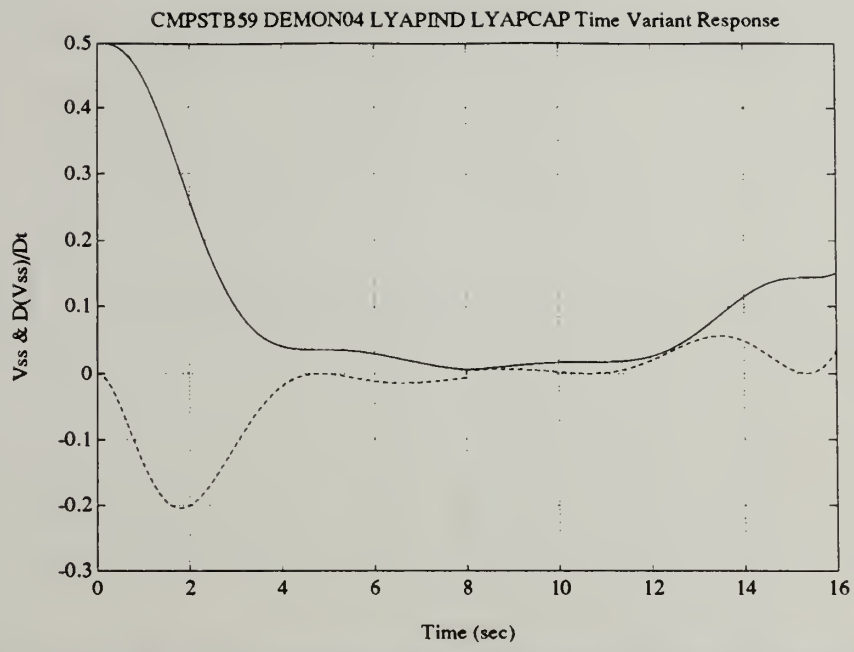

Figure 4.2.29 - Time-Variant Response "Simple Sum" Lyapunov Output (V_{ss} and $D(V_{ss})/Dt$ vs. Time)

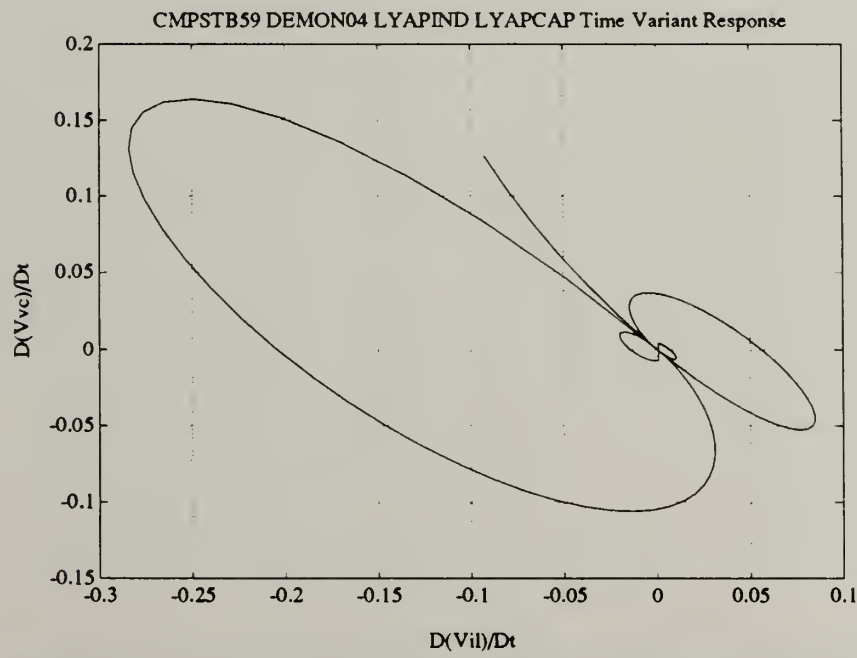

Figure 4.2.30 - Time-Variant Response Lyapunov Space Trajectory ($D(V_2)/Dt$ vs. $D(V_1)/Dt$)

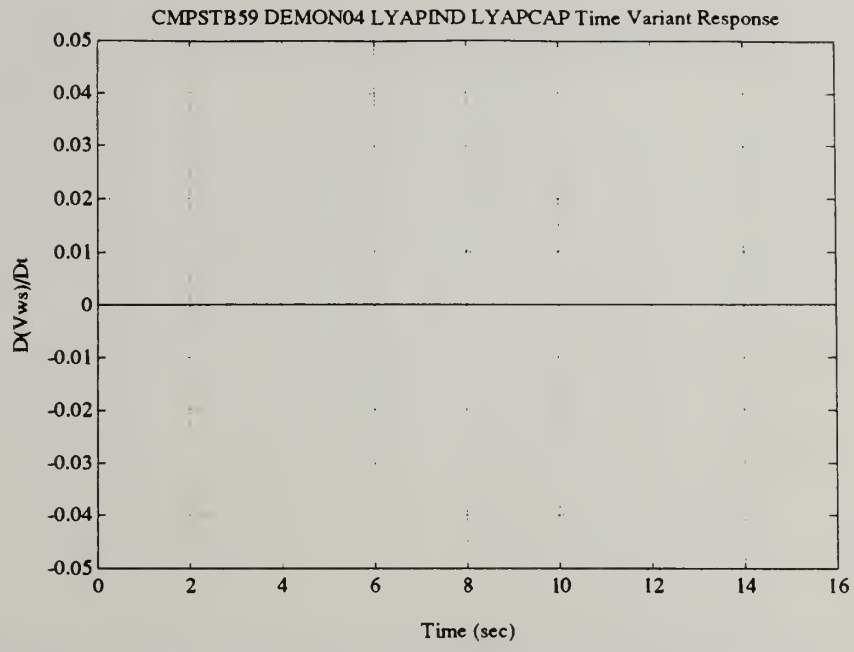

Figure 4.2.31 - Time-Variant Response "Time-Variant Weighted-Sum" Lyapunov Derivative ($D(V_{ws})/Dt$ vs. Time)

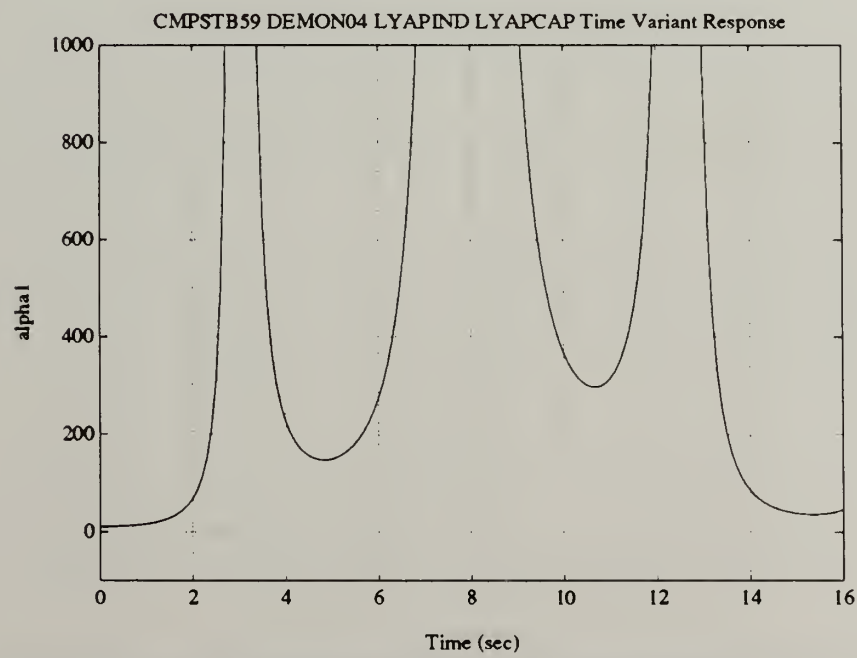

Figure 4.2.32 - Time-Variant Response Time-Variant Weighting Factor (α_1 vs. Time)

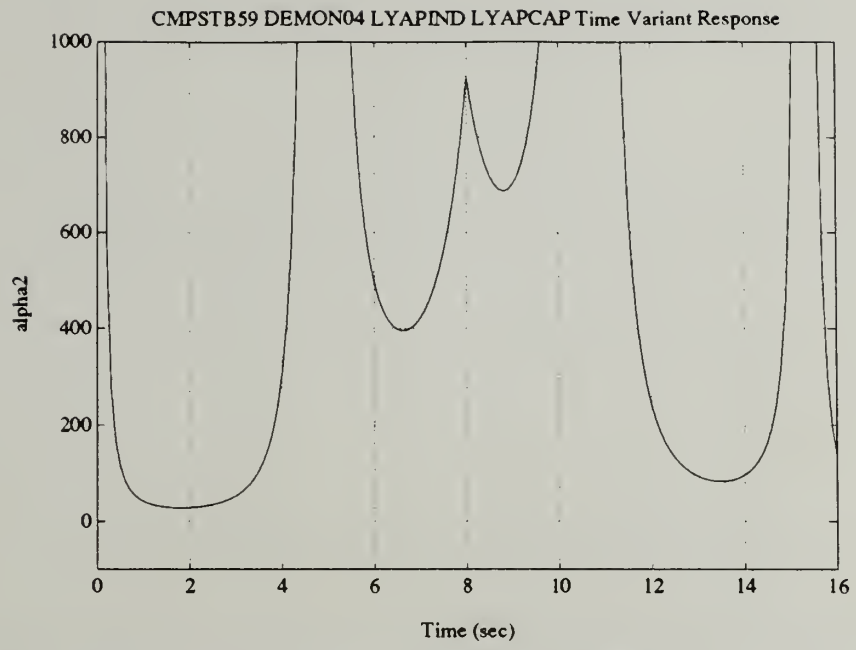

Figure 4.2.33 - Time-Variant Response Time-Variant Weighting Factor (α_2 vs. Time)

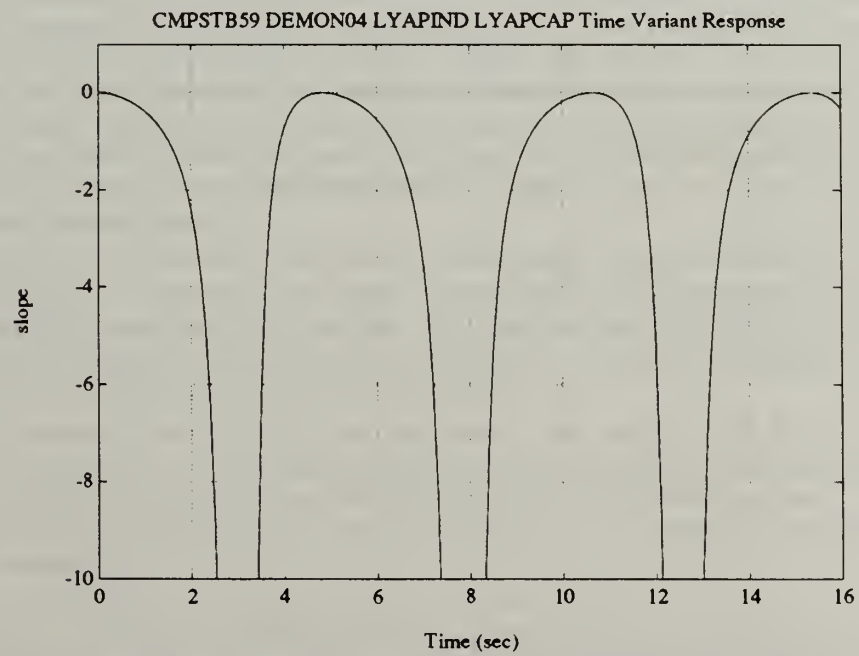

Figure 4.2.34 - Time-Variant Response Stability Region Slope (Slope vs. Time)

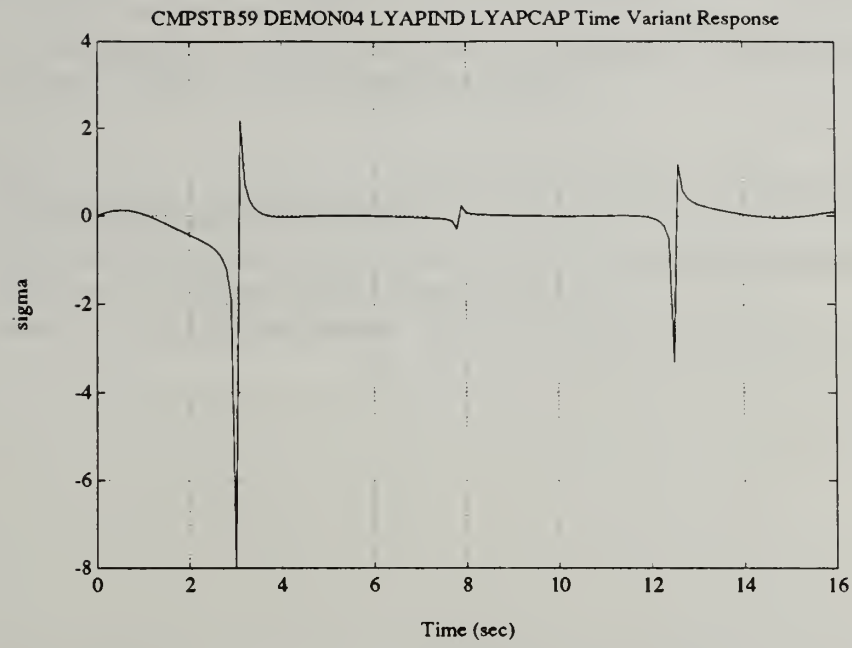

Figure 4.2.35 - Time-Variant Response Stability Region Intercept (Sigma vs. Time)

Figure 4.2.26 shows the behaviour of the inductor current and capacitor voltage, the two state variables. The response for the first 8.0 seconds of the simulation is the same as for the unforced system in section 4.2.1. The response for the second 8.0 seconds of the simulation shows increasing values of the state variables. Figure 4.2.27 shows the output of the inductor's "stability organ", the stored energy and its convective derivative over time. Figure 4.2.28 shows the same quantities for the capacitor. Both "stability organs" indicate decreasing, underdamped, oscillatory behaviour at first, then increasing, oscillatory behaviour later. As expected, the zero points of the Lyapunov function (stored energy) coincide with positive going zero points of the Lyapunov function's convective derivative.

Figure 4.2.29 shows the "simple sum" composite Lyapunov function and its convective derivative. This sum's convective derivative is certainly negative semi-definite for the period of time when R is positive. It is positive semi-definite for the period of time when R is negative. Based upon the "simple sum" criterion, stability can be concluded before R becomes negative but not after.

The curve in figure 4.2.30 is the Lyapunov space trajectory of the composite RLC system. The behaviour of this time-variant RLC circuit does not meet the element wise criterion for stability. It does meet the "simple sum", weighted-sum, and "indeterminately-weighted-sum" criterions of section 3.2.1 when R is positive, but not when R is negative.

As with the other simulations, the convective derivative of the "time-variant weighted-sum" Lyapunov function should be identically zero for all time, despite the repeated, though temporary, incursions into the 'first quadrant' of Lyapunov space. Figure 4.2.31 shows that this is so. Figures 4.2.32 and 4.2.33 show the respective time-variant weighting factors, the α's.

For this simulation, the slope and y-intercept of the boundary of the stable region in Lyapunov space are shown in figures 4.2.34 and 4.2.35 respectively. The slope and intercept are described in figure 3.2.6.

The points where the α'*s* grow asymptotically large are once again seen to be the points where the Lyapunov function itself goes to zero.

4.3 References

4.1 Kirtley, James L. Jr. "Synchronous Machine Dynamic Models." LEES Technical Report TR-87-008. Cambridge, MA: M.I.T. 1987.

4.2 Fitzgerald, A.E., Charles Kingsley Jr. and Stephen D. Umans. Electric Machinery. 4th ed. New York, NY: McGraw-Hill Book Company. 1983.

4.3 Bergen, A. Power Systems Analysis. Englewood Cliffs, NJ: Prentice-Hall, Inc. 1986.

5 Multi-Generator System Response

This chapter uses both the "stability organ" and "stability demon", developed in chapter 3 and tested in chapter 4, to gauge the "large-signal" stability of a two generator system. The two generator system has one conventional generator and one superconducting generator. The motivation for studying this type of system is threefold.

The first reason for examining the two generator system is to use the coenergy-based "stability organ" for 3-phase synchronous machines with the "stability demon" to assess the stability or a two generator system undergoing a short-circuit fault. Such a system requires no other Lyapunov functions than the one developed. Having only two generators also limits the applicable Lyapunov space to an n=2 space, allowing easy visualisation.

The second reason for examining a system containing both a conventional generator and a superconducting generator is that the effect on stability of having these two different types of machine present and in proximity will become an important issue as superconducting machinery starts to be employed in commercial electric power systems. Several studies have been conducted on what the effect on stability will be, references [5.1] - [5.3]. It is still an issue beggaring research.

The third reason for examining a system of two disparate generators, one of which is superconducting, is that it is of some relevance to naval electric power systems for two reasons. First, superconducting machinery offers great promise for reductions in size and weight of generation and propulsion machinery. This is a valuable attribute in such a size-conscious pursuit as naval combatant design. Second, even advanced naval electric power systems comprised solely of conventional generators may contain disparate types of generators. Hence, a stability analysis tool capable of analysing such a system would be valuable.

The first section of this chapter discusses the system to be analysed. The second section treats the results provided by the "stability organ" and "stability demon". The final section provides a discussion of the results.

5.1 Description of System

The system analysed here is based upon the transient stability example in reference [5.1]. There are some important differences, though. Figure 5.1.1 shows the example system.

The generators used here are those used in reference [5.1]. Their parameters are given in table 5.1. These values are an adaptation of the parameters given in the reference.

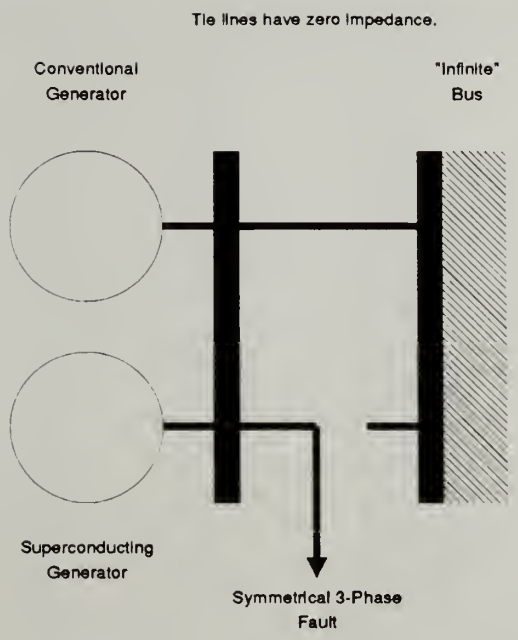

Figure 5.1.1 - Example Two-Generator System

Unlike the system of reference [5.1], the symmetrical fault is applied directly at the terminals of the bus connecting the generators.--There is no snub reactance. This absence will have a significant effect on any critical clearing times. The effect of the pre-fault reactance of the tie line between the infinite bus and the generators' bus on the initial conditions is accounted for by adjusting the initial difference in voltage angle between the two buses to reflect the presence of the reactance.

As well as neglecting line reactances, the voltage regulator and power system stabiliser models included in the system of reference [5.1] are neglected in this research. The effect of these omissions is not addressed. The system used here, though, is much simpler. The field voltage is held constant, as is the mechanical torque input.

Table 5.1 - Generator Parameters

Machine parameters are taken from reference [5.1].

Parameter	Symbol	Conventional	Superconducting	Units
d-axis mutual reactance	xad	2.02	0.197	pu
q-axis mutual reactance	xaq	1.89	0.197	pu
stator leakage reactance	xal	0.1	0.1	pu
field leakage reactance	xfl	0.144	0.244	pu
d-axis damper leakage	xkdl	0.078	0.017	pu
q-axis damper leakage	xkql	0.078	0.017	pu
stator resistance	rs	0.0038	0.0019	pu
field resistance	rf	0.00115	7.9e-7	pu
d-axis damper resistance	rkd	0.00570	0.000365	pu
q-axis damper resistance	rkq	0.392	0.000365	pu
inertia constant	H	3.134	2.456	sec
pole pairs	PP	1	1	
machine base voltage	VB	19596	19596	Volts,peak,l-n
machine base power	PB	907M	907M	Watts
base frequency	wB	376.991	376.991	1/sec
system base voltage	VsB	19596	19596	Volts,peak,l-n
system base power	PsB	907M	907M	Watts

5.2 Stability Analysis of System

The measure of stability sought here is a short-circuit critical clearing time. The two generators are operating in parallel. They are supplying rated voltage and current at unity power factor to an infinite bus through a tie line with 0.2 per-unit reactance prior to the fault. The phase terminals of the two different generators are shorted together, with no external reactances, at time zero. Mechanical torque input and field voltages are held constant. Initial conditions and input quantities are shown in table 5.2.

Table 5.2 - Initial Conditions and Inputs

Parameter	Symbol	Conventional	Superconducting	Units
d-axis current	id_0	-1.040	-0.3481	pu
q-axis current	iq_0	-0.5303	-1.1742	pu
"o" current	io_0	0.0	0.0	pu
field current	ifd_0	1.4072	6.4967	pu
d-axis damper current	ikd_0	0.0	0.0	pu
q-axis damper current	ikq_0	0.0	0.0	pu
rotor electrical angle	θ_{re}	-0.4478	-1.2826	
terminal voltage	vt	0.827	0.827	pu
rotor mechanical speed	ω_{rm}	377.0	377.0	1/sec
mechanical torque input	Tm	1.0	1.0	pu
field voltage	vfd	0.00162	5.13e-6	pu

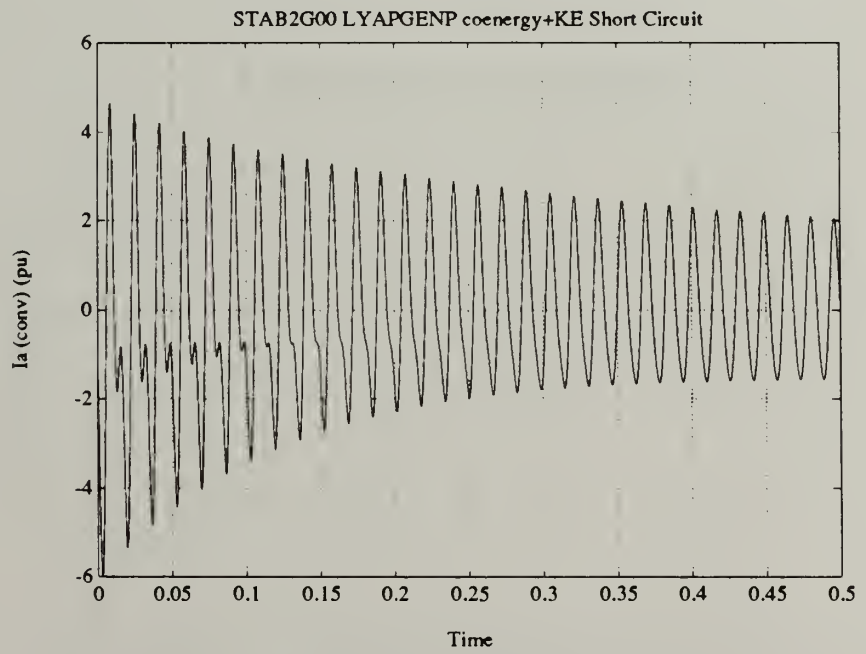

Figure 5.2.1 - Conventional Generator a-Phase Current (I_{ac}) vs. Time (seconds)

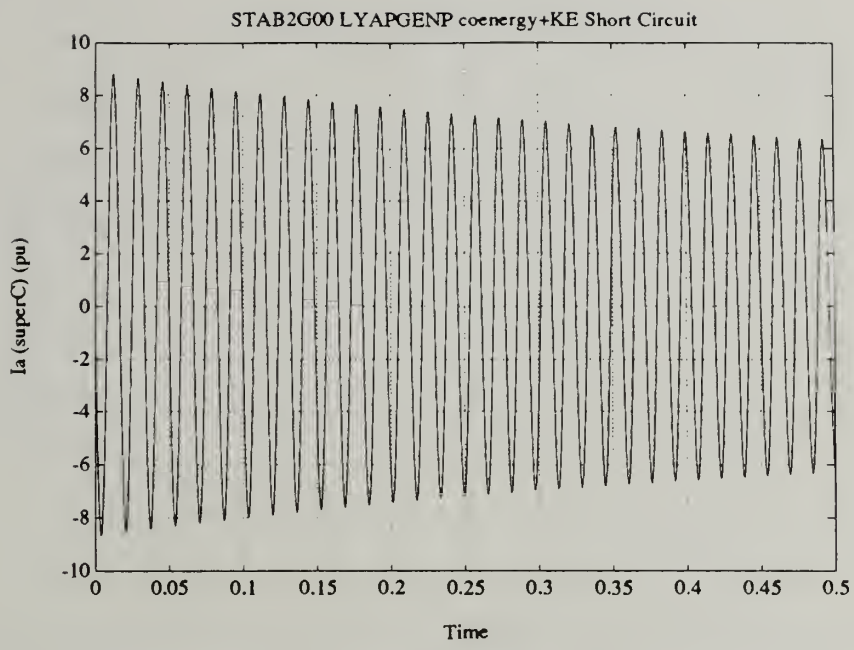

Figure 5.2.2 - Superconducting Generator a-Phase Current (I_{as}) vs. Time (seconds)

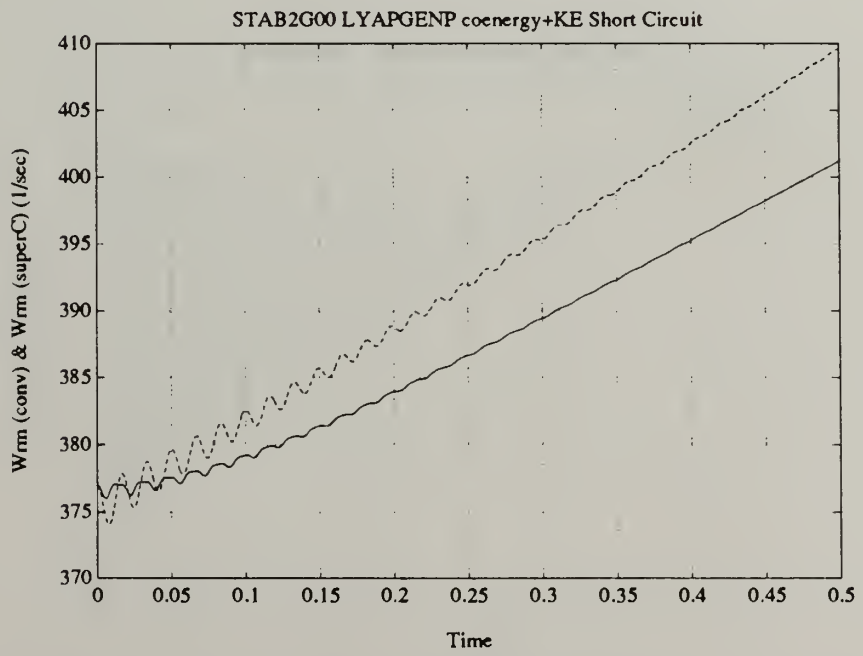

Figure 5.2.3 - Two Generators' Rotor Mechanical Speeds (ω_{rmc} & ω_{rms}) vs. Time (seconds)

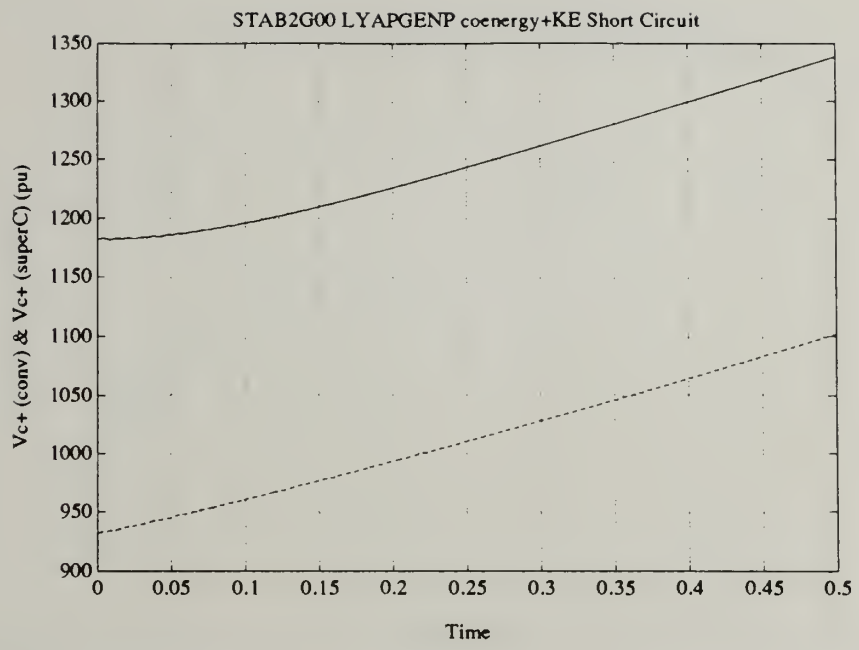

Figure 5.2.4 - Two Generators' Lyapunov Functions, V_c(Coenergy+K.E.) and V_s(Coenergy+K.E.) vs. Time (seconds)

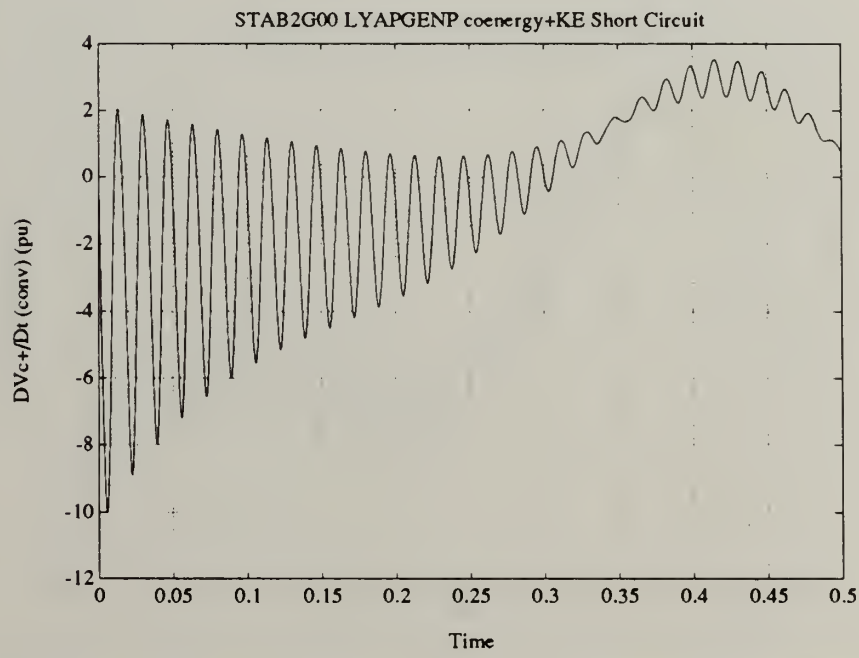

Figure 5.2.5 - Conventional Generator Lyapunov Derivative, DV_c(Coenergy+K.E.)/Dt vs. Time (seconds)

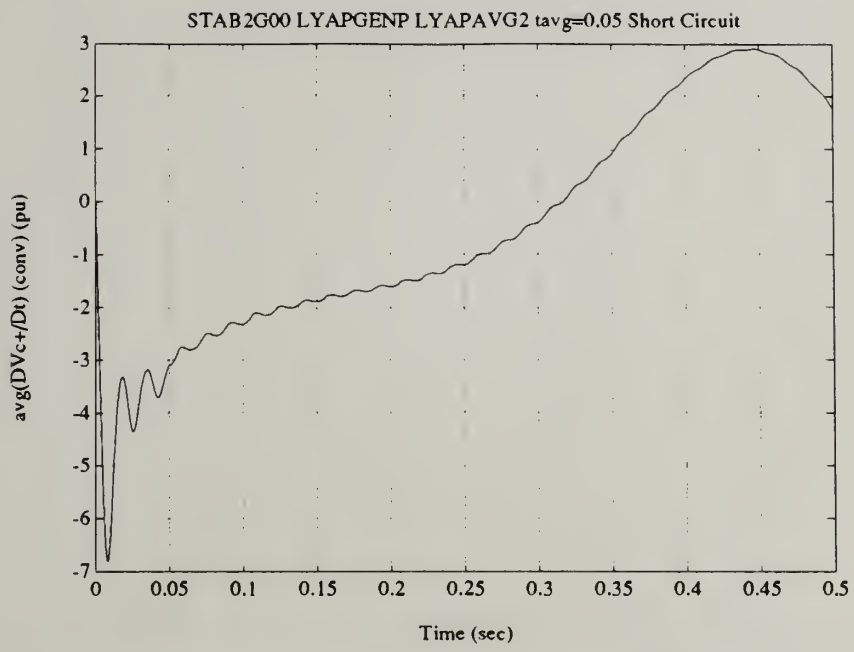

Figure 5.2.6 - Conventional Generator Averaged Lyapunov Derivative avg(DV_c(Coenergy+K.E.)/Dt) vs. Time (t_{avg}=0.05 seconds)

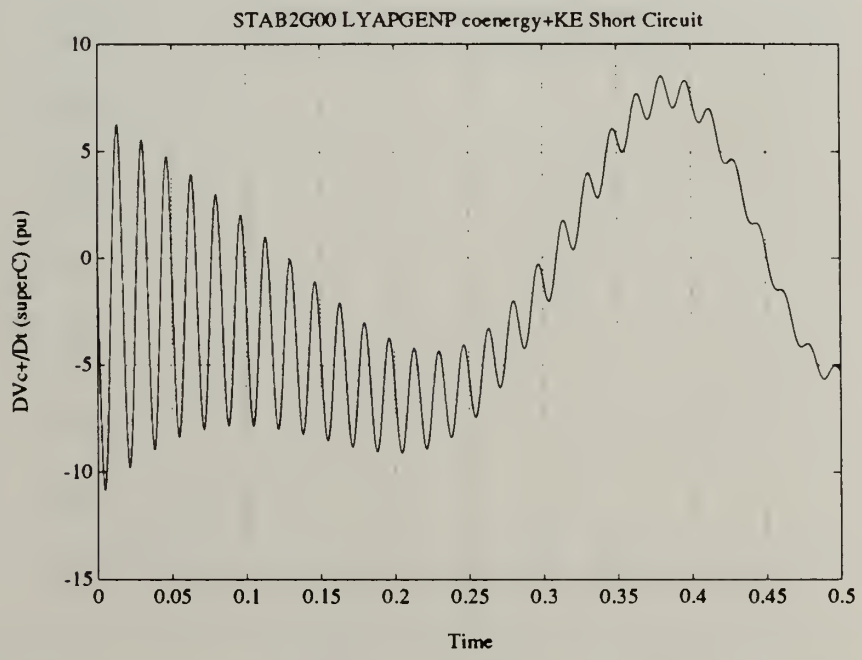

Figure 5.2.7 - Superconducting Generator Lyapunov Derivative DV_s(Coenergy+K.E.)/Dt vs. Time (seconds)

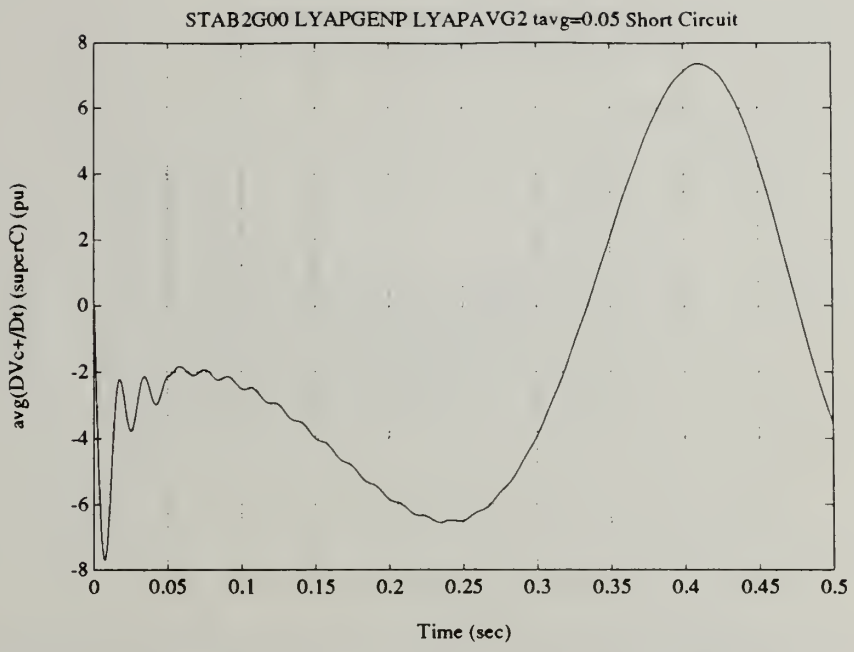

Figure 5.2.8 - Superconducting Generator Averaged Lyapunov Derivative avg(DV_s(Coenergy+K.E.)/Dt) vs. Time (t_{avg}=0.05 seconds)

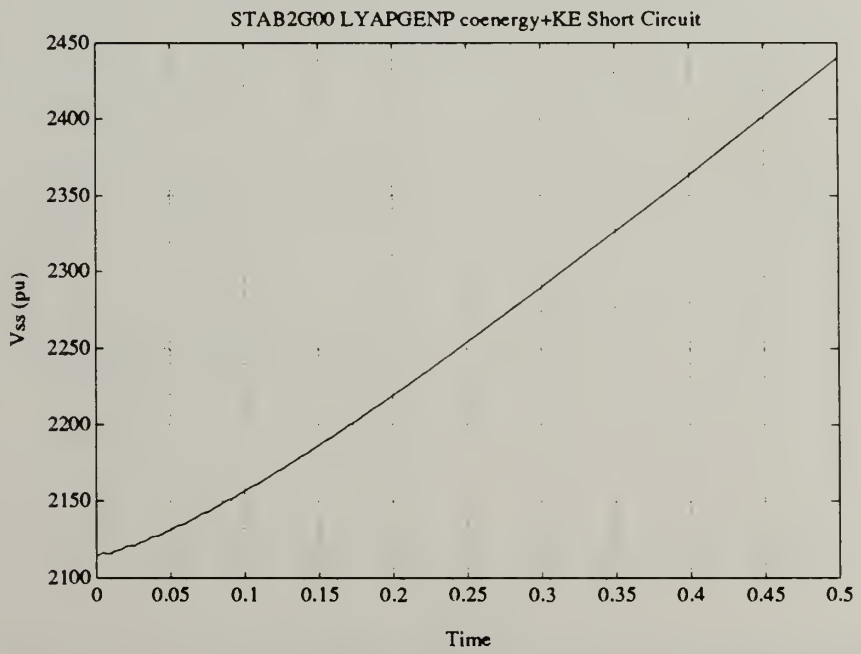

Figure 5.2.9 - Simple Sum Lyapunov Function, V_{ss} vs. Time (seconds)

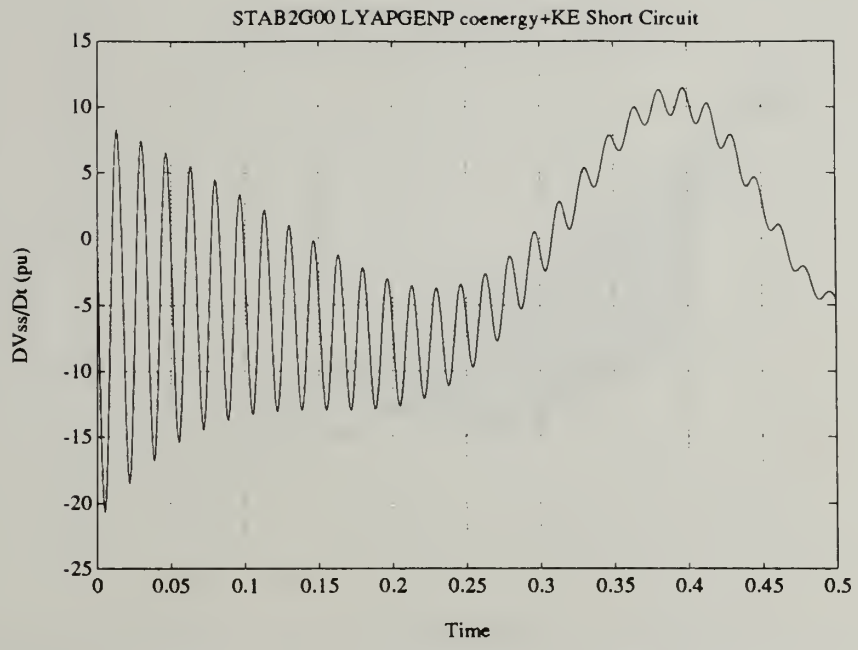

Figure 5.2.10 - Simple Sum Lyapunov Derivative, DV_{ss}/Dt vs. Time (seconds)

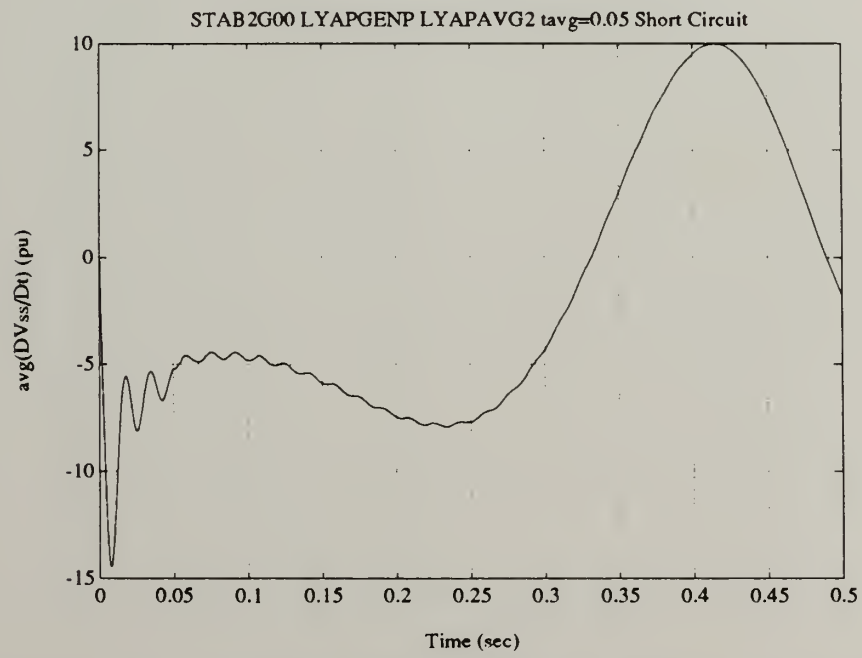

Figure 5.2.11 - Simple Sum Averaged Lyapunov Derivative, $avg(DV_{ss}/Dt)$ vs. Time (t_{avg}=0.05 seconds)

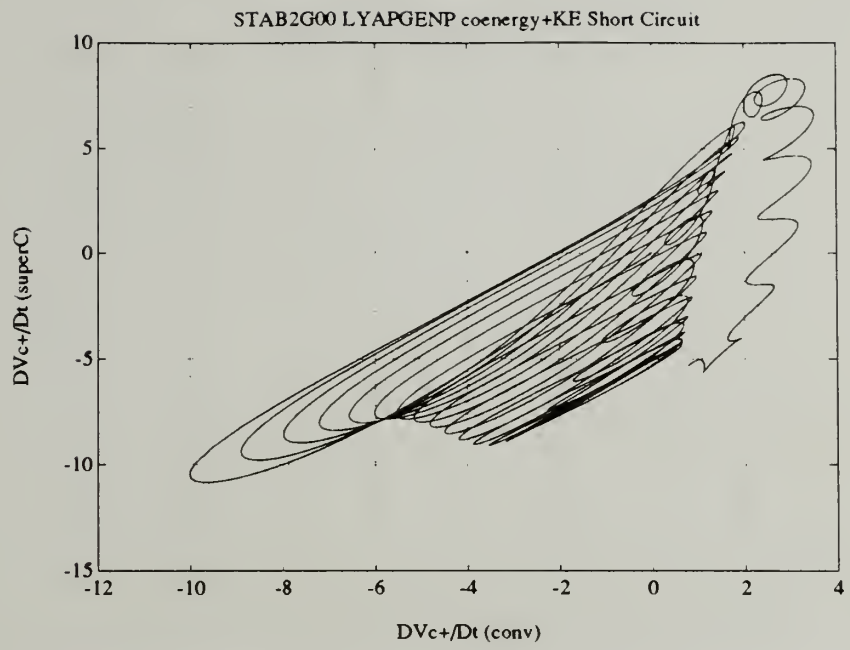

Figure 5.2.12 - Two Generator System Lyapunov Space Trajectory, DV_s/Dt vs. DV_c/Dt

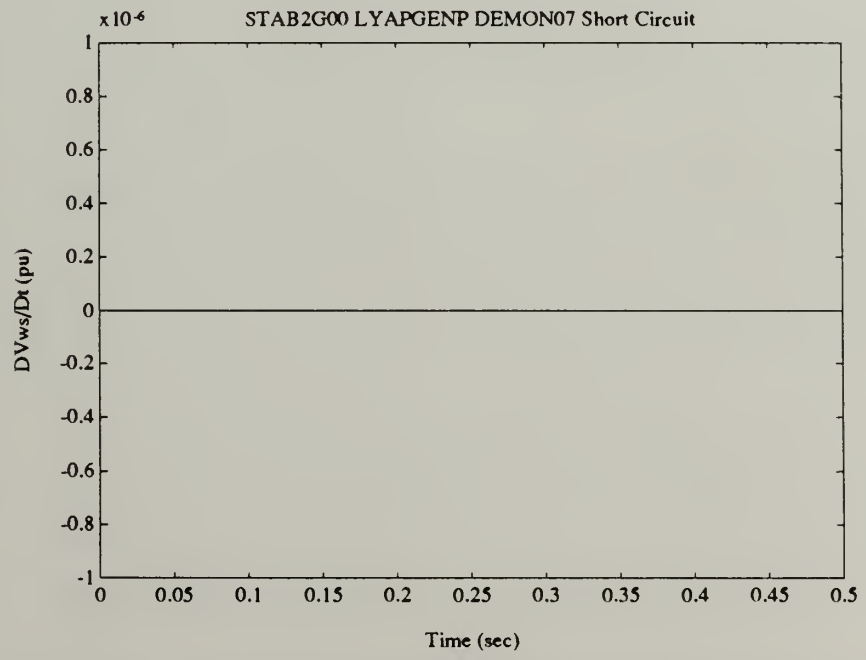

Figure 5.2.13 - Two Generator System "Time-Variant Weighted-Sum" Lyapunov Derivative, DV_{ws}/Dt vs. Time

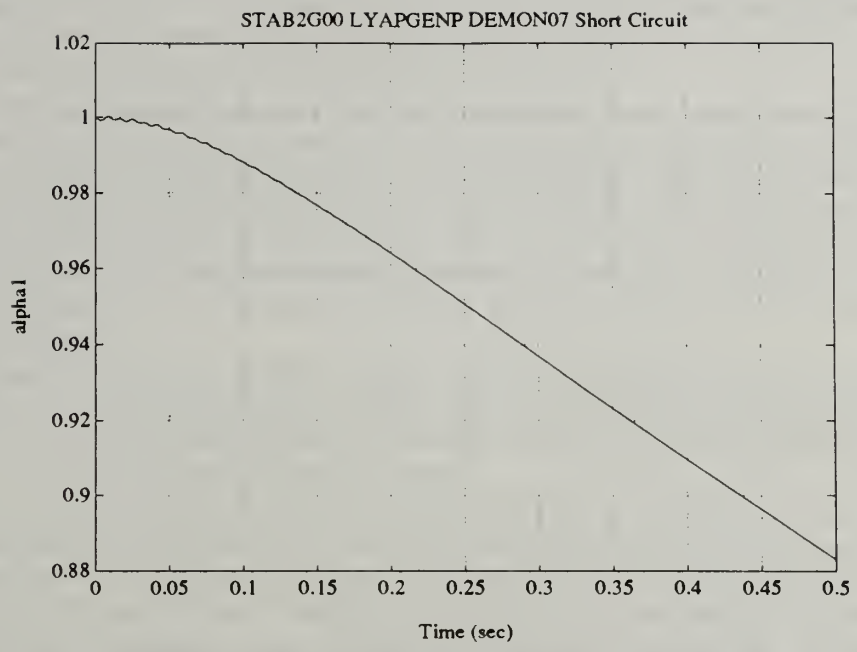

Figure 5.2.14 - Two Generator System Time-Variant Weighting Factor, α_1 vs. Time

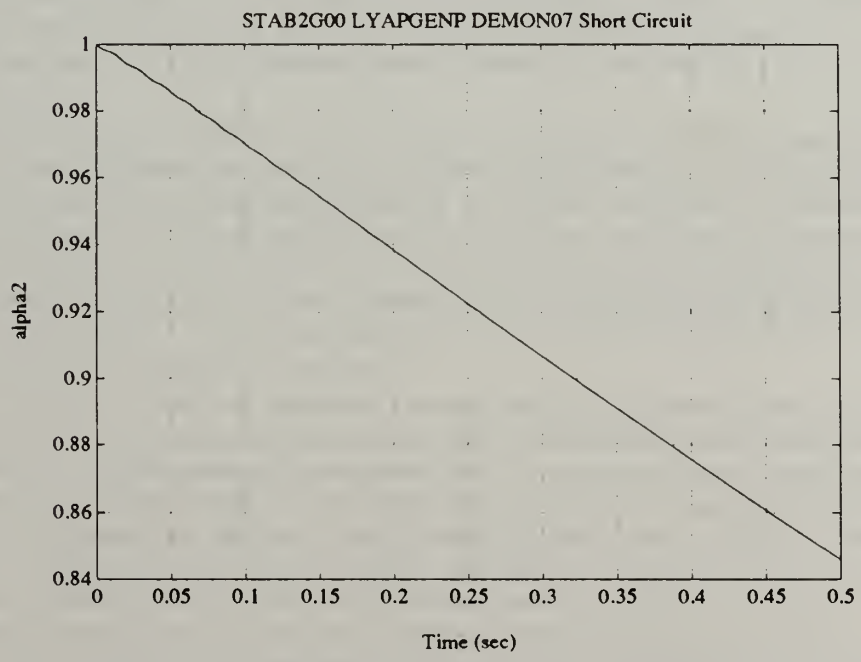

Figure 5.2.15 - Two Generator System Time-Variant Weighting Factor, α_2 vs. Time

The plot of the short-circuit current of the conventional generator, figure 5.2.1, shows the conventional generator having initially, times less than 0.1 seconds, a pronounced negative offset. The offset shifts to a positive one for the second half of the simulation. The superconducting generator's current, on the other hand, has a slight positive offset initially which then tapers off, figure 5.2.2.

The rotor mechanical speeds of the two generators show the effects of oscillating torques, damping and inertia, figure 5.2.3. The conventional generator, with its lower current levels and greater inertia, displays smaller oscillations in speed than the superconducting generator with its larger currents and less inertia. Having greater inertia, the conventional generator does not accelerate as quickly. The effect of damping is also very obvious. Oscillations in the conventional generator's speed have virtually died out by the end of the simulation. The superconducting generator's speed oscillations are larger and more persistent.

The output of the two "stability organs" for this simulation is the sum of the coenergy and kinetic energy, equation (3.1.66). These two Lyapunov functions are shown in figure 5.2.4. Some small oscillations are present; however, the dominant trend, observed in section 4.1, is the increase in inertial energy.

As this simulation involves concern about the ability of the two generators to supply power upon fault clearance, the "re-connected" version of the convective derivative of the Lyapunov function is used, figures 5.2.5 and 5.2.7. In both cases, no conclusions regarding stability can be made. Rather significant energy oscillations are present.

Time-scale averaging is used to attenuate the energy oscillations. Figures 5.2.6 and 5.2.8 are the time-scale averaged versions of the Lyapunov derivatives. Here the chosen time-scale for averaging is 0.05 seconds. The armature time constants for the conventional and superconducting machines are 0.122 seconds and 0.162 seconds respectively. The averaging here involves three 60Hz cycles. The time-scale averaging does, in fact, eliminate the oscillations in stored energy. Interpretation of figure 5.2.6 would suggest a critical clearing time of about 0.315 seconds for the conventional generator. Similarly, figure 5.2.8 suggests a critical clearing time of about 0.33 seconds for the superconducting generator.

The first composite system stability criterion applied to this two generator system is the "simple sum" criterion, section 3.2.1. Figure 5.2.9 shows that the simple sum of the conventional and superconducting generators' Lyapunov functions is positive definite, and increasing with very small oscillations. As with the individual Lyapunov derivatives, the derivative of the "simple sum" Lyapunov function has significant oscillations which obscure a stability conclusion, figure 5.2.10. Time-scale averaging of the "simple sum" derivative, figure 5.2.11, would suggest a critical clearing time for the composite system of slightly less than 0.33 seconds.

The trajectory of the two generator system through Lyapunov space, figure 5.2.12, shows that the two generator system does not meet the element wise, "simple sum", weighted-sum or "indeterminately-weighted-sum" composite system criterions. The trajectory is initially at the origin. It travels around the inside of the 'basket' until it reaches the bottom. The trajectory begins a rapid, spiraling climb back out of the 'basket', spills over the 'rim', then crosses through the first quadrant of Lyapunov space and so on. Qualitatively speaking, the behaviour within the 'basket' appears convergent until the origin is passed on the way up and out. Subsequent behaviour is not so easily characterised. Of note, the length of the segments of the trajectory through the first quadrant are finite.

Figure 5.2.13 shows the "time-variant weighted-sum" Lyapunov derivative. This Lyapunov derivative is calculated using DEMON07.m and DEMONPRO.m, listed in Appendix B. The weighting factors are based upon the "component neutral" relationship. Figure 5.2.13 is zero throughout the simulation.

Figures 5.2.14 and 5.2.15 are the weighting factors calculated by the "stability demon". These α's are valid, being positive and non-zero. Unlike the examples in section 4.2, at no time does either α "blow up". This is because the state variables do not approach their equilibrium values which correspond to the zero value of their Lyapunov function. The quantitative interpretation of the weighting factors is that they are decreasing over the second half of the simulation, indicating decreasing stability.

5.3 Interpretations

The values for critical clearing time given in the previous section are certainly near the values given in reference [5.1]. The fact that the critical clearing times suggested by the time-scale averaged Lyapunov derivatives are slightly larger than the critical clearing times given in reference [5.1] is consistent with the absence of a snub reactance. Without running other analyses, further quantitative statements about the effect on stability of having the two disparate generators operating together are not possible.

The implications of this analysis of a two generator system for the "stability organ" and "stability demon" notions affirm their utility. Namely, both items provided the information that they were supposed to provide. The information is relevant as well. Aside from a determination of a critical clearing time measure based upon the Lyapunov function which underlies the "stability organ", the "stability demon" provides a quantity which is related to the stability of a composite system, the weighting factors. In this instance, the meaning of the precise magnitude of the weighting factors is uncertain.-- Their behaviour with time carries a distinct message.

5.4 References

5.1 Kirtley, J.L. Jr. "System Interaction Characteristics of Superconducting Generators." Draft submitted to: Proceedings of the IEEE. Cambridge, MA: M.I.T. February 10, 1992.

5.2 Taniguchi, H., M.Asada, M.Takasaki, Y.Kitauchi and M.Koike. "Power System Stability Improvement by Superconducting Generators." SM-100, International Conference on the Evolution and Modern Aspects of Synchronous Machines. Zurich, CH. August 27-29, 1991.

5.3 Osheiba, A.M. "Comparative Stability Behaviour of Superconducting and Conventional Synchronous Generators." SM-100, International Conference on the Evolution and Modern Aspects of Synchronous Machines. Zurich, CH. August 27-29, 1991.

6 Conclusions

6.1 Comment on Results

Assessing the merit of the coenergy-based "stability organ" is somewhat complex. The original intent was to develop a measure of stability margin for synchronous generators. Instead, a Lyapunov function which represents the actual stored energy of the machine was developed. Four particular conclusions can be made regarding the utility of the "stability organ" developed in this research.

1) The critical clearing time question really asks, "How long can the fault be imposed before synchronisation is lost?" The coenergy-based "stability organ" answers the question, "How long can the fault be imposed before the generator's stored energy grows?" There is a definite correlation between the two questions. When evaluation of the Lyapunov function convective derivative includes the effect of the system inputs to which the given device would be "re-connected", then answering the second question answers the first as well. The existing issue is selecting the correct version of the convective derivative.

2) The coenergy-based Lyapunov function captures all of the energy dynamics admitted by the underlying 7^{th} order model. This includes energy stored in armature leakages and damper windings. The longer term dynamics of the field winding are included as well. If an analyst deems any of these dynamics to be superfluous, then selection of a simplified model would remove their effects. A reformulation of the expression describing the coenergy is necessary in such a case.

This research offers time-scale averaging of the Lyapunov derivative as a means to include all dynamic effects admitted by the model. However, it allows oscillations to be attenuated over an arbitrary time-scale. The difference between a simplified model formulation and ex post facto time-scale averaging hinges upon flexibility. If it is known a priori that good time-scale separation exists within a system, then a simplified model is a more elegant approach. However, if the separation of dynamics' characteristic times is not pronounced, or even known, then averaging results permits an adaptive means of dealing with unwanted oscillations. The existing issue is selecting the correct time-scale over which to average the convective derivative. The algorithm for averaging which is used in this research is very simplistic.

3) The fact that the coenergy-based Lyapunov function's convective derivative frequently displays oscillatory behaviour rather than strict negative semi-definite behaviour does not disqualify its usefulness. This is particularly true when it is used within a composite system. In a composite system where the Lyapunov functions representing each component account for energy in a consistent manner, components with increasing energy can be matched with components whose energy is decreasing.--The effect on the composite system's stability would be neutral. This is illustrated in the unforced RLC example. That the coenergy-based "stability organ" developed in this research does not doggedly pursue proving negative semi-definiteness and yet provides meaningful information about stability is a victory for engineering-based Lyapunov functions. The existing issue is selecting the correct stored energy relationship upon which to base "stability organs" for additional components and ensuring consistency between different components.

4) Were stabilising generator controls to be based upon the Lyapunov derivative output of the "stability organ", then the controller would tend to ensure that the generator is supplying a load before increasing the inputs to the generator. Such an attribute is important for naval electric power systems.

The original goal of finding a stability 'margin' has been achieved for synchronous machines. It is not the metric of location within stable regions of state-space which was initially envisioned. Rather, it offers a metric of the degree to which input quantities can change before stability can no longer be concluded.

Another important point needs to be made about the "stability organ" as implemented.--It provides a continuous output. The goal of critical clearing time simulations is to obtain a single number, t_{cr}, which characterises a specific configuration with specific initial conditions and a specific perturbation. In a sense, this t_{cr} is static. Knowing what a generator's t_{cr} is will not keep it from losing synchronisation if t_{cr} is exceeded. The "stability organ" provides a quantity which gives an instantaneous indication of stability regardless of configuration or initial conditions. It is more useful than t_{cr} in terms of offering information which a controller can use to ensure the generator's stability. An aside, representing an improvement over indirect methods for determining t_{cr}, the "stability organ's" determination of t_{cr} can be accomplished with just one simulation.

Assessing the merit of the composite system "stability demon" is also somewhat complex. The original intent was to develop a measure of stability margin for a composite system. When composite system criterions are compared in Lyapunov space because of the high dimensionality of state-space for a composite system, development of a "time-variant weighted-sum" criterion offered the largest region of stability. The notion of a state-space oriented stability margin was forsaken for a notion of margin in Lyapunov space. Five particular conclusions can be made regarding the utility of the "stability demon" developed in this research.

1) The time-variant weighting vector is constructive. One needs only to exist for stability to be concluded. Assuming that at least one exists, a multitude of methods for selecting the weighting factors are possible. Finding a weighting vector which is 'best', in some sense, is an open issue. Another existing issue is ensuring that an algorithm finds legitimate weighting vectors.

2) Time-variant weighting vectors allow expansion of the stability region in Lyapunov space into the 'first quadrant' for finite segments of the composite system's Lyapunov space trajectory. This is an important expansion of the region of stability. A system with oscillating stored energy levels will, by the definition of oscillating, experience periods of increasing energy and decreasing energy. Does a finite period of increasing energy constitute instability? The issue existing here too is ensuring that the algorithm finds valid weighting factors.

3) The "component neutral" relationship which is developed and implemented in this research offers at least a partial means of computing valid time-variant weighting vectors. It is not, by itself, a correct indicator of stability. The "component neutral" relationship does not yield a valid "time-variant weighted-sum" Lyapunov function in the neighbourhood of the equilibrium at the origin of the particular component's state space. Dealing with this infinite singularity of the "component neutral" relationship is a surmountable problem, though.

4) Detecting asymptotic stability in a composite system requires an aggressive "stability demon" which uses a relationship that goes beyond the allowances of the "component neutral" relationship. The "component neutral" relationship is based upon a given component having no effect on the composite system's stability.--Simple stability in the sense of Lyapunov is the sole possible conclusion.

5) Finding a valid weighting vector requires an algorithm. This algorithm is based upon some relationship between the weighting vector and the Lyapunov derivative. The Lyapunov derivative is a function of the components' states and inputs. Hence, some relationship, however involuted, exists between the derived weighting vector and inputs. Further, in controllable systems, the components' states can be made respond to inputs in some desired way. Hence, adjusting inputs to yield desired states and desired, valid weighting factors constitutes stabilising control.

Were a component's controller based upon such a premise as the "component neutral" relationship and it was correctly implemented to ensure valid weighting factors, then the composite system's stability would be ensured by ensuring each components' stability contribution.--This constitutes a decentralised approach to composite system stabilising control.

Asymptotic stability of the composite system, on the other hand, requires that the "time-variant weighted-sum" Lyapunov derivative have a negative value. Achieving this in an oscillatory system may well require coordination between components. A convergent system's weighting vector be must kept away from the bounding axes of Lyapunov space. It must also be almost static, thus forcing the Lyapunov space trajectory out of the 'first quadrant'.

Just as with the "stability organ", the "stability demon" does not produce a static measure of stability, such as t_{cr}. It does produce a "time-variant weighted-sum" Lyapunov derivative for the composite system. It also produces a time-variant weighting factor for each component. Such outputs are continuous, instantaneous and appropriate for use in either component-level, decentralised stabilising controllers or a supervisory-level, centralised (varying degrees of centralisation are admitted) stabilising controller.

This research has illustrated the potential of "time-variant weighted-sum" Lyapunov functions, albeit with a simplistic algorithm within the "stability demon". Implementation of the "stability organ" for 3-phase synchronous generators and the "stability demon" increases the analyses which can be performed within the WAVESIM simulation environment.

6.2 Future Research

Two broad areas of follow-on research exist.

"Stability organs" need to be developed for all of the relevant naval electric power system components. For electromechanical devices, an adaptation of the coenergy-based Lyapunov function developed in this research may be the best approach. Meaningful, engineering-oriented Lyapunov functions for power electric equipment must also be developed. Highly controllable, power electronic equipment is a likely candidate for taking stabilising actions based on a stability-optimised controller which incorporates aspects of the "stability demon" developed in this research.

The specific analytic form of "stability demon" calculation of weighting factors beggars reconciliation with nonlinear control strategies. This is perhaps the greatest contribution of this research. Namely, the weighting factors are a quantity which can be the basis for a stability optimisation within a system control strategy. This would ensure that transitions between operating regimes are carried out in a stable manner. Perhaps a system with poor inherent stability performance but a good stabilising controller is preferable to a system with good inherent stability performance but no stabilising controls.

7 References

7.1 Books

1. Bergen, A. Power Systems Analysis. Englewood Cliffs, NJ: Prentice-Hall, Inc. 1986.
2. Bureau of Naval Personnel. Principles of Naval Engineering. (NAVPERS 10788-B). Washington, D.C.: U.S. Government Printing Office, 1970.
3. Cesari, L. Asymptotic Behavior and Stability Problems in Ordinary Differential Equations. 2nd ed. Springer-Verlag. 1963.
4. Dahlquist, Germund and Ake Bjork. Translated by Ned Anderson. Numerical Methods. Englewood Cliffs, NJ: Prentice-Hall, Inc. 1974.
5. Department of Defense. Interface Standard for Shipboard Systems, Section 300A, Electric Power, Alternating Current (Metric). (MIL-STD-1399(NAVY)). Washington, D.C. 13 October 1987.
6. Department of Defense. (MIL-STD-901(NAVY)). Washington, D.C.
7. Department of the Navy, Naval Sea Systems Command. General Specifications for Ships of the United States Navy, Section 300, General Requirements for Electric Plant and Section 320, General Requirements for Electric Power Distribution Systems. Washington, D.C.: Naval Sea Systems Command, 1987.
8. Division of Engineering & Weapons, U.S.N.A. Introduction to Naval Engineering Systems. Annapolis, MD: U.S. Naval Academy, January 1980.
9. Fitzgerald, A.E., Charles Kingsley Jr. and Stephen D. Umans. Electric Machinery. 4th ed. New York, NY: McGraw-Hill Book Company. 1983.
10. Gungor, Behic R. Power Systems. New York, NY: Harcourt Brace Jovanovich, Publishers. 1988.
11. Hahn, W. Theory & Application of Liapunov's Direct Method. Englewood Cliffs, NJ: Prentice-Hall, Inc. 1963.
12. Krause, Paul C. Analysis of Electric Machinery. New York, NY: McGraw-Hill Book Company. 1986.
13. Krause, Paul C. and Oleg Wasynczuk. Electromechanical Motion Devices. New York, NY: McGraw-Hill Book Company. 1989.
14. Matsch, Leander W. Electromagnetic and Electromechanical Machines. 2nd ed. New York, NY: Harper & Row, Publishers. 1977.
15. Pai, M. Energy Function Analysis for Power System Stability. Kluwer Academic Publications.
16. Papoulis, Athanasios. Circuits and Systems A Modern Approach. New York, NY: Holt, Rinehart and Winston, Inc. 1980.
17. Vidyasagar, M. Nonlinear Systems Analysis. Englewood Cliffs, NJ: Prentice-Hall, Inc. 1978.
18. Woodson, H.H. and J.R. Melcher. Electromechanical Dynamics Part I: Discrete Systems. New York, NY: John Wiley & Sons. 1968.

7.2 Papers

1. Abed, E.H. and P.P. Varaiya. "Nonlinear oscillations in power systems." Electrical Power and Energy Systems. 1981. pp 37-43.
2. Araki, M. and B. Kondo. "Stability and Transient Behavior of Composite Nonlinear Systems." IEEE Transactions on Automatic Control. Vol. 17. August 1972. pp. 537-541.
3. Araposthatis, A., S. Sastry, and P. Varaiya. "Analysis of power-flow equation." Electrical Power and Energy Systems. Vol. 3. No. 3. July 1981.
4. Araposthatis, A., S. Sastry, and P. Varaiya. "Global Analysis of Swing Dynamics." IEEE Transactions on Circuits and Systems. Vol. CAS-29. No. 10. October 1982.

5. Bailey, F.N. "The Application of Lyapunov's Second Method to Interconnected Systems." SIAM Journal of Control. Ser. A. Vol. 3. No. 3. 1965. pp. 443-462.

6. Bellman, R. "Vector Lyapunov Functions." SIAM Journal of Control. Ser. A. Vol. 1. No. 1. 1962. pp. 32-34.

7. Casey, John P. "AC Electric Drive Machinery Design." The Society of Naval Architects and Marine Engineers 1990 Chesapeake Marine Engineering Symposium. Arlington, VA. March 14, 1990. (A Technical Speech Reprint, GE).

8. Chae, S. and Z. Bien. "Techniques for Decentralized Control for Interconnected Systems." Control and Dynamic Systems. Vol. 41. Academic Press. April 1991. pp. 273-315.

9. Chiang, H.D., F.F. Wu and P.P. Varaiya. "Foundations of Direct Methods for Power System Transient Stability Analysis." IEEE Transactions on Circuits and Systems. Vol. CAS-34. No. 2. February 1987. pp. 160-173.

10. DeMarco, C.L. and C.A. Canizares. "A Vector Energy Function Approach for Security Analysis of AC/DC Systems." IEEE/PES 1991 Summer Meeting. 91 SM 421-8 PWRS. San Diego, CA. 28 July - 1 August 1991.

11. DeMarco, C.L. and R.X. Qian. "An Optimal Control Approach to Construction of Lyapunov Functions for Power System Models." Proceedings of the 1989 American Control Conference.

12. Doerry, Norbert H. "ASMS Advanced Surface Machinery Systems." Annapolis, MD, December 13, 1991. (Presented at Naval Reserve Training Lecture.)

13. Dommel, H.W. and N. Sato. "Fast Transient Stability Solutions." IEEE 1972 Winter Meeting. T72 137-3. New York, NY. 30 January - 4 February 1972. pp. 1643-1650.

14. Gareis, G.E., Paul C. Krause, and O. Wasynczuk. "Modeling of Shipboard Electric Power Distribution System." Interim Technical Report for DTRC. SBIR2-DT-R1. October 18, 1989.

15. Grujic, L.T., M. Darwish and J. Fantin. "Coherence, Vector Liapunov Functions, and Large-Scale Power Systems." International Journal of System Science. Vol. 10. 1979. pp. 351-362.

16. Grujic, L.T. and D.D. Siljak. "On Stability of Discrete Composite Systems." IEEE Transactions on Automatic Control. Vol. 18. October 1973. pp. 522-524.

17. Hultgren, Kenneth J. "VSCF Cycloconverter Power Equipment." The American Society of Naval Engineers 1990 Destroyer, Cruiser and Frigate Technology Symposium. Biloxi, MS. September 27, 1990. (A Technical Speech Reprint, GE).

18. IEEE Working Group on Computer Modelling of Excitation Systems. "Excitation System Models for Power System Stability Studies." IEEE Transactions on Power Apparatus and Systems. Vol. PAS-100. No. 2. 1981. pp. 494-509.

19. Ilic, M. and J. Zaborszky. "Concepts of Stability." IEEE Tutorial Course. Course Text 87EH0262-6-PWR.

20. Kastner, G.A., A. Davidson, and W.A.B. Hills. "Frigate Electric Cruise Propulsion and Ship's Service Power from a Common Distribution Network." SNAME Transactions. Vol. 90. 1982. pp. 391-414.

21. Kirtley, J.L. Jr. "Per-Unit Reactances of Superconducting Synchronous Machinery." Electric Power Systems Engineering Laboratory. Cambridge, MA: M.I.T.

22. Kirtley, J.L. Jr. "Synchronous Machine Dynamic Models." LEES Technical Report TR-87-008. June 5, 1987.

23. Kirtley, J.L. Jr. "System Interaction Characteristics of Superconducting Generators." Draft submitted to: Proceedings of the IEEE. Cambridge, MA: M.I.T. February 10, 1992.

24. Kwatny, Harry G., Leon Y. Bahar, Arun K. Pasrija. "Energy-Like Lyapunov Functions for Power System Stability Analysis." IEEE Transactions on Circuits and Systems. Vol. CAS-32. No. 11. November 1985.

25. Kwatny, Harry G., Leon Y. Bahar, Arun K. Pasrija. "Static Bifurcations in Electric Power Networks: Loss of Steady-State Stability and Voltage Collapse." IEEE Transactions on Circuits and Systems. Vol. CAS-33. No. 10. October 1986.

26. Mak, F.K. and M.D. Ilic. "Towards Most Effective Control of Reactive Power Reserves in Electric Machines."

27. Matrosov, V.M. "The Method of Vector Lyapunov Functions in Analysis of Interconnected Distributed Systems (A Survey)." Avtomatische Telemechkanika. No. 1. 1973. pp. 5-22.

28. Matrosov, V.M. "The Method of Vector Lyapunov Functions in Feedback Systems." Avtomatische Telemechkanika. No. 9. 1972. pp. 63-75.

29. Michel, A.N. "Stability and Trajectory Behavior of Composite Systems." IEEE Transactions on Circuits and Systems. Vol. CAS-22. No. 4. April 1975. pp. 305-312.

30. Michel, A.N. and D.W. Porter. "Stability Analysis of Composite Systems." IEEE Transactions on Automatic Control. Vol. 17. April 1972. pp. 222-226.

31. Miyagi, H. and A.R. Bergen. "Stability Studies of Multimachine Power Systems with the Effects of Automatic Voltage Regulators." IEEE Transactions on Automatic Control. Vol. AC-31. No. 3. March 1986. pp. 210-215.

32. Narasimhamurthi, Natarajan, Mohamed T. Musavi. "A Generalized Energy Function for Transient Stability Analysis of Power Systems." IEEE Transactions on Circuits and Systems. Vol. CAS-31. No. 7. July 1984.

33. Naval Sea Systems Command. Design Data Sheet 310-1 Electrical System Load and Power Analysis for Surface Ships. Washington, D.C.: Naval Sea Systems Command, 1 July 1980.

34. Osheiba, A.M. "Comparative Stability Behaviour of Superconducting and Conventional Synchronous Generators." SM-100, International Conference on the Evolution and Modern Aspects of Synchronous Machines. Zurich, CH. August 27-29, 1991.

35. Piontkovskii, A.A. and L.D. Rutkovskaya. "Investigation of Certain Stability-Theory Problems by the Vector Lyapunov Function Method." Automation and Remote Control. Vol. 10. 1967. pp. 1422-1429.

36. Rahimi, F.A., M.G. Lauby, J.N. Wrubel and K.L. Lee. "Evaluation of the Transient Energy Function Method for On-Line Dynamic Security Analysis." IEEE/PES 1992 Winter Meeting. 92 WM 148-7 PWRS. New York, NY. 26-30 January 1992.

37. Reed, M.R. "Integrated Electric Drive (IED) - Program Overview." Naval Sea Systems Command (Code 05Z) Presentation, Washington D.C., March 27, 1990.

38. Siljak, D.D. "Stability of Large-Scale Systems Under Structural Perturbations." IEEE Transactions on Systems, Man, and Cybernetics. Vol. SMC-2. No. 5. November 1972. pp. 657-663.

39. Stott, B. "Power System Dynamic Response Calculations." Proceedings of the IEEE. Vol. 67. No. 2. February 1979. pp. 219-241.

40. Taniguchi, H., M.Asada, M.Takasaki, Y.Kitauchi and M.Koike. "Power System Stability Improvement by Superconducting Generators." SM-100, International Conference on the Evolution and Modern Aspects of Synchronous Machines. Zurich, CH. August 27-29, 1991.

41. Tavora, Carlos J., Otto J.M. Smith. "Stability Analysis of Power Systems." IEEE Power Engineering Society 1971 Summer Meeting. Portland, Oregon. July 18-23, 1971. 71 TP 591-PWR.

42. Thompson, W.E. "Exponential Stability of Interconnected Systems." IEEE Transactions on Automatic Control. Vol. 15. August 1970. pp. 504-506.

43. Tsolas, Nikos A., Aristotle Arapostathis, and Pravin P. Varaiya. "A Structure Preserving Energy Function for Power System Transient Stability Analysis." IEEE Transactions on Circuits and Systems. Vol. CAS-32. No. 10. October 1985.

44. Verghese, George C., Jeffrey H. Lang, and Leo F. Casey. "Analysis of Instability in Electrical Machines." IEEE Transactions on Industry Applications. Vol. IA-22, No. 5. September/October 1986.

45. Werbos, P.J. "Backpropagation Through Time: What It Does and How to Do It." Proceedings of IEEE. Vol. 78. No. 10. October 1990. pp. 1550-1560.

46. Willems, Jacques L. "Direct Methods for Transient Stability Studies in Power System Analysis." IEEE Transactions on Automatic Control. Vol. AC-16. No. 4. August 1971.

47. Wyatt, J. "Qualitative Dynamics of Autonomous Differential Equations. Part II: Stability of Equilibria Via Lyapunov Functions." Lecture 22. Unpublished Paper from Lectures on Nonlinear Circuit Theory. M.I.T. VLSI Memo No. 84-158. August 1984.

7.3 Theses

1. Doerry, Norbert Henry. "Computer Simulation of Shipboard Electrical Distribution Systems." Thesis. M.I.T. May 1989.

2. Doerry, Norbert Henry. "Advanced Numerical Methods for Simulating Nonlinear Multirate Lumped Parameter Models." Thesis, PhD. M.I.T. May 1991.

3. Weil, S. "Simulation of Inverter-Driven Six-Phase Synchronous Machines." Thesis, M.S. in E.E. M.I.T. October, 1987.

A Device Objects With Stability Organ

A.1 Synchronous Generator with Stability Organ

A.1.1 Full Order Generator Model

The following is a listing of the .def file for the synchronous generator "device object".

```
% This is a device.def for a 3-phase synchronous machine.
% It is based on the model in 3_PH_WM which uses currents as states.
% It exports one Lyapunov function and its convective
% derivative.  Parameter values are from DTRC's turbine emulator
% system.
%
% Revision 8 - 24 February 1992 John V. Amy Jr.
%
%
DEVICE LYAPGENH
    TERMINAL 1  POTENTIAL    Va IMPORT
    TERMINAL 1  FLOW         Ia EXPORT 1
    TERMINAL 2  POTENTIAL    Vb IMPORT
    TERMINAL 2  FLOW         Ib EXPORT 1
    TERMINAL 3  POTENTIAL    Vc IMPORT
    TERMINAL 3  FLOW         Ic EXPORT 1
    TERMINAL 4  POTENTIAL    Vn IMPORT
    TERMINAL 4  FLOW         In EXPORT 1
    TERMINAL 5  INFORMATION  Wrm IMPORT
    TERMINAL 6  INFORMATION  Tm IMPORT
    TERMINAL 7  INFORMATION  Vf IMPORT
    TERMINAL 8  INFORMATION Wrmp EXPORT
    TERMINAL 9  INFORMATION  Ifd EXPORT
    TERMINAL 10  INFORMATION   vt EXPORT
    TERMINAL 11  INFORMATION   Ly EXPORT
    TERMINAL 12  INFORMATION  Lyp EXPORT
    PARAMETER xad      1.4648
    PARAMETER xaq      0.7668
    PARAMETER xal      0.0632
    PARAMETER xfl      0.1545
    PARAMETER xkdl     0.3676
    PARAMETER xkql     0.0771
    PARAMETER rs       0.0031
    PARAMETER rf       0.00226
    PARAMETER rkd      0.00673
    PARAMETER rkq      0.0224
    PARAMETER H        1.29
    PARAMETER B        0.6156
    PARAMETER PP       2
    PARAMETER VB       367.4
    PARAMETER PB    625000.0
    PARAMETER wB       377.0
    PARAMETER VsB      367.4
    PARAMETER PsB   625000.0
    STATE id_S  0.0
    STATE iq_S  0.0
    STATE io_S  0.0
    STATE if_S  0.0
    STATE ikd_S 0.0
    STATE ikq_S 0.0
    STATE Ore_S 0.0
    STATE vt_S  0.0
    FUNCTION lyapgenh
    STRUCTURAL JACOBIAN ALL
        NNNNN0N
        NNNNN0N
        NNNNN0N
```

```
        NNNNN0N
        NNNNDDN
        NNNNN0N
        NNNN000
        NNNNN0N
        NNNNN0N
    END
END
%
%
```

The following is a listing of the .m file for the synchronous generator "device object".

```
function [e , jacob, s1, tt1] = lyapgenh(stype,i,par,s0,tt,alpha)
%
% 3PH SYNCHRONOUS MACHINE WITH STABILITY ORGAN, 1st Model
%
% VERSION 1.8 of 24 February 1992
% (C) Copyright 1991, 1992 by John V. Amy Jr.
%
% [e , jacob , s1, tt1] = lyapgenh(stype,i,par,s0,tt,alpha)
%
% LYAPGENh creates the values and jacobian matrix for a
% 3 phase synchronous machine. It is based upon the model in
% Kirtley's LEES Technical Paper adapted for sinusoidal inputs
% with currents as states. The mechanical terminal of the generator
% is modelled here by two information terminals. This allows the
% modelling of "constant torque" sources without causing singularities
% in the Newton-Raphson solver. LYAPGENH calculates the rotor's
% acceleration and exports it to another device object which integrates
% the acceleration and returns the speed to LYAPGENh as in import.
% See the INTWRM device object. LYAPGENh also provides an information
% export variable for input to a voltage regulator. Added
% to this version is Lyapunov function export variables. The
% "stability organ" Lyapunov function and its convective derivative are
% returned.
%
% stype = 1 data points
%       = 2 fourier series
%       = 3 legendre series
%       = 4 polynomial
%
%    i = [Va, Vb, Vc, Vn, Wrm, Tm, Vf] where these are the import
%        variable waveform column vectors.
%         Va = Va (pu-system's base) a-phase voltage
%         Vb = Vb (pu-system's base) b-phase voltage
%         Vc = Vc (pu-system's base) c-phase voltage
%         Vn = Vn (pu-system's base) neutral voltage
%        Wrm = Wrm (radians / sec) rotor mechanical speed (info)
%         Tm = Tm (pu-system's base) mechanical torque (information)
%         Vf = Vf (pu-machine's base) field voltage (information)
%
%   par =  [ xad d-axis mutual reactance (pu-machine's base)
%          xaq q-axis mutual reactance (pu-machine's base)
%          xal stator leakage reactance (pu-machine's base)
%          xfl field leakage reactance (pu-machine's base)
%         xkdl d-axis damper leakage reactance (pu-machine's base)
%         xkql q-axis damper leakage reactance (pu-machine's base)
%          rs stator resistance (pu-machine's base)
%          rf field resistance (pu-machine's base)
%         rkd d-axis damper resistance (pu-machine's base)
%         rkq q-axis damper resistance (pu-machine's base)
%          H inertia constant (sec)
%          B damping constant (N-m-sec)
%          pp number of pole pairs
```

```
%            VB machine base voltage (Volts, peak, l-n)
%            PB machine base power (Watts)
%            wB system base frequency (rad/sec)
%           VsB system base voltage (Volts, peak, l-n)
%           PsB system base power (Watts) ]
%
%    s0 = [id_S, iq_S, io_S, ifd_S, ikd_S, ikq_S, Ore_S, vt_S]
%          where these are the initial values of the states, at t0.
%            id d-axis current (pu-machine's base)
%            iq q-axis current (pu-machine's base)
%            io o-axis current (pu-machine's base)
%           ifd field current (pu-machine's base)
%           ikd d-axis damper current (pu-machine's base)
%           ikq q-axis damper current (pu-machine's base)
%           Ore rotor electrical angle (radians, "theta sub[re]")
%            vt terminal voltage (pu-machine's base)
%
%    tt = [t0, t1, adt]
%           t0 = initial time of the interval
%           t1 = final time of the interval
%          adt = averaging time increment
%
%  alpha = continuation parameter (0 linear, 1 nonlinear)
%
%     e = [Ia, Ib, Ic, In, Wrmp, Ifd, vt, Ly, Lyp]
%          where these are the export variable waveform column vectors.
%            Ia (pu-system's base) a-phase terminal current
%            Ib (pu-system's base) b-phase terminal current
%            Ic (pu-system's base) c-phase terminal current
%            In (pu-system's base) neutral terminal current
%          Wrmp (1/sec^2) rotor acceleration (information)
%           Ifd (pu-machine's base) field current (information)
%            vt (pu-machine's base) terminal voltage (information)
%            Ly (pu-system's base) "stability organ" Lyapunov func. (info)
%           Lyp (pu-system's base) derivative of Ly (information)
%
%  jacob = Jacobian matrix of e with respect to i
%
%    s1 = [id_S, iq_S, io_S, ifd_S, ikd_S, ikq_S, Ore_S, vt_S]
%          where these are the final values of the states, at t1.
%
%   tt1 = [nt1, ntt] where
%          nt1 is the recommended recomputation time this interval, and
%          ntt is the recommended ending time next interval.
%
% Structural Jacobian
%
%          VVVVWTV
%          abcnmmf
%
%    Ia     NNNNN0N
%    Ib     NNNNN0N
%    Ic     NNNNN0N
%    In     NNNNN0N
%    Wmp    NNNNDDN
%    If     NNNNN0N
%    Vt     NNNN000
%    Ly     NNNNN0N
%    Lyp    NNNNN0N
%
%
```

```
% READ IN ALL INPUTS.
%
[n, nc] = size(i);
%
xad  = par(1);
xaq  = par(2);
xal  = par(3);
xfl  = par(4);
xkdl = par(5);
xkql = par(6);
rs   = par(7);
rf   = par(8);
rkd  = par(9);
rkq  = par(10);
H    = par(11);
B    = par(12);
pp   = par(13);
VB   = par(14);
PB   = par(15);
wB   = par(16);
VsB  = par(17);
PsB  = par(18);
%
t0 = tt(1);
t1 = tt(2);
adt = tt(3);
%
id_S0  = s0(1);
iq_S0  = s0(2);
io_S0  = s0(3);
ifd_S0 = s0(4);
ikd_S0 = s0(5);
ikq_S0 = s0(6);
Ore_S0 = s0(7);
vt_S0  = s0(8);
%
Va  = i(:,1);
Vb  = i(:,2);
Vc  = i(:,3);
Vn  = i(:,4);
Wrm = i(:,5);
Tm  = i(:,6);
Vf  = i(:,7);
%
%
% GENERATE THE "S" MATRIX.
%
dt = (t1 - t0) / 2;
dummy_wave = zeros(n,1);
[dummy1, SM1] = w_int(dummy_wave, n, stype, 0);
S = SM1 * dt;
%
%
% GENERATE IDENTITY MATRICES.
%
I  = eye(n);
I6 = eye(6*n);
%
%
% GENERATE AN NxN ZEROS MATRIX.
%
Z   = zeros(n,n);
Z51 = zeros(5*n,n);
%
```

```
%
% COMPUTE BASE QUANTITIES.
%
IsB  = (2/3) * (PsB / VsB);
TqsB = (PsB / wB);
EsB  = TqsB;
IB   = (2/3) * (PB / VB);
TqB  = pp * (PB / wB);
EB   = (PB / wB);
%
%
% GENERATE TIME OUTPUT.
%
tt1 = [t1, t0];
%
%
% GENERATE THE Wre AND Ore WAVEFORMS.
%
Wre = Wrm * pp;
[dummy1, M_Wre, dummy2] = wmult(Wre, Wre, n, stype);
%
Ore_0 = wconvert(Ore_S0, n, 1, stype);
Ore = S * Wre + Ore_0;
%
%
% CALCULATE cos AND sin MATRICES.
%
COS_THETA_A = wcos(Ore, n, stype);
THETA_B     = waddc(Ore, -2.094395102, n, stype);
COS_THETA_B = wcos(THETA_B, n, stype);
THETA_C     = waddc(Ore, 2.094395102, n, stype);
COS_THETA_C = wcos(THETA_C, n, stype);
SIN_THETA_A = wsin(Ore, n, stype);
SIN_THETA_B = wsin(THETA_B, n, stype);
SIN_THETA_C = wsin(THETA_C, n, stype);
[dummy1, MCOS_B, MCOS_A] = wmult(COS_THETA_A, COS_THETA_B, n, stype);
[dummy1, MSIN_A, MCOS_C] = wmult(COS_THETA_C, SIN_THETA_A, n, stype);
[dummy1, MSIN_C, MSIN_B] = wmult(SIN_THETA_B, SIN_THETA_C, n, stype);
%
%
% CALCULATE THE UNITARY PARK'S TRANSFORMATION MATRIX, Tue, AND ITS
INVERSE.
%
T1(1:n,1:n)           = MCOS_A;
T1(1:n,n+1:2*n)       = MCOS_B;
T1(1:n,2*n+1:3*n)     = MCOS_C;
T1(n+1:2*n,1:n)       = -MSIN_A;
T1(n+1:2*n,n+1:2*n)   = -MSIN_B;
T1(n+1:2*n,2*n+1:3*n) = -MSIN_C;
T1(2*n+1:3*n,1:n)     = 0.7071067812 * I;
T1(2*n+1:3*n,n+1:2*n) = 0.7071067812 * I;
T1(2*n+1:3*n,2*n+1:3*n) = 0.7071067812 * I;
T1(3*n+1:4*n,3*n+1:4*n) = 1.224744871 * I;
T1(4*n+1:5*n,4*n+1:5*n) = 1.224744871 * I;
T1(5*n+1:6*n,5*n+1:6*n) = 1.224744871 * I;
%
Tue = 0.8164965809 * T1;
%
dT_dWrm(1:n,1:n)           = pp * 0.8164965809 * (-MSIN_A) * S;
dT_dWrm(1:n,n+1:2*n)       = pp * 0.8164965809 * (-MSIN_B) * S;
dT_dWrm(1:n,2*n+1:3*n)     = pp * 0.8164965809 * (-MSIN_C) * S;
dT_dWrm(n+1:2*n,1:n)       = pp * 0.8164965809 * (-MCOS_A) * S;
dT_dWrm(n+1:2*n,n+1:2*n)   = pp * 0.8164965809 * (-MCOS_B) * S;
dT_dWrm(n+1:2*n,2*n+1:3*n) = pp * 0.8164965809 * (-MCOS_C) * S;
```

```
dT_dWrm(2*n+1:6*n,1:6*n)    = zeros(4*n,6*n);
%
T1t(1:n,1:n)          = MCOS_A;
T1t(1:n,n+1:2*n)      = -MSIN_A;
T1t(1:n,2*n+1:3*n)    = 0.7071067812 * I;
T1t(n+1:2*n,1:n)      = MCOS_B;
T1t(n+1:2*n,n+1:2*n)  = -MSIN_B;
T1t(n+1:2*n,2*n+1:3*n) = 0.7071067812 * I;
T1t(2*n+1:3*n,1:n)    = MCOS_C;
T1t(2*n+1:3*n,n+1:2*n) = -MSIN_C;
T1t(2*n+1:3*n,2*n+1:3*n) = 0.7071067812 * I;
T1t(3*n+1:4*n,3*n+1:4*n) = 1.224744871 * I;
T1t(4*n+1:5*n,4*n+1:5*n) = 1.224744871 * I;
T1t(5*n+1:6*n,5*n+1:6*n) = 1.224744871 * I;
%
Tuet = 0.8164965809 * T1t;
%
dTt_dWrm(1:n,1:n)          = pp * 0.8164965809 * (-MSIN_A) * S;
dTt_dWrm(1:n,n+1:2*n)      = pp * 0.8164965809 * (-MCOS_A) * S;
dTt_dWrm(1:n,2*n+1:3*n)    = Z;
dTt_dWrm(n+1:2*n,1:n)      = pp * 0.8164965809 * (-MSIN_B) * S;
dTt_dWrm(n+1:2*n,n+1:2*n)  = pp * 0.8164965809 * (-MCOS_B) * S;
dTt_dWrm(n+1:2*n,2*n+1:3*n) = Z;
dTt_dWrm(2*n+1:3*n,1:n)    = pp * 0.8164965809 * (-MSIN_C) * S;
dTt_dWrm(2*n+1:3*n,n+1:2*n) = pp * 0.8164965809 * (-MCOS_C) * S;
dTt_dWrm(2*n+1:3*n,2*n+1:3*n) = Z;
dTt_dWrm(3*n+1:6*n,1:6*n)  = zeros(3*n,6*n);
%
%
% CALCULATE PARAMETERS AND ELECTRICAL EQUATION MATRICES.
%
xD  = xad + xal;
xQ  = xaq + xal;
xF  = xad + xfl;
xKD = xad + xkdl;
xKQ = xaq + xkql;
%
lDQ(1:n,1:n)          = xD  * I;
lDQ(1:n,3*n+1:4*n)    = xad * I;
lDQ(1:n,4*n+1:5*n)    = xad * I;
lDQ(n+1:2*n,n+1:2*n)  = xQ  * I;
lDQ(n+1:2*n,5*n+1:6*n) = xaq * I;
lDQ(2*n+1:3*n,2*n+1:3*n) = xal * I;
lDQ(3*n+1:4*n,1:n)    = xad * I;
lDQ(3*n+1:4*n,3*n+1:4*n) = xF  * I;
lDQ(3*n+1:4*n,4*n+1:5*n) = xad * I;
lDQ(4*n+1:5*n,1:n)    = xad * I;
lDQ(4*n+1:5*n,3*n+1:4*n) = xad * I;
lDQ(4*n+1:5*n,4*n+1:5*n) = xKD * I;
lDQ(5*n+1:6*n,n+1:2*n) = xaq * I;
lDQ(5*n+1:6*n,5*n+1:6*n) = xKQ * I;
%
lDQ_inv = inv(lDQ);
%
l(1:n,1:n)          = xal  * I;
l(n+1:2*n,n+1:2*n)  = xal  * I;
l(2*n+1:3*n,2*n+1:3*n) = xal  * I;
l(3*n+1:4*n,3*n+1:4*n) = xfl  * I;
l(4*n+1:5*n,4*n+1:5*n) = xkdl * I;
l(5*n+1:6*n,5*n+1:6*n) = xkql * I;
%
ldq = lDQ - l;
%
```

```
r(1:n,1:n)           = rs  * I;
r(n+1:2*n,n+1:2*n)   = rs  * I;
r(2*n+1:3*n,2*n+1:3*n) = rs  * I;
r(3*n+1:4*n,3*n+1:4*n) = rf  * I;
r(4*n+1:5*n,4*n+1:5*n) = rkd * I;
r(5*n+1:6*n,5*n+1:6*n) = rkq * I;
%
b(1:n,n+1:2*n)      = -xQ  * I;
b(1:n,5*n+1:6*n)    = -xaq * I;
b(n+1:2*n,1:n)      =  xD  * I;
b(n+1:2*n,3*n+1:4*n) =  xad * I;
b(n+1:2*n,4*n+1:5*n) =  xad * I;
b(2*n+1:6*n,1:6*n)  =  zeros(4*n,6*n);
%
bIP = (2 / 3) * b;
%
M6_Wre(1:n,1:n)           = M_Wre;
M6_Wre(n+1:2*n,n+1:2*n)   = M_Wre;
M6_Wre(2*n+1:3*n,2*n+1:3*n) = M_Wre;
M6_Wre(3*n+1:4*n,3*n+1:4*n) = M_Wre;
M6_Wre(4*n+1:5*n,4*n+1:5*n) = M_Wre;
M6_Wre(5*n+1:6*n,5*n+1:6*n) = M_Wre;
%
bVP = (1 / wB) * M6_Wre * b;
%
S6(1:n,1:n)           = S;
S6(n+1:2*n,n+1:2*n)   = S;
S6(2*n+1:3*n,2*n+1:3*n) = S;
S6(3*n+1:4*n,3*n+1:4*n) = S;
S6(4*n+1:5*n,4*n+1:5*n) = S;
S6(5*n+1:6*n,5*n+1:6*n) = S;
%
%
% PER-UNITISE THE IMPORT VARIABLES ON MACHINE'S BASE.
%
Imsc(1:n,1:n) = (VsB / VB) * I;
Imsc(n+1:2*n,n+1:2*n) = (VsB / VB) * I;
Imsc(2*n+1:3*n,2*n+1:3*n) = (VsB / VB) * I;
Imsc(3*n+1:4*n,3*n+1:4*n) = (VsB / VB) * I;
Imsc(4*n+1:5*n,4*n+1:5*n) = I;
%
ImV = [Va,
     Vb,
     Vc,
     Vn,
     Vf];
%
Imv = Imsc * ImV;
%
va = Imv(1:n,:);
vb = Imv(n+1:2*n,:);
vc = Imv(2*n+1:3*n,:);
vn = Imv(3*n+1:4*n,:);
vf = Imv(4*n+1:5*n,:);
%
Incv = [ I Z Z (-I) Z,
       Z I Z (-I) Z,
       Z Z I (-I) Z,
       Z Z Z Z I,
       Z Z Z Z Z,
       Z Z Z Z Z];
%
vph = Incv * Imv;
%
```

```
van = vph(1:n,:);
vbn = vph(n+1:2*n,:);
vcn = vph(2*n+1:3*n,:);
vfn = vph(3*n+1:4*n,:);
vkd = vph(4*n+1:5*n,:);
vkq = vph(5*n+1:6*n,:);
%
[dummy1, Mvan, Mvbn] = wmult(vbn, van, n, stype);
[dummy1, Mvcn, Mvfn] = wmult(vfn, vcn, n, stype);
[dummy1, Mvkd, Mvkq] = wmult(vkq, vkd, n, stype);
%
Mvph = [Mvan,
        Mvbn,
        Mvcn,
        Mvfn,
        Mvkd,
        Mvkq];
%
%
% TRANSFORM THE PHASE VOLTAGES TO d-q VOLTAGES.
%
vdq = Tue * vph;
%
vd  = vdq(1:n,:);
vq  = vdq(n+1:2*n,:);
vo  = vdq(2*n+1:3*n,:);
vfd = vdq(3*n+1:4*n,:);
vkD = vdq(4*n+1:5*n,:);
vkQ = vdq(5*n+1:6*n,:);
%
[dummy1, Mvd, Mvq] = wmult(vq, vd, n, stype);
[dummy1, Mvo, Mvfd] = wmult(vfd, vo, n, stype);
[dummy1, MvkD, MvkQ] = wmult(vkQ, vkD, n, stype);
%
Mvdqt = [Mvd, Mvq, Mvo, Mvfd, MvkD, MvkQ];
%
Mvdq = [Mvd,
        Mvq,
        Mvo,
        Mvfd,
        MvkD,
        MvkQ];
%
%
% GENERATE THE INITIAL CONDITION VECTOR.
%
id_0  = wconvert(id_S0, n, 1, stype);
iq_0  = wconvert(iq_S0, n, 1, stype);
io_0  = wconvert(io_S0, n, 1, stype);
ifd_0 = wconvert(ifd_S0, n, 1, stype);
ikd_0 = wconvert(ikd_S0, n, 1, stype);
ikq_0 = wconvert(ikq_S0, n, 1, stype);
%
IC_0 = [ id_0,
         iq_0,
         io_0,
         ifd_0,
         ikd_0,
         ikq_0];
%
%
% SOLVE NOW FOR THE CURRENTS WHICH ARE STATES.
%
A = I6 + wB * (S6 * lDQ_inv * (r + bVP));
```

```
%
dA_dWrm = pp * (S6 * lDQ_inv * b);
%
bu = (wB * S6 * lDQ_inv * vdq) + IC_0;
%
dbu_dWrm = wB * S6 * lDQ_inv * dT_dWrm * Mvph;
%
A_inv = inv(A);
%
xi = A_inv * bu;
%
dxi_dImV = wB * A_inv * S6 * lDQ_inv * Tue * Incv * Imsc;
%
id  = xi(1:n,:);
iq  = xi(n+1:2*n,:);
io  = xi(2*n+1:3*n,:);
ifd = xi(3*n+1:4*n,:);
ikd = xi(4*n+1:5*n,:);
ikq = xi(5*n+1:6*n,:);
%
[dummy1,  Mid,  Miq] = wmult(iq, id, n, stype);
[dummy1,  Mio, Mifd] = wmult(ifd, io, n, stype);
[dummy1, Mikd, Mikq] = wmult(ikq, ikd, n, stype);
%
Mxit = [Mid, Miq, Mio, Mifd, Mikd, Mikq];
Mxi  = [Mid,
        Miq,
        Mio,
        Mifd,
        Mikd,
        Mikq];
%
dxi_dWrm = A_inv * (dbu_dWrm - dA_dWrm * Mxi);
%
iph = Tuet * xi;
%
Inci = [  I   Z   Z  Z Z Z,
          Z   I   Z  Z Z Z,
          Z   Z   I  Z Z Z,
         (-I) (-I) (-I) Z Z Z,
          Z   Z   Z  I Z Z];
%
Exi = Inci * iph;
%
Isc = [ ((IB / IsB) * I) Z Z Z Z,
        Z ((IB / IsB) * I) Z Z Z,
        Z Z ((IB / IsB) * I) Z Z,
        Z Z Z ((IB / IsB) * I) Z,
        Z Z Z Z I];
%
ExI = Isc * Exi;
%
Ia  = ExI(1:n,:);
Ib  = ExI(n+1:2*n,:);
Ic  = ExI(2*n+1:3*n,:);
In  = ExI(3*n+1:4*n,:);
Ifd = ExI(4*n+1:5*n,:);
%
%
%   Calculate the portions of the jacobian.
%
dExI_dImV = (Isc * Inci * Tuet * dxi_dImV);
%
```

```
dExI_dWrm = Isc * Inci * (dTt_dWrm * Mxi + Tuet * dxi_dWrm);
%
%
% SOLVE THE ROTOR ACCELERATION NOW.
%
Tmpu = (TqsB / TqB) * Tm;
%
Tdam = (B / TqB) * Wrm;
%
Wrmp  = (wB / (2 * pp * H)) * (Tmpu + (Mxit * bIP * xi) - Tdam);
%
%
%   Calculate the portions of the jacobian.
%
dWrmp_dImV =  (wB / (2 * pp * H)) * (Mxit * bIP * dxi_dImV);
%
dWrmp_dWrm = -(wB / (2 * pp * H)) * (B / TqB) * I;
%
dWrmp_dTm  =  (wB / (2 * pp * H)) * (TqsB / TqB) * I;
%
%
% CALCULATE THE TERMINAL VOLTAGE, A RECTIFIED AND AVERAGED VERSION.
%
%   Convert to a data point representation of the waveform.
%
[vad, dvad_dva] = wconvert(van, 5*n, stype, 1);
[vbd, dvbd_dvb] = wconvert(vbn, 5*n, stype, 1);
[vcd, dvcd_dvc] = wconvert(vcn, 5*n, stype, 1);
%
%   The following portion serves as the actual "rectifier".
%
for i=1:5*n,
 if vad(i,1) >= vbd(i,1),
  if vad(i,1) >= vcd(i,1),
   vtd(i,1) = vad(i,1);
   dvtd_dvad(i,i) = 1.0;
   dvtd_dvbd(i,i) = 0.0;
   dvtd_dvcd(i,i) = 0.0;
  else
   vtd(i,1) = vcd(i,1);
   dvtd_dvad(i,i) = 0.0;
   dvtd_dvbd(i,i) = 0.0;
   dvtd_dvcd(i,i) = 1.0;
  end
 else
  if vbd(i,1) >= vcd(i,1),
   vtd(i,1) = vbd(i,1);
   dvtd_dvad(i,i) = 0.0;
   dvtd_dvbd(i,i) = 1.0;
   dvtd_dvcd(i,i) = 0.0;
  else
   vtd(i,1) = vcd(i,1);
   dvtd_dvad(i,i) = 0.0;
   dvtd_dvbd(i,i) = 0.0;
   dvtd_dvcd(i,i) = 1.0;
  end
 end
end
%
%   Now the data point waveform is averaged and converted to stype.
%
[vta, dvta_dvtd] = w_ave(vtd, 1, 1, 1);
vtb = [1, 0]' * vt_S0 + [0, 1]' * vta;
```

```
[vtc, dvtc_dvtb] = wconvert(vtb, n, 1, 4);
[vt, dvt_dvtc] = wconvert(vtc, n, 4, stype);
%
%
%   Calculate the portions of the jacobian.
%
dvphd_dvph = [dvad_dva Z51 Z51 Z51 Z51 Z51,
          Z51 dvbd_dvb Z51 Z51 Z51 Z51,
          Z51 Z51 dvcd_dvc Z51 Z51 Z51,
          Z Z Z Z Z Z,
          Z Z Z Z Z Z,
          Z Z Z Z Z Z];
%
dvphd_dImV = dvphd_dvph * Incv * Imsc;
%
dvtd_dImV  = [dvtd_dvad, dvtd_dvbd, dvtd_dvcd, Z51, Z51, Z51] * dvphd_dImV;
%
dvt_dImV   = dvt_dvtc * dvtc_dvtb * [0, 1]' * dvta_dvtd * dvtd_dImV;
%
%
% CALCULATE THE "STABILITY ORGAN" LYAPUNOV FUNCTION AND ITS DERIVATIVE.
%
% % coenergy
% * coenergy + KEdiff ('equal power' normalisation)
% ^ coenergy + KE ('equal power' normalisation)
% & coenergy + KE
% $ coenergy + KEdiff
%
%*Wb = wconvert(wB/pp, n, 1, stype);
%*Wdiff = Wrm - Wb;
%*[Wsqr, MWdiff, dummy2]  = wmult(Wdiff, Wdiff, n, stype);
%&[Wsqr, MWrm, dummy2]  = wmult(Wrm, Wrm, n, stype);
%$Wrr = wconvert(wB/pp, n, 1, stype);
%$Wdiff = Wrm - Wrr;
%$[Wsqr, MWdiff, dummy2]  = wmult(Wdiff, Wdiff, n, stype);
%^
[Wsqr, MWrm, dummy2]  = wmult(Wrm, Wrm, n, stype);
%
%%ly = (1 / 3) * Mxit * ldq * xi;
%*ly = (1 / 3) * Mxit * lDQ * xi + (pp^2 / wB^2) * Wsqr;
%&ly = (1 / 3) * Mxit * lDQ * xi + H * wB * (pp / wB)^2 * Wsqr;
%$ly = (1 / 3) * Mxit * lDQ * xi + H * wB * (pp / wB)^2 * Wsqr;
%^
ly = (1 / 3) * Mxit * lDQ * xi + (pp / wB)^2 * Wsqr;
%
Ly = (EB / EsB) * ly;
%
%%lyp = (2 / 3) * wB * Mxit * ldq * lDQ_inv * (vdq - ((r + bVP) * xi));
%*lyp = (2/3)*wB* Mxit * (vdq - ((r + bVP) * xi)) +2*(pp/wB)^2* MWdiff * Wrmp;
%&lyp = (2/3)* Mxit * (vdq - (r * xi)) + (pp/wB)*(MWrm * Tmpu - (B/TqB)* Wsqr);
%$lypa = (2 / 3) * Mxit * (vdq - (r * xi));
%$lypb = (pp / wB) * (MWdiff * Tmpu - (B / TqB) * MWdiff * Wrm);
%$lypc = Mxit * bIP * xi;
%$lyp = lypa + lypb + lypc;
%^
lyp = (2/3)*wB * Mxit * (vdq - ((r + bVP) * xi)) +2*(pp/wB)^2 * MWrm * Wrmp;
%
Lyp = (PB / PsB) * lyp;
%
%
%   Calculate the portions of the jacobian.
%    These are for the coenergy Lyapunov function only.
%
%dLy_dImV = (EB / EsB) * (2 / 3) * Mxit * ldq * dxi_dImV;
```

```
dLy_dImV = (EB / EsB) * (2 / 3) * Mxit * lDQ * dxi_dImV;
%
%dLy_dWrm = (EB / EsB) * (2 / 3) * Mxit * ldq * dxi_dWrm;
dLy_dWrm = (EB / EsB) * (2 / 3) * Mxit * lDQ * dxi_dWrm;
%
%dlypa_dImV = Mxit * ldq * lDQ_inv * Tue * Incv * Imsc;
%dlypb_dImV = Mvdqt * ldq * lDQ_inv * dxi_dImV;
%dlypc_dImV = 2 * Mxit * ldq * lDQ_inv * (r + bVP) * dxi_dImV;
%dLyp_dImV  = (PB/PsB) * (2/3) * wB * (dlypa_dImV + dlypb_dImV - dlypc_dImV);
%dlypa_dWrm = Mxit * ldq * lDQ_inv * dT_dWrm * Mvph;
%dlypb_dWrm = Mvdqt * ldq * lDQ_inv * dxi_dWrm;
%dlypc_dWrm = 2 * Mxit * ldq * lDQ_inv * (r + bVP) * dxi_dWrm;
%dLyp_dWrm  = (PB/PsB) * (2/3) * wB * (dlypa_dWrm + dlypb_dWrm - dlypc_dWrm);
%
dlypa_dImV = Mxit * Tue * Incv * Imsc;
dlypb_dImV = Mvdqt * dxi_dImV;
dlypc_dImV = 2 * Mxit * (r + bVP) * dxi_dImV;
dLyp_dImV  = (PB/PsB) * (2/3) * wB * (dlypa_dImV + dlypb_dImV - dlypc_dImV);
dlypa_dWrm = Mxit * dT_dWrm * Mvph;
dlypb_dWrm = Mvdqt * dxi_dWrm;
dlypc_dWrm = 2 * Mxit * (r + bVP) * dxi_dWrm;
dLyp_dWrm  = (PB/PsB) * (2/3) * wB * (dlypa_dWrm + dlypb_dWrm - dlypc_dWrm);
%
% COLLECT THE EXPORT VARIABLES.
%
e = [Ia, Ib, Ic, In, Wrmp, Ifd, vt, Ly, Lyp];
%
%
% COLLECT THE FINAL STATES.
%
%
%  Return modulo 2 pi values for THETA at end of interval.
%
Ore_S1a = w_at_one(Ore, stype);
if ( (Ore_S1a > 6.283185307) | (Ore_S1a < -6.283185307) ),
  Ore_S1 = rem(Ore_S1a, 6.283185307);
else
  Ore_S1 = Ore_S1a;
end
%
id_S1  = w_at_one(id, stype);
iq_S1  = w_at_one(iq, stype);
io_S1  = w_at_one(io, stype);
ifd_S1 = w_at_one(ifd, stype);
ikd_S1 = w_at_one(ikd, stype);
ikq_S1 = w_at_one(ikq, stype);
%
s1 = [id_S1, iq_S1, io_S1, ifd_S1, ikd_S1, ikq_S1, Ore_S1, vta]';
%
%
% COLLECT THE JACOBIAN.
%
   jacob(1:4*n,1:4*n) = dExI_dImV(1:4*n,1:4*n);
%
   jacob(1:4*n,4*n+1:5*n) = dExI_dWrm(1:4*n,:);
%
   jacob(1:4*n,5*n+1:6*n) = [Z,
                             Z,
                             Z,
                             Z];
%
   jacob(1:4*n,6*n+1:7*n) = dExI_dImV(1:4*n,4*n+1:5*n);
%
```

```
   jacob(4*n+1:5*n,1:4*n) = dWrmp_dImV(:,1:4*n);
%
   jacob(4*n+1:5*n,4*n+1:5*n) = dWrmp_dWrm;
%
   jacob(4*n+1:5*n,5*n+1:6*n) = dWrmp_dTm;
%
   jacob(4*n+1:5*n,6*n+1:7*n) = dWrmp_dImV(:,4*n+1:5*n);
%
   jacob(5*n+1:6*n,1:4*n) = dExI_dImV(4*n+1:5*n,1:4*n);
%
   jacob(5*n+1:6*n,4*n+1:5*n) = dExI_dWrm(4*n+1:5*n,:);
%
   jacob(5*n+1:6*n,5*n+1:6*n) = Z;
%
   jacob(5*n+1:6*n,6*n+1:7*n) = dExI_dImV(4*n+1:5*n,4*n+1:5*n);
%
   jacob(6*n+1:7*n,1:4*n) = dvt_dImV(:,1:4*n);
%
   jacob(6*n+1:7*n,4*n+1:5*n) = Z;
%
   jacob(6*n+1:7*n,5*n+1:6*n) = Z;
%
   jacob(6*n+1:7*n,6*n+1:7*n) = Z;
%
   jacob(7*n+1:8*n,1:4*n) = dLy_dImV(:,1:4*n);
%
   jacob(7*n+1:8*n,4*n+1:5*n) = dLy_dWrm;
%
   jacob(7*n+1:8*n,5*n+1:6*n) = Z;
%
   jacob(7*n+1:8*n,6*n+1:7*n) = dLy_dImV(:,4*n+1:5*n);
%
   jacob(8*n+1:9*n,1:4*n) = dLyp_dImV(:,1:4*n);
%
   jacob(8*n+1:9*n,4*n+1:5*n) = dLyp_dWrm;
%
   jacob(8*n+1:9*n,5*n+1:6*n) = Z;
%
   jacob(8*n+1:9*n,6*n+1:7*n) = dLyp_dImV(:,4*n+1:5*n);
%
```

A.1.2 Generator Model With the "Re-connected" Version of Lyapunov Derivative

The following is a listing of the .def file for the synchronous generator "device object".

```
% This is a device.def for a 3-phase synchronous machine.
% It is based on the model in 3_PH_WM which uses currents as states.
% It exports one Lyapunov function and its convective
% derivative.  Parameter values are from DTRC's turbine emulator
% system.
%
% Revision 8 - 25 March 1992 John V. Amy Jr.
%
%
DEVICE LYAPGENP
      TERMINAL  1  POTENTIAL    Va IMPORT
      TERMINAL  1  FLOW         Ia EXPORT 1
      TERMINAL  2  POTENTIAL    Vb IMPORT
      TERMINAL  2  FLOW         Ib EXPORT 1
      TERMINAL  3  POTENTIAL    Vc IMPORT
      TERMINAL  3  FLOW         Ic EXPORT 1
      TERMINAL  4  POTENTIAL    Vn IMPORT
      TERMINAL  4  FLOW         In EXPORT 1
      TERMINAL  5  INFORMATION  Vai IMPORT
      TERMINAL  6  INFORMATION  Vbi IMPORT
```

```
    TERMINAL  7  INFORMATION  Vci IMPORT
    TERMINAL  8  INFORMATION  Wrm IMPORT
    TERMINAL  9  INFORMATION   Tm IMPORT
    TERMINAL 10  INFORMATION   Vf IMPORT
    TERMINAL 11  INFORMATION Wrmp EXPORT
    TERMINAL 12  INFORMATION  Ifd EXPORT
    TERMINAL 13  INFORMATION   vt EXPORT
    TERMINAL 14  INFORMATION   Ly EXPORT
    TERMINAL 15  INFORMATION  Lyp EXPORT
    PARAMETER xad      1.4648
    PARAMETER xaq      0.7668
    PARAMETER xal      0.0632
    PARAMETER xfl      0.1545
    PARAMETER xkdl     0.3676
    PARAMETER xkql     0.0771
    PARAMETER rs       0.0031
    PARAMETER rf       0.00226
    PARAMETER rkd      0.00673
    PARAMETER rkq      0.0224
    PARAMETER H        1.29
    PARAMETER B        0.6156
    PARAMETER PP       2
    PARAMETER VB       367.4
    PARAMETER PB       625000.0
    PARAMETER wB       377.0
    PARAMETER VsB      367.4
    PARAMETER PsB      625000.0
    STATE id_S   0.0
    STATE iq_S   0.0
    STATE io_S   0.0
    STATE if_S   0.0
    STATE ikd_S  0.0
    STATE ikq_S  0.0
    STATE Ore_S  0.0
    STATE vt_S   0.0
    FUNCTION lyapgenp
    STRUCTURAL JACOBIAN ALL
        NNNN000N0N
        NNNN000N0N
        NNNN000N0N
        NNNN000N0N
        NNNN000DDN
        NNNN000N0N
        NNNN000000
        NNNN000N0N
        NNNNNNNN0N
  END
END
%
%
```

The following is a listing of the .m file for the synchronous generator "device object".

```
function [e , jacob, s1, tt1] = lyapgenp(stype,i,par,s0,tt,alpha)
%
% 3PH SYNCHRONOUS MACHINE WITH STABILITY ORGAN, 1st Model
%
% VERSION 2.6 of 25 March 1992
% (C) Copyright 1991, 1992 by John V. Amy Jr.
%
% [e , jacob , s1, tt1] = lyapgenp(stype,i,par,s0,tt,alpha)
%
% LYAPGENp creates the values and jacobian matrix for a
% 3 phase synchronous machine.  It is based upon the model in
% Kirtley's LEES Technical Paper adapted for sinusoidal inputs
```

```
% with currents as states. The mechanical terminal of the generator
% is modelled here by two information terminals. This allows the
% modelling of "constant torque" sources without causing singularities
% in the Newton-Raphson solver. LYAPGENH calculates the rotor's
% acceleration and exports it to another device object which integrates
% the acceleration and returns the speed to LYAPGENh as an import.
% See the INTWRM device object. LYAPGENh also provides an information
% export variable for input to a voltage regulator. Added
% to this version are Lyapunov function export variables. The
% "stability organ's" Lyapunov function and its convective derivative are
% returned. This particular Lyapunov function uses information import
% variables to calculate what the Lyapunov derivative would be if the
% machine were reconnected at the given instant.
%
%  stype = 1 data points
%        = 2 fourier series
%        = 3 legendre series
%        = 4 polynomial
%
%     i = [Va, Vb, Vc, Vn, Vai, Vbi, Vci, Wrm, Tm, Vf] These are the import
%          variable waveform column vectors.
%           Va = Va (pu-system's base) a-phase voltage
%           Vb = Vb (pu-system's base) b-phase voltage
%           Vc = Vc (pu-system's base) c-phase voltage
%           Vn = Vn (pu-system's base) neutral voltage
%          Vai = Vai (pu-system's base) "system" a-phase voltage
%          Vbi = Vbi (pu-system's base) "system" b-phase voltage
%          Vci = Vci (pu-system's base) "system" c-phase voltage
%          Wrm = Wrm (radians / sec) rotor mechanical speed (info)
%           Tm = Tm (pu-system's base) mechanical torque (information)
%           Vf = Vf (pu-machine's base) field voltage (information)
%
%    par =  [ xad d-axis mutual reactance (pu-machine's base)
%           xaq q-axis mutual reactance (pu-machine's base)
%           xal stator leakage reactance (pu-machine's base)
%           xfl field leakage reactance (pu-machine's base)
%          xkdl d-axis damper leakage reactance (pu-machine's base)
%          xkql q-axis damper leakage reactance (pu-machine's base)
%            rs stator resistance (pu-machine's base)
%            rf field resistance (pu-machine's base)
%           rkd d-axis damper resistance (pu-machine's base)
%           rkq q-axis damper resistance (pu-machine's base)
%             H inertia constant (sec)
%             B damping constant (N-m-sec)
%            pp number of pole pairs
%            VB machine base voltage (Volts, peak, l-n)
%            PB machine base power (Watts)
%            wB system base frequency (rad/sec)
%           VsB system base voltage (Volts, peak, l-n)
%           PsB system base power (Watts) ]
%
%     s0 = [id_S, iq_S, io_S, ifd_S, ikd_S, ikq_S, Ore_S, vt_S]
%          where these are the initial values of the states, at t0.
%            id d-axis current (pu-machine's base)
%            iq q-axis current (pu-machine's base)
%            io o-axis current (pu-machine's base)
%           ifd field current (pu-machine's base)
%           ikd d-axis damper current (pu-machine's base)
%           ikq q-axis damper current (pu-machine's base)
%           Ore rotor electrical angle (radians, "theta sub[re]")
%            vt terminal voltage (pu-machine's base)
%
%     tt = [t0, t1, adt]
%            t0 = initial time of the interval
```

```
%            t1 = final time of the interval
%           adt = averaging time increment
%
%  alpha = continuation parameter (0 linear, 1 nonlinear)
%
%     e = [Ia, Ib, Ic, In, Wrmp, Ifd, vt, Ly, Lyp]
%          where these are the export variable waveform column vectors.
%           Ia (pu-system's base) a-phase terminal current
%           Ib (pu-system's base) b-phase terminal current
%           Ic (pu-system's base) c-phase terminal current
%           In (pu-system's base) neutral terminal current
%          Wrmp (1/sec^2) rotor acceleration (information)
%          Ifd (pu-machine's base) field current (information)
%           vt (pu-machine's base) terminal voltage (information)
%           Ly (pu-system's base) "stability organ" Lyapunov func. (info)
%          Lyp (pu-system's base) derivative of Ly (information)
%
%  jacob = Jacobian matrix of e with respect to i
%
%     s1 = [id_S, iq_S, io_S, ifd_S, ikd_S, ikq_S, Ore_S, vt_S]
%          where these are the final values of the states, at t1.
%
%    tt1 = [nt1, ntt] where
%          nt1 is the recommended recomputation time this interval, and
%          ntt is the recommended ending time next interval.
%
% Structural Jacobian
%
%          VVVVVVVWTV
%          abcnabcmmf
%            iii
%    Ia     NNNNZZZN0N
%    Ib     NNNNZZZN0N
%    Ic     NNNNZZZN0N
%    In     NNNNZZZN0N
%    Wmp     NNNNZZZDDN
%    If     NNNNZZZN0N
%    Vt      NNNNZZZ000
%    Ly      NNNNZZZN0N
%    Lyp      NNNNNNNN0N
%
%
% READ IN ALL INPUTS.
%
[n, nc] = size(i);
%
xad  = par(1);
xaq  = par(2);
xal  = par(3);
xfl  = par(4);
xkdl = par(5);
xkql = par(6);
rs   = par(7);
rf   = par(8);
rkd  = par(9);
rkq  = par(10);
H    = par(11);
B    = par(12);
pp   = par(13);
VB   = par(14);
PB   = par(15);
wB   = par(16);
VsB  = par(17);
```

```
PsB  = par(18);
%
t0  = tt(1);
t1  = tt(2);
adt = tt(3);
%
id_S0  = s0(1);
iq_S0  = s0(2);
io_S0  = s0(3);
ifd_S0 = s0(4);
ikd_S0 = s0(5);
ikq_S0 = s0(6);
Ore_S0 = s0(7);
vt_S0  = s0(8);
%
Va  = i(:,1);
Vb  = i(:,2);
Vc  = i(:,3);
Vn  = i(:,4);
Vai = i(:,5);
Vbi = i(:,6);
Vci = i(:,7);
Wrm = i(:,8);
Tm  = i(:,9);
Vf  = i(:,10);
%
%
% GENERATE THE "S" MATRIX.
%
dt = (t1 - t0) / 2;
dummy_wave = zeros(n,1);
[dummy1, SM1] = w_int(dummy_wave, n, stype, 0);
S = SM1 * dt;
%
%
% GENERATE IDENTITY MATRICES.
%
I  = eye(n);
I6 = eye(6*n);
%
%
% GENERATE AN NxN ZEROS MATRIX.
%
Z   = zeros(n,n);
Z51 = zeros(5*n,n);
%
%
% COMPUTE BASE QUANTITIES.
%
IsB  = (2/3) * (PsB / VsB);
TqsB = (PsB / wB);
EsB  = TqsB;
IB   = (2/3) * (PB / VB);
TqB  = pp * (PB / wB);
EB   = (PB / wB);
%
%
% GENERATE TIME OUTPUT.
%
tt1 = [t1, t0];
%
%
% GENERATE THE Wre AND Ore WAVEFORMS.
%
```

```
Wre = Wrm * pp;
[dummy1, M_Wre, dummy2] = wmult(Wre, Wre, n, stype);
%
Ore_0 = wconvert(Ore_S0, n, 1, stype);
Ore = S * Wre + Ore_0;
%
%
% CALCULATE cos AND sin MATRICES.
%
COS_THETA_A = wcos(Ore, n, stype);
THETA_B     = waddc(Ore, -2.094395102, n, stype);
COS_THETA_B = wcos(THETA_B, n, stype);
THETA_C     = waddc(Ore, 2.094395102, n, stype);
COS_THETA_C = wcos(THETA_C, n, stype);
SIN_THETA_A = wsin(Ore, n, stype);
SIN_THETA_B = wsin(THETA_B, n, stype);
SIN_THETA_C = wsin(THETA_C, n, stype);
[dummy1, MCOS_B, MCOS_A] = wmult(COS_THETA_A, COS_THETA_B, n, stype);
[dummy1, MSIN_A, MCOS_C] = wmult(COS_THETA_C, SIN_THETA_A, n, stype);
[dummy1, MSIN_C, MSIN_B] = wmult(SIN_THETA_B, SIN_THETA_C, n, stype);
%
%
% CALCULATE THE UNITARY PARK'S TRANSFORMATION MATRIX, Tue, AND ITS
INVERSE.
%
T1(1:n,1:n)          = MCOS_A;
T1(1:n,n+1:2*n)      = MCOS_B;
T1(1:n,2*n+1:3*n)    = MCOS_C;
T1(n+1:2*n,1:n)      = -MSIN_A;
T1(n+1:2*n,n+1:2*n)  = -MSIN_B;
T1(n+1:2*n,2*n+1:3*n) = -MSIN_C;
T1(2*n+1:3*n,1:n)    = 0.7071067812 * I;
T1(2*n+1:3*n,n+1:2*n) = 0.7071067812 * I;
T1(2*n+1:3*n,2*n+1:3*n) = 0.7071067812 * I;
T1(3*n+1:4*n,3*n+1:4*n) = 1.224744871 * I;
T1(4*n+1:5*n,4*n+1:5*n) = 1.224744871 * I;
T1(5*n+1:6*n,5*n+1:6*n) = 1.224744871 * I;
%
Tue = 0.8164965809 * T1;
%
dT_dWrm(1:n,1:n)          = pp * 0.8164965809 * (-MSIN_A) * S;
dT_dWrm(1:n,n+1:2*n)      = pp * 0.8164965809 * (-MSIN_B) * S;
dT_dWrm(1:n,2*n+1:3*n)    = pp * 0.8164965809 * (-MSIN_C) * S;
dT_dWrm(n+1:2*n,1:n)      = pp * 0.8164965809 * (-MCOS_A) * S;
dT_dWrm(n+1:2*n,n+1:2*n)  = pp * 0.8164965809 * (-MCOS_B) * S;
dT_dWrm(n+1:2*n,2*n+1:3*n) = pp * 0.8164965809 * (-MCOS_C) * S;
dT_dWrm(2*n+1:6*n,1:6*n)  = zeros(4*n,6*n);
%
T1t(1:n,1:n)          = MCOS_A;
T1t(1:n,n+1:2*n)      = -MSIN_A;
T1t(1:n,2*n+1:3*n)    = 0.7071067812 * I;
T1t(n+1:2*n,1:n)      = MCOS_B;
T1t(n+1:2*n,n+1:2*n)  = -MSIN_B;
T1t(n+1:2*n,2*n+1:3*n) = 0.7071067812 * I;
T1t(2*n+1:3*n,1:n)    = MCOS_C;
T1t(2*n+1:3*n,n+1:2*n) = -MSIN_C;
T1t(2*n+1:3*n,2*n+1:3*n) = 0.7071067812 * I;
T1t(3*n+1:4*n,3*n+1:4*n) = 1.224744871 * I;
T1t(4*n+1:5*n,4*n+1:5*n) = 1.224744871 * I;
T1t(5*n+1:6*n,5*n+1:6*n) = 1.224744871 * I;
%
Tuet = 0.8164965809 * T1t;
%
dTt_dWrm(1:n,1:n)          = pp * 0.8164965809 * (-MSIN_A) * S;
```

```
dTt_dWrm(1:n,n+1:2*n)       = pp * 0.8164965809 * (-MCOS_A) * S;
dTt_dWrm(1:n,2*n+1:3*n)     = Z;
dTt_dWrm(n+1:2*n,1:n)       = pp * 0.8164965809 * (-MSIN_B) * S;
dTt_dWrm(n+1:2*n,n+1:2*n)   = pp * 0.8164965809 * (-MCOS_B) * S;
dTt_dWrm(n+1:2*n,2*n+1:3*n) = Z;
dTt_dWrm(2*n+1:3*n,1:n)     = pp * 0.8164965809 * (-MSIN_C) * S;
dTt_dWrm(2*n+1:3*n,n+1:2*n) = pp * 0.8164965809 * (-MCOS_C) * S;
dTt_dWrm(2*n+1:3*n,2*n+1:3*n) = Z;
dTt_dWrm(3*n+1:6*n,1:6*n)   = zeros(3*n,6*n);
%
%
% CALCULATE PARAMETERS AND ELECTRICAL EQUATION MATRICES.
%
xD  = xad + xal;
xQ  = xaq + xal;
xF  = xad + xfl;
xKD = xad + xkdl;
xKQ = xaq + xkql;
%
lDQ(1:n,1:n)          = xD  * I;
lDQ(1:n,3*n+1:4*n)    = xad * I;
lDQ(1:n,4*n+1:5*n)    = xad * I;
lDQ(n+1:2*n,n+1:2*n)  = xQ  * I;
lDQ(n+1:2*n,5*n+1:6*n) = xaq * I;
lDQ(2*n+1:3*n,2*n+1:3*n) = xal * I;
lDQ(3*n+1:4*n,1:n)    = xad * I;
lDQ(3*n+1:4*n,3*n+1:4*n) = xF  * I;
lDQ(3*n+1:4*n,4*n+1:5*n) = xad * I;
lDQ(4*n+1:5*n,1:n)    = xad * I;
lDQ(4*n+1:5*n,3*n+1:4*n) = xad * I;
lDQ(4*n+1:5*n,4*n+1:5*n) = xKD * I;
lDQ(5*n+1:6*n,n+1:2*n)  = xaq * I;
lDQ(5*n+1:6*n,5*n+1:6*n) = xKQ * I;
%
lDQ_inv = inv(lDQ);
%
l(1:n,1:n)          = xal  * I;
l(n+1:2*n,n+1:2*n)  = xal  * I;
l(2*n+1:3*n,2*n+1:3*n) = xal  * I;
l(3*n+1:4*n,3*n+1:4*n) = xfl  * I;
l(4*n+1:5*n,4*n+1:5*n) = xkdl * I;
l(5*n+1:6*n,5*n+1:6*n) = xkql * I;
%
ldq = lDQ - l;
%
r(1:n,1:n)          = rs  * I;
r(n+1:2*n,n+1:2*n)  = rs  * I;
r(2*n+1:3*n,2*n+1:3*n) = rs  * I;
r(3*n+1:4*n,3*n+1:4*n) = rf  * I;
r(4*n+1:5*n,4*n+1:5*n) = rkd * I;
r(5*n+1:6*n,5*n+1:6*n) = rkq * I;
%
b(1:n,n+1:2*n)      = -xQ  * I;
b(1:n,5*n+1:6*n)    = -xaq * I;
b(n+1:2*n,1:n)      =  xD  * I;
b(n+1:2*n,3*n+1:4*n) =  xad * I;
b(n+1:2*n,4*n+1:5*n) =  xad * I;
b(2*n+1:6*n,1:6*n)  =  zeros(4*n,6*n);
%
bIP = (2 / 3) * b;
%
M6_Wre(1:n,1:n)          = M_Wre;
M6_Wre(n+1:2*n,n+1:2*n)  = M_Wre;
```

```
M6_Wre(2*n+1:3*n,2*n+1:3*n) = M_Wre;
M6_Wre(3*n+1:4*n,3*n+1:4*n) = M_Wre;
M6_Wre(4*n+1:5*n,4*n+1:5*n) = M_Wre;
M6_Wre(5*n+1:6*n,5*n+1:6*n) = M_Wre;
%
bVP = (1 / wB) * M6_Wre * b;
%
S6(1:n,1:n)           = S;
S6(n+1:2*n,n+1:2*n)   = S;
S6(2*n+1:3*n,2*n+1:3*n) = S;
S6(3*n+1:4*n,3*n+1:4*n) = S;
S6(4*n+1:5*n,4*n+1:5*n) = S;
S6(5*n+1:6*n,5*n+1:6*n) = S;
%
%
% PER-UNITISE THE IMPORT VARIABLES ON MACHINE'S BASE.
%
Imsc(1:n,1:n) = (VsB / VB) * I;
Imsc(n+1:2*n,n+1:2*n) = (VsB / VB) * I;
Imsc(2*n+1:3*n,2*n+1:3*n) = (VsB / VB) * I;
Imsc(3*n+1:4*n,3*n+1:4*n) = (VsB / VB) * I;
Imsc(4*n+1:5*n,4*n+1:5*n) = I;
%
Imsci(1:n,1:n) = (VsB / VB) * I;
Imsci(n+1:2*n,n+1:2*n) = (VsB / VB) * I;
Imsci(2*n+1:3*n,2*n+1:3*n) = (VsB / VB) * I;
%
ImV = [Va,
     Vb,
     Vc,
     Vn,
     Vf];
%
ImVi = [Vai,
      Vbi,
      Vci];
%
Imv = Imsc * ImV;
%
Imvi = Imsci * ImVi;
%
va = Imv(1:n,:);
vb = Imv(n+1:2*n,:);
vc = Imv(2*n+1:3*n,:);
vn = Imv(3*n+1:4*n,:);
vf = Imv(4*n+1:5*n,:);
%
vai = Imvi(1:n,:);
vbi = Imvi(n+1:2*n,:);
vci = Imvi(2*n+1:3*n,:);
%
Incv = [ I Z Z (-I) Z,
       Z I Z (-I) Z,
       Z Z I (-I) Z,
       Z Z Z Z I,
       Z Z Z Z Z,
       Z Z Z Z Z];
%
Incvi = [ I Z Z,
        Z I Z,
        Z Z I,
        Z Z Z,
        Z Z Z,
        Z Z Z];
```

```
%
vph = Incv * Imv;
%
van = vph(1:n,:);
vbn = vph(n+1:2*n,:);
vcn = vph(2*n+1:3*n,:);
vfn = vph(3*n+1:4*n,:);
vkd = vph(4*n+1:5*n,:);
vkq = vph(5*n+1:6*n,:);
%
[dummy1, Mvan, Mvbn] = wmult(vbn, van, n, stype);
[dummy1, Mvcn, Mvfn] = wmult(vfn, vcn, n, stype);
[dummy1, Mvkd, Mvkq] = wmult(vkq, vkd, n, stype);
%
vphi = [vai,
        vbi,
        vci,
        vfn,
        vkd,
        vkq];
%
[dummy1, Mvai, Mvbi] = wmult(vbi, vai, n, stype);
[dummy1, Mvci, dummy2] = wmult(vci, vci, n, stype);
%
Mvph = [Mvan,
        Mvbn,
        Mvcn,
        Mvfn,
        Mvkd,
        Mvkq];
%
Mvphi = [Mvai,
         Mvbi,
         Mvci,
         Mvfn,
         Mvkd,
         Mvkq];
%
%
% TRANSFORM THE PHASE VOLTAGES TO d-q VOLTAGES.
%
vdq = Tue * vph;
%
vdqi = Tue * vphi;
%
vd  = vdq(1:n,:);
vq  = vdq(n+1:2*n,:);
vo  = vdq(2*n+1:3*n,:);
vfd = vdq(3*n+1:4*n,:);
vkD = vdq(4*n+1:5*n,:);
vkQ = vdq(5*n+1:6*n,:);
%
vdi  = vdqi(1:n,:);
vqi  = vdqi(n+1:2*n,:);
voi  = vdqi(2*n+1:3*n,:);
vfdi = vdqi(3*n+1:4*n,:);
vkDi = vdqi(4*n+1:5*n,:);
vkQi = vdqi(5*n+1:6*n,:);
%
[dummy1, Mvd, Mvq] = wmult(vq, vd, n, stype);
[dummy1, Mvo, Mvfd] = wmult(vfd, vo, n, stype);
[dummy1, MvkD, MvkQ] = wmult(vkQ, vkD, n, stype);
%
```

```
[dummy1, Mvdi, Mvqi] = wmult(vqi, vdi, n, stype);
[dummy1, Mvoi, Mvfdi] = wmult(vfdi, voi, n, stype);
[dummy1, MvkDi, MvkQi] = wmult(vkQi, vkDi, n, stype);
%
Mvdqt = [Mvd, Mvq, Mvo, Mvfd, MvkD, MvkQ];
%
Mvdqti = [Mvdi, Mvqi, Mvoi, Mvfdi, MvkDi, MvkQi];
%
Mvdq = [Mvd,
      Mvq,
      Mvo,
      Mvfd,
      MvkD,
      MvkQ];
%
Mvdqi = [Mvdi,
       Mvqi,
       Mvoi,
       Mvfdi,
       MvkDi,
       MvkQi];
%
%
% GENERATE THE INITIAL CONDITION VECTOR.
%
id_0  = wconvert(id_S0, n, 1, stype);
iq_0  = wconvert(iq_S0, n, 1, stype);
io_0  = wconvert(io_S0, n, 1, stype);
ifd_0 = wconvert(ifd_S0, n, 1, stype);
ikd_0 = wconvert(ikd_S0, n, 1, stype);
ikq_0 = wconvert(ikq_S0, n, 1, stype);
%
IC_0 = [ id_0,
       iq_0,
       io_0,
       ifd_0,
       ikd_0,
       ikq_0];
%
%
% SOLVE NOW FOR THE CURRENTS WHICH ARE STATES.
%
A = I6 + wB * (S6 * lDQ_inv * (r + bVP));
%
dA_dWrm = pp * (S6 * lDQ_inv * b);
%
bu = (wB * S6 * lDQ_inv * vdq) + IC_0;
%
dbu_dWrm = wB * S6 * lDQ_inv * dT_dWrm * Mvph;
%
A_inv = inv(A);
%
xi = A_inv * bu;
%
dxi_dImV = wB * A_inv * S6 * lDQ_inv * Tue * Incv * Imsc;
%
id  = xi(1:n,:);
iq  = xi(n+1:2*n,:);
io  = xi(2*n+1:3*n,:);
ifd = xi(3*n+1:4*n,:);
ikd = xi(4*n+1:5*n,:);
ikq = xi(5*n+1:6*n,:);
%
[dummy1,  Mid,  Miq] = wmult(iq, id, n, stype);
```

```
[dummy1,  Mio, Mifd] = wmult(ifd, io, n, stype);
[dummy1, Mikd, Mikq] = wmult(ikq, ikd, n, stype);
%
Mxit = [Mid, Miq, Mio, Mifd, Mikd, Mikq];
Mxi  = [Mid,
      Miq,
      Mio,
      Mifd,
      Mikd,
      Mikq];
%
dxi_dWrm = A_inv * (dbu_dWrm - dA_dWrm * Mxi);
%
iph = Tuet * xi;
%
Inci = [  I   Z   Z  Z Z Z,
        Z   I   Z  Z Z Z,
        Z   Z   I  Z Z Z,
       (-I) (-I) (-I) Z Z Z,
        Z   Z   Z  I Z Z];
%
Exi = Inci * iph;
%
Isc = [ ((IB / IsB) * I) Z Z Z Z,
      Z ((IB / IsB) * I) Z Z Z,
      Z Z ((IB / IsB) * I) Z Z,
      Z Z Z ((IB / IsB) * I) Z,
      Z Z Z Z I];
%
ExI = Isc * Exi;
%
Ia  = ExI(1:n,:);
Ib  = ExI(n+1:2*n,:);
Ic  = ExI(2*n+1:3*n,:);
In  = ExI(3*n+1:4*n,:);
Ifd = ExI(4*n+1:5*n,:);
%
%
%   Calculate the portions of the jacobian.
%
dExI_dImV = (Isc * Inci * Tuet * dxi_dImV);
%
dExI_dWrm = Isc * Inci * (dTt_dWrm * Mxi + Tuet * dxi_dWrm);
%
%
% SOLVE THE ROTOR ACCELERATION NOW.
%
Tmpu = (TqsB / TqB) * Tm;
%
Tdam = (B / TqB) * Wrm;
%
Wrmp  = (wB / (2 * pp * H)) * (Tmpu + (Mxit * bIP * xi) - Tdam);
%
%
%   Calculate the portions of the jacobian.
%
dWrmp_dImV =  (wB / (2 * pp * H)) * (Mxit * bIP * dxi_dImV);
%
dWrmp_dWrm = -(wB / (2 * pp * H)) * (B / TqB) * I;
%
dWrmp_dTm  =  (wB / (2 * pp * H)) * (TqsB / TqB) * I;
%
%
```

```
% CALCULATE THE TERMINAL VOLTAGE, A RECTIFIED AND AVERAGED VERSION.
%
%   Convert to a data point representation of the waveform.
%
[vad, dvad_dva] = wconvert(van, 5*n, stype, 1);
[vbd, dvbd_dvb] = wconvert(vbn, 5*n, stype, 1);
[vcd, dvcd_dvc] = wconvert(vcn, 5*n, stype, 1);
%
%   The following portion serves as the actual "rectifier".
%
for i=1:5*n,
 if vad(i,1) >= vbd(i,1),
  if vad(i,1) >= vcd(i,1),
   vtd(i,1) = vad(i,1);
   dvtd_dvad(i,i) = 1.0;
   dvtd_dvbd(i,i) = 0.0;
   dvtd_dvcd(i,i) = 0.0;
  else
   vtd(i,1) = vcd(i,1);
   dvtd_dvad(i,i) = 0.0;
   dvtd_dvbd(i,i) = 0.0;
   dvtd_dvcd(i,i) = 1.0;
  end
 else
  if vbd(i,1) >= vcd(i,1),
   vtd(i,1) = vbd(i,1);
   dvtd_dvad(i,i) = 0.0;
   dvtd_dvbd(i,i) = 1.0;
   dvtd_dvcd(i,i) = 0.0;
  else
   vtd(i,1) = vcd(i,1);
   dvtd_dvad(i,i) = 0.0;
   dvtd_dvbd(i,i) = 0.0;
   dvtd_dvcd(i,i) = 1.0;
  end
 end
end
%
%   Now the data point waveform is averaged and converted to stype.
%
[vta, dvta_dvtd] = w_ave(vtd, 1, 1, 1);
vtb = [1, 0]' * vt_S0 + [0, 1]' * vta;
[vtc, dvtc_dvtb] = wconvert(vtb, n, 1, 4);
[vt, dvt_dvtc] = wconvert(vtc, n, 4, stype);
%
%
%   Calculate the portions of the jacobian.
%
dvphd_dvph = [dvad_dva Z51 Z51 Z51 Z51 Z51,
          Z51 dvbd_dvb Z51 Z51 Z51 Z51,
          Z51 Z51 dvcd_dvc Z51 Z51 Z51,
          Z Z Z Z Z Z,
          Z Z Z Z Z Z,
          Z Z Z Z Z Z];
%
dvphd_dImV = dvphd_dvph * Incv * Imsc;
%
dvtd_dImV  = [dvtd_dvad, dvtd_dvbd, dvtd_dvcd, Z51, Z51, Z51] * dvphd_dImV;
%
dvt_dImV   = dvt_dvtc * dvtc_dvtb * [0, 1]' * dvta_dvtd * dvtd_dImV;
%
%
% CALCULATE THE "STABILITY ORGAN" LYAPUNOV FUNCTION AND ITS DERIVATIVE.
%
```

```
% % coenergy
% * coenergy + KEdiff ('equal power' normalisation)
% ^ coenergy + KE ('equal power' normalisation)
% & coenergy + KE
% $ coenergy + KEdiff
%
%*Wb = wconvert(wB/pp, n, 1, stype);
%*Wdiff = Wrm - Wb;
%*[Wsqr, MWdiff, dummy2]  = wmult(Wdiff, Wdiff, n, stype);
%&
[Wsqr, MWrm, dummy2]  = wmult(Wrm, Wrm, n, stype);
%$Wrr = wconvert(wB/pp, n, 1, stype);
%$Wdiff = Wrm - Wrr;
%$[Wsqr, MWdiff, dummy2]  = wmult(Wdiff, Wdiff, n, stype);
%^[Wsqr, MWrm, dummy2]  = wmult(Wrm, Wrm, n, stype);
%
%%ly = (1 / 3) * Mxit * ldq * xi;
%*ly = (1 / 3) * Mxit * lDQ * xi + (pp^2 / wB^2) * Wsqr;
%&
ly = (1 / 3) * Mxit * lDQ * xi + H * wB * (pp / wB)^2 * Wsqr;
%$ly = (1 / 3) * Mxit * lDQ * xi + H * wB * (pp / wB)^2 * Wsqr;
%^ly = (1 / 3) * Mxit * lDQ * xi + (pp / wB)^2 * Wsqr;
%
Ly = (EB / EsB) * ly;
%
%%lyp = (2 / 3) * wB * Mxit * ldq * lDQ_inv * (vdqi - ((r + bVP) * xi));
%*lyp = (2/3)*wB* Mxit * (vdqi - ((r + bVP) * xi)) +2*(pp/wB)^2* MWdiff * Wrmp;
%&
lyp = (2/3)* Mxit * (vdqi - (r * xi)) + (pp/wB)*(MWrm * Tmpu - (B/TqB)* Wsqr);
%$lypa = (2 / 3) * Mxit * (vdqi - (r * xi));
%$lypb = (pp / wB) * (MWdiff * Tmpu - (B / TqB) * MWdiff * Wrm);
%$lypc = Mxit * bIP * xi;
%$lyp = lypa + lypb + lypc;
%^lyp = (2/3)*wB * Mxit * (vdqi - ((r + bVP) * xi)) +2*(pp/wB)^2 * MWrm * Wrmp;
%
Lyp = (PB / PsB) * lyp;
%
%
%   Calculate the portions of the jacobian.
%    These are for the coenergy Lyapunov function only.
%    The jacobians for the "i" voltages are not complete either.
%
%dLy_dImV = (EB / EsB) * (2 / 3) * Mxit * ldq * dxi_dImV;
dLy_dImV = (EB / EsB) * (2 / 3) * Mxit * lDQ * dxi_dImV;
%
%dLy_dWrm = (EB / EsB) * (2 / 3) * Mxit * ldq * dxi_dWrm;
dLy_dWrm = (EB / EsB) * (2 / 3) * Mxit * lDQ * dxi_dWrm;
%
%dlypa_dImVi = Mxit * ldq * lDQ_inv * Tue * Incvi * Imsci;
%dlypb_dImVi = Mvdqti * ldq * lDQ_inv * dxi_dImV;
%dlypc_dImVi = 2 * Mxit * ldq * lDQ_inv * (r + bVP) * dxi_dImV;
%dLyp_dImVi  = (PB/PsB) * (2/3) * wB * (dlypa_dImV + dlypb_dImV - dlypc_dImV);
%dlypa_dWrm = Mxit * ldq * lDQ_inv * dT_dWrm * Mvphi;
%dlypb_dWrm = Mvdqti * ldq * lDQ_inv * dxi_dWrm;
%dlypc_dWrm = 2 * Mxit * ldq * lDQ_inv * (r + bVP) * dxi_dWrm;
%dLyp_dWrm  = (PB/PsB) * (2/3) * wB * (dlypa_dWrm + dlypb_dWrm - dlypc_dWrm);
%
dlypa_dImV = Mxit * Tue * Incv * Imsc;
dlypb_dImV = Mvdqt * dxi_dImV;
dlypc_dImV = 2 * Mxit * (r + bVP) * dxi_dImV;
dLyp_dImV = (PB/PsB) * (2/3) * wB * (dlypa_dImV + dlypb_dImV - dlypc_dImV);
dlypa_dWrm = Mxit * dT_dWrm * Mvph;
dlypb_dWrm = Mvdqt * dxi_dWrm;
```

```
dlypc_dWrm = 2 * Mxit * (r + bVP) * dxi_dWrm;
dLyp_dWrm  = (PB/PsB) * (2/3) * wB * (dlypa_dWrm + dlypb_dWrm - dlypc_dWrm);
%
% COLLECT THE EXPORT VARIABLES.
%
e = [Ia, Ib, Ic, In, Wrmp, Ifd, vt, Ly, Lyp];
%
%
% COLLECT THE FINAL STATES.
%
%
%  Return modulo 2 pi values for THETA at end of interval.
%
Ore_S1a = w_at_one(Ore, stype);
if ( (Ore_S1a > 6.283185307) | (Ore_S1a < -6.283185307) ),
  Ore_S1 = rem(Ore_S1a, 6.283185307);
else
  Ore_S1 = Ore_S1a;
end
%
id_S1  = w_at_one(id, stype);
iq_S1  = w_at_one(iq, stype);
io_S1  = w_at_one(io, stype);
ifd_S1 = w_at_one(ifd, stype);
ikd_S1 = w_at_one(ikd, stype);
ikq_S1 = w_at_one(ikq, stype);
%
s1 = [id_S1, iq_S1, io_S1, ifd_S1, ikd_S1, ikq_S1, Ore_S1, vta]';
%
%
% COLLECT THE JACOBIAN.
%
   jacob(1:4*n,1:4*n) = dExI_dImV(1:4*n,1:4*n);
%
   jacob(1:4*n,4*n+1:7*n) = zeros(4*n,3*n);
%
   jacob(1:4*n,7*n+1:8*n) = dExI_dWrm(1:4*n,:);
%
   jacob(1:4*n,8*n+1:9*n) = [Z,
                             Z,
                             Z,
                             Z];
%
   jacob(1:4*n,9*n+1:10*n) = dExI_dImV(1:4*n,4*n+1:5*n);
%
   jacob(4*n+1:5*n,1:4*n) = dWrmp_dImV(:,1:4*n);
%
   jacob(4*n+1:5*n,4*n+1:7*n) = zeros(n,3*n);
%
   jacob(4*n+1:5*n,7*n+1:8*n) = dWrmp_dWrm;
%
   jacob(4*n+1:5*n,8*n+1:9*n) = dWrmp_dTm;
%
   jacob(4*n+1:5*n,9*n+1:10*n) = dWrmp_dImV(:,4*n+1:5*n);
%
   jacob(5*n+1:6*n,1:4*n) = dExI_dImV(4*n+1:5*n,1:4*n);
%
   jacob(5*n+1:6*n,4*n+1:7*n) = zeros(n,3*n);
%
   jacob(5*n+1:6*n,7*n+1:8*n) = dExI_dWrm(4*n+1:5*n,:);
%
   jacob(5*n+1:6*n,8*n+1:9*n) = Z;
%
```

```
   jacob(5*n+1:6*n,9*n+1:10*n) = dExI_dImV(4*n+1:5*n,4*n+1:5*n);
%
   jacob(6*n+1:7*n,1:4*n) = dvt_dImV(:,1:4*n);
%
   jacob(6*n+1:7*n,4*n+1:10*n) = zeros(n,6*n);
%
   jacob(7*n+1:8*n,1:4*n) = dLy_dImV(:,1:4*n);
%
   jacob(7*n+1:8*n,4*n+1:7*n) = zeros(n,3*n);
%
   jacob(7*n+1:8*n,7*n+1:8*n) = dLy_dWrm;
%
   jacob(7*n+1:8*n,8*n+1:9*n) = Z;
%
   jacob(7*n+1:8*n,9*n+1:10*n) = dLy_dImV(:,4*n+1:5*n);
%
   jacob(8*n+1:9*n,1:4*n) = [I, I, I, I];
%
   jacob(8*n+1:9*n,4*n+1:7*n) = [I, I, I];
%
   jacob(8*n+1:9*n,7*n+1:8*n) = I;
%
   jacob(8*n+1:9*n,8*n+1:9*n) = Z;
%
   jacob(8*n+1:9*n,9*n+1:10*n) = I;
%
```

A.1.3 Reduced Order Generator Model

The following is a listing of the .def file for the synchronous generator "device object".

```
% This is a device.def for an open-circuited 3-phase synchronous machine.
% It is based on the model in Kirtley's LEES report.
% It exports one Lyapunov function and its convective
% derivative. Parameter values are from the LEES report.
%
% Revision 1 - 2 March 1992 John V. Amy Jr.
%
%
DEVICE LYAPGENK
      TERMINAL  1  INFORMATION delta IMPORT
      TERMINAL  2  INFORMATION eaf   IMPORT
      TERMINAL  3  INFORMATION Tm    IMPORT
      TERMINAL  4  INFORMATION Wre   EXPORT
      TERMINAL  5  INFORMATION Ly    EXPORT
      TERMINAL  6  INFORMATION Lyp   EXPORT
      PARAMETER XD        2.0
      PARAMETER XQ        1.8
      PARAMETER XDP       0.4
      PARAMETER XDPP      0.2
      PARAMETER XQPP      0.2
      PARAMETER XAL       0.02
      PARAMETER TDOP      5.0
      PARAMETER TDOPP     0.2
      PARAMETER TQOPP     0.2
      PARAMETER TAD       0.003
      PARAMETER H         3.0
      PARAMETER PP        1
      PARAMETER wB        377.0
      PARAMETER tcl       0.0
      STATE EQPP_S  0.0
      STATE EDPP_S  0.0
      STATE EQP_S   0.0
      STATE Wrm_S   0.0
      STATE ifd_S   0.0
```

```
    STATE ikd_S  0.0
    STATE ikq_S  0.0
    FUNCTION lyapgenk
    STRUCTURAL JACOBIAN ALL
        NNI
        NN0
        NN0
    END
END
%
%
```

The following is a listing of the .m file for the synchronous generator "device object".

```
function [e , jacob, s1, tt1] = lyapgenk(stype,i,par,s0,tt,alpha)
%
% 3PH SYNCHRONOUS MACHINE with stability organ
%
% VERSION 2.1 of 4 March 1992
% (C) Copyright 1992 by John V. Amy Jr.
%
% [e , jacob , s1, tt1] = lyapgenk(stype,i,par,s0,tt,alpha)
%
% LYAPGENk creates the values and jacobian matrix for a
% 3 phase synchronous machine.  It is based upon the model in
% Kirtley's LEES Report.  It also provides an information
% export variable for input to a stability demon.  This is for
% the open circuited portion of the critical clearing time simulation.
% What psid and psiq are differs from LYAPGENj.
%
%  stype = 1 data points
%        = 2 fourier series
%        = 3 legendre series
%        = 4 polynomial
%
%      i = [delta, eaf, Tm]
%          delta = rotor angle (radians)
%            eaf = field excitation (pu)
%             Tm = mechanical torque input (pu)
%
%    par =    [ XD Synchronous Reactance (pu)
%              XQ Negative Sequence Reactance (pu)
%             XDP Transient Reactance (pu)
%            XDPP D-axis Subtransient Reactance (pu)
%            XQPP Q-axis Subtransient Reactance (pu)
%             XAL Armature Leakage Reactance (pu)
%            TDOP Transient Open Circuit Time Constant (sec)
%           TDOPP D-axis Subtransient Open Circuit Time Constant (sec)
%           TQOPP Q-axis Subtransient Open Circuit Time Constant (sec)
%            TAD Armature Time Constant (sec)
%              H Inertia Constant (sec)
%             PP Number of Pole Pairs
%             wB Base Frequency (1/sec)
%            tcl fault clear time (sec)  ]
%
%     s0 = [EQPP_S, EDPP_S, EQP_S, Wrm_S, ifd_S, ikd_S, ikq_S]
%          these are the initial values of the states, at t0.
%          EQPP = "q"-axis voltage behind subtransient reactance (pu)
%          EDPP = "d"-axis voltage behind subtransient reactance (pu)
%           EQP = "q"-axis voltage behind transient reactance (pu)
%           Wrm = rotor mechanical speed (1/sec)
%                 rotor currents (pu)
%
%     tt = [t0, t1, adt]
%               t0 = initial time of the interval
```

```
%              t1 = final time of the interval
%             adt = averaging time increment
%
%  alpha = continuation parameter (0 linear, 1 nonlinear)
%
%     e = [Wre, Ly, Lyp]
%         Wre = rotor electrical frequency (1/sec)
%          Ly = coupling field Lyapunov function (pu)
%         Lyp = D(coupling field Lyapunov function)/Dt (pu)
%
%    s1 = [EQPP_S, EDPP_S, EQP_S, Wrm_S, ifd_S, ikd_S, ikq_S]
%           these are the final values of the states, at t1.
%
%   tt1 = [nt1, ntt] where
%           nt1 is the recommended recomputation time this interval, and
%           ntt is the recommended ending time next interval.
%
% Structural Jacobian
%
%           NNI
%           NN0
%           NN0
%
% READ IN ALL INPUTS.
%
[n,nc] = size(i);
%
XD   = par(1);
XQ   = par(2);
XDP  = par(3);
XDPP = par(4);
XQPP = par(5);
XAL  = par(6);
TDOP = par(7);
TDOPP = par(8);
TQOPP = par(9);
TAD  = par(10);
H    = par(11);
PP   = par(12);
wB   = par(13);
tcl  = par(14);
%
t0  = tt(1);
t1  = tt(2);
adt = tt(3);
%
EQPP_S0 = s0(1);
EDPP_S0 = s0(2);
EQP_S0  = s0(3);
Wrm_S0  = s0(4);
ifd_S0  = s0(5);
ikd_S0  = s0(6);
ikq_S0  = s0(7);
%
delta = i(:,1);
eaf   = i(:,2);
Tm    = i(:,3);
%
%
% START CALCULATIONS.--GENERATE TIME OUTPUTS.
%
dt = (t1 - t0) / 2;
%
```

```
% I - CALCULATE PARAMETERS AND ELECTRICAL EQUATION MATRICES.
%
ALPHA = ((XD - XDPP) / (XDP - XDPP));
XAD   = XD - XAL;
XAQ   = XQ - XAL;
XF    = ((XAD * XAD) / (XD - XDP));
RF    = (XF / (wB * TDOP));
XKD   = ((XAD * XAD) / (XD - XDPP));
RKD   = (XKD / (ALPHA * wB * TDOPP));
XKQ   = ((XAQ * XAQ) / (XQ - XQPP));
RKQ   = (XKQ / (wB * TQOPP));
%
% Generate the "S" matrix.
%
dummy_wave = zeros(n,1);
[dummy1, SM1] = w_int(dummy_wave, n, stype, 0);
S = SM1 * dt;
%
% Generate an identity matrix.
%
I = eye(n);
%
% Generate a zero matrix.
%
Z = zeros(n,n);
%
% Generate the rotor inductance matrix.
%
lDQR(1:n,1:n)           = XF * I;
lDQR(1:n,n+1:2*n)       = XAD * I;
lDQR(n+1:2*n,1:n)       = XAD * I;
lDQR(n+1:2*n,n+1:2*n)   = XKD * I;
lDQR(2*n+1:3*n,2*n+1:3*n) = XKQ * I;
%
lDQR_inv = inv(lDQR);
%
% Generate the coupling field inductance matrix.
%
ldqR(1:n,1:n)           = XAD * I;
ldqR(1:n,n+1:2*n)       = XAD * I;
ldqR(n+1:2*n,1:n)       = XAD * I;
ldqR(n+1:2*n,n+1:2*n)   = XAD * I;
ldqR(2*n+1:3*n,2*n+1:3*n) = XAQ * I;
%
% Generate the rotor resistance matrix.
%
rR(1:n,1:n) = RF * I;
rR(n+1:2*n,n+1:2*n) = RKD * I;
rR(2*n+1:3*n,2*n+1:3*n) = RKQ * I;
%
% Generate the initial condition vector.
%
EQPP_0 = wconvert(EQPP_S0, n, 1, stype);
EDPP_0 = wconvert(EDPP_S0, n, 1, stype);
EQP_0  = wconvert(EQP_S0, n, 1, stype);
%
b_0 = [ EQPP_0,
      EDPP_0,
      EQP_0];
%
%
```

```
% II - CALCULATE ELECTRICAL STATES AND CURRENTS
%       Determine whether OPEN CIRCUIT assumptions are valid.
%
 if t0 < tcl,
%
% OPEN CIRCUIT FLUX ASSUMPTIONS ARE PRESENT.
%  Generate the A matrix.
%
  A(1:n,1:n)      = I + S * (1.0 / TDOPP);
  A(1:n,n+1:2*n)  = Z;
  A(1:n,2*n+1:3*n) = - S / TDOPP;
%
  A(n+1:2*n,1:n)      = Z;
  A(n+1:2*n,n+1:2*n)  = I + S * (1.0 / TQOPP);
  A(n+1:2*n,2*n+1:3*n) = Z;
%
  A(2*n+1:3*n,1:n)      = - S * ( ( ALPHA - 1 ) / TDOP );
  A(2*n+1:3*n,n+1:2*n)  = Z;
  A(2*n+1:3*n,2*n+1:3*n) = I + S * ( ALPHA / TDOP );
%
%  Invert the A matrix.
%
  A_INV = inv(A);
%
%  Generate the b matrix.
%
  b(1:n,1)      = zeros(n,1);
  b(n+1:2*n,1)  = zeros(n,1);
  b(2*n+1:3*n,1) = (1 / TDOP) * S * eaf;
%
  db_ddelta = [Z,
               Z,
               Z];
  db_deaf   = [Z,
               Z,
               ((1 / TDOP) * S)];
%
%  Calculate the electrical states.
%
  b_sum = b + b_0;
%
  x = A_INV * b_sum;
%
  EQPP = x(1:n,:);
  EDPP = x((n+1):2*n,:);
  EQP  = x((2*n+1):3*n,:);
%
  [dummy1, MEQPP, MEDPP] = wmult(EDPP, EQPP, n, stype);
  [dummy1, MEQP, dummy2] = wmult(EQP, EQP, n, stype);
%
  dx_ddelta = A_INV * db_ddelta;
  dx_deaf   = A_INV * db_deaf;
%
  if t1 < tcl,
%   The fault has not yet been cleared. Do not pass a break point.
    tt1 = [t1, t0];
    Tnet = Tm;
    dTnet_ddelta = Z;
    dTnet_deaf = Z;
    dTnet_dTm = I;
  else
%   The fault is cleared during the present increment. Pass a break time.
    tt1 = [tcl, t0];
    Tnet = Tm;
```

```
    dTnet_ddelta = Z;
    dTnet_deaf = Z;
    dTnet_dTm = I;
  end
 else
% The fault has been cleared. Do not pass a break point.
  tt1 = [t1, t0];
%
% OPEN CIRCUIT ASSUMPTIONS ARE NOT PRESENT.
%  Generate the A matrix.
%
  A(1:n,1:n)      = I + S * ( XDP / ( TDOPP * XDPP ) );
  A(1:n,n+1:2*n)  = Z;
  A(1:n,2*n+1:3*n) = - S / TDOPP;
%
  A(n+1:2*n,1:n)      = Z;
  A(n+1:2*n,n+1:2*n)  = I + S * XQ / ( TQOPP * XQPP );
  A(n+1:2*n,2*n+1:3*n) = Z;
%
  A(2*n+1:3*n,1:n)      = - S * ( ( ALPHA - 1 ) / TDOP );
  A(2*n+1:3*n,n+1:2*n)  = Z;
  A(2*n+1:3*n,2*n+1:3*n) = I + S * ( ALPHA / TDOP );
%
%  Invert the A matrix.
%
  A_INV = inv(A);
%
%  Generate the b matrix.
%
  [psid, dpsid_ddelta] = wcos(delta, n, stype);
  [psiq, dpsiq_ddelta] = wsin(-1.0 * delta, n, stype);
%
  [dummy1, Mpsiq, Mpsid] = wmult(psid, psiq, n, stype);
%
  b(1:n,1) = ( ( XDP - XDPP ) / ( TDOPP * XDPP ) ) * S * psid;
  b(n+1:2*n,1) = - ( ( XQ - XQPP ) / ( TQOPP * XQPP ) ) * S * psiq;
  b(2*n+1:3*n,1) = (1 / TDOP) * S * eaf;
%
  db_ddelta = [(((XDP - XDPP) / (TDOPP * XDPP)) * S * dpsid_ddelta),
           (-((XQ - XQPP) / (TQOPP * XQPP)) * S * dpsiq_ddelta),
           Z];
  db_deaf  = [Z,
           Z,
           ((1 / TDOP) * S)];
%
%  Calculate the electrical states.
%
  b_sum = b + b_0;
%
  x = A_INV * b_sum;
%
  EQPP = x(1:n,:);
  EDPP = x((n+1):2*n,:);
  EQP  = x((2*n+1):3*n,:);
%
  [dummy1, MEQPP, MEDPP] = wmult(EDPP, EQPP, n, stype);
  [dummy1, MEQP, dummy2] = wmult(EQP, EQP, n, stype);
%
  dx_ddelta = A_INV * db_ddelta;
  dx_deaf  = A_INV * db_deaf;
%
% Calculate the electromagnetic torque.
%
  Tepu = (1 / XQPP) * Mpsid * EDPP + (1 / XDPP) * Mpsiq * EQPP;
```

```
%
  dTepu_ddelta1 = (1/XQPP)*(dpsid_ddelta*MEDPP + Mpsid*dx_ddelta(n+1:2*n,:));
  dTepu_ddelta2 = (1/XDPP)*(dpsiq_ddelta*MEQPP + Mpsiq*dx_ddelta(1:n,:));
  dTepu_ddelta = dTepu_ddelta1 + dTepu_ddelta2;
%
  dTepu_deaf1 = (1/XQPP) * Mpsid * dx_deaf(n+1:2*n,:);
  dTepu_deaf2 = (1/XDPP) * Mpsiq * dx_deaf(1:n,:);
  dTepu_deaf = dTepu_deaf1 + dTepu_deaf2;
%
%  Calculate the net torque on the rotor.
%
  Tnet = Tm + Tepu;
  dTnet_ddelta = dTepu_ddelta;
  dTnet_deaf = dTepu_deaf;
  dTnet_dTm = I;
 end
%
%
%  Generate a rotor voltage vector.
%
vfd = (RF / XAD) * sqrt(1.5) * eaf;
%
vR = [vfd,
    zeros(2*n,1)];
%
dvR_deaf = [(RF / XAD) * sqrt(1.5) * I,
         Z,
         Z];
%
%
%  Calculate machine currents.
%
C(1:n,1:n)      = (XD - XDPP) * I;
C(1:n,n+1:2*n)  = XAD * I;
C(1:n,2*n+1:3*n) = Z;
%
C(n+1:2*n,1:n)      = Z;
C(n+1:2*n,n+1:2*n)  = Z;
C(n+1:2*n,2*n+1:3*n) = -XAQ * I;
%
C(2*n+1:3*n,1:n)      = XAD * I;
C(2*n+1:3*n,n+1:2*n)  = (XD - XDP) * I;
C(2*n+1:3*n,2*n+1:3*n) = Z;
%
C_inv = inv(C);
%
iR = C_inv * x;
%
iRm = sqrt(1.5) * iR;
%
ifdm = iRm(1:n,:);
ikdm = iRm(n+1:2*n,:);
ikqm = iRm(2*n+1:3*n,:);
%
[dummy1, Mifdm, Mikdm]  = wmult(ikdm, ifdm, n, stype);
[dummy1, Mikqm, dummy2] = wmult(ikqm, ikqm, n, stype);
MiRmt = [Mifdm, Mikdm, Mikqm];
MiRm = [Mifdm,
      Mikdm,
      Mikqm];
%
%
iRmdot = wB * lDQR_inv * (vR - (rR * iRm));
%
```

```
difdm = iRmdot(1:n,:);
dikdm = iRmdot(n+1:2*n,:);
dikqm = iRmdot(2*n+1:3*n,:);
%
[dummy1, Mdifdm, Mdikdm] = wmult(dikdm, difdm, n, stype);
[dummy1, Mdikqm, dummy2] = wmult(dikqm, dikqm, n, stype);
MiRmdott = [Mdifdm, Mdikdm, Mdikqm];
%
diRm_ddelta = sqrt(1.5) * C_inv * dx_ddelta;
diRm_deaf   = sqrt(1.5) * C_inv * dx_deaf;
diRm_deaft = [diRm_deaf(1:n,:), diRm_deaf(n+1:2*n,:), diRm_deaf(2*n+1:3*n,:)];
%
diRmdot_ddelta = - wB * sqrt(1.5) * lDQR_inv * rR * C_inv * dx_ddelta;
diRmdot_deaf  = wB * lDQR_inv * (dvR_deaf - rR * sqrt(1.5) * C_inv * dx_deaf);
%
%
% III - Calculate the rotor's electrical frequency.
%
Wrm_0 = wconvert(Wrm_S0, n, 1, stype);
%
Wrm = (wB / (2 * PP * H)) * S * Tnet + Wrm_0;
%
Wre = PP * Wrm;
%
dWre_ddelta = (wB / (2 * H)) * S * dTnet_ddelta;
dWre_deaf   = (wB / (2 * H)) * S * dTnet_deaf;
dWre_dTm    = (wB / (2 * H)) * S * dTnet_dTm;
%
%
% IV - Calculate the "coupling field" coenergy Lyapunov function waveforms.
%
% % coenergy + KEdiff(scaled)    # coenergy + KE(scaled)
%
% * coenergy  ^ coenergy + KEdiff  & coenergy + KE  $ coenergy + KE^2/KErtd
%   COENTST1   COENTST2          COENTST3       COENTST4
%
%%
Wb = wconvert(wB/PP, n, 1, stype);
%%
Wdiff = Wrm - Wb;
%%
[Wsqr, MWdiff, dummy2]  = wmult(Wdiff, Wdiff, n, stype);
%%
Wrmdot = (wB / (2 * PP * H)) * Tnet;
%*
%^Wb = wconvert(wB/PP, n, 1, stype);
%^Wdiff = Wrm - Wb;
%^[Wsqr, MWdiff, dummy2]  = wmult(Wdiff, Wdiff, n, stype);
%&[Wsqr, MWrm, dummy2]  = wmult(Wrm, Wrm, n, stype);
%$[Wsqra, MWrm, dummy2]  = wmult(Wrm, Wrm, n, stype);
%$Wrr = wconvert(wB/PP, n, 1, stype);
%$[Wsqrb, MWrr, dummy2]  = wmult(Wrr, Wrr, n, stype);
%$Wdiff_2 = Wsqra - Wsqrb;
%$[Wsqrc, MWdiff_2, dummy2] = wmult(Wdiff_2, Wdiff_2, n, stype);
%#Wrmdot = (wB / (2 * PP * H)) * Tnet;
%#[Wsqr, MWrm, dummy2]  = wmult(Wrm, Wrm, n, stype);
%
%%
Ly = (1 / 3) * MiRmt * lDQR * iRm + (PP / wB)^2 * Wsqr;
%*Ly = (1 / 3) * MiRmt * lDQR * iRm;
%^Ly = (1 / 3) * MiRmt * lDQR * iRm + H * wB * (PP / wB)^2 * Wsqr;
%&Ly = (1 / 3) * MiRmt * lDQR * iRm + H * wB * (PP / wB)^2 * Wsqr;
%$Ly = (1 / 3) * MiRmt * lDQR * iRm + H * wB * (PP / wB)^4 * Wsqrc;
```

```
%#Ly = (1 / 3) * MiRmt * lDQR * iRm + (PP / wB)^2 * Wsqr;
%
%%
Lyp = (2 / 3) * MiRmt * lDQR * iRmdot + 2 * (PP / wB)^2 * MWdiff * Wrmdot;
%*Lyp = (2 / 3) * MiRmt * (vR - (rR * iRm));
%^Lyp = (2 / 3) * MiRmt * (vR - (rR * iRm)) + (PP / wB) * MWdiff * Tm;
%&Lyp = (2 / 3) * MiRmt * (vR - (rR * iRm)) + (PP / wB) * MWrm * Tm;
%$Lyp = (2/3) * MiRmt * (vR - (rR * iRm)) + 2*(PP/wB)^3 * MWdiff_2 * MWrm * Tm;
%#Lyp = (2 / 3) * MiRmt * lDQR * iRmdot + 2 * (PP / wB)^2 * MWrm * Wrmdot;
%
dLy_ddelta = (2 / 3) * MiRmt * ldqR * diRm_ddelta;
dLy_deaf   = (2 / 3) * MiRmt * ldqR * diRm_deaf;
%
dLyp_ddelta1 = (2 / 3) * MiRmt * ldqR * diRmdot_ddelta;
dLyp_ddelta2 = (2 / 3) * MiRmdott * ldqR * diRm_ddelta;
dLyp_ddelta  = dLyp_ddelta1 + dLyp_ddelta2;
%
dLyp_deaf1 = (2 / 3) * MiRmt * ldqR * diRmdot_deaf;
dLyp_deaf2 = (2 / 3) * MiRmdott * ldqR * diRm_deaf;
dLyp_deaf  = dLyp_deaf1 + dLyp_deaf2;
%
%
% Identify the export variables.
%
e = [Wre, Ly, Lyp];
%
%
% Collect the Jacobian.
%
jacob(1:n,1:n)      = dWre_ddelta;
jacob(1:n,n+1:2*n)  = dWre_deaf;
jacob(1:n,2*n+1:3*n) = dWre_dTm;
%
jacob(n+1:2*n,1:n)      = dLy_ddelta;
jacob(n+1:2*n,n+1:2*n)  = dLy_deaf;
jacob(n+1:2*n,2*n+1:3*n) = Z;
%
jacob(2*n+1:3*n,1:n)      = dLyp_ddelta;
jacob(2*n+1:3*n,n+1:2*n)  = dLyp_deaf;
jacob(2*n+1:3*n,2*n+1:3*n) = Z;
%
%
% Calculate values of states at the end of the time interval.
%
[EQPP_S1, dummy1] = w_at_one(EQPP, stype);
[EDPP_S1, dummy1] = w_at_one(EDPP, stype);
[EQP_S1,  dummy1] = w_at_one(EQP, stype);
[Wrm_S1,  dummy1] = w_at_one(Wrm, stype);
[ifd_S1,  dummy1] = w_at_one(ifdm, stype);
[ikd_S1,  dummy1] = w_at_one(ikdm, stype);
[ikq_S1,  dummy1] = w_at_one(ikqm, stype);
%
s1 = [EQPP_S1, EDPP_S1, EQP_S1, Wrm_S1, ifd_S1, ikd_S1, ikq_S1]';
```

A.2 Inductor with Stability Organ

The following is a listing of the .def file for the inductor "device object".

```
%
% This is the .def file for a device object which represents a simple
% inductor.  In addition to providing current as a function of the
% terminal voltages, two information export variables are provided.
% These two export waveforms represent the stored energy of the inductor
% and the rate of change of the stored energy.
%
```

```
% 23 January 1992  John V. Amy Jr.
%
DEVICE LYAPIND
  TERMINAL 1 POTENTIAL   V1  IMPORT
  TERMINAL 1 FLOW        I1  EXPORT 1
  TERMINAL 2 POTENTIAL   V2  IMPORT
  TERMINAL 2 FLOW        I2  EXPORT 1
  TERMINAL 3 INFORMATION LF  EXPORT
  TERMINAL 4 INFORMATION LFp EXPORT
  PARAMETER L 1e-15
  STATE IL_S 0.0
  FUNCTION lyapind
  STRUCTURAL JACOBIAN ALL
          LL
          LL
          NN
          NN
  END
END
```

The following is a listing of the .m file for the inductor "device object".

```
function [e , jacob, s1, tt1] = lyapind(stype,i,par,s0,tt,alpha)
%
% INDUCTOR with a LYAPUNOV Function Export Variable
%
% VERSION 1.0 of 23 January 1992
% (C) Copyright 1990, 1991, 1992 by Norbert H. Doerry, John V. Amy Jr.
%
% [e , jacob , s1, tt1] = lyapind(stype,i,par,s0,tt,alpha)
%
% LYAPIND  creates the values and jacobian matrix for an INDUCTOR
% with a Lyapunov function export variable.  The Lyapunov function
% is the energy stored in the inductor.
%
%
%     stype = 1 data points
%           = 2 fourier series
%           = 3 legendre series
%           = 4 polynomial
%
%     i    = [V1, V2] where V1 and V2 are column vectors
%              V1 = terminal 1 potential
%              V2 = terminal 2 potential
%
%     par  = [L]  where L = inductance
%
%     s0   = [IL_S] where IL_S0 = Initial value for IL_S
%
%     tt   = [t0, t1, adt]
%              t0   = initial time of the interval
%              t1   = final time of the interval
%             adt   = averaging time increment
%
%     alpha = continuation parameter (0 linear 1 nonlinear)
%
%     e    = [I1, I2, LF, LFp] where I1 and I2 are column vectors
%              I1 = terminal 1 flow
%              I2 = terminal 2 flow
%              LF = Lyapunov function (information)
%             LFp = Convective derivative of LF (information)
%
%     jacob = Jacobian matrix of e with respect to i
%
%     s1   = [IL_S]
```

```
%
%      tt1   = [nt1 ntt] where
%              nt1 recommended recomputation time this interval
%              ntt recommended ending time next interval
%
%      structural jacobian
%
%      L L
%      L L
%           N N
%           N N
%
%  READ ALL INPUTS.
%
[n, nc] = size(i);
%
L = par(1);
%
t0  = tt(1);
t1  = tt(2);
adt = tt(3);
%
IL_S0 = s0(1);
%
V1 = i(:,1);
V2 = i(:,2);
%
%
%  GENERATE TIME VARIABLES AND OUTPUTS.
%
dt = (t1 - t0) / 2;
%
tt1 = [t1 t0];
%
%
% GENERATE THE "S" MATRIX.
%
dt = (t1 - t0) / 2;
dummy_wave = zeros(n,1);
[dummy1, SM1] = w_int(dummy_wave, n, stype, 0);
S = SM1 * dt;
%
%
%  CALCULATE EXPORT VARIABLES, CURRENTS FIRST.
%
Vdiff = (V1 - V2);
[dummy1, MVdiff, likewise] = wmult(Vdiff, Vdiff, n, stype);
%
IL_0 = wconvert(IL_S0, n, 1, stype);
I1 = (1 / L) * S * Vdiff + IL_0;
I2 = -I1;
%
[IL2, MI1, likewise] = wmult(I1, I1, n, stype);
LF = (L / 2) * IL2;
%
LFp = wmult(I1, Vdiff, n, stype);
%
e = [I1, I2, LF, LFp];
%
%
%  CALCULATE THE FINAL STATE.
%
IL_S1 = w_at_one(I1, stype);
%
```

```
s1 = [IL_S1]';
%
%
% CALCULATE THE JACOBIAN.
%
jacob(1:n,1:n)          =  (1 / L) * S;
jacob(1:n,n+1:2*n)      = - jacob(1:n,1:n);
jacob(n+1:2*n,1:n)      = - jacob(1:n,1:n);
jacob(n+1:2*n,n+1:2*n)  =  jacob(1:n,1:n);
jacob(2*n+1:3*n,1:n)    =  L * MI1 * jacob(1:n,1:n);
jacob(2*n+1:3*n,n+1:2*n) = - L * MI1 * jacob(1:n,1:n);
jacob(3*n+1:4*n,1:n)    =  MI1 + MVdiff * jacob(1:n,1:n);
jacob(3*n+1:4*n,n+1:2*n) = - MI1 - MVdiff * jacob(1:n,1:n);
```

A.3 Capacitor with Stability Organ

The following is a listing of the .def file for the capacitor "device object".

```
%
% This is the .def file for a device object which represents a simple
% capacitor. In addition to providing currents and voltages as
% functions of the terminal voltages and currents, two information
% export variables are provided. These two export waveforms represent
% the stored energy of the inductor and the rate of change of the
% stored energy.
%
% 29 January 1992  John V. Amy Jr.
%
DEVICE LYAPCAP
  TERMINAL 1 POTENTIAL   V1  EXPORT
  TERMINAL 1 FLOW        I1  EXPORT 1
  TERMINAL 2 POTENTIAL   V2  IMPORT
  TERMINAL 2 FLOW        I2  IMPORT 1
  TERMINAL 3 INFORMATION LF  EXPORT
  TERMINAL 4 INFORMATION LFp EXPORT
  PARAMETER C 1e-15
  STATE VC_S 0.0
  FUNCTION lyapcap
  STRUCTURAL JACOBIAN ALL
          IL
          0D
          NN
          NN
  END
END
```

The following is a listing of the .m file for the capacitor "device object".

```
function [e , jacob, s1, tt1] = lyapcap(stype,i,par,s0,tt,alpha)
%
% CAPACITOR with a LYAPUNOV Function Export Variable
%
% VERSION 1.0 of 29 January 1992
% (C) Copyright 1990, 1991, 1992 by Norbert H. Doerry, John V. Amy Jr.
%
% [e , jacob, s1, tt1] = lyapcap(stype,i,par,s0,tt,alpha)
%
% LYAPCAP creates the values and jacobian matrix for a CAPACITOR
% with a Lyapunov function export variable.  The Lyapunov function
% is the energy stored in the capacitor.
%
%
%     stype = 1 data points
%           = 2 fourier series
%           = 3 legendre series
%           = 4 polynomial
```

```
%
%     i    = [V2, I2] where V2 and I2 are column vectors
%              V2 = terminal 2 potential
%              I2 = terminal 2 flow
%
%     par  = [C] where C = Capacitance
%
%     s0   = [VC_S] where VC_S = initial value of (V1 - V2)
%
%     tt   =  [t0 t1 dt]
%              t0 = initial time of the interval
%              t1 = final time of the interval
%             adt = averaging increment
%
%     alpha = continuation parameter
%
%     e    = [V1, I1, LF, LFp] where the column vectors are
%              V1 = terminal 1 potential
%              I1 = terminal 1 flow
%              LF = Lyapunov function (information)
%             LFp = Convective Derivative of LF (information)
%
%     jacob = Jacobian matrix of e with respect to i
%
%     s1   = [VC_S]
%
%     tt1  = [nt1, ntt] where
%              nt1 recommended recomputation time this interval
%              ntt recommended ending time next interval
%
%
%     structural jacobian
%
%              I L
%              0 D
%              N N
%              N N
%
% READ ALL INPUTS.
%
[n, nc] = size(i);
%
C = par(1);
%
t0  = tt(1);
t1  = tt(2);
adt = tt(3);
%
VC_S0 = s0(1);
%
V2 = i(:,1);
I2 = i(:,2);
%
%
% GENERATE TIME VARIABLES AND OUTPUTS.
%
dt = (t1 - t0) / 2;
%
tt1 = [t1, t0];
%
%
% GENERATE AN "S" MATRIX.
%
dummy_wave = zeros(n,1);
```

```
[dummy1, SM1] = w_int(dummy_wave, n, stype, 0);
S = SM1 * dt;
%
%
%  CALCULATE EXPORT VARIABLES.
%
I1 = - I2;
%
VC_0 = wconvert(VC_S0, n, 1, stype);
V1 = (1 / C) * S * I1 + V2 + VC_0;
%
Vc = V1 - V2;
[Vc_2, MVc, likewise]  = wmult(Vc, Vc, n, stype);
LF = (C / 2) * Vc_2;
%
[LFp, MI1, sameabove] = wmult(Vc, I1, n, stype);
%
e = [V1, I1, LF, LFp];
%
I = eye(n,n);
Z = zeros(n,n);
%
%
%  CALCULATE THE JACOBIAN.
%
jacob(1:n,1:n)         =  I;
jacob(1:n,n+1:2*n)     = - (1 / C) * S;
jacob(n+1:2*n,1:n)     =  Z;
jacob(n+1:2*n,n+1:2*n)  = - I;
jacob(2*n+1:3*n,1:n)    = - C * MVc;
jacob(2*n+1:3*n,n+1:2*n) = - MVc * S;
jacob(3*n+1:4*n,1:n)    = - MI1;
jacob(3*n+1:4*n,n+1:2*n) = - (1 / C) * S * MI1 - MVc;
%
%
VC_S1 = w_at_one(Vc, stype);
%
s1 = [VC_S1]';
```

A.4 Time-Scale Averaging Function

```
[nrr, ncc] = size(data_t);
delt = 0.05;
v1dasum = zeros(nrr,1);
v2dasum = zeros(nrr,1);
v1davg  = zeros(nrr,1);
v2davg  = zeros(nrr,1);
for i=1:nrr,
 if (data_t(i,1) - delt) < t0,
  p = 1;
 else
  is = i;
  while data_t(is,1) >= (data_t(i,1) - delt),
   is = is - 1;
  end
  p = is + 1;
 end
%
 V1dotsum = 0.0;
 V2dotsum = 0.0;
 for j=p:i-1,
  deltat = data_t(j+1,1) - data_t(j,1);
  V1dotsum = V1dotsum + deltat * V1dot(j,1);
  V2dotsum = V2dotsum + deltat * V2dot(j,1);
```

```
  end
  if i==1,
    actdt = data_t(2,1) - data_t(1,1);
  else
    actdt = data_t(i,1) - data_t(p,1);
  end
  V1dotavg(i,1) = V1dotsum / actdt;
  V2dotavg(i,1) = V2dotsum / actdt;
%
end
plot(data_t, V1dotavg, data_t, V2dotavg);
```

B Stability Demon

B.1 Component Neutral Relationship Based Stability Demon

The following is a listing of the .def file for the stability demon "device object".

```
%
% This is the .def file for a device object which is the fifth
% stability demon.
%
% 17 March 1992  John V. Amy Jr.
%
DEVICE DEMON04
  TERMINAL 1 INFORMATION V1   IMPORT
  TERMINAL 2 INFORMATION V1d  IMPORT
  TERMINAL 3 INFORMATION V2   IMPORT
  TERMINAL 4 INFORMATION V2d  IMPORT
  TERMINAL 5 INFORMATION a1   EXPORT
  TERMINAL 6 INFORMATION a1d  EXPORT
  TERMINAL 7 INFORMATION a2   EXPORT
  TERMINAL 8 INFORMATION a2d  EXPORT
  TERMINAL 9 INFORMATION Vwsd EXPORT
  PARAMETER delta1 1e-6
  PARAMETER delta2 1e-6
  FUNCTION demon04
  STRUCTURAL JACOBIAN ALL
          N000
          NN00
          00N0
          00NN
          NNNN
  END
END
```

The following is a listing of the .m file for the stability demon "device object".

```
function [e , jacob, s1, tt1] = demon04(stype,i,par,s0,tt,alpha)
%
% DEMON04 is the fifth Stability Demon Implemented
%
% VERSION 5.0 of 17 March 1992
% (C) Copyright 1992 by John V. Amy Jr.
%
% [e , jacob , s1, tt1] = demon05(stype,i,par,s0,tt,alpha)
%
% DEMON05 is the fifth stability demon to be written.  It uses a time varying
% alpha vector to assess stability.  The rate of change of alpha is adjusted
% only for its own component, the "component neutral" algorithm is used.  This
% demon is designed to work on data points to avoid harmonics problems which
% arise when computing exponentials as a finite series.  See 16 March
% notes for specific equations.  This demon only treats two organs' inputs.
%
%
%     stype = 1 data points  ****** This demon is made only for data points.
%           = 2 fourier series
%           = 3 legendre series
%           = 4 polynomial
%
%     i    = [V1, V1d, V2, V2d] where V1, V1d, V2, V2d are column vectors.
%              V1 = Lyapunov function of component 1
%             V1d = D(Lyapunov function)/Dt of component 1
%              V2 = Lyapunov function of component 2
%             V2d = D(Lyapunov function)/Dt of component 2
%
%     par  = [delta1, delta2]
%             delta#n is a (positive) constant relating a#n and 1/V#n.
```

```
%
%     s0   = []
%
%     tt   = [t0, t1, adt]
%            t0 = initial time of the interval
%            t1 = final time of the interval
%           adt = averaging time increment
%
%     alpha = continuation parameter (0 linear 1 nonlinear)
%
%     e    = [a1, a1dot, a2, a2dot, DVws_Dt]
%              a1  = component 1 alpha
%            a1dot = D(alpha1)/Dt
%              a2  = component 2 alpha
%            a2dot = D(alpha2)/Dt
%           DVws_Dt = D(Vws)/Dt
%
%     jacob = Jacobian matrix of e with respect to i
%
%     s1   = []
%
%     tt1  = [nt1 ntt] where
%            nt1 recommended recomputation time this interval
%            ntt recommended ending time next interval
%
%     structural jacobian
%
%            N000
%            NN00
%            00N0
%            00NN
%            NNNN
%
%
%  Read all inputs.
%
[n, nc] = size(i);
%
t0  = tt(1);
t1  = tt(2);
adt = tt(3);
%
delta1 = par(1);
delta2 = par(2);
%
V1    = i(:,1);
V1dot = i(:,2);
V2    = i(:,3);
V2dot = i(:,4);
%
%
%  Generate some required terms.
%
e_delta1 = exp(delta1);
e_delta2 = exp(delta2);
%
Z = zeros(n,n);
%
%
% Calculate the a#n's using the "component neutral" algorithm.
%
% Carry out the calculation term by term.
for i=1:n,
% First remove near singularities from swamping out other information.
```

```
 if V1(i,1) == 0,
  denom1 = 1e-16;
  if sign(V1dot(i,1)) == -1,
   numer1 = -1e-16;
  else
   numer1 = 1e-16;
  end
 else
  denom1 = V1(i,1);
  numer1 = V1dot(i,1);
 end
%
%  if abs(V1dot(i,1)) < 1e-6,
%   if sign(V1dot(i,1)) == -1,
%    numer1 = -1e-6;
%   else
%    numer1 = 1e-6;
%   end
%  else
%   numer1 = V1dot(i,1);
%  end
% Calculate alpha1 and d(alpha1)/dt using "component neutral".
 a1(i,1)          =    e_delta1 / denom1;
 da1_dV1(i,i)     =   - e_delta1 / denom1^2;
%
 a1dot(i,1)       =   - e_delta1 * numer1 / denom1^2;
 da1dot_dV1(i,i)  = 2 * e_delta1 * numer1 / denom1^3;
 da1dot_dV1dot(i,i) =  - e_delta1 / denom1^2;
%
% Remove near singularities from swamping out other information.
 if V2(i,1) == 0,
  denom2 = 1e-16;
  if sign(V2dot(i,1)) == -1,
   numer2 = -1e-16;
  else
   numer2 = 1e-16;
  end
 else
  denom2 = V2(i,1);
  numer2 = V2dot(i,1);
 end
%
%  if V2dot(i,1) < 1e-6,
%   if sign(V2dot(i,1)) == -1,
%    numer2 = -1e-6;
%   else
%    numer2 = 1e-6;
%   end
%  else
%   numer2 = V2dot(i,1);
%  end
%
 a2(i,1)          =    e_delta2 / denom2;
 da2_dV2(i,i)     =   - e_delta2 / denom2^2;
%
 a2dot(i,1)       =   - e_delta2 * numer2 / denom2^2;
 da2dot_dV2(i,i)  = 2 * e_delta2 * numer2 / denom2^3;
 da2dot_dV2dot(i,i) =  - e_delta2 / denom2^2;
%
 sum1(i,1)      = a1(i,1) * V1dot(i,1) + V1(i,1) * a1dot(i,1);
 dsum1_dV1(i,i) = da1_dV1(i,i)*V1dot(i,1)+a1dot(i,1)+V1(i,1)*da1dot_dV1(i,i);
 dsum1_dV1dot(i,i) = a1(i,1) + V1(i,1) * da1dot_dV1dot(i,i);
%
 sum2(i,1)   = a2(i,1) * V2dot(i,1) + V2(i,1) * a2dot(i,1);
```

```
 dsum2_dV2(i,i)  = da2_dV2(i,i)*V2dot(i,1)+a2dot(i,1)+V2(i,1)*da2dot_dV2(i,i);
 dsum2_dV2dot(i,i) = a2(i,1) + V2(i,1) * da2dot_dV2dot(i,i);
%
 DVws_Dt(i,1)       = sum1(i,1) + sum2(i,1);
 dDVws_Dt_dV1(i,i)   = dsum1_dV1(i,i);
 dDVws_Dt_dV1dot(i,i) = dsum1_dV1dot(i,i);
 dDVws_Dt_dV2(i,i)   = dsum2_dV2(i,i);
 dDVws_Dt_dV2dot(i,i) = dsum2_dV2dot(i,i);
%
end
%
%
% Collect the export variables, final states, time intervals and jacobian.
%
e = [a1, a1dot, a2, a2dot, DVws_Dt];
%
s1 = []';
%
tt1 = [t1, t0];
%
%
%  Collect the portions of the Jacobian.
%
jacob(1:n,1:n)          = da1_dV1;
jacob(1:n,n+1:2*n)       = Z;
jacob(1:n,2*n+1:3*n)     = Z;
jacob(1:n,3*n+1:4*n)     = Z;
%
jacob(n+1:2*n,1:n)       = da1dot_dV1;
jacob(n+1:2*n,n+1:2*n)    = da1dot_dV1dot;
jacob(n+1:2*n,2*n+1:3*n)  = Z;
jacob(n+1:2*n,3*n+1:4*n)  = Z;
%
jacob(2*n+1:3*n,1:n)     = Z;
jacob(2*n+1:3*n,n+1:2*n)  = Z;
jacob(2*n+1:3*n,2*n+1:3*n) = da2_dV2;
jacob(2*n+1:3*n,3*n+1:4*n) = Z;
%
jacob(3*n+1:4*n,1:n)     = Z;
jacob(3*n+1:4*n,n+1:2*n)  = Z;
jacob(3*n+1:4*n,2*n+1:3*n) = da2dot_dV2;
jacob(3*n+1:4*n,3*n+1:4*n) = da2dot_dV2dot;
%
jacob(4*n+1:5*n,1:n)     = dDVws_Dt_dV1;
jacob(4*n+1:5*n,n+1:2*n)  = dDVws_Dt_dV1dot;
jacob(4*n+1:5*n,2*n+1:3*n) = dDVws_Dt_dV2;
jacob(4*n+1:5*n,3*n+1:4*n) = dDVws_Dt_dV2dot;
```

B.2 Component Neutral Based Stability Demon for Two Generator Analysis

The following is a listing of the .m file for the stability demon "device object".

```
%function [e , jacob, s1, tt1] = demon07(stype,i,par,s0,tt,alpha)
%
%  DEMON07 is the eighth Stability Demon Implemented
%
%  VERSION 8.0 of 31 March 1992
%  (C) Copyright 1992 by John V. Amy Jr.
%
%  [e , jacob , s1, tt1] = demon07(stype,i,par,s0,tt,alpha)
%
%  DEMON07 is the eighth stability demon to be written.  It uses a time varying
%  alpha vector to assess stability.  The rate of change of alpha is adjusted
%  only for its own component, the "component neutral" algorithm is used.  This
%  demon is designed to work on data points to avoid harmonics problems which
```

```
% arise when computing exponentials as a finite series. See 16 March
% notes for specific equations. This demon only treats two organs' inputs.
%
%
%     stype = 1 data points  ****** This demon is made only for data points.
%           = 2 fourier series
%           = 3 legendre series
%           = 4 polynomial
%
%     i    = [V1, V1d, V2, V2d] where V1, V1d, V2, V2d are column vectors.
%              V1 = Lyapunov function of component 1
%             V1d = D(Lyapunov function)/Dt of component 1
%              V2 = Lyapunov function of component 2
%             V2d = D(Lyapunov function)/Dt of component 2
%
%     par  = [delta1, delta2]
%            delta#n is a (positive) constant relating a#n and 1/V#n.
%
%     s0   = []
%
%     tt   = [t0, t1, adt]
%              t0 = initial time of the interval
%              t1 = final time of the interval
%             adt = averaging time increment
%
%     alpha = continuation parameter (0 linear 1 nonlinear)
%
%     e    = [a1, a1dot, a2, a2dot, DVws_Dt]
%                a1  = component 1 alpha
%              a1dot = D(alpha1)/Dt
%                a2  = component 2 alpha
%              a2dot = D(alpha2)/Dt
%             DVws_Dt = D(Vws)/Dt
%
%     jacob = Jacobian matrix of e with respect to i
%
%     s1   = []
%
%     tt1  = [nt1 ntt] where
%              nt1 recommended recomputation time this interval
%              ntt recommended ending time next interval
%
%     structural jacobian
%
%           N000
%           NN00
%           00N0
%           00NN
%           NNNN
%
%
% Read all inputs.
%
[n, nc] = size(i);
%
t0  = tt(1);
t1  = tt(2);
adt = tt(3);
%
delta1 = par(1);
delta2 = par(2);
%
V1    = i(:,1);
V1dot = i(:,2);
```

```
V2    = i(:,3);
V2dot = i(:,4);
%
%
%  Generate some required terms.
%
e_delta1 = exp(delta1);
e_delta2 = exp(delta2);
%
Z = zeros(n,n);
%
%
% Calculate the a#n's using the "component neutral" algorithm.
%
% Carry out the calculation term by term.
%for i=1:n,
% First remove near singularities from swamping out other information.
 if V1(i,1) == 0,
   denom1 = 1e-16;
   if sign(V1dot(i,1)) == -1,
     numer1 = -1e-16;
   else
     numer1 = 1e-16;
   end
 else
   denom1 = V1(i,1);
   numer1 = V1dot(i,1);
 end
%
%%  if abs(V1dot(i,1)) < 1e-6,
%%    if sign(V1dot(i,1)) == -1,
%%      numer1 = -1e-6;
%%    else
%%      numer1 = 1e-6;
%%    end
%%  else
%%    numer1 = V1dot(i,1);
%%  end
% Calculate alpha1 and d(alpha1)/dt using "component neutral".
 a1(i,1)          =    e_delta1 / denom1;
%  da1_dV1(i,i)     =  - e_delta1 / denom1^2;
%
 a1dot(i,1)       =  - e_delta1 * numer1 / denom1^2;
%  da1dot_dV1(i,i)   = 2 * e_delta1 * numer1 / denom1^3;
%  da1dot_dV1dot(i,i) =  - e_delta1 / denom1^2;
%
% Remove near singularities from swamping out other information.
 if V2(i,1) == 0,
   denom2 = 1e-16;
   if sign(V2dot(i,1)) == -1,
     numer2 = -1e-16;
   else
     numer2 = 1e-16;
   end
 else
   denom2 = V2(i,1);
   numer2 = V2dot(i,1);
 end
%
%%  if V2dot(i,1) < 1e-6,
%%    if sign(V2dot(i,1)) == -1,
%%      numer2 = -1e-6;
%%    else
%%      numer2 = 1e-6;
```

```
%%   end
%% else
%%   numer2 = V2dot(i,1);
%% end
%
 a2(i,1)         =    e_delta2 / denom2;
%  da2_dV2(i,i)      =   - e_delta2 / denom2^2;
%
 a2dot(i,1)       =   - e_delta2 * numer2 / denom2^2;
%  da2dot_dV2(i,i)   = 2 * e_delta2 * numer2 / denom2^3;
%  da2dot_dV2dot(i,i) =   - e_delta2 / denom2^2;
%
 sum1(i,1)      = a1(i,1) * V1dot(i,1) + V1(i,1) * a1dot(i,1);
%  dsum1_dV1(i,i)  = da1_dV1(i,i)*V1dot(i,1)+a1dot(i,1)+V1(i,1)*da1dot_dV1(i,i);
%  dsum1_dV1dot(i,i) = a1(i,1) + V1(i,1) * da1dot_dV1dot(i,i);
%
 sum2(i,1)   = a2(i,1) * V2dot(i,1) + V2(i,1) * a2dot(i,1);
%  dsum2_dV2(i,i)  = da2_dV2(i,i)*V2dot(i,1)+a2dot(i,1)+V2(i,1)*da2dot_dV2(i,i);
%  dsum2_dV2dot(i,i) = a2(i,1) + V2(i,1) * da2dot_dV2dot(i,i);
%
 DVws_Dt(i,1)       = sum1(i,1) + sum2(i,1);
%  dDVws_Dt_dV1(i,i)   = dsum1_dV1(i,i);
%  dDVws_Dt_dV1dot(i,i) = dsum1_dV1dot(i,i);
%  dDVws_Dt_dV2(i,i)   = dsum2_dV2(i,i);
%  dDVws_Dt_dV2dot(i,i) = dsum2_dV2dot(i,i);
%
%end
%
%
% Collect the export variables, final states, time intervals and jacobian.
%
%e = [a1, a1dot, a2, a2dot, DVws_Dt];
%
%s1 = []';
%
%tt1 = [t1, t0];
%
%
%  Collect the portions of the Jacobian.
%
%jacob(1:n,1:n)          = da1_dV1;
%jacob(1:n,n+1:2*n)       = Z;
%jacob(1:n,2*n+1:3*n)     = Z;
%jacob(1:n,3*n+1:4*n)     = Z;
%
%jacob(n+1:2*n,1:n)       = da1dot_dV1;
%jacob(n+1:2*n,n+1:2*n)    = da1dot_dV1dot;
%jacob(n+1:2*n,2*n+1:3*n)  = Z;
%jacob(n+1:2*n,3*n+1:4*n)  = Z;
%
%jacob(2*n+1:3*n,1:n)     = Z;
%jacob(2*n+1:3*n,n+1:2*n)  = Z;
%jacob(2*n+1:3*n,2*n+1:3*n) = da2_dV2;
%jacob(2*n+1:3*n,3*n+1:4*n) = Z;
%
%jacob(3*n+1:4*n,1:n)     = Z;
%jacob(3*n+1:4*n,n+1:2*n)  = Z;
%jacob(3*n+1:4*n,2*n+1:3*n) = da2dot_dV2;
%jacob(3*n+1:4*n,3*n+1:4*n) = da2dot_dV2dot;
%
%jacob(4*n+1:5*n,1:n)     = dDVws_Dt_dV1;
%jacob(4*n+1:5*n,n+1:2*n)  = dDVws_Dt_dV1dot;
%jacob(4*n+1:5*n,2*n+1:3*n) = dDVws_Dt_dV2;
%jacob(4*n+1:5*n,3*n+1:4*n) = dDVws_Dt_dV2dot;
```

The previous .m file is streamlined for ex post facto analysis of simulation results.

```
[n, nc] = size(data_t);
%
delta1 = log(data_nd_14(1,1));
delta2 = log(data_nd_23(1,1));
%
%
%  Generate some required terms.
%
e_delta1 = exp(delta1);
e_delta2 = exp(delta2);
%
%
% Calculate the a#n's using the "component neutral" algorithm.
%
% Carry out the calculation term by term.
%
for i=1:n,
%
V1(i,1)    = data_nd_14(i,1);
V1dot(i,1) = data_nd_15(i,1);
V2(i,1)    = data_nd_23(i,1);
V2dot(i,1) = data_nd_24(i,1);
%
% First remove near singularities from swamping out other information.
 if V1(i,1) == 0,
   denom1 = 1e-16;
   if sign(V1dot(i,1)) == -1,
     numer1 = -1e-16;
   else
     numer1 = 1e-16;
   end
 else
   denom1 = V1(i,1);
   numer1 = V1dot(i,1);
 end
%
% Calculate alpha1 and d(alpha1)/dt using "component neutral".
 a1(i,1)          =    e_delta1 / denom1;
%
 a1dot(i,1)       =  - e_delta1 * numer1 / denom1^2;
%
% Remove near singularities from swamping out other information.
 if V2(i,1) == 0,
   denom2 = 1e-16;
   if sign(V2dot(i,1)) == -1,
     numer2 = -1e-16;
   else
     numer2 = 1e-16;
   end
 else
   denom2 = V2(i,1);
   numer2 = V2dot(i,1);
 end
%
 a2(i,1)   =    e_delta2 / denom2;
%
 a2dot(i,1) =   - e_delta2 * numer2 / denom2^2;
%
 sum1(i,1)  = a1(i,1) * V1dot(i,1) + V1(i,1) * a1dot(i,1);
%
 sum2(i,1)  = a2(i,1) * V2dot(i,1) + V2(i,1) * a2dot(i,1);
%
```

```
  DVws_Dt(i,1) = sum1(i,1) + sum2(i,1);
%
end
```

Thesis
A438547 Amy
c.1 Composite system stability methods applied to advanced shipboard electric power systems.